Mathematical modelling and control of perennial plant phytopathogens

Clotilde Djuikem

UNIVERSITÉ CÔTE D'AZUR

ÉCOLE DOCTORALE
SCIENCES ET TECHNOLOGIES DE L'INFORMATION ET DE LA COMMUNICATION

THÈSE DE DOCTORAT

Modélisation mathématique et contrôle de phytopathogènes de plantes pérennes

Clotilde DJUIKEM

BIOCORE, Centre Inria d'Université Côte d'Azur

Présentée en vue de l'obtention du grade de docteur en
Automatique, Traitement du Signal et des Images
d'Université Côte d'Azur

Dirigée par :
Jean-Luc GOUZÉ

Co-encadrée par :
Frédéric GROGNARD
Suzanne TOUZEAU
Samuel BOWONG

Devant le jury, composé de :
Julien ARINO, Professeur, University of Manitoba, Canada
Samuel BOWONG, Professeur, Université de Douala, Cameroun
Arnaud DUCROT, Professeur, Université Le Havre Normandie
Jean-luc GOUZÉ, Directeur de recherche, Inria
Frédéric GROGNARD, Chargé de recherche, Inria
Fabien HALKETT, Chargé de recherche, INRAE
Béatrice LAROCHE, Directrice de recherche, INRAE
Jean Jules TEWA, Professeur, Université de Yaoundé I, Cameroun
Suzanne TOUZEAU, Chargée de recherche, INRAE

Soutenue le : 5 janvier 2023

Inria

Modélisation mathématique et contrôle de phytopathogènes de plantes pérennes

Jury :

Président du jury
Julien ARINO, Professeur, University of Manitoba, Canada

Rapporteurs :
Arnaud DUCROT, Professeur, Université Le Havre Normandie
Jean Jules TEWA, Professeur, Université de Yaoundé I, Cameroun

Examinateurs/Examinatrice :
Samuel BOWONG, Professeur, Université de Douala, Cameroun
Jean-Luc GOUZÉ, Directeur de recherche, Inria
Fabien HALKETT, Chargé de recherche, INRAE
Béatrice LAROCHE, Directrice de recherche, INRAE
Suzanne TOUZEAU, Chargée de recherche, INRAE

Invité :
Frédéric GROGNARD, Chargé de recherche, Inria

Dedication

To my mother NGOULLA Thérèse.

Acknowledgments

This work like others could not have been realised without the numerous consultation of scholarly works and collaboration from different people. I was always thought not to say «thank you» but to know how to show gratefulness to those who gave you support. I would therefore show my thankfulness to all those who supported me throughout this work.

First of all, I thank the Almighty God for giving me the strength to finish my three-year thesis despite the surgeries I went through.

I would like to thank Jean-Luc Gouzé for accepting to direct my thesis. Thank you for your help over the years.

I would like to express my particular gratitude to supervisors Suzanne Touzeau and Frédéric Grognard for years of incredible collaboration with them in rigorous scientific research. Moreover, I want to express my gratitude to them for acting as my parents over the years by assisting me during my surgeries and driving me to and from the research facilities and to my hospital appointments. Again, I thank them for the wonderful environment they helped to develop during my journey at Inria in Sophia Antipolis.

I am grateful to Samuel Bowong for his advices and support during all my academic and research period. Thank you for believing in me and encouraging me in this way. On a daily basis, I much value your advises.

I would want to express my gratitude to Ludovic Mailleret and Fabien Hallket for agreeing to lead my Individual Survival Committee. Your advises was really helpful in completing my thesis.

I would like to thank the jury's members composed of Julien Arino as President, Jean Jules Tewa, Arnaud Ducrot the Rapporteur and Beatrice and Fabien Hallket as members of this jury, for their high contribution in the improvement of the quality of this manuscript.

I would like to thank all the members of my team (Biocore), as well as all those who exchanged a smile, a sweet word, in the hallway or at lunch. A special thank goes to the Team Leader Olivier Bernard.

Johan Monagnat deserves a special thank you for being there all these years and welcoming me into his house as his own daughter. I am grateful to you and Suzanne for welcoming me back after these operations. The completion of my thesis would not have been feasible without your help throughout the years.

I appreciate and will never forget the people I made at Inria, Inrae and others place who kept the three years pleasant and lighthearted : Bruno, Yan, Ali, Ignacio, Juan-Carlos, Lucie, Alesia, Carlos, Nicolas, Elena, Lamberto, Agústin, Walid, Israël, Nicolás, Yan, Ali, Ignacio, Juan-Carlos, Adel, Odile, Joseph, Fransheca, Jineth, David, Ludovic, Josué, Pauline, Méline, Hannah, Adel, David, Maxime, Marine, Beryl, Tehreem . Thank you for our time spending together at the volleyball beach and coffee break.

I would also like to warmly thank Marielle for her friendship, advice, presence at my several hospital appointments, and her role as Stella's aunty during this time.

A special thank you to Masimba for his friendship and advice on how to improve my English during these three years.

A special thank you to Yves for being there from the beginning of this experience with his assistance concerning my health issues and his scientific advice during my internship.

A special thanks to my mother Thérèse Ngoulla for all the sacrifices and efforts made during all these years to encourage her children to go as far as possible in their achievement. Your character as a hard-working woman helped me to better understand life and its difficulties.

I would like to thank Stella, my lovely daughter for the strength and the support she gives me everyday by her presence here in my life.

I am indebted to my brothers and sisters Cyrille, Delphine, Gilbertine, Aubin, Rodrigue, Carole, Chanceline who are dearest in my heart. Thanks for their support and permanent assistance. It is a blessing to have a family that supports you in what you do and values what you do. My brothers and sisters, this journey today is made possible in part by you, since your adventures motivate me every day, and you are my first role models of success.

A special thanks to Yvon for being there, for encouraging me, and for reminding me when things get tough that I can accomplish anything.

Special thanks go to Fanou for his advices, support and encouragements in all my undertakings.

A particular thanks to Marc, my physiotherapist ; the several operations I had throughout my thesis years required a patient and attentive individual to enhance my health, and you were such person.

A particular thank you to my best friend Gaïtan, who I affectionately call Gaï ; you are one of those people who has been there since the beginning of this study experience, since Babété, and who is always there to encourage me and provide a helping hand when required.

I cannot my friends Daniel, Rodin, Naomie, Foutse, Charles, Vanessa, Irène, Auriole, Ralph, Mitterand, Anita, Myriam, Damarique, Crepin, Roméo, Guerlaine, Bienvenu, Cedric, Camelle, Arantes, Pablo, Jerry, Léon, Harold, Franklin, Arnold, Alphonse, Pierre who also stand by me in one way and the other during these years.

To everyone whose is not mentioned here, your prayers, encouragements, patience and tolerance will always be remembered.

Modélisation mathématique et contrôle de phytopathogènes de plantes pérennes

Résumé Les maladies fongiques causent d'importants dégâts dans les cultures et menacent la sécurité alimentaire mondiale. Les fongicides chimiques sont couramment utilisés, mais ils sont nocifs pour l'environnement, la santé humaine et peuvent entraîner des résistances des pathogènes. Il est donc nécessaire de développer des méthodes de contrôle plus durables. Pour aborder cette question, nous avons développé des modèles mathématiques représentant l'interaction plante-champignon, afin de proposer des méthodes alternatives. Nous avons obtenu des résultats qualitatifs génériques, qui ont été appliqués à la rouille orangée du caféier causée par *Hemileia vastatrix*, une importante maladie du café. Cette culture de rente faisant vivre de nombreux petits producteurs et leurs familles, le contrôle de cette maladie est un enjeu socio-économique majeur.

Tout d'abord, nous avons développé un modèle représentant l'interaction plante-champignon en utilisant des équations différentielles ordinaires. Comme dans les modèles épidémiologiques classiques, la population hôte a été subdivisée par état de santé, l'individu étant la feuille de la plante. L'infection étant transmise par les spores libérées par le champignon, leur dynamique a également été incluse. De plus, les feuilles jeunes et matures ont été différenciées, pour tenir compte de variations d'agressivité du champignon selon l'âge de l'hôte. Nous avons calculé le taux de reproduction de base $\mathcal{R}_0$, qui détermine classiquement la stabilité de l'équilibre sans maladie. Ce modèle a exhibé des propriétés asymptotiques complexes, différentes des modèles classiques : $\mathcal{R}_0 < 1$ ne suffisait pas à obtenir la stabilité de l'équilibre sans maladie, un équilibre endémique stable pouvant exister ; $\mathcal{R}_0 > 1$ ne garantissait pas l'existence et la stabilité d'un équilibre endémique, car de fortes valeurs de $\mathcal{R}_0$ pouvaient conduire à la destruction de la plantation.

Puis, les spores de champignons tels que *H. vastatrix* étant dispersées par le vent, nous avons considéré un modèle spatio-temporel décrivant la propagation de la maladie dans une plantation pendant la saison des pluies et la saison sèche, à base d'équations aux derivées partielles. Nous avons calculé deux seuils, les taux de reproduction de base en saison des pluies et saison sèche, qui caractérisent la stabilité des équilibres des sous-systèmes saisonniers. Pour illustrer ces résultats théoriques, des simulations numériques ont été réalisées, en utilisant une méthode non-standard de différences finies pour intégrer le modèle. Nous avons également étudié numériquement l'impact d'un agent de biocontrôle qui réduit la reproduction du champignon. Nous avons déterminé son seuil d'efficacité afin d'assurer l'éradication de la maladie.

Enfin, nous avons développé un modèle multi-saison, avec des dynamiques continues pour l'hôte et le champignon en saisons des pluies et des événements discrets pour les dynamiques plus simples des saisons sèches. En outre, nous avons implémenté une stratégie de biocontrôle fondée sur des hyperparasites se nourrissant de spores, dont la dynamique a été explicitement représentée. Les hyperparasites étaient lâchés une ou plusieurs fois pendant les saisons des pluies. Des études analytiques et semi-numériques ont été réalisées afin de déterminer la quantité et la fréquence des lâchers nécessaires pour contrôler efficacement la maladie. Nous avons montré que la meilleure stratégie dépendait de la mortalité des hyperparasites : les parasites à faible mortalité ne devaient être introduits qu'une fois par an, tandis que les parasites avec une mortalité élevée devaient l'être plus fréquemment afin d'assurer leur persistance dans la plantation.

Grâce à la modélisation mathématique, ce travail fournit des bases qualitatives et quantitatives pour la compréhension des interactions plante-champignon, ainsi que pour la mise en place d'alternatives aux fongicides chimiques afin de lutter contre les maladies fongiques de cultures pérennes.

Mots-clés: modélisation mathématique, épidémiologie végétale, culture pérenne, champignon phytopathogène, rouille orangée du caféier, méthodes de lutte durables

Mathematical modelling and control of perennial plant phytopathogens

Abstract Fungal diseases cause serious damages in crops, which threatens food security worldwide. In response, chemical fungicides are commonly used, yet they are harmful to the environment and human health and they may induce fungus resistance. There is a definite need for more sustainable control methods. To tackle this issue, our approach consisted in developing mathematical models representing crop-fungus interactions, in order to design alternative control methods. We obtained generic qualitative results, which we applied to coffee leaf rust caused by *Hemileia vastatrix*, a major coffee disease. Coffee being an important cash crop which provides a living for numerous small producers and their family, controlling coffee leaf rust is hence a major socio-economic issue.

First, we developed a crop-fungus interaction model using ordinary differential equations. As in classical epidemiological models, the host population was subdivided by health status, considering the crop leaf as an individual. The infection being mediated by fungus spores released in the plantation, their dynamics were also included. Moreover, this model differentiated between young and mature leaves, to take into account variations in fungus aggressiveness according to host development. We computed the basic reproduction number $\mathcal{R}_0$, which classically determines the stability of the disease free equilibrium. This model exhibited complex asymptotic properties, that differed from classical epidemiological models: $\mathcal{R}_0 < 1$ was not sufficient to obtain the stability of the disease free equilibrium, as a stable endemic equilibrium could exist; $\mathcal{R}_0 > 1$ did not guarantee the existence and stability of an endemic equilibrium, because high $\mathcal{R}_0$ values could lead to the destruction of the plantation.

Then, based on the knowledge that spores of fungi such as *H. vastatrix* are dispersed by wind, we considered a spatio-temporal model describing the disease propagation in a plantation during the rainy and dry seasons, using partial differential equations. We computed two threshold parameters, the rainy and dry period basic reproduction numbers, that characterised the stability of the equilibria for seasonal subsystems. To illustrate these theoretical results, numerical simulations were performed, using a non-standard finite method to integrate the pest model. We also numerically investigated the impact of a biocontrol agent which reduces the reproduction of the fungus. We determined its efficiency threshold in order to ensure disease eradication.

Finally, we developed a multi-seasonal model, alternating continuous crop-fungus dynamics during the rainy seasons and discrete events to represent the simpler dynamics during the dry seasons. Moreover, we implemented a biocontrol strategy based on hyperparasites, whose dynamics were explicitly represented. Hyperparasites were introduced through one or more discrete events over the rainy seasons. Analytical and semi-numerical studies were performed to determine how much and how frequently hyperparasites had to be introduced to efficiently control the disease. We showed that the best strategy depended on the hyperparasite mortality: low mortality parasites needed be released only once a year, while high mortality parasites had to be released more frequently to ensure their persistence in the plantation.

Through mathematical modelling, this work hence provides qualitative and quantitative bases for the understanding of interactions between a crop and a phytopathogenic fungus, as well as for the implementation of alternatives to chemical fungicides for the control of fungal diseases in perennial crops.

Keywords: mathematical modelling, plant epidemiology, perennial crop, phytopathogenic fungus, coffee leaf rust, sustainable control methods

Modélisation mathématique et contrôle de phytopathogènes de plantes pérennes

Résumé grand public Les maladies fongiques causent d'importants dégâts dans les cultures et menacent ainsi la sécurité alimentaire mondiale. Les fongicides sont largement utilisés, malgré leur impact négatif sur l'environnement et la santé humaine. En outre, ils induisent des résistances qui limitent leur utilisation à long terme. Des méthodes de lutte alternatives et durables doivent donc être développées. Cette thèse contribue à cet enjeu par une approche de modélisation mathématique. Les modèles représentent les dynamiques saisonnières des interactions plante-champignon et intègrent une méthode de lutte biologique par des lâchers d'hyperparasites. Les résultats obtenus ont permis de déterminer la quantité et la fréquence de lâchers nécessaires pour contrôler la maladie. Ils ont été appliqués à la rouille orangée du caféier, une importante maladie du café. Cette culture de rente faisant vivre de nombreux petits producteurs, le contrôle de cette maladie est un enjeu socio-économique majeur.

Mathematical modelling and control of perennial plant phytopathogens

Lay summary Fungal diseases cause significant damages in crops and thus threaten global food security. Fungicides are widely used, despite their negative impact on the environment and human health. In addition, they induce resistance that limits their long-term use. Alternative and sustainable control methods therefore need to be developed. This thesis contributes to this issue through a mathematical modelling approach. The models represent the seasonal dynamics of plant-fungus interactions and integrate a biological control method using hyperparasite releases. The results obtained allowed to determine the quantity and frequency of releases necessary to control the disease. These results were applied to coffee leaf rust, a major coffee disease. Coffee being an important cash crop which provides a living for numerous small producers, controlling coffee leaf rust is a major socio-economic issue.

Contents

List of Figures

List of Tables

Chapter 1

Introduction

Contents

1.1 Context

1.1.1 Socio-economic impact of crop pests and diseases

Agriculture plays a key role in reducing poverty, raising incomes and improving food security [110]. The rapid growth of global population raises the need for agricultural production while simultaneously increasing the need for agricultural land. As agriculture struggles to feed this growing population, climate change, pest and crop diseases reduce quantity and quality of crop production [110, 53, 3]. According to FAO estimates, up to 40% of the world crop production is lost each year due to pests, and plant diseases cost the global economy more than $220 billion yearly [46]. Global yield losses for crops that dominate the world in production, such as rice, wheat, barley, maize, potatoes, soybeans, cotton, and coffee in various regions and countries range from 20% to 40% [117]. Due to the intricate interactions between social and economic issues, the primary problem facing agriculture is ensuring food security while increasing production and reducing environmental cost [127]. In order to boost productivity, it is necessary to manage pests and plant diseases, but due to the resilience of them, these efforts are not only expensive but also incredibly difficult. Consequently, it is necessary to continuously develop the control methods.

Control of crop diseases and pests is a major issue, particularly in African countries such as Cameroon, where agriculture is a very important sector in terms of income and employment. More precisely, Cameroon's tropical climate is very favourable to agriculture. With 21% of agricultural land, this sector represents 30% of the country export revenues and 14% of its GDP [47, 118]. It employs almost 62% of the working population. The main export crops are cocoa (4^{th} largest producing country in 2016, 15% of exports), bananas and plantains (7.2%), cotton (4.2%) and coffee (1.5%). Food crops include bananas and plantains, cassava, yam, maize, sorghum, millet, etc. Amount these crops, coffee is an economically important crop in the tropics and subtropics. Globally, more than 50 countries across Latin America, Africa, Asia and Oceania grow coffee on a commercial scale [126]. Coffee exports are a significant source of income for developing countries, and the worldwide green coffee market is expected to increase from $35.40 billion in 2021 to $47.22 billion in 2028 [51]. However, the production of coffee was attacked by many pests and pathogens.

1.1.2 Coffee pests and diseases

Coffee is grown in practically every tropical country [177]. Optimal coffee-growing conditions include cold to warm tropical climates, rich soils, and theses optimal conditions favour pests or diseases. The world coffee belt spans the globe along the equator, with cultivation in North, Central, and South America; the Caribbean; Africa; the Middle East; and Asia. Brazil is now the world largest coffee-producing country, accounting for one-third of all the coffee produced worldwide [171]. The climate change increased intense heat waves, drought, and excessive rainfall in some coffee cultivation areas which make more difficult to grow coffee, and increase the pathogens and pests that affect it. The list provided here does not include all of the diseases and pests that are damaging coffee farms around the world, but it does represent a significant portion of them. We classify two category, coffee pests and diseases [170].

Coffee pests

- The coffee berry borer (CBB), whose scientific name is *Hypothenemus Hampei*, is an insect of the *Scolytidae* family that feeds and grows at the expense of the berries. According to historical records, this insect pest was originally identified in Gabon in Central Africa in 1901. But this pest currently presents a risk to every coffee plantation in the world, starting in Africa [74]. Accidental introductions of CBB in coffee plantations have led to its rapid geographical expansion worldwide. This insect can adapt to a variety of environmental circumstances and defy a variety of eradication programmes implemented by coffee growers since it spends the most of its life inside a berry [52, 138].

- Root knot nematodes (*Meloidogyne spp.*) develop inside the roots of plants, their impact reduce the ability of the coffee tree to absorb water and nutrients. This is in turn reflected in a decline in the general health and vigour of the tree and hence yield and bean quality [41, 138].

- Nursery disease, caused by *Rhizoctonia solani*, occurs on seedlings of 1-3 months age in the nursery if the conditions are favourable for the fungus growth [41].

- *Monochamus leuconotus*, commonly named white coffee stem borer, is a pest whose larvae, by feeding on the bark and tunnelling into the wood, cause serious damage to the tree.

This pest is endemic to Africa and has been reported in many coffee-growing countries [138].

- *Coccus viridis*, named green scale, is an important widespread coffee scale present in most coffee-producing countries. It affects plants during any stage of their growth, whether vegetative, flowering, fruiting, or post-harvest [138].

- *Pseudococcus coffeae*, named coffee root mealybug, is a tiny insect that consumes plants by draining the sap from their roots. Mealybugs can multiply rapidly, especially in dry weather. Root mealybugs have been known to cause severe damage to the crop, especially in Kenya [138].

Coffee diseases

- Coffee berry disease (CBD) is a disease caused by fungus *Colletotrichum kahawae* that produces areas of black necrosis and premature dropping of the green coffee berries. High humidity, relatively warm temperatures, and high altitude are ideal for disease formation [98]. The first report of CBD dates back to 1922 in western Kenya, where it led to the destruction of coffee plantations [103]. It has only been found to date in African production zones, as in the west of Cameroon [17], and it can lead to 60% harvest losses [99].

- Coffee leaf rust (CLR) is a disease caused by an obligate fungus, *Hemileia vastatrix*, which attacks leaves and reduces the photosynthesis rate by either defoliating the plant or covering a portion of the leaf surface area. It has an impact on yield because berry production is correlated with the amount of foliage [87]. It was first reported by an English explorer on wild *Coffea* species in the Lake Victoria region of East Africa in 1861 [171]. Since this initial report, CLR has continued to cause significant economic losses. As of 1990, CLR has become endemic in all major coffee-producing countries [171]. In 2012, ten nations in Latin America and the Caribbean experienced a severe CLR outbreak. The disease spread rapidly, and the consequent crop losses caused the supply to drop significantly. Between 2012 and 2014, CLR damaged over $1 billion and impacted over 2 million people in Latin America [160]. During this period in Honduras, 80,000 hectares of coffee farms were infected [175]. Coffee crops in Guatemala were ruined and a state of emergency was declared in February 2013 [13]. Sanitary emergency was also declared in Peru by the government. In the Hawaiian Islands, coffee leaf rust was reported in January 2021 [66].

- There are four different root diseases that affect coffee plants: brown root disease, red root disease (by *Poria hypolateritia*), black root disease (by *Rosellinia bunodes*) and Santavery root disease (by *Fusarium oxysporum*). These diseases damage the tree roots: they stop the trunk supply of nutrients and water, which kills the tree [41].

- The soil-borne fungus *Fusarium stilbioides*, which causes coffee bark disease, only seems to affect *Coffea arabica*. It was initially identified in Tanzania in 1932, then later in Malawi, where it significantly damaged the economy of the country [138].

- Coffee wilt disease, also known as “fusarium wilt”, is a vascular disease caused by fungus *Fusarium xylarioides*. The fungus blocks the xylem system, causing host reactions that progressively lead to plant death [50]. Coffee wilt disease was first observed in the Central

African Republic in 1928 where it developed slowly and went on to cause two epidemics between the 1930s and the 1960s [138].

- American leaf spot of coffee is a disease caused by gemmiferous fungus *Mycena citricolor* [7].
- The coffee brown-eye spot, a disease caused by the fungus *Cercospora coffeicola*, has been reported in all coffee-growing countries. The disease is usually a problem when coffee plants are not growing well, because of poor nutrition or too little shade. In nurseries, it can cause leaf fall of seedlings and, in severe cases, stem dieback. Generally, it is less important on mature plants, although epidemics may occur on well-maintained trees [41].
- Powdery rust of coffee is a disease caused by fungus *Hemileia coffeicola*. It was first recorded on *Coffea arabica* in Cameroon in 1932. Infected leaves eventually turn yellow and are desiccated [100].

In contrast to other harmful coffee diseases like coffee berry disease, which is more common in Africa, CLR affects all coffee plantations worldwide. Moreover, new epidemics still happen nowadays, as was the case in Hawaii in 2021 [66]. A major epidemic like the one that struck America in 2012 could occur at any time and bring about the collapse of the coffee industry, in addition to the losses that the disease continues to cause today. Estimates of yield loss due to CLR vary by country and might be as high as 80% [171]. The costs of controlling the disease are also high. They are largely due to the reliance on fungicides, which are estimated, globally, between US$1 billion and US$3 billion per year [138]. This is why we chose to concentrate on CLR.

1.2 Biology of coffee leaf rust (CLR)

1.2.1 Coffee development

The coffee tree is a tropical perennial plant of the *Rubiaceae* genus. There are around 100 species of this plant. The two main species of coffee tree cultivated worldwide are *Coffea arabica* (arabica) and *Coffea canephora* (robusta) [30]. Less cultivated species include *Coffea liberica* and *Coffea excelsa*, which are mainly restricted to West Africa and Asia, and account for only 1-2% of the global production [177]. The taxonomic classification has become increasingly complex due to the discovery of several new species during the twentieth century in West Africa, Central Africa, Madagascar, and East Africa [30]. The growth of a coffee plant from seed to first flowering and fruit production takes around five years. The fruit of the coffee tree is called a cherry or berry. The beans that grow within the berry are used to make roast and grind coffee, soluble coffee powders, coffee liquor, etc. The economic lifespan of a coffee plantation is rarely more than 30 years, although a well-managed coffee tree can be productive for 80 years or more, but fruit production decreases over time [177]. There are two main periods in the life cycle of a coffee tree, described below.

- Growth period: from the germination of the seed until adulthood. The coffee bean may be seeded fast and can germinate right away after harvest. After germination it takes around three to seven years to become an adult plant [28]. The coffee tree often has an upright

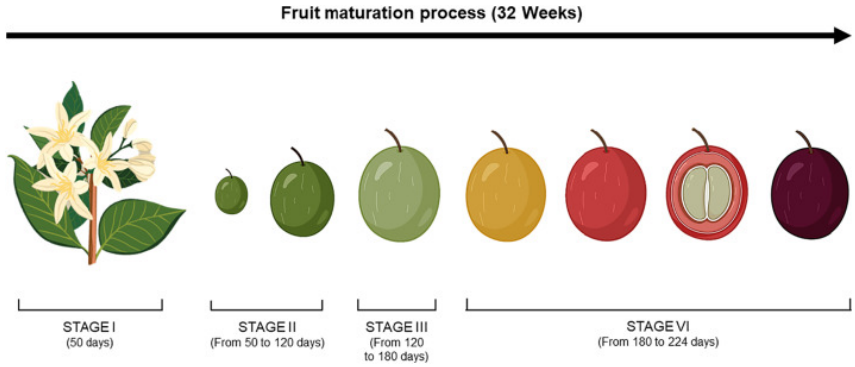

Figure 1.1: Coffee maturation, from flower to ripe frui – from [159].

main shoot (trunk) with lateral branches that are classified as primary, secondary, and tertiary. On the sides of the main stem and branches of the coffee tree, leaves develop on petioles in opposing pairs [31].

- Productivity period: from the time the coffee tree initially flowers until it dies. The flowers begin to form in the axils of the leaves at the age of three. There are 15 to 50 blossoms at each node, which consists of two leaves [28, 177]. After pollination, 65% of flowers will produce fruit. However, this proportion varies among species and trees, ranging from 3 to 91% [31, 177]. Figure 1.1 shows the fruiting period, which ranges from flowering to fruit maturity, for a single season of coffee production.

  Usually, the number of fruits is higher for arabica than robusta, due to the fact that the former is self-fertile, while the latter is self-sterile [28]. Varieties of coffee differ in the size and shape of the coffee bean (seed) but, on average, beans are approximately 10 mm long and 6 mm wide. The weight of a seed is 0.45–0.50 g for arabica and 0.37–0.40 g for robusta [177].

1.2.2 Fungus *Hemileia vastatrix*

Coffee leaf rust (CLR) is caused by the fungus known scientifically as *Hemileia vastatrix*. This fungus is an obligate parasite of coffee, meaning that it can only complete its life cycle on plants of the *Coffea* genus.

1.2.2.1 History of *Hemileia vastatrix*

After the first report in 1861, CLR was detected in 1867 on the Island of Ceylon (now Sri Lanka), where it decimated all coffee trees [5]. In Figure 1.2, which depicts the progression of CLR worldwide since its first report until 2014, we can see that practically all of the nations that produce coffee have been affected.

Cameroon went through an epidemic from 1930 to 1935, Brazil in 1970, Costa Rica in 1989, Nicaragua in 1995, El Salvador from 2002 to 2003, Colombia from 2008 to 2013, Peru from 2008 to 2011, and Ecuador in 2013. Coffee production declined in many nations in 2012 as a result of the serious CLR outbreak in Central America. El Salvador, the nation most affected, reported a 70% decrease in coffee yields, and Honduras, whose production had reached a record level in 2012, saw a 23% decrease between 2012 and 2013. In Guatemala, production dropped by 18% between 2012 and 2014, while Nicaragua, the country least affected, met an 11% decline between

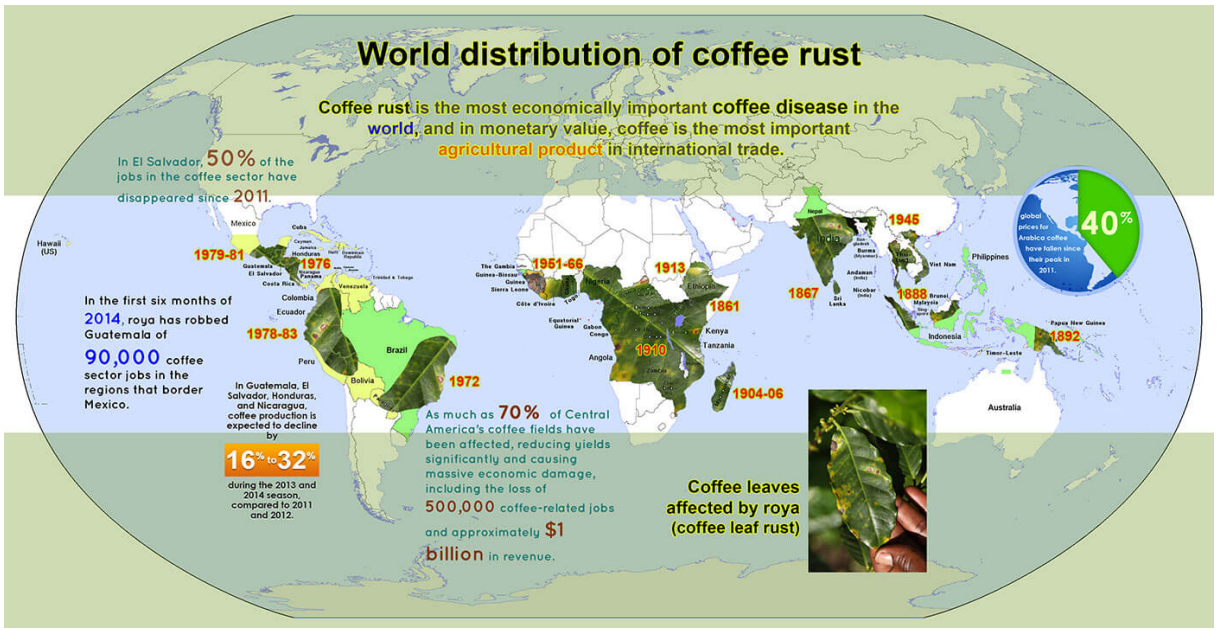

Figure 1.2: World distribution of coffee leaf rust. Source: Bionovelus, 2014.

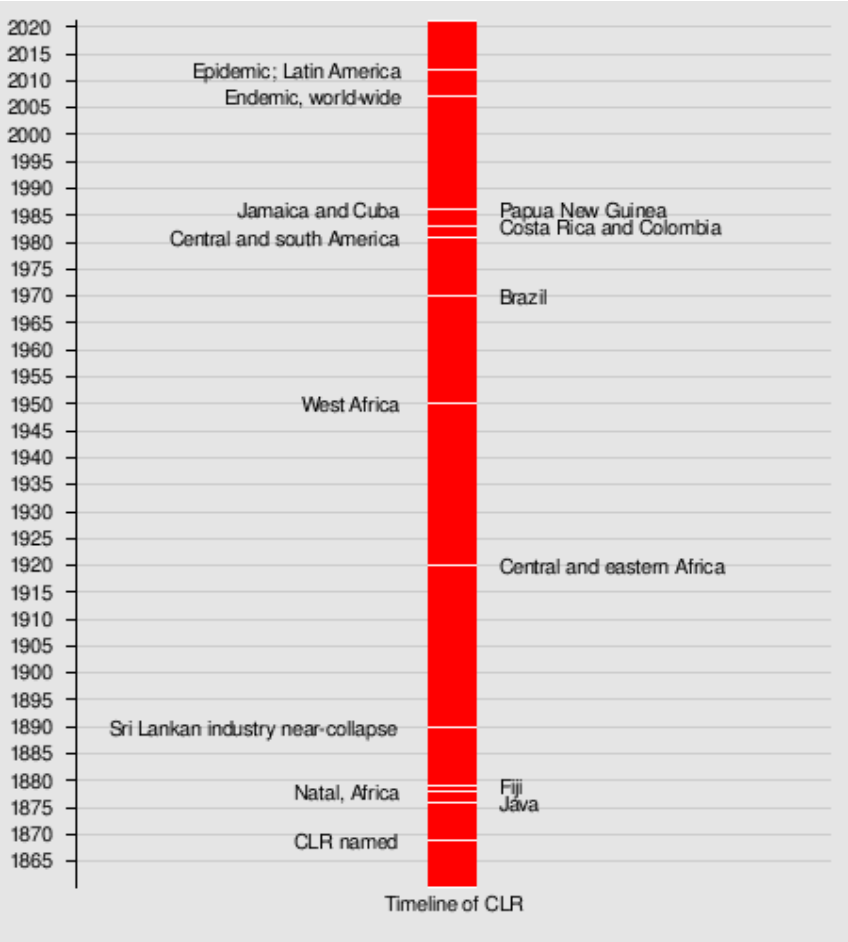

Figure 1.3: Timeline of coffee leaf rust, from 1865 to 2020 – from [176].

2012 and 2014 [8]. The first CLR reports in Hawaii appeared in 2020 [66, 4]. Figure 1.3 presents the timeline of CLR since its discovery.

1.2.2.2 Life cycle of *Hemileia vastatrix*

The life cycle of fungus *H. vastatrix* involves several steps, presented in Figure 1.4.

Step 1: Uredospore dispersal is generally caused by wind, rain, human impact, or a combination of these factors [153].

Step 2: Under favourable conditions uredospores germinate. Although temperature and moisture are key factors for infection, dispersal, and colonisation, plant resistance is also important in determining whether *H. vastatrix* will penetrate the leaves [153].

Step 3: The germinal tubes of the uredospores penetrate the open stomata, which are present only on the underside of the leaves. In order to create a biotrophic connection, the fungus colonises the leaf through an intercellular mycelium[1] growth hypha[2] that forms haustoria[3] within the host cells [153].

Step 4: Within 24–48 hours, infection is completed. A successful infection will cause yellow

[1]The mycelium is a root-like structure of a fungus
[2]The hypha is a long, branching, filamentous structure of a fungus
[3]The haustoria is a rootlike structure that grows into another structure to absorb water or nutrients

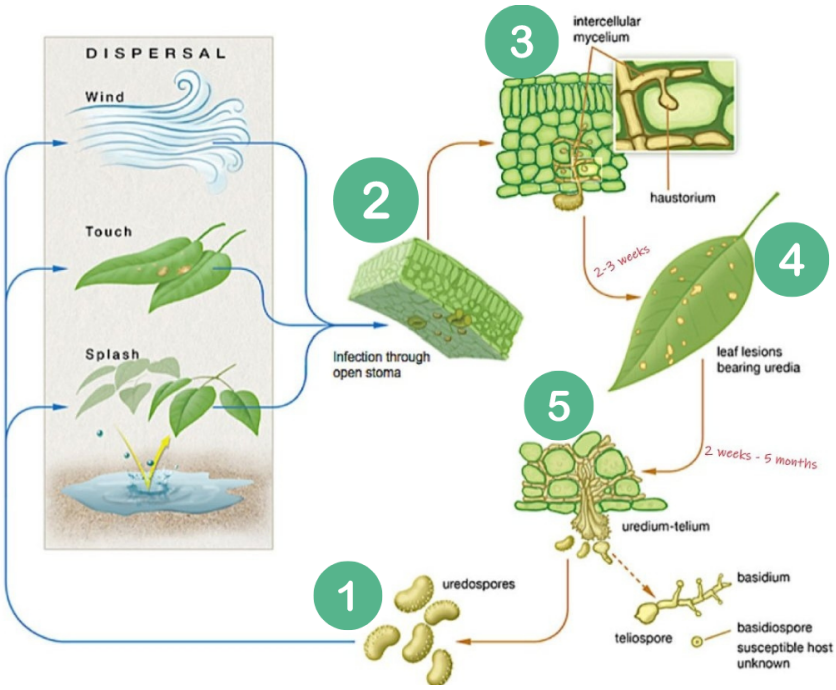

Figure 1.4: Life cycle of fungus *H. vastatrix*: (1) Dissemination, (2) germination, (3) intercellular mycelium, (4) yellow spots and (5) sporulation – adapted from [77].

lesions to appear on the leaf within 2-3 weeks, and these lesions will colonise and produce spores. Each lesion is made up of multiple pustules that will continue to develop for several months [87].

Step 5: Fungus *H. vastatrix* produces uredospores asexually and teliospores sexually. However, because teliospores do not infect coffee leaves and have no known hosts, there is no evidence for an active sexual reproductive cycle [136].

1.2.2.3 Impact of coffee leaf rust

Coffee leaf rust has direct and indirect economic impacts on coffee production. Direct impacts include decreased quantity and quality of yield produced by the diseased plants. Indeed, CLR cause:

- premature defoliation of leaves, which reduces the plant ability to derive energy through photosynthesis [87];
- abortion of flowers and fruits at the premature stage, which decreases their quantity and quality, and which ultimately reduces the beverage quality [123];
- desiccation of young shoots and branches, which reduces the production for the following years [8].

Indirect impacts include increased costs to control the disease [102].

1.2.3 CLR control methods

Farmers use integrated pest management to reduce the spread of rust. Integrated pest management is a combination of biological, biotechnological, chemical, physical, cultural methods, as well as the use of resistant cultivars [145]. CLR control methods can be classified into five categories.

Quarantine During more than a century, strict quarantine measures prevented coffee rust from invading the Americas. In Central America, new infections were removed by spraying diseased coffee plants as well as asymptomatic plants within 30 metres with a herbicide mixed with diesel fuel [5]. The downside is that coffee plant take several years to produce. Thus, removing infected plants implies to wait at least three years before the replacement plants start producing coffee.

Chemical control Among the chemical fungicides available, the ones usually used against CLR are copper fungicides and dithiocarbamate, which must be present on the leaves before the infection occurs [25]. One disadvantage of using fungicides, beside the cost, is that the copper accumulates in the soil, particularly in the organic matter, and can reach levels toxic to plants and to other organisms in the environment [5]. Furthermore, the application of fungicides leads to resistance of fungi over time, which considerably limits their effectiveness and disqualifies them as sustainable control methods [93, 109].

Cultural practices Although cultural practices are crucial, there are no clear-cut guidelines to follow. Nutrition is an important aspect in CLR management, since the susceptibility to rust is associated with the nutritional status of the plant. Fertilisation with nitrogen and phosphorus tends to reduce susceptibility to rust, but excessive potassium increases susceptibility [5]. One of

the key cultural management decisions is to produce coffee either in full sun or with some degree of shade [90]. This decision is often more sociopolitical than agronomic. Some say that rust is easier to control on properly spaced plants in full sun, since they dry faster and, therefore, have shorter periods of leaf wetness. Others argue that coffee in the shade has less rust because the closed canopy prevents the formation of dew on coffee leaves and thus reduces the infection. Sun may hinder the development of the pathogen, but it increases the plant productivity. The plant then needs an extra input of nutrients, particularly nitrogen. Furthermore, a higher production may provide more scope to the spread of CLR [177].

Biological control It is an approach that employs natural pest enemies. Several biological agents have been tested to control CLR, among which various bacteria. Antagonist bacteria *Bacillus subtilis* isolated from the rhizosphere of coffee crops significantly decreased uredospore development (up to 68%) in vitro [34]. In greenhouse and field conditions, antagonist bacteria *Pseudomonas putida* (P286) and *Bacillus thuringiensis* (B157) completely inhibited uredospore germination; electron microscopy revealed that the B157 isolate prevented the production of germination tubes. An investigation done in Ervália in 2007 revealed that isolate B157 decreased rust intensity as efficiently as copper hydroxide. As a result, it is being investigated as a possible biocontrol agent for coffee rust in organic agricultural systems in Brazil [62]. Forty endophytic bacteria isolates were tested for their capacity to inhibit *H. vastatrix* uredospore germination, among which twenty three reduced more than 40% of the germination; in general, the endophytes were more effective when applied before the inoculation of *H. vastatrix* uredospores [146].

Other investigations on biocontrol focused on hyperparasites, which are parasites whose host, often an insect, is also a parasite. Several potential hyperparasites emerged to be natural enemies of fungus *H. vastatrix*, among which *Verticillium psalliotae*, shown to reduce the germination of uredospores [95, 91], and fungus *Cladosporium hemileiae*, which inhibits the evolution of *H. vastatrix* mycelium [149]. Fungus *Lecanicillium lecanii* (previously called *Verticillium lecanii*) affects the viability of *H. vastatrix* uredospores and was reported as a promising biocontrol agent in several studies [168, 73, 44]. In southern Ethiopia, investigations conducted during the dry and wet seasons for three consecutive years at 60 showed that *L. lecanii* inhibits the rust growth when the seasons change from wet to dry [181]. Finally, the larvae of some *Mycodiplosis* insect species can feed on spores of rust fungus *H. vastatrix* and can therefore be considered as rust spore predators [139, 63, 67].

Resistant cultivars Recent biotechnology advances made it possible to detect and choose the best cultivars for coffee farming that should be resistant to fungus *H. vastatrix* [145] and to other fungi [141]. Combining CLR resistance with desirable agronomic traits and high calibre coffee is a problem for breeders. The next issue is to use these resistance genes such that new strains of *H. vastatrix* do not quickly overcome them. The Major resistant cultivars were developed from hybridisation between *C. arabica* and *C. canephora* or their descendants [177]. There are several types of resistant coffee, with varying degrees of CLR resistance (high, moderate, or low) [142]. Some resistant cultivars are cited below.

- Hibrido de Timor is the result of natural hybridisation between *C. arabica* and *C. canephora* [135] and grown widely on the island of Timor. It is the most important progenitor for resistance to coffee leaf rust.

- S288, S333, S795 and BA selections of the Balehonnur Coffee Research Station in India are resistant to many rust races and are believed to have originated from a natural hybrid between *C. arabica* and *C. canephora* [31].
- Icatú is a backcross[4] between *C. canephora* and Bourbon Vermelho. Its has a resistance genes to many rust races of *H. vastatrix* [43].
- Sarchimor is a cross between the Timor Hybrid and Costa Rican Villa Sarchi that is commonly cultivated in both Costa Rica and India [142].
- Catimor is a cross between the Caturra and the Timor Hybrid. The ideal combination of high yields, excellent disease resistance, and tiny plant size was discovered by scientists in Portugal in 1959. In Brazil, Catimor was initially introduced in 1970 [31].

It is important to remember that the disease has a probability of getting past even these defences. For long-lasting resistance, it is advised to combine several resistance genes in a single cultivar. There are signs that *H. vastatrix* is sometimes unable to combine certain virulence components; when the rust is still able to overcome resistance based on multiple genes, the resulting virulence is anticipated to be modest [43, 31].

1.3 Mathematical models for fungal disease propagation

1.3.1 Models for fungal crop diseases

Due to the increased spread of fungal diseases, researchers have developed several mathematical models to understand the dynamics of these pathogens, but also to propose control strategies against these diseases. Plant pathogens can be generally divided into two main groups: the necrotrophs which kill their host and feed on their content, and the biotrophs which establish a long term feeding relationship with the living cells of the host [111]. During the infection stage, the penetrating necrotrophic fungi release a group of fungal enzymes which disrupt the cell integrity of the host tissue, causing the cell death which thereby constitutes the food supply. In contrast biotrophic fungi form specialised physiological and morphological adaptations to the living host to ensure the supply of nutrients [150]. Biotrophic fungi also require a living host to complete their life cycle. The existing mathematical models are based on the life cycle of pathogens and their interactions with their host (cf. Section 1.2.2.2). Many of these models are rooted in the epidemic SIR models developed by pioneers Hamer [65], Ross [137], and Kermack and McKendrick [80] as the disease is transmitted by spores produced on infected plants and carried by wind, water, insects, human and impact currents and deposited on new susceptible host plants.

The first models describing the temporal progress of a plant disease epidemic was developed by Van der Plank in the 1960s [163, 164]. Since then, mathematical models of fungal diseases have received a lot of attention from researchers. For instance, Van den Bosch et al. developed a framework for modelling the continental spread of focal plant disease. Therefore, they restricted their first attempt at modelling pandemic spread to simple parameter-sparse submodels. The authors conclude that the simple analytically tractable models, are useful tools to gain qualitative

[4]Backcrossing aims at transferring one or two major genes.

insight. But they have also been able to conclude that a parameter-rich models is difficult to study due to parameter dependence of the velocity of pandemic spread [161]. Fleming used a mathematical model to prove that a complex of polyphagous non-synchronised predators and parasites is likely to control only low-density cereal rust populations. He also prove that control at low rust density can delay epidemic development and thus substantially reduce yield losses. However, the model only describes the dynamics of pathogen and it is not possible to estimate the impact on the cereal production [49]. Pivonia et al. studied the seasonal appearance of rusts in the United States, in particular soybean rust. The authors used the mathematical models developed by Gumpert et al. [59] and Van der Plank's [163] to proved the existence of the potential lag period which favours a development of different rusts over a time [124]. Ravigné et al. looked at the impact of sexual and asexual reproduction on the epidemiological dynamics of fungal plant parasites and showed that they could induce cyclic persistence of the disease, which can occur with Sigatoka diseases of banana [130].

Among the models that have focused on airborne spread of these fungal diseases, one can cite the DDAL framework developed by Papaïx et al. that focuses on the deployment of susceptible and resistant crop hosts in an agricultural landscape. The authors proposed a modelling approach for landscape epidemiology that takes advantage of theoretical results developed in the metapopulation context while considering realistic landscape structures [120]. Burie et al. developed two models coupling host and pathogen dynamics for mildew infestation in a vineyard. First, they investigated the structure of travelling waves of the PDE [22]. In a second instance, the authors proved the existence of solutions of their model, the stability of the disease free equilibrium and showed numerically that the disease establishes [23]. Based on this last work, Mammeri et al. studied the impact of spatial heterogeneities on the spread and control of grapevine powdery mildew, but only during a cropping season [97]. Burie et al. proposed a field scale model for the spread of a powdery mildew epidemic over a large vineyard and showed the well-posedness of the asymptotic model and obtained a convergence result confirmed by numerical simulations [24]. Sapoukhina et al. developed a model to simulate the propagation of a fungal disease in a 2D field, including a reaction-diffusion model for short-distance disease dispersal, and a stochastic model for long-distance dispersal. The authors demonstrated that the spatial arrangement of the mixture components in both agro-ecosystems and forestry has to accord with the modes of pathogen dispersal if the efficacy of crop diversification is to be maximized [140]. Mustapha et al. proposed and analysed a mathematical model for describing the dispersal by wind of fungal pathogens in plant populations. The authors modelled the dispersal of pathogen spores using a non-local diffusion equation which took into account variations in wind velocity components [42]

Plant growth and disease spread may be affected by seasonal patterns, which then need to be included in epidemiological models. Among these models, one can cite Rimbaud et al. who investigated how the spatial deployment of resistant cultivars affects the resistance efficiency and durability, using a demogenetic model, for a seasonal crop infected by a fungal-like pathogen [134]. Desprez-Loustau et al. developed a seasonal eco-evolutionary model of oak powdery mildew in Europe, based on a within-season and between-season transmission trade-off, which captures the main features of the disease, that is seasonality and pathogen species coexistence [36]. Maupetit et al. tested which of these factors have a dominant effect on the pathogens development and applied to the particular case of poplar rust [101]. For the crops cultivated in temperate climates or tropical regions that alternate dry and rainy seasons, the pathogens dynamics can substantially differ between the seasons with possibly rapid transitions. Impulsive or semi-discrete models have

been developed for several plant fungal diseases. Among these models, one can also cite Nembot et al. who built a model of cocoa black pod rot disease, caused by *Phytophthora megakarya*, and showed the impact of periodic impulsive sanitary harvests on the disease dynamics [113]. Blériot Tchienkou-Tchiengang et al. build two multi-seasonal mathematical models to show the impact of Maize Stalk Borer (*Busseola fusca*) on maize tissues [157]. Tankam-Chedjou et al. developed a model to describe and control the dynamics of a banana soilborne pest in a multi-seasonal framework, optimising the fallow period durations between cropping seasons [155]. Periodic patterns are not necessarily linked to seasonality and can also be due to impulsive control strategies introduced in the epidemiological models. For instance, in the biological control framework, Nundloll et al. studied the periodic release of predators, natural enemies of the plant pest of interest, and determined the minimal predator rate required to eradicate the pest [115]. Xinzhu et al. formulated and analysed a model with continuous cultural control and with impulsive cultural control strategies such as replanting and/or removing diseased plants; they concluded that impulsive removing of diseased plants is more efficient and more economic than continuous removing [105].

Among these models presented in this subsection, we have detailed three cases, which represent the modelling approaches that we have considered in the different chapters of the thesis.

1.3.1.1 A cereal rust model

Fleming proposed a simple model that describes the dynamics of the population densities of the cereal rust (in pustules/area) [49]. The model considers low-density rust dynamics in an aerobiological zone, then the population density of the cereal rust N (in pustules/area) is described as

$$\frac{dN}{dT} = G(N) - L(N)$$

where $G(N)$ and $L(N)$ are the rates per unit area at which the rust population gains and loses pustules, respectively. Time is represented by T.

The rate at which the rust population gains is defined by

$$G(N) = B \cdot f(N) \cdot T_L + IT_I,$$

where B, T_L and T_I are, respectively, the rate of spore production per pustule, the transmission factors for local and immigrant spores. Author suppose that $f(N) = N$ is the effective number of pustules per unit area. I is the density-independent rate of spore immigration per unit area.

The density-dependent loss rate is defined by

$$L(N) = f_\mathrm{D}(N) + f_\mathrm{E}(N) + f_\mathrm{P}(N),$$

where $f_\mathrm{D}(N) = DN$ is the sum of losses due to natural host deaths and D is the intrinsic rate of natural rust mortality. $f_\mathrm{B}(N) = EN$ is the sum of losses due to the essentially passive and wind-mediated process of emigration and E is the instantaneous rate of emigration. The function $f_\mathrm{P}(N) = AN(Z+N)^{-1}$ is a sum of losses of the rust fungi to the complex of background predators and parasites, A is the maximum attack rate (pustules/time) and Z is the rust density at which the rate of losses to the complex of background predators and parasites is $A/2$.

Finally the model is given

$$\frac{dN}{dT} = (BT_L - D - E)\,N + IT_I - AN(Z+N)^{-1} \tag{1.1}$$

Fleming used this mathematical model to prove that a complex of polyphagous non-synchronised predators and parasites is likely to control only low-density cereal rust populations. However, the model only describes the dynamics of the pathogen and it is not possible to estimate the impact on the cereal production. This model can be adapted to the dynamics of the uredospores of fungus *H. vastatrix* but we still need to couple it with the dynamics of coffee tree development.

1.3.1.2 A model of mildew in a vineyard

Burie et al. proposed a model of the dynamics of mildew in a vineyard [23]. Their modelling hypotheses are that, when spores fall upon the plant tissue, they may create a new colony which will produce spores after some latency period and during some sporulating period. They assumed for simplicity that the time variation of the surface of a colony can be neglected.

The authors proposed a SEIR model in which the total density N of sites than can host a colony of fungus at location x and time t is divided into four categories: healthy H, latent L, sporulating I, and removed (postinfectious) R. The total spore density is separated into two categories according to the range of dispersal: short range $S_1(x,t)$ and longer range $S_2(x,t)$. A sporulating colony produces them at a rate of $r_p > 0$, and they can spread over short distances with a probability of $F \in [0,1]$ and over longer distances with a probability of $(1-F)$. The authors assumed that the spores disperse according to a diffusion process with Fickian diffusion coefficient $D_1 > 0$ (short range) or $D_2 > D_1 > 0$ (long range). Spores fall upon the vineyard with some deposition rate $\delta_1 > 0$ or $\delta_2 > 0$ ($\delta_1 = \delta_2$ in numerical simulations). The authors thus obtain the equations that describe the production of spores by the colonies and their dispersal:

$$\begin{cases} \frac{\partial S_1}{\partial t}(x,t) = \nabla \cdot (D_1 \nabla S_1(x,t)) - \delta_1 S_1(x,t) + r_p F I(x,t) \\ \frac{\partial S_2}{\partial t}(x,t) = \nabla \cdot (D_2 \nabla S_2(x,t)) - \delta_2 S_2(x,t) + r_p (1-F) I(x,t) \end{cases}$$

for $x \in \Omega$,a regular spatial domain and $t > 0$.

Moreover, they assumed that no spores come from outside the vineyard, so that they imposed Dirichlet conditions on the boundary:

$$S_1(x,t) = S_2(x,t) = 0 \text{ for } x \in \partial\Omega \text{ and } t > 0$$

with non-negative initial conditions:

$$S_1(x,0) = S_1^0(x) \geq 0, S_2(x,0) = S_2^0(x) \geq 0 \text{ for } x \in \Omega$$

The set $\Omega_r \subset \Omega$ denotes the area covered by the vine rows. They devised their model in such a way that for all $t > 0$ and $x \in \Omega, N(x,t)$ equals 0 if $x \notin \Omega_r$.

According to the authors, the host development is unaffected by the powdery mildew outbreak. New places become accessible for colonisation as a result of this increase. They examined the epidemic over the period of a single season and made the assumption that the logistic rule

governs the variation in time of the total number of colony sites inside the rows.

$$\frac{\partial N}{\partial t}(x,t) = rN(x,t)\left(1 - \frac{N(x,t)}{K}\right), \text{ for } x \in \Omega_r$$

where $r > 0$ is the growth rate and $K > 0$ the carrying capacity.

The local evolution of the disease at some point $x \in \Omega_r$ (inside a row) then obeys the classical SEIR model, whereas we set $N(x,t) = L(x,t) = I(x,t) = R(x,t) = 0$ for $t \geq 0$ if $x \notin \Omega_r$. Let p and i denote the mean duration of the latency and infectious period respectively. Let E be the inoculum effectiveness (probability for the spores succeed in creating a new colony upon a site). The second set of equations of the model for $x \in \Omega_r$ is then

$$\begin{cases} \frac{\partial H}{\partial t}(x,t) = -E\left(\delta_1 S_1(x,t) + \delta_2 S_2(x,t)\right)\frac{H(x,t)}{N(x,t)} + rN(x,t)\left(1 - \frac{N(x,t)}{K}\right) \\ \frac{\partial L}{\partial t}(x,t) = +E\left(\delta_1 S_1(x,t) + \delta_2 S_2(x,t)\right)\frac{H(x,t)}{N(x,t)} - \frac{1}{p}L(x,t) \\ \frac{\partial I}{\partial t}(x,t) = +\frac{1}{p}L(x,t) - \frac{1}{i}I(x,t) \\ \frac{\partial R}{\partial t}(x,t) = +\frac{1}{i}I(x,t) \end{cases}$$

supplemented with non-negative initial conditions

$$H(x,0) = H^0(x) \geq 0, L(x,0) = L^0(x) \geq 0$$
$$I(x,0) = I^0(x) \geq 0, R(x,0) = R^0(x) \geq 0 \text{ for } x \in \Omega_r$$

Burie et al. proved the existence of solutions of the full model, computed the basic reproduction number and concluded about the stability of the disease free equilibrium. The model would probably be a good starting point for CLR dynamics modelling, but the authors only showed numerically that the epidemic reach a maximal rate of infection. Their model has to be reduced for the global mathematical analysis because it is difficult, especially with the Fickian diffusion.

1.3.1.3 A multi-seasonal model

Madden and Van den Bosch developed a coupled differential equation model for the multi-seasonal dynamics of plant disease for annual crops in the early 2000s [94]. Their model is a semi-discrete SEIR model of a plant disease introduced in an annual cropping system. They looked at the possibility of using plant infections as biological weapons and described the circumstances in which they may endure from season to season. Naming S the disease free plant individuals, E the latent infected individuals, I the infectious individuals, such that $Y = E + I + R$ is the total diseased individual, and naming P the abundance of pathogen inoculum, the model of Madden and Van den Bosch is given by the following equation :

$$\begin{cases} \frac{dS}{dt} = -\nu SP - \beta SI \\ \frac{dE}{dt} = \nu SP + \beta SI - \sigma E \\ \frac{dI}{dt} = \sigma E - \gamma I \\ \frac{dR}{dt} = \gamma I \\ \frac{dP}{dt} = -\left(\mu'_g + \nu'\right)P \end{cases} \tag{1.2}$$

where $P(0) = P_0, S(0) = S_0$. The constant ν is the primary infection rate parameter, such that νSP is the rate of occurrence of new infections, and νS is the mean number of new infected plant individuals produced per unit of inoculum per time. Infectious plants are first in latent

state and become infectious at rate σ. Infectious plants become post-infectious or remove from the epidemic at the rate γ. New infection occurs from infectious plants at a rate βSI, with β being the secondary infection rate parameter. Thus, βS is the mean number of new infected individuals per infected individual per time.

The inoculum decays exponentially at a natural mortality rate $\mu_g P$ and a depletion rate $\nu' P$. In the latter expression, $\mu' = \mu$ because each unit of inoculum that produces a plant infecting is one less unit of inoculum available for infecting another plant.

In this model, an epidemic ends at $t = T_g$, the time of crop harvest. All abundances are set to 0 immediately after T_g: $E\left(T_g^+\right) = I\left(T_g^+\right) = R\left(T_g^+\right) = S\left(T_g^+\right) = 0$; where the "+" and the "-" superscript represent the instant after the end of the season and the instant before the end of the season, respectively.

Diseased individuals E, I and R produce each an amount of pathogen inoculum at the end of the growing season. If $\theta_E, \theta_I, \theta_R$ represent the amount of pathogen inoculum produced per diseased individuals, then $k_E = \theta_E E\left(T_g^-\right), k_I = \theta_I I\left(T_g^-\right), k_R = \theta_R R\left(T_g^-\right)$ represent the total amount of inoculum at $t = T_g^+$ from latent, infectious and removed diseased individuals at time $t = T_g^-$. Hence, $P\left(T_g^+\right) = k_P + k_E + k_I + k_R$; $k_p = P_0 \exp -\left(\nu' + \mu_g\right) T_g^-$, where k_p is the inoculum from the beginning of the season left at the end of the season.

Between growing seasons, P decays exponentially with the rate $\mu_b(\varepsilon)$. This correspond to $dP/dt = -\mu_b(\varepsilon)P$. As a result, the single-season model (1.2) is extended to account for several seasons, with initial susceptible individuals set to S_0 and new inoculum of the growing season provided by the inoculum that survived from the previous season.

Madden and Van den Bosch determined the basic reproduction number and the infection persistence thresholds using this model. This model, that covers multiple seasons, can be adapted to CLR but would not be sufficient as it does not contain a spore compartment.

1.3.2 CLR models

Coffee leaf rust epidemics are based on a seemingly simple infection cycle, but develop polycyclic epidemics in a season and polyetic epidemics over successive seasons. To study these outbreaks, several authors have published results of their investigations about the germination of the uredospores of *H. vastatrix*, the propagation of CLR in the whole plantation and many other approaches in order to understand the dynamics of the pathogen and to control it.

Modelling coffee rust epidemics necessitates a variety of approaches, thus CLR models in the literature represent a range of scales, from the individual coffee bush to the country or even the continent. Kushalappa developed a method to quantify the rate of CLR development using a linear model. Stepwise regression identified combination of biological and meteorological variables that explained significant variation in the rate of CLR development [86]. Kashalappa et al. used equations for predicting the rate of coffee rust development based on net survival ratio for monocyclic process of *Hemileia vastatrix* [84]. Later, they analysed the development of CLR in the field and using the proportion of infected leaves, pustules/leaf and percentage of infected area to determine the intensity of *H. vastatrix* [85]. Avelino et al. used multivariate analysis to show that CLR development is linked to three sets of factors: the environment, plant growth and development, and grower's practices. The authors used a statistical segmentation technique to define some recommendation domains to control CLR in Honduras, based on these three sets of factors [11]. Avelino et al. also sowed how other trees affect CLR at the field and landscape

scales. The authors identified several canopy characteristics and leaf traits that can help manage coffee leaf rust at the plot scale: namely, thin canopies with high openness, short base height, horizontal branching, and small, dentate leaves [9]. Bebber et al. developed a model of germination and infection risk, and drove this model using estimates of leaf wetness duration and canopy temperature. They modelled germination and infection as Weibull functions with different temperature optima, based upon existing experimental data. They found that the germination and infection risks do not depend on the climate in Colombia and neighbouring countries. They concluded that biological modelling need to improve using spatial resolution and accuracy of climate reanalyses [15]. Beasley et al. developed a probabilistic model to simulate within-patch and between-patch transmission using a random walk with spore movement inhibited by canopy cover. The authors concluded that increasing the spacing between coffee farms and reducing forest fragmentation in coffee-growing regions can benefit biodiversity conservation and reduce the economic impacts of coffee rust [14]. Merle et al. statistically identified the complex combinations of microclimatic variables responsible for changes in lesion status to construct three models predicting lesion emergence probability, lesion sporulation probability and growth of its infectious area [107]. Vandermeer et al. studied the interaction between the regional and local dynamics of CLR model by representing the evolution of the proportion of infected bushes and farms. The model suggested that it could be the larger ecological structure of the agro-ecosystem, both local and regional aspects, that needs to be considered [169]. Vandermeer et al. also represented the CLR dynamics in a coffee farm in Chiapas using an SI epidemiological model of the host. They showed that the network approach can be a useful way of gaining qualitative insight on spatial disease dynamics [165].

Several researchers were intrigued by the incorporation of integrated crop management methods into coffee rust models. A survey conducted in Honduras illustrated how crop management, different combinations of shade, coffee tree density, fertilisation and pruning may strongly influence coffee rust epidemics [10]. Hannah et al. used Gompertz growth model to describe CLR epidemics. Their forecast system showed to be promising for recommending sprays for coffee plantations in Brazil; but authors argue that more field trials are essential to evaluate its performance in other coffee regions and under different fungicide management situations [69]. To study biological control of CLR using hyperpasites, Vandermeer et King used a basic Lotka–Volterra model, with a consumer depending on two resources, one fixed, another renewable [167]. They applied the model to the particular case of the fungus *H. vastatrix*, coffee green scales and a mycoparasite *Lecanicillium lecanii* which predates the former two [166]. Arroyo et al. developed a stochastic model based on [167] that considers the interactions between bacteria *B. thuringiensis* B157 and fungus *H. vastatrix*. They studied the effect of the spatial distribution of the disease and its spread on the overall dynamics of the disease. The authors found that at equilibrium, the proportion of tree leaves infected with coffee rust is directly proportional to how much the coffee rust both grows and spreads inside the coffee plantation, and inversely proportional to how much bacteria population is present in each tree [6]. Zewdie et al. studied CLR dynamics in the presence of hyperparasites during the dry and wet seasons for three consecutive years at 60 sites across the southwestern Ethiopia. Their findings highlight the potential of the hyperparasite to suppress the rust growth rate from the wet season to dry season transition when the rust severity could otherwise be at its peak. However, they argue that more detailed knowledge is needed on the interaction of these species to assess its importance for reducing rust induced yield losses or the risk of rust outbreaks [181].

All these existing CLR models do not explicitly incorporate coffee plant development. In particular, the differences between young and mature leaves are not considered while they clearly have an impact on the severity of infection. In fact, the mature leaves become infected more quickly than the young ones and it is only the latter that produce the coffee berries [122, 106].

1.4 Objectives

World agriculture is still affected by serious fungal diseases. Even though several studies have been conducted and a variety of management strategies have been developed, crop losses caused by these diseases are still quite severe. Sometimes the pathogen dynamics are poorly understood and they also become more resistant over time to the chemical fungicides that are still widely used, which makes the disease control more challenging. As a result, the focus of this thesis is to employ mathematical techniques to understand and manage fungal diseases.

The initial goal of the thesis is to develop rigorous mathematical model of plant-pathogen interactions. The models range from ordinary differential equations, which represent the global dynamics of plants and pathogens, to partial differential equations which study aerial dispersal and to hybrid models with discrete jumps, which represent (almost) instantaneous events like harvesting, the introduction of biocontrol agents or seasonality. The qualitative analysis of these models helps to understand their asymptotic behaviour. Additionally, numerical simulations of the models illustrate these theoretical findings and help to better understand the disease transient phases.

The thesis ultimate goal is to develop efficient and long-lasting control strategies that reduce the fungal development and preserve the yield. We favour biological control methods, which are less harmful for the environment and human health than chemical fungicides.

In this thesis, we examine the specific case of coffe leaf rust. Indeed, due to the economic importance of coffee, particularly for developing countries like Cameroon, managing this rust is still a major problem. Latin America and the Caribbean suffered from a major outbreak in 2012 despite the many management measures implemented. The emergency rust summit meeting held in Guatemala in April 2013 compiled a comprehensive list of shortcomings, among which a lack of resources to combat CLR and inefficient fungicide application methods [13]. In this thesis, we will explore alternative control approaches such as the release of hyperparasites. Different hyperparasites have been identified for CLR: for instance fungus *Lecanicillium lecanii* [181] and insect *Mycodiplosis* [67], which feed on CLR spores.

1.5 Thesis structure

The thesis is divided into 5 chapters:

- Introduction 1 reviews the impact of fungal diseases and pests in agriculture, and presents different existing fungal disease models. It also describes the biological background on coffee leaf rust, paying special attention to recent developments and CLR modelling.
- Chapter 2 presents some major mathematical tools that were used in the thesis.
- In Chapter 3, we built our baseline model, an ODE model in which the host population is subdivided by health status, considering the crop leaf as an individual. The infection being

mediated by fungus spores released in the plantation, their dynamics were also included. Moreover, this model differentiated between young and mature leaves, to take into account variations in fungus aggressiveness according to host development. We then studied analytically the existence and the stability of the equilibria. We also explored numerically the disappearance or persistence of CLR in the plantation, or the whole destruction of the coffee plantation by CLR.

- Chapter 4 is based on the ODE model of Chapter 3, which was simplified by combining young and mature leaves into branches. We introduced spore dispersal and we took into account the seasonality which is important factor of coffee production by distinguishing between dry and rainy seasons. The well-posedness of the PDE model with seasonality obtained was addressed. We studied analytically the existence and the stability of the equilibria. We investigated the CLR control by varying a parameter which reduces spore production.

- In Chapter 5, we presented a seasonal model which does not distinguish between young and mature leaves. The dynamics are continuous during the rainy seasons and represented by discrete events during the rainy seasons. For the biological control of the disease, we included the dynamics of hyperparasites which feed on uredospores. We used Floquet theory to analyse the stability of the periodic disease free solution. We used semi-numerical analysis to find the frequency and quantity of predators to release to control the disease.

- Chapter 6 presents the main results and the perspectives resulting from this work.

Chapter 2

Mathematical preliminaries

Contents

In this chapter, we present the main mathematical tools that are used in this thesis. As evidenced by the table of content, they are at the crossing point between mathematical epidemiology, dynamical systems and partial differential equations.

2.1 Stability of epidemiological models

The transmission of diseases in animal (underlay humans) or plants, such as fungi, can be described using epidemiological models. Once the model is established, we can investigate the behaviour of the disease using mathematical analysis.

2.1.1 Computation of the basic reproduction number

The basic reproduction number is computed in classical epidemiological models to determine whether the disease will disappear or establish itself. Here we present a method of Van den Driessche et Watmough [162] to compute that number.

Let us note $x = (x_1, ..., x_n)^t$, with each $x_i \geq 0$, be the number of individuals in each compartment. Let us define the domain

$$X_s = \{x \geq 0 | x_i = 0, i = 1, ..., m\}$$

where the disease is not present.

Let us consider the following epidemiological model with a non-negative initial conditions

$$\dot{x}_i = f_i(x) = \mathcal{F}_i(x) - \mathcal{V}_i(x),\ i = 1, ..., n, \tag{2.1}$$

where $\mathcal{F}_i(x)$ is the rate of appearance of new infections in compartment i, and $\mathcal{V}_i = \mathcal{V}_i^- - \mathcal{V}_i^+$ with $\mathcal{V}_i^+(x)$ is the rate of transfer of individuals into compartment i by all other means, and $\mathcal{V}_i^-(x)$ is the rate of transfer of individuals out of compartment i. It is assumed that each function is continuously differentiable at least twice in each variable.

Let us suppose the following assumptions $(A_1) - (A_5)$

(A_1) if $x \geq 0$, then $\mathcal{F}_i(x), \mathcal{V}_i^+, \mathcal{V}_i^- \geq 0$ for $i = 1, ..., n$.

(A_2) if $x_i = 0$ then $\mathcal{V}_i^- = 0$. In particular, if $x \in X_s$ then $\mathcal{V}_i^- = 0$ for $i = 1, ..., m$.

(A_3) $\mathcal{F}_i = 0$ if $i > m$.

(A_4) if $x \in X_s$ then $\mathcal{V}_i^+ = 0$ for $i = 1, ..., m$.

(A_5) If $\mathcal{F}(x)$ is set to zero, then all eigenvalues of $Df(x_0)$ have negative real parts. where $Df(x_0)$ is the Jacobian matrix $\left(\frac{\partial f_i}{\partial x_j}\right)$ evaluated at a disease free equilibrium (DFE) x_0.

Lemma 2.1. *[162]*

If x_0 is a DFE of equation (2.1) and $f_i(x)$ satisfies assumptions $(A_1)-(A_5)$, then the Jacobian matrices $D\mathcal{F}(x_0)$ and $D\mathcal{V}(x_0)$ are partitioned as

$$D\mathcal{F}(x_0) = \begin{pmatrix} F & 0 \\ 0 & 0 \end{pmatrix} \text{ and } D\mathcal{V}(x_0) = \begin{pmatrix} V & 0 \\ J_3 & J_4 \end{pmatrix}$$

where F and V are the $m \times m$ matrices defined by

$$F = \left(\frac{\partial \mathcal{F}_i}{\partial x_j}(x_0)\right) \text{ and } V = \left(\frac{\partial \mathcal{V}_i}{\partial x_j}(x_0)\right), \text{ with } 1 \leq i, j \leq m.$$

Further, F is non-negative, V is a non-singular M-matrix and all eigenvalues of J_4 have a positive real part.

From these elements, the basic reproduction number is defined:

Definition 2.1. *The basic reproduction number, denoted $\mathcal{R}_0$, is the expected number of secondary cases produced, in a completely susceptible population, by a typical infective individual. $\mathcal{R}_0$ is computed as the spectral radius of matrix FV^{-1}:*

$$\mathcal{R}_0 = \rho(FV^{-1}) \tag{2.2}$$

where FV^{-1} is called the next generation matrix for model (2.1).

We have the following theorem about the local stability of the disease free equilibrium

Theorem 2.1 (Local stability of a DFE)**.** *Consider the disease transmission model given by (2.1) with $f(x)$ satisfying conditions $(A_1) - (A_5)$. If x_0 is a DFE of the model, then x_0 is locally asymptotically stable if $\mathcal{R}_0 < 1$, and unstable if $\mathcal{R}_0 > 1$.*

2.1.2 Bifurcation analysis

The Castillo-Chavez and Song theorem [27] allows for the analysis of the different types of bifurcations that the epidemiological model exhibits, giving then the stability of the disease free and endemic equilibria.

Theorem 2.2. *Consider the following ordinary differential equations, with a parameter ψ:*

$$\frac{dx}{dt} = f(x,\psi), \quad f : \mathbb{R}^n \times \mathbb{R}^n\mathbb{R}^n \quad \text{and} \quad f \in C^2(\mathbb{R}^n \times \mathbb{R}). \tag{2.3}$$

Without loss of generality, it is assumed that 0 is an equilibrium for system (2.3) for all values of the parameter ψ, that is $f(0,\psi) \equiv 0$ for all ψ. Assume

A_1: *$A = D_x f(0,0) = (\frac{\partial f_i}{\partial x_j}(0,0))$ is the linearisation matrix of system (2.3) around the equilibrium 0 with ψ evaluated at 0. Zero is a simple eigenvalue of A and all other eigenvalues of A have negative real parts;*

A_2: *Matrix A has a nonnegative right eigenvector u and a left eigenvector v corresponding to the zero eigenvalue. Let f_k be the k^{th} component of f and*

$$a = \sum_{k,i,j=1}^{n} v_k u_i u_j \frac{\partial^2 f_k}{\partial z_i \partial z_j}(0,0), \quad \text{and} \quad b = \sum_{k,i=1}^{n} v_k u_i \frac{\partial^2 f_k}{\partial z_i \partial \psi}(0,0).$$

The local dynamics of (2.3) around 0 are totally determined by a and b.

1. *$a > 0$, $b > 0$. When $\psi < 0$ with $\|\psi\| \ll 1$, 0 is locally asymptotically stable, and there exists a positive unstable equilibrium; when $0 < \psi \ll 1$, 0 is unstable and there exists a negative and locally asymptotically stable equilibrium;*

2. *$a < 0$, $b < 0$. When $\psi < 0$ with $\|\psi\| \ll 1$, 0 is unstable; when $0 < \psi \ll 1$, 0 is locally asymptotically stable, and there exists a positive unstable equilibrium;*

3. *$a > 0$, $b < 0$. When $\psi < 0$ with $\|\psi\| \ll 1$, 0 is unstable, and there exists a locally asymptotically stable negative equilibrium; when $0 < \psi \ll 1$, 0 is stable, and a positive unstable equilibrium appears;*

4. *$a < 0$, $b > 0$. When ψ changes from negative to positive, 0 changes its stability from stable to unstable. Correspondingly a negative unstable equilibrium becomes positive and locally asymptotically stable.*

2.2 Stability of semi-discrete models

In the present manuscript, semi-discrete models are developed to model the phenomena related to seasonality or the introduction of hyperparasites to control fungal diseases in crop. For example, plant development and plant-pathogen interactions during the wet season may be modelled using continuous dynamics, whereas simpler dynamics during the dry season allow for their modelling as a discrete event. In this work, we consider semi-discrete models in which impulses occur at fixed times, so that they can be described as follows [12]:

$$\begin{cases} \dfrac{dx(t)}{dt} = f(t,x),\ t \neq t_k, \\ \quad \Delta x = I_k(x(t)),\ t = t_k,\ \text{for } k \in \mathbb{Z}. \\ x(t_0^+) = x_0,\ t_0 \geq 0. \end{cases} \tag{2.4}$$

where $\Delta x = x(t_k^+) - x(t_k)$ with t_k^+ denoting the instant just after $t = t_k$ so that $x(t_k^+) = \lim_{h \longrightarrow 0^+} = x(t_k + h)$. f is locally Lipschitz continuous on $\mathbb{R} \times \Omega$, with Ω an open set of $\mathbb{R}^n$, $I_k : \Omega \longrightarrow \Omega$.

In the particular case where $t_k = kT$ define regularly spaced discrete events, we define a periodic solution for such a system (2.4) as a map $x : \mathbb{R}^+ \longrightarrow \mathbb{R}^n$ is said to be a periodic solution of equation (2.4) with period T if it satisfies $x(t+T) = x(t)$ for $t \neq t_k$ and $x(t_k + T^+) = x(t_k^+)$, for $k \in \mathbb{Z}$.

2.2.1 Floquet theory

We apply Floquet's theory to study semi-discrete models. Floquet theory, in general, is a branch of the theory of ordinary differential equations that deals with solutions to periodic linear differential equations. These can arise from semi-discrete systems like (2.4) when f is T-periodic in t and the $t_{k+q} = t_k + T$ for a fixed q. Let us consider the following linear impulsive differential system associated with non-linear model (2.4):

$$\begin{cases} \dfrac{dx(t)}{dt} = A(t)x(t),\ t \neq t_k, \\ x(t_k^+) = x(t_k) + B_k x(t_k),\ t = t_k,\ t_k < t_{k+1}, k \in \mathbb{Z}, \\ x(t_0^+) = x_0,\ t_0 \geq 0. \end{cases} \tag{2.5}$$

where $A(t)$ and B are $n \times n$ matrices. These equations are obtained by linearising system (2.4) around one of its periodic solutions, in order to consider the stability of the periodic solution (the x of (2.5) is then the difference between the x of (2.4) and the periodic solution).

Let us consider the following hypotheses :

H_1: $A(.) \in PC(\mathbb{R}, \mathcal{M}_n)$ and $A(t+T) = A(t)$, where $\mathcal{M}_n$ is the set of $(n \times n)$-matrices

H_2: $B_k \in \mathcal{M}_n$ and $\det(I + B_k) \neq 0$, $k \in \mathbb{Z}$

H_3: there exists $q \in \mathbb{N}$ such that $B_{k+q} = B_k$ and $t_{k+q} = t_k + T$, $k \in \mathbb{Z}$.

where $PC(\mathbb{R}, \mathcal{M}_n)$ denotes the set of functions $h : \mathbb{R} \longrightarrow \mathcal{M}_n$ that are continuous $\forall t \in \mathbb{R}$, $t \neq t_k$, and admitting jump discontinuities at t_k.

Theorem 2.3 (Fundamental matrix [12]). *Suppose that condition $(H_1) - (H_3)$ hold. Then each fundamental matrix of equation (2.5) can be represented in the form $X(t) = \phi(t)e^{\Lambda t}, (t \in \mathbb{R})$ for a non-singular, T-periodic matrix $\phi(.) \in PC^1(\mathbb{R}, \mathcal{M}_n(\mathbb{C}))$ and a constant matrix $\Lambda \in \mathcal{M}_n(\mathbb{C})$.*

Definition 2.2 (Monodromy matrix [12]). *Let $X(t)$ be a fundamental matrix of equation (2.5). Then the matrix $X(t+T)$ is also fundamental, and there corresponds a unique non-singular matrix $\mathrm{M} \in M_n(\mathbb{C})$ such that*

$$X(t+T) = X(t)\mathrm{M},$$

for all $t \in \mathbb{R}$. *Here,* M *is called monodromy matrix of* (2.5) *corresponding to the fundamental matrix* $X(t)$. *All monodromy matrices of equation* (2.5) *are similar and have the same eigenvalues. Their eigenvalues* $\lambda_1, \ldots, \lambda_n$ *are called Floquet multipliers.*

In the order to calculate the Floquet multipliers of (2.5), we have to choose an arbitrary fundamental matrix $X(t)$ and calculate the eigenvalues of the matrix $\mathrm{M} = X(t_0 + T)X^{-1}(t_0)$ where $t_0 \in \mathbb{R}$ is fixed.

If $X(0) = I$ (or $X(0^+) = I$), then we can choose $\mathrm{M} = X(T)$ (or $\mathrm{M} = X(T^+)$) as the monodromy matrix. It follows that for any monodromy matrix M of (2.5), we have by [12]

$$\det \mathrm{M} = \lambda_1 \cdot \lambda_2 \ldots . \lambda_n = \Pi_{k=1}^{q} \det(I + B_k) \exp\left(\int_0^T \mathrm{Tr}\, A(s) ds\right).$$

Under these hypotheses, the following stability result holds.

Theorem 2.4 (Stability [12])**.** *Suppose that the conditions* $(H_1) - (H_3)$ *hold. Then the linear T-periodic impulsive equation* (2.5) *is:*

(1) stable if and only if all Floquet multipliers $\lambda_j, (j = 1, \ldots, n)$ *of equation* (2.5) *satisfy* $|\lambda_j| \leq 1$ *and moreover, to those* λ_j *for which* $|\lambda_k| = 1$*, there corresponds a simple elementary divisor.*

(2) asymptotically stable if and only if all Floquet multipliers $\lambda_j, (j = 1, \ldots, n)$ *of the equation* (2.5) *satisfy the inequality* $|\lambda_j| < 1$.

(3) unstable if there is a Floquet multiplier $\lambda_j, (j = 1, \ldots, n)$ *such that* $|\lambda_j| > 1$.

2.2.2 Jury conditions

Through Floquet theory and the computation of the monodromy matrix, the stability study often requires the analysis of a discrete-time system, corresponding to the map from time kT^+ to time $(k+1)T^+$. To achieve that in dimension 2, we will need a simple tool that circumvent the computation of the eigenvalues, that is the Jury condition.

Let A a 2×2-monodromy matrix for which we are not able to compute explicitly the Floquet multiplications. The conditions for these multipliers to stay in the unit circle can be established using the Jury criteria.

Defining A as

$$A = \begin{pmatrix} a_{11} & a_{12} \\ a_{21} & a_{22} \end{pmatrix}$$

the Jury conditions [173] guarantees that the eigenvalues of matrix A stay inside the unit circle if and only if

$$\begin{cases} -\mathrm{Tr}(A) - \det(A) < 1, \\ \det(A) < 1, \\ \mathrm{Tr}(A) - \det(A) < 1, \end{cases} \tag{2.6}$$

where

$$\begin{cases} \mathrm{Tr}(A) = a_{11} + a_{22}, \\ \det(A) = a_{11}a_{22} - a_{12}a_{21}. \end{cases}$$

2.2.3 Semi-numerical analysis

In order to analyse system (2.5) when it is not possible to compute analytically the Floquet multipliers. For that, we consider the simplified situation where $B_k = B$ and $t_k = kT$. The monodromy matrix associated with system (2.5) is evaluted in two steps: we first compute the state transition matrix of system $\dot{x} = A(t)x$ by numerically solving the linear system (2.5) using the initial conditions $x(0) = e_i$ with e_i the elements of the orthonormal basis. The n solutions evaluated at time T, which is a period, are then put together to obtain the fundamental matrix $\Phi(T)$. Then we use the impulsive condition to obtain the monodromy matrix. We name this method "semi-numerical" as it requires numerical computations, but not extensive simulations of the system [56].

The algorithm is given by the following steps:

- Matrix $A(t)$ is a $n \times n$-matrix
- The fundamental matrix verifies $\frac{d\Phi(t)}{dt} = A(t)\Phi(t)$
- We use initial conditions $\Phi(0) = I$ to compute numerically the fundamental matrix $\Phi(T)$
- The **monodromy matrix** associated with system (2.5) is then

$$x((k+1)T^+) = (I + B)\Phi(T)x(kT^+)$$

- We compute $\mathcal{R}$, the spectral radius of this monodromy matrix
- $\mathcal{R} < 1$ implies stability of the zero solution

The monodromy matrix associated with x is

$$M = (I + B)\Phi(T).$$

2.3 Some results for the analysis and simulation of reaction-diffusion partial differential equations

For the positivity of PDE systemen, we use the following Lemma defined by [119] and given as follow:

Lemma 2.2. *Suppose* $w \in C([0, \mathcal{T}] \times \bar{\Omega}) \cap C^{1,2}((0, \mathcal{T}] \times \Omega)$ *that satisfies:*

$$\begin{cases} w_t - D\Delta w \geq -c(t,x)w(t,x), & x \in \Omega, \quad 0 < t \leqslant \mathcal{T}, \\ \frac{\partial w}{\partial \eta} \geq 0, & on\ \partial\Omega, \\ w(0,x) \geq 0, & x \in \Omega, \end{cases}$$

where $c(t,x)$ *is any bounded function in* $[0, \mathcal{T}] \times \Omega$. *Then,* $w(t,x) \geq 0$ *on* $[0, \mathcal{T}] \times \bar{\Omega}$. *Moreover,* $w(t,x) > 0$ *or* $w \equiv 0$ *in* $(0, \mathcal{T}] \times \Omega$.

2.3.1 Existence of solution

In this section we defined the initial value problem and the existence of solution for the abstract problem following the approach described by Pazy [121].

Let $1 < p < \infty$ and let Ω be a bounded domain with smooth boundary $\partial\Omega$ in $\mathbb{R}^n$. Consider the initial value problem:

$$\begin{cases} \dfrac{\partial u}{\partial t} + A(t,x,D) = f(t,x), \quad \text{in } \Omega \times [0,T], \\ D^\alpha u(t,x) = 0, \ |\alpha| < m, \quad \text{on } \partial\Omega \times [0,T], \\ u(0,x) = u_0(x) \quad \text{in } \Omega \end{cases} \tag{2.7}$$

where

$$A(t,x,D) = \sum_{|\alpha| \leq 2m} a_\alpha(t,x) D^\alpha \tag{2.8}$$

Let us define the following assumptions:

(H_1) The operator $A(t,x,D)$, $t \geq 0$ are uniformly strongly elliptic in Ω.

(H_2) The coefficients $a_\alpha(t,x)$ are smooth functions of the variables $x \in \bar{\Omega}$ for every $0 \leq t \leq T$ and satisfy for some constants $C_1 > 0$ and $0 < \beta \leq 1$

$$|a_\alpha(t,x) - a_\alpha(s,x)| \leq C_1 |t-s|^\beta$$

for $x \in \bar{\Omega}$, $0 \leq s,t \leq T$ and $|\alpha| \leq 2m$

With the family $A(t,x,D)$, $t \in [0,T]$, of strongly elliptic operators, we associate a family of linear operators $A_p(t)$, $t \in [0,T]$, in $\mathcal{L}^p(\Omega)$, $1 < p < \infty$. This is done as follows:

$$D(A_p(t)) = D = W^{2m,p}(\Omega) \cap W_0^{m,p}(\Omega)$$

and

$$A_p(t)u = A(t,x,D)u \text{ for } u \in D.$$

If $u_0 \in \mathcal{L}^p(\Omega)$ and $f(t,x) \in \mathcal{L}^p(\Omega)$ for every $0 \leq t \leq T$ then a classical solution u of the following abstract initial value problem

$$\begin{cases} \dfrac{du}{dt} + A_p(t)u = f, \\ u(0) = u_0 \end{cases} \tag{2.9}$$

in $\mathcal{L}^p(\Omega)$ is defined to be a generalized solution of the initial value problem (2.7).

Theorem 2.5 (Existence of solution [121]). *Let the family $A(t,x,D)$, $0 \leq t \leq T$, satisfy the conditions (H_1) and (H_2) and let $f(t,x) \in \mathcal{L}^p(\Omega)$ for $0 \leq t \leq T$ satisfy*

$$\left(\int_\Omega |f(t,x) - f(s,x)|^p dx \right)^{\frac{1}{p}} \leq C|t-s|^\gamma \tag{2.10}$$

for some constants $C > 0$ and $0 \leq \gamma < 1$. Then for every $u_0(x) \in \mathcal{L}^p(\Omega)$ the evolution equation (2.7) possesses a unique generalized solution $u \in D$.

2.3.2 Nonstandard finite difference scheme for parabolic equations

Here, we present a finite difference scheme for a particular class of reaction-diffusion partial differential equations (PDEs) in dimension one [108]. Consider the following equation

$$\frac{\partial u_i}{\partial t} = D_i \frac{\partial^2 u_i}{\partial x^2} - f_i(u_1, u_2, ..., u_n)u_i + g_i(u_1, u_2, ..., u_n)u_i + \Lambda_i,\ i = 1, 2, ..., n, \tag{2.11}$$

where D_i are nonnegative diffusion coefficients, and the f_i and g_i are polynomial or rational functions of $(u_1, u_2, ..., u_n)$ with positive coefficients. With Neumann boundary condition

$$\frac{\partial u_i}{\partial x} = 0 \tag{2.12}$$

We suppose that,

$$u_i(x, 0) \geq 0 \Longrightarrow u_i(x, t) \geq 0.$$

Let us introduce the notation:

$$t \to t_k = \psi(\Delta t)k, \quad x \to x_m = \phi(\Delta x)m,$$

where k is a non-negative integer, m is an integer; $\psi(\Delta t)$ and $\phi(\Delta x)$ are, respectively, the time and space step-sizes, with ψ and ϕ satisfying

$$\begin{cases} \psi(h) = h + O(h^2) \\ \phi(h) = h^2 + O(h^4). \end{cases} \tag{2.13}$$

The discrete approximations to the dependent variables are

$$u_i(x, t) = [u_i]_m^k, \quad i = 1, 2, \ldots, n.$$

A positivity preserving finite difference scheme is one for which

$$[u_i]_m^k \geq 0 \Rightarrow [u_i]_m^{k+1} \geq 0, \quad i = 1, 2, \ldots, n.$$

One consequence of this requirement is that it can hold only if a functional relation exists between the time and space step-sizes. In particular, for the PDE system given by equation (2.11), the following relation holds:

$$\psi(\Delta t) \leq \alpha(\phi(\Delta x))^2, \tag{2.14}$$

where α is a constant determined by the diffusion coefficients $(D_1, D_2, \ldots, D_n)$.

The discrete forms for the first-order time derivative and the second-order space derivative are given, respectively, by the usual forward Euler and central difference is given by :

$$\begin{aligned} \frac{\partial u_i}{\partial t} &= \frac{[u_i]_m^{k+1} - [u_i]_m^k}{\psi(\Delta t)} + O(\psi(\Delta t)) \\ \frac{\partial^2 u_i}{\partial x^2} &= \frac{[u_i]_{m+1}^k - 2\,[u_i]_m^k + [u_i]_{m-1}^k}{(\phi(\Delta x))^2} + O((\phi(\Delta x))^2). \end{aligned}$$

A non-standard finite difference scheme for the PDE system of equation (2.7) is obtained by making the substitutions of the above expressions. Doing this gives $(i = 1, 2, \ldots, n)$

$$\frac{[u_i]_m^{k+1} - [u_i]_m^k}{\psi(\Delta t)} = D_i \frac{[u_i]_{m+1}^k - 2\,[u_i]_m^k + [u_i]_{m-1}^k}{(\phi(\Delta x))^2} - f_i([u]_m^k)\,[u_i]_m^{k+1} + g_i([u]_m^k)\,[u_i]_m^k + \Lambda_i, \quad (2.15)$$

where $[u]_m^k = ([u_1]_m^k, [u_2]_m^k, \ldots, [u_n]_m^k)$ represent u evaluated at $t = t_k$ and $x = x_m$,

If R_i is defined as

$$R_i \equiv \frac{D_i \psi(\Delta t)}{(\phi(\Delta x))^2}$$

then equation (2.15) can be written as

$$\begin{aligned}\left[1 + \psi(\Delta t) f_i([u]_m^k)\right][u_i]_m^{k+1} = R_i\left([u_i]_{m+1}^k + [u_i]_{m-1}^k\right) + (1 - 2R_i)\,[u_i]_m^k + \psi(\Delta t)\Lambda_i \\ + \psi(\Delta t) g_i([u]_m^k)\,[u_i]_m^k\,.\end{aligned} \quad (2.16)$$

Inspection of the second term in equation (2.16) shows that the positivity condition

$$[u_i]_m^k \geq 0 \Rightarrow [u_i]_m^{k+1} \geq 0$$

is satisfied, provided that

$$\frac{D\psi(\Delta t)}{(\phi(\Delta x))^2} \leq \frac{1}{2}, \quad D = \text{Max}\,(D_1, D_2, \ldots, D_n) \quad (2.17)$$

Then the time-step size should be selected such that the condition given in equation (2.17) holds and the non-standard scheme is (conditionally) stable. However, in general, the solutions of this condition do not satisfy this principle. The imposing of this min-max principle on the solutions to equation (2.17) gives the conditional stability requirement.

Consider Neuman condition in equation (2.12), the discrete form is given by:

$$\begin{cases} \dfrac{\partial u_i}{\partial x}|_{m=0} = \dfrac{[u_i]_{m+1}^k - [u_i]_m^k}{(\phi(\Delta x))^2} = 0 \Longrightarrow [u_i]_1^k = [u_i]_0^k \\ \dfrac{\partial u_i}{\partial x}|_{m=N_x} = \dfrac{[u_i]_{m+1}^k - [u_i]_m^k}{(\phi(\Delta x))^2} = 0 \Longrightarrow [u_i]_{N_x+1}^k = [u_i]_{N_x}^k \end{cases}$$

where N_x is the number of space point. Replacing the above Neumann condition in equation (2.16), we obtain

$$\begin{cases} (1 + \psi(\Delta t) f_i([u]_0^k))\,[u_i]_0^{k+1} = [u_i]_0^k + \psi(\Delta t)(\Lambda_i + g_i([u]_0^k))\,[u_i]_0^k\,, \\ (1 + \psi(\Delta t) f_i([u]_{N_x}^k))\,[u_i]_{N_x}^{k+1} = [u_i]_{N_x}^k + \psi(\Delta t)(\Lambda_i + g_i([u]_{N_x}^k))\,[u_i]_{N_x}^k\,. \end{cases} \quad (2.18)$$

Combining equations (2.16) and (2.18), we obtain a non-standard schemes for a reaction-diffusion partial differential equations with Neumann boundary condition.

Chapter 3

Bifurcation analysis in an epidemiological model of fungal crop disease

In this chapter, we develop an epidemiological host-pathogen model that describes the propagation of a fungal disease, applied to CLR, using the following hypotheses.

H_1: The model is based on a classical epidemiological model, in which the host population is subdivided by health status (susceptible leaves S, latent leaves L, infectious leaves I and dry leaves R), considering the crop leaf as an individual. This model differentiates between young and mature leaves, to take into account variations in fungus aggressiveness according to host development. The model includes crop production (berries B) by mature leaves. The infection being mediated by fungus spores (uredospores U) released in the plantation, their dynamics are also included.

H_2: The model takes into account the non-constant recruitment of young susceptible leaves, which are generated by mature leaves. Due to competition, the dynamics of young leaves are negatively impacted by mature leaves.

H_3: Although the germination rate (which determines the infection success) differs between young and mature leaves, both face the same force of infection. The latter is proportional to the number of uredospores and inversely proportional to the total number of leaves. Thus, the force of infection is density-dependent.

H_4: The model does not take seasonality into account.

H_5: Space is not explicitly taken into account in this model, uredospores are homogeneously distributed on young and mature leaves.

H_6: The model uses an ODE formalism.

H_7: No control methods are implemented.

Based on these hypotheses we obtain a complex ODE model with nine compartments. We use it to understand the dynamics of fungal diseases applied to the particular case of CLR. We study the model behaviour for different values of parameters and initial states of the pathogen.

Contents

Abstract: Most crops are subject to many pests and pathogens, which reduce their yield. In this paper, we develop an SEIR-U epidemiological model for a fungal crop disease, where U stands for spores. The originality of this model is a differentiation between young and mature leaves, that takes into account the impact of host development on the aggressiveness of the pathogen. This is motivated by the particular case of coffee leaf rust (CLR), which can drastically reduce coffee berry production. We compute the basic reproduction number $\mathcal{R}_0$, which classically determines the stability of the disease-free equilibrium (DFE), and identify two bifurcation cases at its threshold value 1. The first classical case corresponds to a forward bifurcation. Above the threshold, the DFE becomes unstable and a stable endemic equilibrium (EE) appears. In the second case, there is backward bifurcation. Below the threshold, there are two EE, one stable and one unstable, and a stable DFE. Above the threshold, the DFE becomes unstable, one EE disappears and the other EE remains stable. In both cases, when $\mathcal{R}_0$ is notably larger than 1, either the EE persists and remains stable or it disappears and the trivial equilibrium becomes stable. This model hence exhibits complex asymptotic properties: $\mathcal{R}_0 < 1$ is not sufficient to eradicate the disease, as a stable EE may exist; moreover, high $\mathcal{R}_0$ values may lead to the destruction of the coffee plantation.

Keywords: Epidemiological model, Host age classes, Coffee leaf rust, Basic reproduction number, Stability, Backward bifurcation

MSC Classification: 92D30, 37N25, 34D20, 34C23, 34C60

3.1 Introduction

Plant pest and pathogens account for up to 40% of yield loss worldwide [21]. In the current context of ever growing population and climate change, this problem needs to be tackled at scale. Hence, the interactions between pest/pathogens and their hosts need to be better understood. Mathematical models of fungal diseases have received a lot of attention from researchers. For instance, [49] used a mathematical model to describe the transition of a cereal rust population from endemic to epidemic densities and prove that natural enemies are likely to control only low-density cereal rust populations. [124] studied the seasonal appearance of rusts in the United States, in particular soybean rust, thanks to a general disease model. [134] investigated how the spatial deployment of resistant cultivars affected the resistance efficiency and durability, using a demogenetic model, for a seasonal crop infected by a fungal-like pathogen.

There are fewer models of fungal diseases that target perennial hosts. For instance, [23] explored the dynamical behaviour of mildew in a vineyard, while [97] studied the impact of spatial heterogeneities on its spread and control during a cropping season. [140] studied susceptible and resistant crop mixtures for a fungal disease propagated by airborne spores in a field. [36] developed a seasonal eco-evolutionary model of oak powdery mildew in Europe, based on a within-season and between-season transmission trade-off, which captures the main features of the disease, that is seasonality and pathogen species coexistence. [130] looked at the impact of sexual and asexual reproduction on the epidemiological dynamics of fungal plant parasites and showed that they could induce cyclic persistence of the disease, which can occur with Sigatoka diseases of banana.

In this paper, we develop an epidemiological model to describe the spread of a fungal disease on a perennial plant in an agriculture context. The originality of this model is that it is structured to represent host developmental stages, as they often impact the aggressiveness of the pathogen, stemming from nutrient availability [32] or presence of different defense compounds [101] in the host.

The present work is motivated by the particular case of coffee leaf rust (CLR) on the coffee tree, which is a perennial plant that is exploited commercially for about 30 years [177]. CLR has a major impact on coffee production [180]. However, our study can be applied to other fungal diseases that target perennial hosts since most fungal diseases present the same type of life cycle, going through spore dispersion for asexual and/or sexual reproduction. CLR is caused by a basidiomycete fungus, *Hemileia vastatrix*, which infects coffee leaves of all stages, and dries them up before they fall down. The life cycle of *H. vastatrix* starts with the dispersion of uredospores, which land on the leaves. They germinate and penetrate the leaf, the infection process requires 48 hours to 10 days [116] depending of the age of the leaf and the climatic conditions [132]. Two to three weeks after the infection, yellow spots appear on the leaves. They grow and sporulate for two weeks to several months to produce two types of spores: uredospores for asexual reproduction and teliospores for sexual reproduction [172]. As the teliospore part of the cycle is not well known, except that these spores do not infect coffee leaves and might even be a dead end [83], it is not included in our model. For other rusts such as poplar rust, this part of the cycle is crucial for overwintering [60].

Mathematical models have been developed to study the epidemiology of CLR. [11] investigated the factors (coffee tree characteristics, crop management patterns, environment) that affect CLR intensity in several plots in Honduras. They showed that coffee rust development is linked

to three sets of factors: the environment, plant growth and development, and grower practices. [15] determined the germination and infection risk depending on the climate in Colombia and neighbouring countries, based upon existing experimental data. [165] represented the CLR dynamics in a coffee farm in Chiapas using an SI epidemiological model of the host. They showed that the network approach can be a useful way of gaining qualitative insight on spatial disease dynamics. They also showed in their study that coffee rust pattern suggests something other than random dispersal of spores. [38] studied the dynamics of CLR in a coffee plantation. However, existing models do not explicitly incorporate coffee plant development. In particular, in these models the differences between young and mature leaves are not considered while they clearly have an impact on the severity of infection. In fact, the mature leaves become infected more quickly than the young ones and it is only the latter that produce the coffee berries [122, 106].

Our aim is hence first to build a mathematical model describing the interactions between a fungal pathogen and a perennial plant, taking into account the development stages of the host and the epidemiological status of the leaves. It is based on the SEIR-U epidemiological model, where U stands for uredospores, presented in [38]. Compared to this previous work, this new model does not include the spatially-explicit spore dispersal, but it differentiates young and mature leaves and the young leaves grow logistically. We explicitly include a berry compartment to study the impact of CLR on crop production. Secondly, we analyse the equilibria of this complex ODE model and their stability.

This paper is organized as follows. Section 3.2 is devoted to the formulation of the model and derive its basic properties. In Section 3.3, we compute the disease free equilibrium and the basic reproduction number which determines its stability. In Section 3.4, we prove the existence of endemic equilibria and study their stability. We also presents different types of bifurcations that occurs in the model. Finally, we conclude the paper and propose several perspectives for future work.

3.2 Model formulation and basic properties

3.2.1 Formulation of the CLR model

Herein, we formulate a mathematical model for the CLR in the coffee plantation. To do so, we propose an ODE coffee–CLR interaction model that take into account a logistic growth of young leaves, the different stages of development of a leaf and the production of uredospores by all types of leaves. More precisely, we consider that in a coffee plantation we can find: susceptible young and mature leaves (J_S and M_S), that have not (yet) been affected, latent young and mature leaves (J_L and M_L), that are infected but not (yet) infectious, infectious young and mature leaves (J_I and M_I), dry leaves (M_R), uredospores (U), which the fungus *H. vastatrix* uses for its asexual reproduction, and berries (B).

Figure 3.1 gives the compartmental representation of the corresponding ODE model.

The process begins with a logistic-like production of susceptible young leaves at rate $r_0 M_1 - r_1 M J_S$. In the first term, $M_1 = M_S + M_L + \varepsilon(M_I + M_R)$ and $\varepsilon < 1$, since all mature leaves can produce young ones, with the infectious and dry leaves producing less due to infection. The second term represents the competition between susceptible young leaves and all mature leaves with $M = M_S + M_L + M_I + M_R$. All young leaves become mature at rate β. Uredospores land on leaves of all leaves at deposition rate ν, with fractions $\frac{J_S}{J+M}$ and $\frac{M_S}{J+M}$ on susceptible

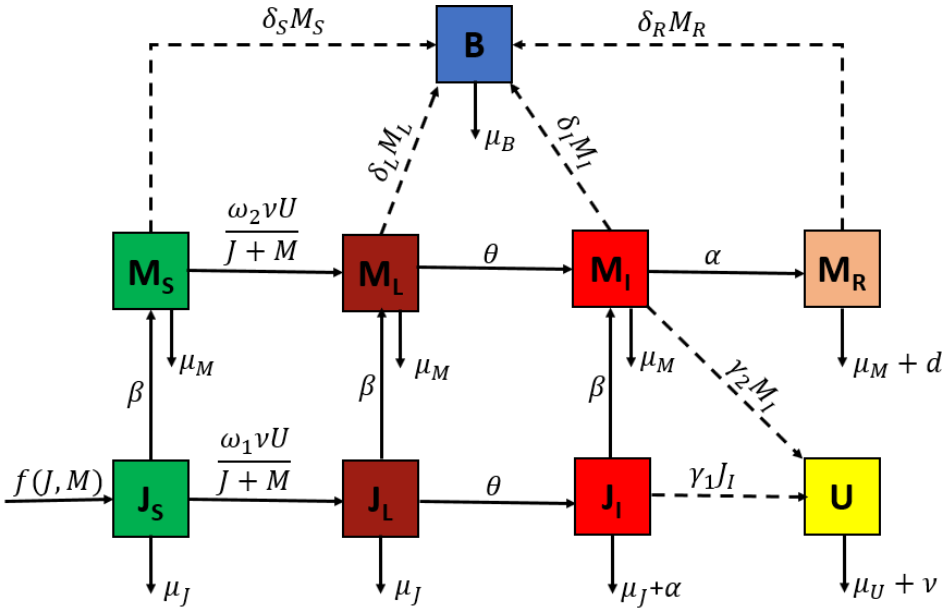

Figure 3.1: Diagram of the CLR propagation in the coffee plantation corresponding to system (3.1). State variables are: susceptible young and mature leaves (J_S and M_S), latent young and mature leaves (J_L and M_L), infectious young and mature leaves (J_I and M_I), dry leaves (M_R), uredospores (U) and berries (B).

young and mature leaves, respectively, with $J = J_S + J_L + J_I$. Uredospores germinate at rates ω_1 and ω_2, respectively. Young and mature latent leaves become infectious at rate θ, where $1/\theta$ corresponds to the average latency period. Infectious leaves sporulate over on average period $1/\alpha$; young leaves then die, while mature ones become dry. All young and mature leaves undergo natural mortality with baseline rate μ_J and μ_M, respectively. Dry leaves have an additional mortality rate d. Uredospores are produced by infectious young and mature leaves at rate γ_1 and γ_2, respectively, and lose their infection ability at rate μ_U. Berries are produced by all types of mature leaves at rates $\delta_S \geq \delta_L \geq \delta_I \geq \delta_R$ and die at rate μ_B.

Table 3.1 summarises the parameter definitions and values of system (3.1).

From the compartmental model in Figure 3.1, we have the following system of ordinary differential equations:

$$\begin{cases} \dot{J}_S &= r_0 M_1 - r_1 M J_S - \frac{\omega_1 \nu U}{J+M} J_S - (\beta + \mu_J) J_S, \\ \dot{J}_L &= \frac{\omega_1 \nu U}{J+M} J_S - (\beta + \theta + \mu_J) J_L, \\ \dot{J}_I &= \theta J_L - (\beta + \alpha + \mu_J) J_I, \\ \dot{M}_S &= \beta J_S - \frac{\omega_2 \nu U}{J+M} M_S - \mu_M M_S, \\ \dot{M}_L &= \beta J_L + \frac{\omega_2 \nu U}{J+M} M_S - (\theta + \mu_M) M_L, \\ \dot{M}_I &= \beta J_I + \theta M_L - (\alpha + \mu_M) M_I, \\ \dot{M}_R &= \alpha M_I - (\mu_M + d) M_R, \\ \dot{U} &= \gamma_1 J_I + \gamma_2 M_I - (\nu + \mu_U) U. \\ \dot{B} &= \delta_1 M_S + \delta_2 M_L + \delta_3 M_I + \delta_4 M_R - \mu_B B, \end{cases} \tag{3.1}$$

Since B is not present in the other equations of system (3.1), we do not consider this state variable in the mathematical analysis. With this in mind, system (3.1) reduces to

Table 3.1: Description and values of parameters for system (3.1)

Symbol	Biological meaning	Value	Source
r_0	Production rate of J_S	2 /day	Assumed
r_1	Competition rate	0.02 /leaf.day	Assumed
ε	Infection-related production ratio	0.06	Assumed
ω_1	Germination rate on J_S	0.055 leaves/spore	ref[1]
ω_2	Germination rate on M_S	0.065 leaves/spore	ref[1]
γ_1	Sporulation rate by J_I	5 spores/leaf.day	ref[2]
γ_2	Sporulation rate by M_I	7 spores/leaf.day	ref[2]
ν	Deposition rate	0.09 /day	ref[2]
β	Maturation rate	0.05 /day	Assumed
θ	1 / duration of latency period	0.033 /day	ref[3]
α	1 / duration of sporulation period	0.066 /day	Assumed
μ_J	Mortality rate of J	0.0054 /day	Assumed
μ_M	Mortality rate of M	0.0034 /day	Assumed
μ_U	Mortality rate of U	0.035 /day	ref[4]
d	Extra mortality rate of M_R	0.056 /day	Assumed
δ_S	Berry production rate by M_S	0.7 berries/leaf.day	ref[5]
δ_L	Berry production rate by M_L	0.5 berries/leaf.day	ref[5]
δ_I	Berry production rate by M_I	0.3 berries/leaf.day	ref[5]
δ_R	Berry production rate by M_R	0.05 berries/leaf.day	ref[5]
μ_B	Mortality rate of B	0.0021 /day	Assumed

ref[1]: [131], ref[2]: [19], ref[3]: [172],
ref[4]: [180] and ref[5]: [29].

$$\begin{cases} \dot{J}_S &= r_0 M_1 - r_1 M J_S - \frac{\omega_1 \nu U}{J+M} J_S - (\beta + \mu_J) J_S, \\ \dot{J}_L &= \frac{\omega_1 \nu U}{J+M} J_S - k_1 J_L, \\ \dot{J}_I &= \theta J_L - k_2 J_I, \\ \dot{M}_S &= \beta J_S - \frac{\omega_2 \nu U}{J+M} M_S - \mu_M M_S, \\ \dot{M}_L &= \beta J_L + \frac{\omega_2 \nu U}{J+M} M_S - k_3 M_L, \\ \dot{M}_I &= \beta J_I + \theta M_L - k_4 M_I, \\ \dot{M}_R &= \alpha M_I - k_5 M_R, \\ \dot{U} &= \gamma_1 J_I + \gamma_2 M_I - k_6 U. \end{cases} \tag{3.2}$$

where

$$k_1 = \beta + \theta + \mu_J, \quad k_2 = \beta + \alpha + \mu_J, \quad k_3 = \theta + \mu_M,$$
$$k_4 = \alpha + \mu_M, \quad k_5 = \mu_M + d, \quad k_6 = \nu + \mu_U,$$

System (3.2) is defined in

$$\Gamma = \mathbb{R}^8_+ \setminus \{(0,0,0,0,0,0,0,U) \text{ with } U \geq 0\}$$

where $\mathbb{R}_+$ is the set of non-negative real numbers.

3.2.2 Basic properties

We obtain the following results for the positivity of solutions of system (3.2).

Lemma 3.1. *For any initial condition in* Γ*, system* (3.2) *has a unique solution in* Γ.

Proof of Lemma 3.1. Let $x = (J_S, J_L, J_I, M_S, M_L, M_I, M_R, U)$ and $x(0)$ be an initial condition in Γ of system (3.2).

Suppose that one of the variables, that we will denote x_i is equal to 0 at some time, with all others being non-negative. A quick analysis shows that $\dot{x}_i \geq 0$ so that x_i cannot become negative. To ensure that any solution remains non-negative, we still need to prove that $J + M$ cannot become negative in finite time.

Using system (3.2), we obtain

$$\begin{aligned}\dot{J} + \dot{M} &= r_0 M_1 - r_1 M J_S - \mu_J J - \mu_M M - \alpha J_I - d M_R, \\ &\geq -r_1 M J_S - \mu_J J - \mu_M M - \alpha J_I - d M_R.\end{aligned}$$

Using the fact that $J_S < J < J + M$, $M < J + M$, $J_I < J + M$ and $M_R < J + M$, one has

$$\widehat{J + M} \geq -r_1 (J + M)^2 - \Upsilon (J + M) \tag{3.3}$$

where $\Upsilon = \mu_J + \mu_M + \alpha + d$. Using the comparison theorem to solve equation (3.3) yields

$$J(t) + M(t) \geq \frac{\Upsilon (J(0) + M(0))}{\Upsilon e^{\Upsilon t} + (J(0) + M(0))(e^{\Upsilon t} - 1)}.$$

The above expression proves that $J(t) + M(t)$ cannot reach 0 in finite time. Therefore, the right hand-side of system (3.2) is Lipschitz continuous along all solutions, which implies that this system admits a unique solution that stays in Γ at all time.

□

We also obtain the following result about the boundedness of solutions of system (3.2).

Lemma 3.2. *All solutions of system (3.2) are bounded.*

Proof of Lemma 3.2.

(1) Firstly we will show that the compact region

$$\Omega = \left\{ \begin{array}{l} (J_S, J_L, J_I, M_S, M_L, M_I, M_R, U) \in \mathbb{R}^8_+, J_S \leq \overline{J_S}, J_L \leq \mathcal{K}_{J_L} \sqrt{U_{\max}}, \\ J_I \leq \mathcal{K}_{J_I} \sqrt{U_{\max}}, M_S \leq \overline{M_S}, M_L \leq \mathcal{K}_{M_L} \sqrt{U_{\max}}, M_I \leq \mathcal{K}_{M_I} \sqrt{U_{\max}}, \\ M_R \leq \mathcal{K}_{M_R} \sqrt{U_{\max}} \quad \text{and} \quad U \leq U_{\max}, \text{with} \quad U_{\max} \geq \mathcal{K}_U \end{array} \right\},$$

is positively invariant for system (3.2), where

$$\begin{aligned} &\overline{J_S} = \max(J_S(0), \frac{r_0}{r_1}), \quad \overline{M_S} = \max\left(M_S(0), \frac{\beta}{\mu_M} \overline{J_S}\right), \quad \mathcal{K}_{J_L} = \sqrt{\frac{\omega_1 \nu \overline{J_S}}{k_1}}, \\ &\mathcal{K}_{J_I} = \frac{\theta \mathcal{K}_{J_L}}{k_2} \quad \mathcal{T}_1 = \sqrt{\beta^2 \mathcal{K}^2_{J_L} + 4 k_3 \omega_2 \nu \overline{M_S}}, \quad \mathcal{K}_{M_L} = \frac{\beta \mathcal{K}_{J_L} + \mathcal{T}_1}{2 k_3}, \\ &\mathcal{K}_{M_I} = \frac{\beta \mathcal{K}_{J_L} + \theta \mathcal{K}_{M_L}}{k_4}, \quad \mathcal{K}_{M_R} = \frac{\alpha \mathcal{K}_{M_I}}{k_5} \quad \mathcal{T}_2 = \gamma_1 \mathcal{K}_{J_I} + \gamma_2 \mathcal{K}_{M_I}, \text{ and } \mathcal{K}_U = \frac{\mathcal{T}_2^2}{k_6^2}. \end{aligned}$$

Consider the first equation of system (3.2):

$$\dot{J}_S = r_0 M_1 - r_1 M J_S - \frac{\omega_1 \nu U}{J + M} J_S - (\beta + \mu_J) J_S.$$

Using the fact that $\frac{\omega_1 \nu U}{J+M} J_S \geq 0$ and $M_1 \leq M$, we obtain the following equation

$$\dot{J}_S \leq r_0 M \left(1 - \frac{J_S}{\frac{r_0}{r_1}}\right) - (\beta + \mu_J) J_S.$$

If $J_S \geq \frac{r_0}{r_1}$, we obtain $\dot{J}_S \leq 0$, this implies that $\forall t \geq 0$, $J_S(t) \leq \overline{J_S}$.
Similarly, let us consider the fourth equation of system (3.2).

$$\dot{M}_S = \beta J_S - \frac{\omega_2 \nu U}{J+M} M_S - \mu_M M_S,$$

Using the fact that $\frac{\omega_2 \nu U}{J+M} M_S \geq 0$ and $J_S \leq \overline{J_S}$, we obtain

$$\dot{M}_S \leq \beta \overline{J_S} - \mu_M M_S.$$

If $M_S \geq \frac{\beta}{\mu_M} \overline{J_S}$, one has $\dot{M}_S \leq 0$, this allows to conclude for all $t \geq 0$ and $M_S(t) \leq \overline{M_S}$.

Now for the boundness of the other variables, we use the hypothesis that $\forall t \geq 0$, $U(t) \leq U_{\max}$ whose validity will be confirmed later. Let us consider the second equation of system (3.2):

$$\dot{J}_L = \frac{\omega_1 \nu U}{J+M} J_S - k_1 J_L$$

Using the fact that $\frac{J_S}{J+M} \leq \frac{\overline{J_S}}{J_L}$ and $U \leq U_{\max}$, we obtain

$$\dot{J}_L \leq \frac{\omega_1 \nu U_{\max} \overline{J_S}}{J_L} - k_1 J_L. \tag{3.4}$$

If $J_L \geq \mathcal{K}_{J_L} \sqrt{U_{\max}}$ in the equation (3.4) we obtain $\dot{J}_L \leq 0$. This implies that, if $J_L(0) \leq \mathcal{K}_{J_L} \sqrt{U_{\max}}$, then $J_L(t) \leq \mathcal{K}_{J_L} \sqrt{U_{\max}}$, for all $t \geq 0$.
Now, replacing the upper-bound value of J_L into the third equation of system (3.2), gives

$$\dot{J}_I \leq \theta \mathcal{K}_{J_L} \sqrt{U_{\max}} - k_2 J_I. \tag{3.5}$$

In the equation (3.5), one can observe that if $J_I \geq \mathcal{K}_{J_I} \sqrt{U_{\max}}$, we have $\dot{J}_I \leq 0$ so that, when $J_I(0) \leq \mathcal{K}_{J_I} \sqrt{U_{\max}} = \frac{\theta \mathcal{K}_{J_L}}{k_2} \sqrt{U_{\max}}$, we obtain $J_I(t) \leq \mathcal{K}_{J_I} \sqrt{U_{\max}}$, for all $t \geq 0$.
Replacing the upper-bound of J_L and U into the fifth equation of system (3.2) and using the fact $\frac{M_S}{J+M} \leq \frac{\overline{M_S}}{M_L}$, yields

$$\begin{aligned} \dot{M}_L &\leq \beta \mathcal{K}_{J_L} \sqrt{U_{\max}} + \frac{\omega_2 \nu U_{\max} \overline{M_S}}{M_L} - (\theta + \mu_M) M_L \\ &= \frac{-k_3 M_L^2 + \beta \mathcal{K}_{J_L} \sqrt{U_{\max}} M_L + \omega_2 \nu U_{\max} \overline{M_S}}{M_L}. \end{aligned} \tag{3.6}$$

The sign of the right-hand side of equation (3.6) is given by the sign of the second order equation of the numerator. Hence, it is negative when M_L is larger than the largest of its two roots. This largest root is given by $\mathcal{K}_{M_L} \sqrt{U_{\max}} = \frac{\beta \mathcal{K}_{J_L} + \mathcal{T}_1}{2k_3} \sqrt{U_{\max}}$. Then, one can conclude that when $M_L(0) \leq \mathcal{K}_{M_L} \sqrt{U_{\max}}$, one has $M_L(t) \leq \mathcal{K}_{M_L} \sqrt{U_{\max}}$ for all $t \geq 0$.

Replacing the upper-bound of J_I and M_L into sixth equation of system (3.2), gives

$$\dot{M}_I \leq \beta\mathcal{K}_{J_L}\sqrt{U_{\max}} + \theta\mathcal{K}_{M_L}\sqrt{U_{\max}} - k_4 M_I. \tag{3.7}$$

In the equation (3.7), one can observe that if $M_I \geq \mathcal{K}_{M_I}\sqrt{U_{\max}} = \frac{\beta\mathcal{K}_{J_L}+\theta\mathcal{K}_{M_L}}{k_4}\sqrt{U_{\max}}$, we have $\dot{M}_I \leq 0$ so that, when $M_I(0) \leq \mathcal{K}_{M_I}\sqrt{U_{\max}}$, we obtain $M_I(t) \leq \mathcal{K}_{M_I}\sqrt{U_{\max}}$, for all $t \geq 0$.

Replacing the upper-bound value of M_I into the seventh equation of system (3.2), yields

$$\dot{M}_R \leq \alpha\mathcal{K}_{M_I}\sqrt{U_{\max}} - k_5 M_R. \tag{3.8}$$

Thus, if $M_R \geq \mathcal{K}_{M_R}\sqrt{U_{\max}} = \frac{\alpha\mathcal{K}_{M_I}}{k_5}\sqrt{U_{\max}}$ in the equation (3.8) we obtain $\dot{M}_R \leq 0$, this implies, if $M_R(0) \leq \mathcal{K}_{M_R}\sqrt{U_{\max}}$, then $M_R(t) \leq \mathcal{K}_{M_R}\sqrt{U_{\max}}$, for all $t \geq 0$.

Replacing the upper-bound value of J_I and M_I into the eighth equation of system (3.2), gives

$$\dot{U} \leq \gamma_1\mathcal{K}_{J_I}\sqrt{U_{\max}} + \gamma_2\mathcal{K}_{M_I}\sqrt{U_{\max}} - k_6 U. \tag{3.9}$$

Let $\mathcal{T}_3 = \gamma_1\mathcal{K}_{J_I} + \gamma_2\mathcal{K}_{M_I}$, from the equation (3.9), one can observe that if $U \geq \frac{\mathcal{T}_3}{k_6}\sqrt{U_{\max}}$, we obtain $\dot{U} \leq 0$. Thus, if $U_{\max} \geq \frac{\mathcal{T}_3^2}{k_6^2}$, we obtain $\dot{U} \leq 0$ for $U = U_{max}$. Hence, the positive invariance of Ω is shown.

(2) Secondly, for any given initial conditions, one can choose $U_{\max}$ large enough i.e

$$U_{\max} \geq \max\left\{\frac{J_L(0)^2}{\mathcal{K}_{J_L}^2}, \frac{J_I(0)^2}{\mathcal{K}_{J_I}^2}, \frac{M_L(0)^2}{\mathcal{K}_{M_L}^2}, \frac{M_I0)^2}{\mathcal{K}_{M_I}^2}, \frac{M_R(0)^2}{\mathcal{K}_{M_R}^2}, \mathcal{K}_U\right\},$$

such that the initial condition belongs to the corresponding positively invariant compact region Ω. Hence the solution initiated there is bounded.

Finally, using these two items one can conclude that all solutions are bounded. This achieves the proof.

□

Remark 3.1. *System (3.2) is not defined for $(J_S, J_L, J_I, M_S, M_L, M_I, M_R) = 0_{\mathbb{R}^7}$ but is extended to the trivial equilibrium $0_{\mathbb{R}^8}$ which makes sense biologically. However, the stability of this trivial equilibrium cannot be analysed as the Jacobian matrix of system (3.2) is not defined at this point.*

3.3 The disease free equilibrium and its stability

The disease free equilibrium (DFE) of system (3.2) occurs in the absence of CLR, so the DFE is

$$x^1 = (J_S^1, 0, 0, M_S^1, 0, 0, 0, 0)$$

where

$$J_S^1 = \frac{r_0\beta - \mu_M(\beta + \mu_J)}{\beta r_1} \qquad \text{and} \qquad M_S^1 = \frac{\beta J_S^1}{\mu_M}. \tag{3.10}$$

The above expression shows that the DFE exists under the following condition:

$$r_0\beta - \mu_M(\beta + \mu_J) > 0. \tag{3.11}$$

If condition (3.11) does not hold, the plantation of coffee cannot survive.

3.3.1 The basic reproduction number and the local stability of the DFE

To compute the basic reproduction number and the study local stability of the DFE of system (3.2), we use the standard method of the next generation matrix developed by [162]. In system (3.2), we consider only the variables in which the infection is in progression and uredospores, i.e. J_L, J_I, M_L, M_I, M_R and U. The corresponding equations can be rewritten in the following way

$$\frac{dx_I}{dt} = \mathcal{F}(x) - \mathcal{V}(x),$$

where $x_I = (J_L, J_I, M_L, M_I, M_R, U)$, $\mathcal{F}_i(x)$ represents the rate of appearance of the new infections in compartment i and $V(x)$ the transfer terms between compartments or the outside. We have

$$\mathcal{F}(x) = \begin{pmatrix} \frac{\omega_1\nu U}{J+M}J_S \\ 0 \\ \frac{\omega_2\nu U}{J+M}M_S \\ 0 \\ 0 \\ 0 \end{pmatrix} \quad \text{and} \quad \mathcal{V}(x) = \begin{pmatrix} k_1 J_L \\ -\theta J_L + k_2 J_I \\ -\beta J_L + k_3 M_L \\ -\beta J_I - \theta M_L + k_4 M_I \\ -\alpha M_I + k_5 M_R \\ -\gamma_1 J_I - \gamma_2 M_I + k_6 U \end{pmatrix}.$$

The Jacobian matrices F of $\mathcal{F}$ and V of $\mathcal{V}$ evaluated at the DFE x^1 are respectively

$$F = \begin{pmatrix} 0 & 0 & 0 & 0 & 0 & \frac{\omega_1\nu J_S^1}{J_S^1+M_S^1} \\ 0 & 0 & 0 & 0 & 0 & 0 \\ 0 & 0 & 0 & 0 & 0 & \frac{\omega_2\nu M_S^1}{J_S^1+M_S^1} \\ 0 & 0 & 0 & 0 & 0 & 0 \\ 0 & 0 & 0 & 0 & 0 & 0 \\ 0 & 0 & 0 & 0 & 0 & 0 \end{pmatrix} \text{ and } V = \begin{pmatrix} k_1 & 0 & 0 & 0 & 0 & 0 \\ -\theta & k_2 & 0 & 0 & 0 & 0 \\ -\beta & 0 & k_3 & 0 & 0 & 0 \\ 0 & -\beta & -\theta & k_4 & 0 & 0 \\ 0 & 0 & 0 & -\alpha & k_5 & 0 \\ 0 & -\gamma_1 & 0 & -\gamma_2 & 0 & k_6 \end{pmatrix}.$$

The basic reproduction number $\mathcal{R}_0$ is obtained as the spectral radius of the positive matrix FV^{-1}, that is

$$\mathcal{R}_0 = \frac{\nu\theta\left[\omega_1\mu_M[\beta\gamma_2(k_2+k_3)+\gamma_1 k_3 k_4] + \beta\omega_2\gamma_2 k_1 k_2\right]}{k_1 k_2 k_3 k_4 k_6(\beta+\mu_M)} \tag{3.12}$$

Moreover, we have the following result about the local stability of the DFE.

Lemma 3.3. *The DFE x^1 of system (3.2) is locally asymptotically stable (LAS) in Γ when $\mathcal{R}_0 < 1$, and unstable if $\mathcal{R}_0 > 1$.*

3.3.2 Global stability of DFE

Using a result obtained by Kamgang and Sallet [78], we have the following result about the global stability of the DFE.

Theorem 3.1. *If* $\mathcal{R}_0 \leq \xi < 1$, *where*

$$\xi = \frac{\mu_M}{\beta + \mu_M}\left(1 + \frac{\nu\theta\omega_2\gamma_2}{k_3k_4k_6}\left(\frac{\beta}{\mu_M} - 1\right)\right),$$

then the DFE x^1 *of system (3.2) is globally asymptotically stable (*GAS*) in* Γ.

Proof of Theorem 3.1. For the proof of this global stability, using the property of DFE, we rewrite system (3.2) in the following compact form

$$\begin{cases} \dot{x}_S = G_{11}(x_S, x_I)(x_S - x_S^1) - G_{12}(x_S, x_I)x_I \\ \dot{x}_I = G_{22}(x_S, x_I)x_I \end{cases} \tag{3.13}$$

where x_S is the vector representing the state of different compartments of non-transmitting leaves (e.g. susceptible leaves) and the vector x_I represents the state of compartments of different transmitting leaves (e.g. infected leaves). Here, we have $x_S = (J_S, M_S)^T$, $x_I = (J_L, J_I, M_L, M_I, M_R, U)^T$, $x_S^1 = (J_S^1, M_S^1)^T$, $x = (x_S, x_I)$,

$$G_{11}(x_S, x_I) = \begin{pmatrix} -r_1M - (\beta + \mu_J) & r_0 - r_1J_S^1 \\ \beta & -\mu_M \end{pmatrix},$$

$$G_{12}(x_S, x_I) = \begin{pmatrix} 0 & 0 & r_0 - r_1J_S^1 & \varepsilon r_0 - r_1J_S^1 & \varepsilon r_0 - r_1J_S^1 & -\frac{\omega_1\nu J_S}{J+M} \\ 0 & 0 & 0 & 0 & 0 & -\frac{\omega_2\nu M_S}{J+M} \end{pmatrix}$$

and

$$G_{22}(x_S, x_I) = \begin{pmatrix} -k_1 & 0 & 0 & 0 & 0 & \frac{\omega_1\nu J_S}{J+M} \\ \theta & -k_2 & 0 & 0 & 0 & 0 \\ \beta & 0 & -k_3 & 0 & 0 & \frac{\omega_2\nu M_S}{J+M} \\ 0 & \beta & \theta & -k_4 & 0 & 0 \\ 0 & 0 & 0 & \alpha & -k_5 & 0 \\ 0 & \gamma_1 & 0 & \gamma_2 & 0 & -k_6 \end{pmatrix}$$

Let $\Omega \subset \mathcal{U} = \mathbb{R}_+^2 \times \mathbb{R}_+^6$. The right-hand side of system (3.13) is of class C^1 on the open set $\mathcal{U}$. Let us verify the following five hypotheses for the application of the Kamgang and Sallet's theorem.

H_1: System (3.13) is defined on a positively invariant set Ω of the nonnegative orthant. System (3.13) is dissipative on Ω

H_2: Subsystem $\dot{x}_I = G_{11}(x_S, 0)(x_S - x_S^1)$ is globally asymptotically stable at the equilibrium $x_S^1 = (J_S^1, M_S^1)$ on the canonical projection $\mathfrak{D} = \Omega \cap (\mathbb{R}_+^2 \times \{0_{\mathbb{R}^6}\})$ of Ω on $\mathbb{R}_+^2$

Indeed, this subsystem can be written as

$$\begin{cases} \frac{dJ_S(t)}{dt} = r_0M_S - r_1J_SM_S - (\beta + \mu_J)J_S, \\ \frac{dM_S(t)}{dt} = \beta J_S - \mu_M M_S \end{cases} \tag{3.14}$$

System (3.14) has two equilibria: a trivial which is unstable and the DFE $x_S^1 = (J_S^1, M_S^1)$, (where the values of J_S^1 and M_S^1 are giving above and exist under the condition (3.11)) which is globally asymptotically stable.

H_3: Matrix $G_{22}(x_S, x_I)$ is Metzler and irreducible for any given $x \in \Omega$.

H_4: There exists an upper-bound matrix $\hat{G}_{22}$ for $\mathfrak{M} = \{G_{22}(x) \in \mathcal{M}_6(\mathbb{R})/x \in \Omega\}$ with the property that either $\hat{G}_{22} \notin \mathfrak{M}$ or if $\hat{G}_{22} \in \mathfrak{M}$, (i.e., $\hat{G}_{22} = \max_{\Omega} \mathfrak{M}$), then for any $\bar{x} \in \Omega$ such that $\hat{G}_{22} = G_{22}(\bar{x})$, $\bar{x} \in \mathbb{R}^2_+ \times \{0\}$.

Indeed, consider the subsystem $\dot{x}_I = G_{22}(x_S, x_I)x_I$, on the matrix $G_{22}(x)$, we have $\frac{J_S}{J+M} \leq 1$ and $\frac{M_S}{J+M} \leq 1$, this implies that $\dot{x}_I \leq \hat{G}_{22}x_I$, where $\hat{G}_{22}$ can be written as $\hat{G}_{22} = \hat{F} - V$, with V given above and

$$\hat{F} = \begin{pmatrix} 0 & 0 & 0 & 0 & 0 & \omega_1\nu \\ 0 & 0 & 0 & 0 & 0 & 0 \\ 0 & 0 & 0 & 0 & 0 & \omega_2\nu \\ 0 & 0 & 0 & 0 & 0 & 0 \\ 0 & 0 & 0 & 0 & 0 & 0 \\ 0 & 0 & 0 & 0 & 0 & 0 \end{pmatrix}.$$

H_5: The spectral radius of the matrix $\hat{G}_{22}$ verify $\sigma(\hat{G}_{22}) \leq 0$

Indeed, consider the following auxiliary problem:

$$\frac{d\hat{x}_I}{dt} = (\hat{F} - V)\hat{x}_I \tag{3.15}$$

The matrix $\hat{F}$ and V verified the condition of Theorem 2 in [162], then we have $\sigma(\hat{G}_{22}) = \sigma(\hat{F} - V) < 0$, which implies that $\mathcal{R}_C = \sigma(\hat{F}V^{-1}) \leq 1$, where $\sigma(\hat{F} - V)$ represents the spectral radius of the matrix $\hat{F} - V$ (i.e. the largest real part of all the eigenvalues of this matrix) and $\hat{F}V^{-1}$ is the next generation matrix. The computation gives

$$\mathcal{R}_C = \frac{\nu\theta\left[\omega_1[\beta\gamma_2(k_2 + k_3) + \gamma_1 k_3 k_4] + \omega_2\gamma_2 k_1 k_2\right]}{k_1 k_2 k_3 k_4 k_6}$$

Thus $\mathcal{R}_C \leq 1$ ensures that all eigenvalues of $\hat{G}_{22}$ have a negative real parts. We have computed $\mathcal{R}_C$ and we have seen that the hypotheses H_1, H_2 , H_3 , H_4 and H_5 are satisfied. Then, by [79], we have proven that the DFE x^1 for the system (3.2) is GAS if $\mathcal{R}_C \leq 1$.

One can observe that

$$\mathcal{R}_0 = \frac{\mu_M}{\beta + \mu_M}\left(\mathcal{R}_C + \frac{\nu\theta\omega_2\gamma_2}{k_3 k_4 k_6}\left(\frac{\beta}{\mu_M} - 1\right)\right),$$

and using the fact that $\mathcal{R}_C \leq 1$, we obtain

$$\mathcal{R}_0 \leq \xi,$$

where

$$\xi = \frac{\mu_M}{\beta + \mu_M}\left(1 + \frac{\nu\theta\omega_2\gamma_2}{k_3 k_4 k_6}\left(\frac{\beta}{\mu_M} - 1\right)\right) < 1.$$

Then, Lemma 3.3 and hypothesis $H_1 - H_5$ allow to conclude that the DFE is GAS if $\mathcal{R}_0 \leq \xi < 1$, where ξ is given above. This completes the proof. □

3.4 Endemic equilibria and their stability

Herein we prove the existence of endemic equilibria (EE) of system (3.2) and analysed their stability.

We denote by λ the force of infection given by

$$\lambda = \frac{\nu U}{J + M}. \tag{3.16}$$

Let $x^* = (J_S^*, J_L^*, J_I^*, M_S^*, M_S^*, M_L^*, M_I^*, M_R^*, U^*)$ be an endemic equilibrium of system (3.2). Setting the right hand side of this system to 0 yields

$$\begin{cases} 0 = r_0 M_1^* - r_1 M^* J_S^* - \omega_1 \lambda^* J_S^* - (\beta + \mu_J) J_S^* \\ J_L^* = \lambda^* \dfrac{\omega_1}{k_1} J_S^*, \\ J_I^* = \lambda^* \dfrac{\theta \omega_1}{k_1 k_2} J_S^*, \\ M_S^* = \dfrac{\beta J_S^*}{(\mu_M + \lambda^* \omega_2)}, \\ M_L^* = \lambda^* \left(\dfrac{\beta \omega_1}{k_1 k_3} J_S^* + \dfrac{\omega_2}{k_3} M_S^* \right), \\ M_I^* = \lambda^* \left(\dfrac{\beta \theta \omega_1 (k_2 + k_3)}{k_1 k_2 k_3 k_4} J_S^* + \dfrac{\theta \omega_2}{k_3 k_4} M_S^* \right), \\ M_R^* = \lambda^* \left(\dfrac{\beta \theta \alpha \omega_1 (k_2 + k_3)}{k_1 k_2 k_3 k_4 k_5} J_S^* + \dfrac{\theta \alpha \omega_2}{k_3 k_4 k_5} M_S^* \right), \\ U^* = \lambda^* \left(\dfrac{\theta \omega_1 (\beta \gamma_2 (k_2 + k_3) + \gamma_1 k_3 k_4)}{k_1 k_2 k_3 k_4 k_6} J_S^* + \dfrac{\theta \gamma_2 \omega_2}{k_3 k_4 k_6} M_S^* \right). \end{cases} \tag{3.17}$$

One can observe that there exists an endemic equilibrium x^* if and only if λ^* and J_S^* are positive.

Substituting the expressions of $J_{\{L,I\}}^*$ and $M_{\{S,L,I,R\}}^*$ into the first equation of system (3.17) and solving this equation for J_S^*, we obtain either $J_S^* = 0$ which corresponds to the trivial equilibrium or

$$J_S^* = \frac{b_2 (\lambda^*)^2 + b_1 \lambda^* + b_0}{\beta r_1 (c_2 (\lambda^*)^2 + c_1 \lambda^* + c_0)}, \tag{3.18}$$

where

$$\begin{cases} b_2 = \omega_1 \omega_2 (\beta r_0 (\theta \varepsilon (\alpha + k_5)(k_2 + k_3) + k_2 k_4 k_5) - k_1 k_2 k_3 k_4 k_5), \\ b_1 = \beta r_0 k_2 \left[(k_5 (\varepsilon \theta + k_4) + \varepsilon \theta \alpha)(k_1 \omega_2 + \mu_M \omega_1) \right] + \beta r_0 \mu_M \theta \varepsilon \omega_1 k_3 (\alpha + k_5), \\ \qquad - k_1 k_2 k_3 k_4 k_5 (\omega_2 (\beta + \mu_J) + \mu_M \omega_1), \\ b_0 = (\beta r_0 - \mu_M (\beta + \mu_J)) k_1 k_2 k_3 k_4 k_5, \\ c_2 = \omega_1 \omega_2 \left[\theta (k_2 + k_3)(\alpha + k_5) + k_2 k_4 k_5 \right], \\ c_1 = k_2 (k_1 \omega_2 + \mu_M \omega_1) \left[k_5 (\theta + k_4) + \alpha \theta \right] + \mu_M \theta \omega_1 k_3 (\alpha + k_5), \\ c_0 = k_1 k_2 k_3 k_4 k_5. \end{cases}$$

Note that, in the equation (3.18) when λ^* is positive, the sign of J_S^* is determined by it numerator in (3.18), as all $c_.$ are positive.

Firstly, let us study the positivity of λ^*. From equation (3.16) one has

$$\lambda^* = \frac{\nu U^*}{J^* + M^*} \Rightarrow (J^* + M^*) = \frac{\nu U^*}{\lambda^*},$$

Replacing the expression of U^* given in system (3.17), we obtain

$$J^* + M^* = \nu\theta \left[\frac{\omega_1[\beta\gamma_2(k_2+k_3) + \gamma_1 k_3 k_4]}{k_1 k_2 k_3 k_4 k_6} + \frac{\beta\omega_2\gamma_2}{k_3 k_4 k_6(\mu_M + \lambda^*\omega_2)} \right] J_S^*.$$

As $J^* + M^* = J_S^* + J_L^* + J_I^* + M_S^* + M_L^* + M_I^* + M_R^*$, replacing the expressions given in equation (3.17) into the left-hand side of the above equation, we obtain either $J_S^* = 0$ or the following second degree polynomial governed by λ^*:

$$P(\lambda^*) = m_2(\lambda^*)^2 + m_1\lambda^* + m_0 \tag{3.19}$$

where

$$\begin{cases} m_2 = \omega_1\omega_2 \left[\frac{\theta+k_2}{k_1k_2} + \frac{\beta}{k_1k_3} + \frac{\beta\theta(k_2+k_3)(\alpha+k_5)}{k_1k_2k_3k_4k_5} \right], \\ m_1 = \mu_M \frac{a_2}{\omega_2} + \omega_2 \left[1 + \frac{\beta}{k_3} + \frac{\beta\theta(\alpha+k_5)}{k_3k_4k_5} \right] - \frac{\theta\omega_1\omega_2\nu[\beta\gamma_2(k_2+k_3)+\gamma_1k_3k_4]}{k_1k_2k_3k_4k_6}, \\ m_0 = (\beta + \mu_M)(1 - \mathcal{R}_0). \end{cases}$$

Now, using the Descartes sign rules for λ-polynomial (3.19), the number of positive solutions is given in Table 3.2.

Table 3.2: Descartes rule for λ-polynomial (3.19).

m_2	m_1	m_0	$\mathcal{R}_0$	Number of positive solutions
+	+	+	$\mathcal{R}_0 < 1$	No solution
+	-	+	$\mathcal{R}_0 < 1$	No or two solutions
+	+	-	$\mathcal{R}_0 > 1$	One solution
+	-	-	$\mathcal{R}_0 > 1$	One solution

A positive value for λ^* is not sufficient to obtain an endemic equilibrium of system (3.2). We also need to verify if the corresponding value of J_S^*, determined from equation (3.18), is positive. If both λ^* and J_S^* are positive, according to system (3.17), all state variables are positive, so it corresponds to an endemic equilibrium.

From the above proof we have the following Lemma

Lemma 3.4. *If $\mathcal{R}_0 > 1$ and $J^* > 0$, the system (3.2) has one endemic equilibrium*

3.4.1 Bifurcation analysis

To study the stability of the endemic equilibria around $\mathcal{R}_0$, we use Theorem 2.2 given in Subsection 2.1.2. We first introduce a positive parameter η and set $\gamma_2 = \eta\gamma_1$. We then use γ_1 as bifurcation parameter, as its variations cover all $\mathcal{R}_0$ values. Indeed,

$$\frac{\mathcal{R}_0}{\gamma_1} = \frac{\nu\theta(\omega_1\mu_M(\beta\eta(k_2+k_3) + k_3k_4) + \beta\omega_2\eta k_1k_2)}{k_1k_2k_3k_4k_6(\beta+\mu_M)} := \frac{1}{\zeta} > 0. \tag{3.20}$$

The linearisation of system (3.2) in the neighbourhood of DFE x^1 and around $\mathcal{R}_0 = 1$, using expression in equation (3.20) setting γ_1 to ζ, yields

$$\frac{dx(t)}{dt} = J(x^1)x(t), \tag{3.21}$$

where

$$J(x^1) = \begin{pmatrix} -\frac{r_0\beta}{\mu_M} & 0 & 0 & \frac{\mu_M(\beta+\mu_J)}{\beta} & \frac{\mu_M(\beta+\mu_J)}{\beta} & \mathcal{Q} & \mathcal{Q} & -\frac{\omega_1\nu\mu_M}{\beta+\mu_M} \\ 0 & -k_1 & 0 & 0 & 0 & 0 & 0 & \frac{\omega_1\nu\mu_M}{\beta+\mu_M} \\ 0 & \theta & -k_2 & 0 & 0 & 0 & 0 & 0 \\ \beta & 0 & 0 & -\mu_M & 0 & 0 & 0 & -\frac{\omega_2\nu\beta}{\beta+\mu_M} \\ 0 & \beta & 0 & 0 & -k_3 & 0 & 0 & \frac{\omega_2\nu\beta}{\beta+\mu_M} \\ 0 & 0 & \beta & 0 & \theta & -k_4 & 0 & 0 \\ 0 & 0 & 0 & 0 & 0 & \alpha & -k_5 & 0 \\ 0 & 0 & \zeta & 0 & 0 & \eta\zeta & 0 & -k_6 \end{pmatrix},$$

where $\mathcal{Q} = \frac{\mu_M(\beta+\mu_J)+r_0(\varepsilon-1)\beta}{\beta}$.

The matrix $J(x^1)$ admits $\rho = 0$ as eigenvalue, the other eigenvalues still having a negative real part. Thereby, assumption A_1 of Theorem 4.3 is verified.

Let us now verify assumption A_2. We need to compute the left and right eigenvectors of matrix $J(x^1)$ associated to the eigenvalue $\rho = 0$. The left eigenvector, denoted by $v = (v_1, v_2, v_3, v_4, v_5, v_6, v_7, v_8)$, satisfies $vJ(x^1) = \mathbf{0}$

Solving the above equation, yields

$$\begin{cases} v_1 = 0, \\ v_2 = \dfrac{\zeta\theta[\beta\eta(k_2+k_3)+k_3k_4]}{k_1k_2k_3k_4}v_8, \\ v_3 = \dfrac{\zeta(\beta\eta+k_4)}{k_2k_4}v_8, \\ v_4 = 0, \\ v_5 = \dfrac{\eta\zeta\theta}{k_3k_4}v_8, \\ v_6 = \dfrac{\eta\zeta}{k_4}v_8, \\ v_7 = 0,\ v_8 > 0. \end{cases}$$

Similarly, the right eigenvector of matrix $J(x^1)$, denoted by $u = (u_1, u_2, u_3, u_4, u_5, u_6, u_7, u_8)^T$, satisfies $J(x^1)u = \mathbf{0}$,

Solving the above equation, we obtain

$$\begin{cases} u_1 = \dfrac{u_8\nu\mu_M\mathcal{X}}{(\beta+\mu_M)((\beta+\mu_M)\mu_M - r_0\beta)k_1k_2k_3k_4k_5}, \\ u_2 = \dfrac{\omega_1\nu\mu_M}{(\beta+\mu_M)k_1}u_8, \\ u_3 = \dfrac{\theta\omega_1\nu\mu_M}{(\beta+\mu_M)k_1k_2}u_8, \\ u_4 = \dfrac{\beta(-\nu\omega_2u_8 + (\beta+\mu_M)u_1)}{(\beta+\mu_M)\mu_M} \\ u_5 = \dfrac{\beta\nu(\mu_M\omega_1+\omega_2k_1)}{(\beta+\mu_M)k_1k_3}u_8, \\ u_6 = \dfrac{\beta\nu\theta(\mu_M\omega_1(k_2+k_3)+\omega_2k_1k_2)}{(\beta+\mu_M)k_1k_2k_3k_4}u_8, \\ u_7 = \dfrac{\nu\theta\alpha\beta(\mu_M\omega_1(k_2+k_3)+\omega_2k_1k_2)}{(\beta+\mu_M)k_1k_2k_3k_4k_5}u_8, \\ u_8 > 0. \end{cases}$$

where

$$\begin{cases} \mathcal{X} = \mathcal{X}_1 + \mathcal{X}_2 + \mathcal{X}_3 + \mathcal{X}_4, \\ \mathcal{X}_1 = (\beta+\mu_J)\omega_1((k_2+k_3)(\alpha+k_5)\theta + k_2k_4k_5)\mu_M^2, \\ \mathcal{X}_2 = ((r_0(\varepsilon-1)\omega_1 + k_1\omega_2)k_2 + \omega_1k_3r_0(\varepsilon-1))\beta + \mu_J\omega_2k_1k_2, \\ \mathcal{X}_3 = ((\alpha+k_5)\theta + k_1k_2k_4k_5(\beta\omega_2 - k_3\omega_1 + \mu_J\omega_2))\mu_M, \\ \mathcal{X}_4 = k_1\omega_2k_2(\beta r_0(\varepsilon-1)(\alpha+k_5)\theta - k_3k_4k_5(\beta+\mu_J)). \end{cases}$$

The expression b defined in Assumption A_2 of Theorem 2.2 for system (3.2) is rewritten by

$$b = \sum_{k,i=1}^{8} v_k u_i \frac{\partial^2 F_k}{\partial x_i \partial\gamma_1}(x^1, \zeta),$$

where $F_k = \dot{x}_k$ with $k = 1, 2, ..., 8$ corresponding to system (3.2).

The only term of partial derivative that is non-null corresponds to

$$v_8\frac{\partial^2 F_8}{\partial x_3\partial\gamma_1}(x^1,\zeta) = v_8 \quad \text{and} \quad v_8\frac{\partial^2 F_8}{\partial x_6\partial\gamma_1}(x^1,\zeta) = v_8\eta.$$

Substituting the above expression into the expression of b, yields

$$b = v_8u_3\frac{\partial^2 F_8}{\partial x_3\partial\gamma_1}(x^1,\zeta) + v_8u_6\frac{\partial^2 F_8}{\partial x_6\partial\gamma_1}(x^1,\zeta) = v_8(u_3+u_6\eta),$$

Then

$$b = v_8(u_3 + u_6\eta) > 0 \tag{3.22}$$

Let us compute the expression of a, defined in Assumption A_2 of Theorem 2.2 for system (3.2),

which is

$$a = \sum_{i,j,k=1}^{8} v_k u_i u_j \frac{\partial^2 F_k}{\partial x_i \partial x_j}(x^1, \zeta).$$

The only terms that are non-null correspond to

$$\begin{aligned}
v_2 \frac{\partial^2 F_2}{\partial x_1 \partial x_8}(x^1,\zeta) &= v_2 \frac{\partial^2 F_2}{\partial x_8 \partial x_1}(x^1,\zeta) = \frac{\omega_1 \nu M_S^1}{(J_S^1 + M_S^1)^2} v_2 \\
v_2 \frac{\partial^2 F_2}{\partial x_i \partial x_8}(x^1,\zeta) &= v_2 \frac{\partial^2 F_2}{\partial x_8 \partial x_j}(x^1,\zeta) = -\frac{\omega_1 \nu J_S^1}{(J_S^1 + M_S^1)^2} v_2 \quad \text{for } i,j = 2,...,7. \\
v_5 \frac{\partial^2 F_5}{\partial x_4 \partial x_8}(x^1,\zeta) &= v_5 \frac{\partial^2 F_5}{\partial x_8 \partial x_4}(x^1,\zeta) = \frac{\omega_2 \nu J_S^1}{(J_S^1 + M_S^1)^2} v_5 \\
v_2 \frac{\partial^2 F_5}{\partial x_i \partial x_8}(x^1,\zeta) &= v_5 \frac{\partial^2 F_5}{\partial x_8 \partial x_j}(x^1,\zeta) = -\frac{\omega_2 \nu M_S^1}{(J_S^1 + M_S^1)^2} v_5 \quad \text{for } i,j = 2,...,7.
\end{aligned}$$

Substituting these above expressions into the expression of a, yields

$$\begin{aligned}
a &= 2u_8 \left[v_2 \sum_{j=1}^{7} u_j \frac{\partial^2 F_2}{\partial x_j \partial x_8}(x^1,\zeta) + v_5 \sum_{j=1}^{7} u_j \frac{\partial^2 F_5}{\partial x_j \partial x_8}(x^1,\zeta) \right], \\
&= 2u_8 v_2 \left(\frac{\omega_1 \nu M_S^1}{(J_S^1 + M_S^1)^2} u_1 - \frac{\omega_1 \nu J_S^1}{(J_S^1 + M_S^1)^2} (u_2 + u_3 + u_4 + u_5 + u_6 + u_7) \right) \\
&+ 2u_8 v_5 \left(\frac{\omega_2 \nu J_S^1}{(J_S^1 + M_S^1)^2} u_1 - \frac{\omega_2 \nu M_S^1}{(J_S^1 + M_S^1)^2} (u_2 + u_3 + u_4 + u_5 + u_6 + u_7) \right).
\end{aligned}$$

Replace the values of J_S^1, M_S^1, v_2 and v_5, we obtain

$$\begin{aligned}
a = &\frac{2\zeta \mu_M r_1 \omega_1 \nu \beta \theta u_8 v_8 (\mu_M \sum_{i=2}^{7} u_i - \beta u_1)(\gamma_{1r} k_4 k_3 + \gamma_{2r} \beta (k_2 + k_3))}{k_1 k_2 k_3 k_4 (\beta + \mu_M)^2 ((\beta + \mu_J)\mu_M - \beta r_0))} \\
&+ \frac{2 r_1 \theta \mu_M \zeta \beta \nu \omega_2 u_8 v_8 \gamma_{2r} (\beta(u_1 + u_2 + u_3 + u_5 + u_6 + u_7) - \mu_M u_4)}{(\beta + \mu_M)^2 ((\beta + \mu_J)\mu_M - \beta r_0) k_3 k_4}.
\end{aligned} \tag{3.23}$$

The expression b given in equation (3.22) is always positive, then the direction of bifurcation depends on the sign of a given by (3.23). This means that we are in the cases **1** and **4** of Theorem 2.2. Then, the direction of the bifurcation is determined by the sign of parameter a defined in equation (3.23). Using parameter values in Table 3.1, with $\eta = 7/5$, lead to $a < 0$ which corresponds to a forward bifurcation.

3.4.2 Forward bifurcation and stability

Using Maple to calculate the solutions of the λ-polynomial in equation (3.19), we obtain Table 3.3.

From this table, one can conclude that system (3.2) has one endemic equilibrium when $\mathcal{R}_0 > 1$ and that the DFE always exists.

According to the results in Section 3.4.1, when the bifurcation parameter changes from $\gamma_1 < \zeta$ to $\gamma_1 > \zeta$, i.e. the basic reproduction number changes from $\mathcal{R}_0 < 1$ to $\mathcal{R}_0 > 1$, the DFE changes from LAS to unstable. Moreover, the endemic equilibrium $J_{S,1}^*$ in Table 3.3 appears and is locally asymptotically stable.

To complement this analytical result, Figure 3.2 shows the existence of equilibria and their

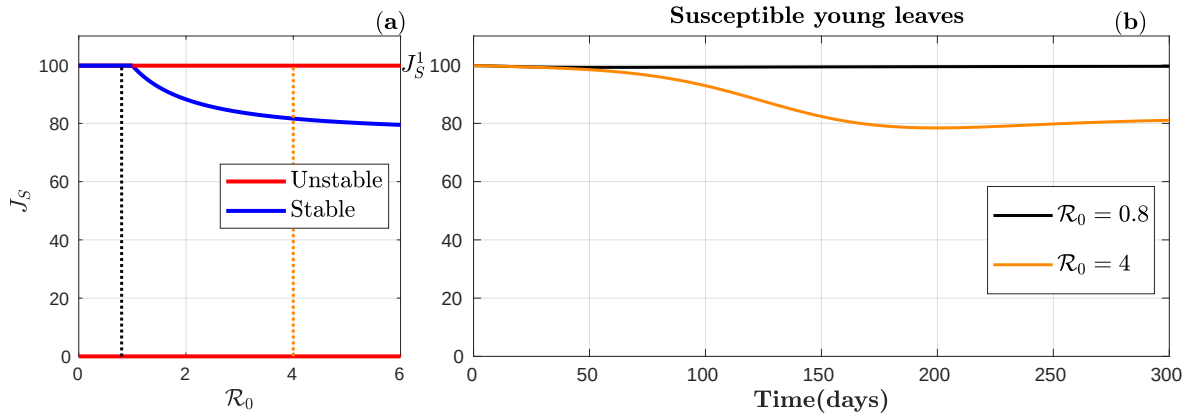

Figure 3.2: Bifurcation diagram and dynamics of susceptible young leaves for the forward bifurcation case. Subplot (a) presents the $(\mathcal{R}_0, J_S)$-bifurcation diagram with stable (blue curve) and unstable (red curve) equilibria of system (3.1). Subplot (b) shows the dynamics of susceptible young leaves J_S for parameter values $\mathcal{R}_0 = 0.8$ (black curve) and $\mathcal{R}_0 = 4$ (orange curve) corresponding to the dotted lines in subplot (a). Bifurcation parameter is γ_1, $\mathcal{R}_0 = \gamma_1/\zeta$ and $\gamma_2 = \eta\gamma_1$, with ζ defined in equation (3.20) and $\eta = 7/5$. All remaining parameters are given in Table 3.1, leading to $\zeta = 1.185$ spores/leaf.day and initial conditions defined by (3.24) with $U_0 = 1000$ spores.

Table 3.3: Force of infection λ and susceptible young leaves J_S at equilibrium using parameter values in Table 3.1.

$\mathcal{R}_0$	Equilibrium values for: λ	J_S
$\mathcal{R}_0 = 0.8$		$J_S^0 = 0$
	$\lambda_0 = 0$	$J_S^1 = 99.81$
	$\lambda_1^* < 0$	$J_{S,1}^* < 0$
	$\lambda_2^* < 0$	$J_{S,2}^* < 0$
$\mathcal{R}_0 = 4$		$J_S^0 = 0$
	$\lambda_0 = 0$	$J_S^1 = 99.81$
	$\lambda_1^* = 1.27$	$J_{S,1}^* = 81.94$
	$\lambda_2^* < 0$	$J_{S,2}^* < 0$

stability. The initial conditions are chosen to be

$$x(0) = \left\{ \begin{array}{l} J_S(0) = J_S^1,\ J_L(0) = J_I(0) = 0,\ M_S(0) = M_S^1, \\ M_L(0) = M_I(0) = M_R(0) = 0,\ U(0) = U_0 > 0\ , B(0) = 0 \end{array} \right\}. \tag{3.24}$$

They correspond to the DFE except for the initial presence of uredospores and absence of berries.

For $\mathcal{R}_0 = 0.8 < 1$ (black curves), subplot (a) shows that system (3.1) has two equilibria, the DFE which is stable and the trivial equilibrium which we showed to be unstable numerically; subplot (b) shows the convergence of susceptible young leaves to their DFE value J_S^1.

For $\mathcal{R}_0 = 4 > 1$ (orange curves), subplot (a) shows that system (3.1) has three equilibria: the trivial equilibrium which is unstable, the DFE which is unstable and the endemic equilibrium which is stable; subplot (b) shows the convergence of susceptible young leaves to their endemic equilibrium value $J_{S,1}^*$.

Figure 3.3 shows the convergence of system (3.1), initially at the disease free equilibrium, towards the endemic equilibrium for different initial uredospore values. Susceptible leaves decrease over time. Infected leaves and uredospores overshoot their endemic steady state values. There are globally less leaves at the endemic equilibrium, compared to the initial disease free state. Compared to the DFE value ($B^1 = 48929$ berries), the number of berry at endemic equilibrium ($B^* = 8212$ berries) is drastically reduced by 83%.

Figure 3.4 differentiates CLR impact between young and mature leaves. Young leaves are less susceptible to the disease and hence less affected. There are globally less young leaves, but more young susceptible leaves than mature susceptible leaves at the endemic equilibrium. Indeed, as there are less mature leaves, young leaves are less impacted by the competition with mature leaves.

3.4.3 Backward bifurcation and stability

In this subsection we study the behavior of system (3.1) when there is a backward bifurcation, corresponding to $a > 0$ in equation (3.23). We choose ad hoc parameters given in Table 3.4.

Firstly, using Maple to calculate the equilibria of system (3.2), we obtain Table 3.5. In this table, negative or complex values of λ^* and/or J_S^* are included (text in gray), but they do not correspond to biological equilibria.

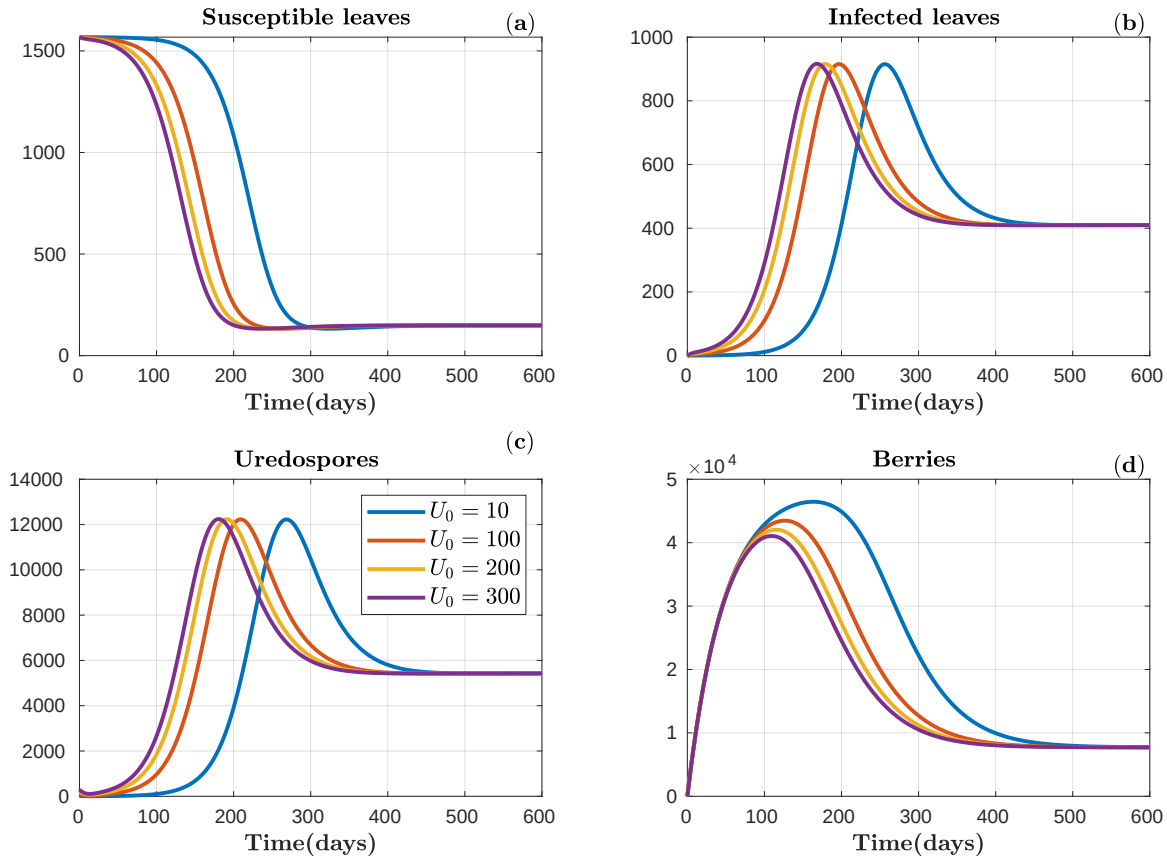

Figure 3.3: Persistence of CLR in the coffee plantation. Simulations of system (3.1) for $\mathcal{R}_0 = 4.218$, using initial conditions (3.24) with $U_0 = 10$ (blue curves), $U_0 = 100$ (red curves), $U_0 = 200$ (yellow curves) and $U(0) = 300$ spores (purple curves): (a) susceptible leaves $J_S + M_S$, (b) infected leaves $J_L + J_I + M_L + M_I + M_R$, (c) uredospores U and (d) berries B. All parameter values are given in Table 3.1.

Table 3.4: Parameter values of system (3.1) chosen to obtain a backward bifurcation.

Symbol	Value	Symbol	Value
r_0	0.7094 /day	θ	0.2336 /day
r_1	0.0065 /day	α	0.8261 /day
ω_1	0.5092 leaves/spore	μ_J	0.0114 /day
ω_2	0.4709 leaves/spore	μ_M	0.0236 /day
η	0.0396	μ_U	0.0931 /day
ν	0.6269 /day	d	0.8961 /day
β	0.0555 /day	ε	0.9953 /day

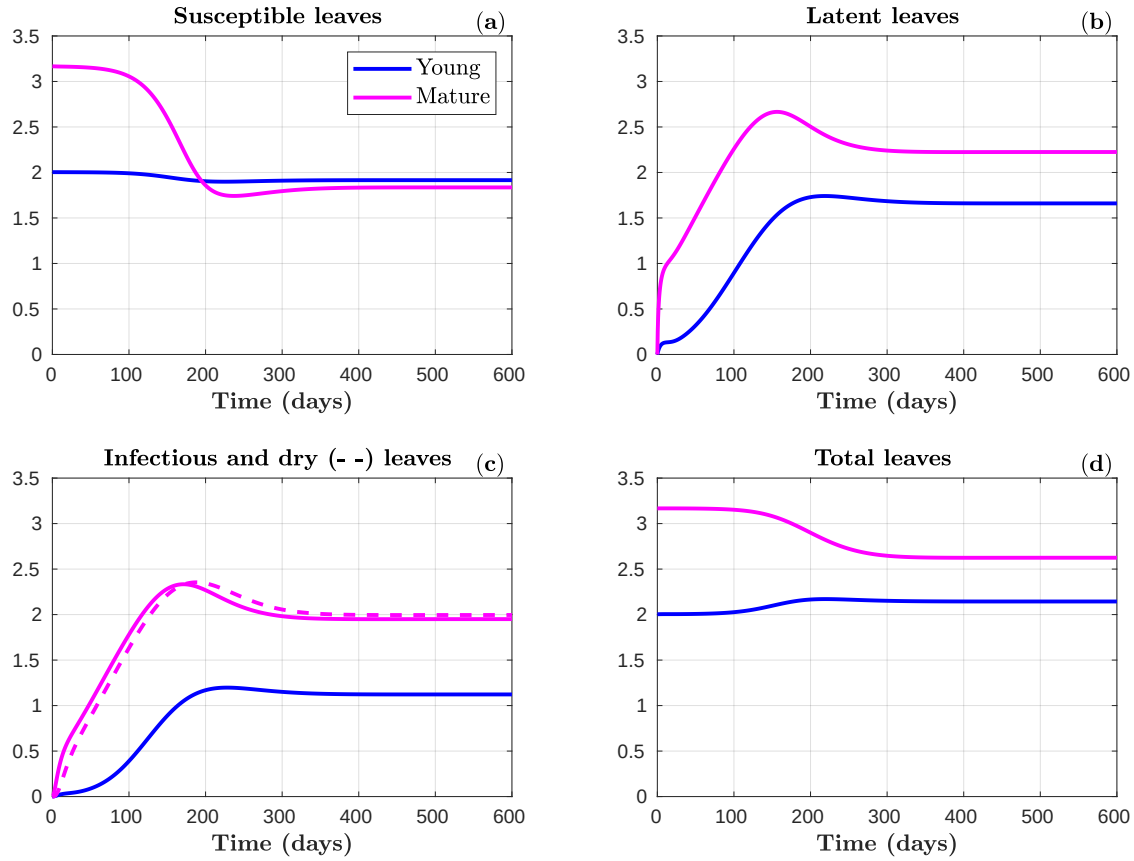

Figure 3.4: CLR impact according to host development. Simulations of system (3.1) for $\mathcal{R}_0 = 4.218$, using initial conditions (3.24) with $U_0 = 300$: (a) susceptible young J_S and mature M_S leaves, (b) latent young J_L and mature M_L leaves, (c) infectious young J_I, infectious M_I and dry M_R mature leaves, and (d) total young $J = J_S + J_L + J_I$ and mature $M = M_S + M_L + M_I + M_R$ leaves. Leaves are represented in a log scale that preserves 0 ($\log(1 + J_S)$ instead of J_S). All parameter values are given in Table 3.1.

Table 3.5: Force of infection λ and susceptible young leaves J_S at equilibrium using parameter values in Table 3.4.

$\mathcal{R}_0$	Equilibrium values for:	
	λ	J_S
$\mathcal{R}_0 = 0.3$		$J_S^0 = 0$
	$\lambda_0 = 0$	$J_S^1 = 104.76$
	λ_1^* complex	$J_{S,1}^*$ complex
	λ_2^* complex	$J_{S,2}^*$ complex
$\mathcal{R}_0 = 0.8$		$J_S^0 = 0$
	$\lambda_0 = 0$	$J_S^1 = 104.76$
	$\lambda_1^* = 0.31$	$J_{S,1}^* = 65.75$
	$\lambda_2^* = 0.039$	$J_{S,2}^* = 100.11$
$\mathcal{R}_0 = 2$		$J_S^0 = 0$
	$\lambda_0^* = 0$	$J_S^1 = 104.76$
	$\lambda_1^* = 1.70$	$J_{S,1}^* = 8.18$
	$\lambda_2^* < 0$	$J_{S,2}^* < 0$
$\mathcal{R}_0 = 4$		$J_S^0 = 0$
	$\lambda_0 = 0$	$J_S^1 = 104.76$
	$\lambda_1^* = 3.92$	$J_{S,1}^* = -6.46$
	$\lambda_2^* < 0$	$J_{S,2}^* < 0$

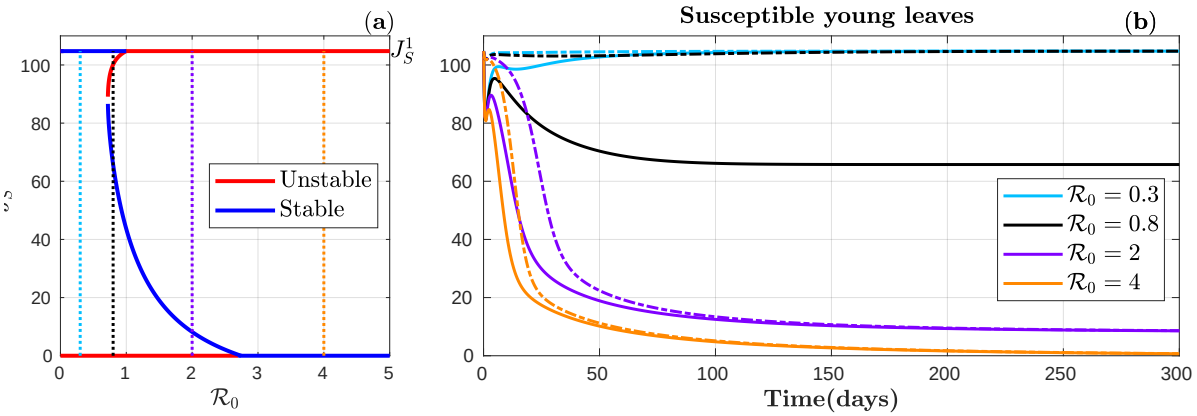

Figure 3.5: Bifurcation diagram and dynamics of susceptible young leaves for the backward bifurcation case. Subplot (a) presents the $(\mathcal{R}_0, J_S)$-bifurcation diagram with stable (blue curve) and unstable (red curve) equilibria of system (3.1). Subplot (b) shows the dynamics of susceptible young leaves J_S for parameter values $\mathcal{R}_0 = 0.3$ (blue curves), $\mathcal{R}_0 = 0.8$ (black curves), $\mathcal{R}_0 = 2$ (purple curves) and $\mathcal{R}_0 = 4$ (orange curves) corresponding to the dotted lines in subplot (a). The bifurcation parameter is γ_1, $\mathcal{R}_0 = \gamma_1/\zeta$ and $\gamma_2 = \eta\gamma_1$, with ζ defined in equation (3.20). All remaining parameters are given in Table 3.4, leading to $\zeta = 7.771$ spores/leaf.day and initial conditions defined by (3.24) with $U_0 = 100$ (dashed curves) and $U_0 = 1000$ spores (solid curves).

From this table, we conclude that system (3.2) has two endemic equilibria when $\mathcal{R}_0 < 1$ and one endemic equilibrium when $\mathcal{R}_0 > 1$.

When $\mathcal{R}_0 < 1$, the DFE is stable. Moreover, according to the results in Section 3.4.1, when $\mathcal{R}_0$ is close to one, there exist two endemic equilibria among which one is stable and the other unstable. When $\mathcal{R}_0 > 1$, the DFE is unstable. Moreover, when $\mathcal{R}_0$ is close to one, there is a unique endemic equilibrium, which is stable. For larger $\mathcal{R}_0$ values, the endemic equilibrium disappears.

Figure 3.5 illustrates the existence of the endemic equilibria and their stability. The diagram in subplot (a) presents a sequence of three bifurcations: a saddle-node bifurcation in $\mathcal{R}_0 \approx 0.7$, a backward transcritical bifurcation in $\mathcal{R}_0 = 1$ and an other transcritical bifurcation in $\mathcal{R}_0 \approx 2.7$. Subplot (b) presents the dynamics of susceptible young leaves J_S for representative parameter values.

For $\mathcal{R}_0 = 0.3$ (blue curves), subplot (a) shows that system (3.1) has two equilibria: the trivial equilibrium which we showed to be unstable numerically and the DFE which is stable; subplot (b) shows the convergence of susceptible young leaves to their DFE value J_S^1.

For $\mathcal{R}_0 = 0.8$ (black curves), subplot (a) shows that system (3.1) has four equilibria: the trivial equilibrium which is unstable, the DFE which is stable, the endemic equilibrium $J_{S,1}^*$ which is stable and the endemic equilibrium $J_{S,2}^*$ which is unstable; subplot (b) shows the convergence of susceptible young leaves to their DFE value J_S^1 (for $U_0 = 100$ spores) and to their endemic equilibrium value $J_{S,1}^*$ (for $U_0 = 1000$ spores).

For $\mathcal{R}_0 = 2$ (orange curves), subplot (a) shows that system (3.1) has three equilibria: the trivial equilibrium which is unstable, the DFE which is unstable and the endemic equilibrium which is stable; subplot (b) shows the convergence of susceptible young leaves to their endemic equilibrium value $J_{S,1}^*$.

For $\mathcal{R}_0 = 4$ (orange curves), subplot (a) shows that system (3.1) has three equilibria: the trivial equilibrium which is stable and the DFE is unstable; subplot (b) shows the convergence

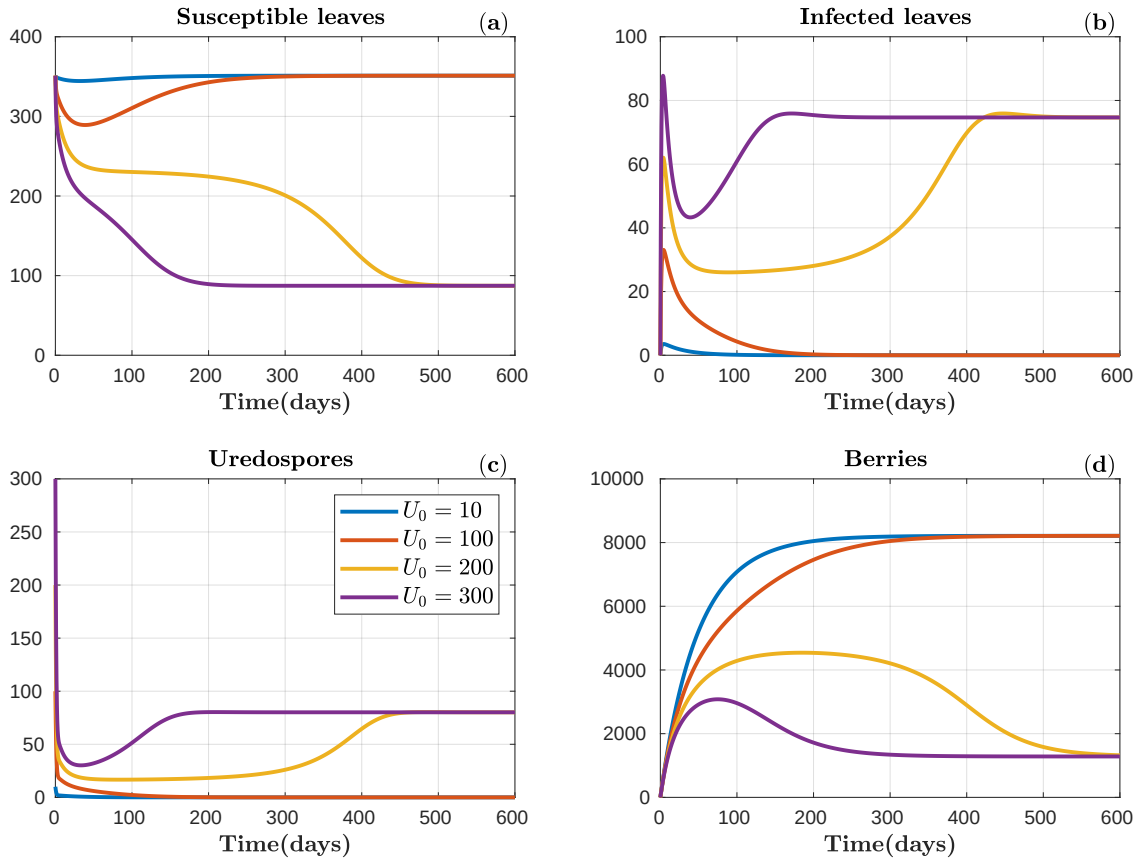

Figure 3.6: Extinction and persistence of CLR in the coffee plantation. Simulations of model (3.1) for $\mathcal{R}_0 = 0.8$, using initial conditions (3.24) with $U_0 = 10$ (blue curves), $U_0 = 100$ (red curves), $U_0 = 200$ (yellow curves) and $U(0) = 300$ spores (purple curves): (a) susceptible leaves $J_S + M_S$, (b) infected leaves $J_L + J_I + M_L + M_I + M_R$, (c) uredospores U and (d) berries B. All parameter values are given in Table 3.4 except $\gamma_1 = 6.2171$ spores/leaf.day.

of susceptible young leaves to their value at trivial equilibrium.

For $\mathcal{R}_0 = 0.8$, Figure 3.6 shows the convergence of system (3.1) towards the DFE and towards the stable endemic equilibrium for different initial uredospore values. For $U_0 = 10$ (blue curves) and $U_0 = 100$ spores (red curves), susceptible leaves decrease and then increase towards their DFE values. Simultaneously, the infected leaves and uredospores decrease towards zero and the berries increase. This convergence corresponds to the local stability of the DFE. For $U_0 = 200$ (yellow curves) and $U(0) = 300$ spores (purple curves), susceptible leaves decrease towards their endemic values. Infected leaves and uredospores first decrease, as for smaller initial uredospore values, and then increase towards their endemic values. Berries increase and then decrease towards their endemic values. This convergence corresponds to the local stability of one of the two endemic equilibria.

For $\mathcal{R}_0 = 4$, Figure 3.7 shows the convergence of system (3.1) towards the trivial equilibrium for different initial uredospore values. Susceptible leaves decrease over time towards zero. Infected leaves, uredospores and berries first increase and then decrease towards zero. This shows the stability of the trivial equilibrium. This case corresponds to a very virulent pathogen that totally destroys the coffee plantation. Note that the dynamics does not depend on the initial conditions, except for the berries whose dynamics are amplified by the small differences

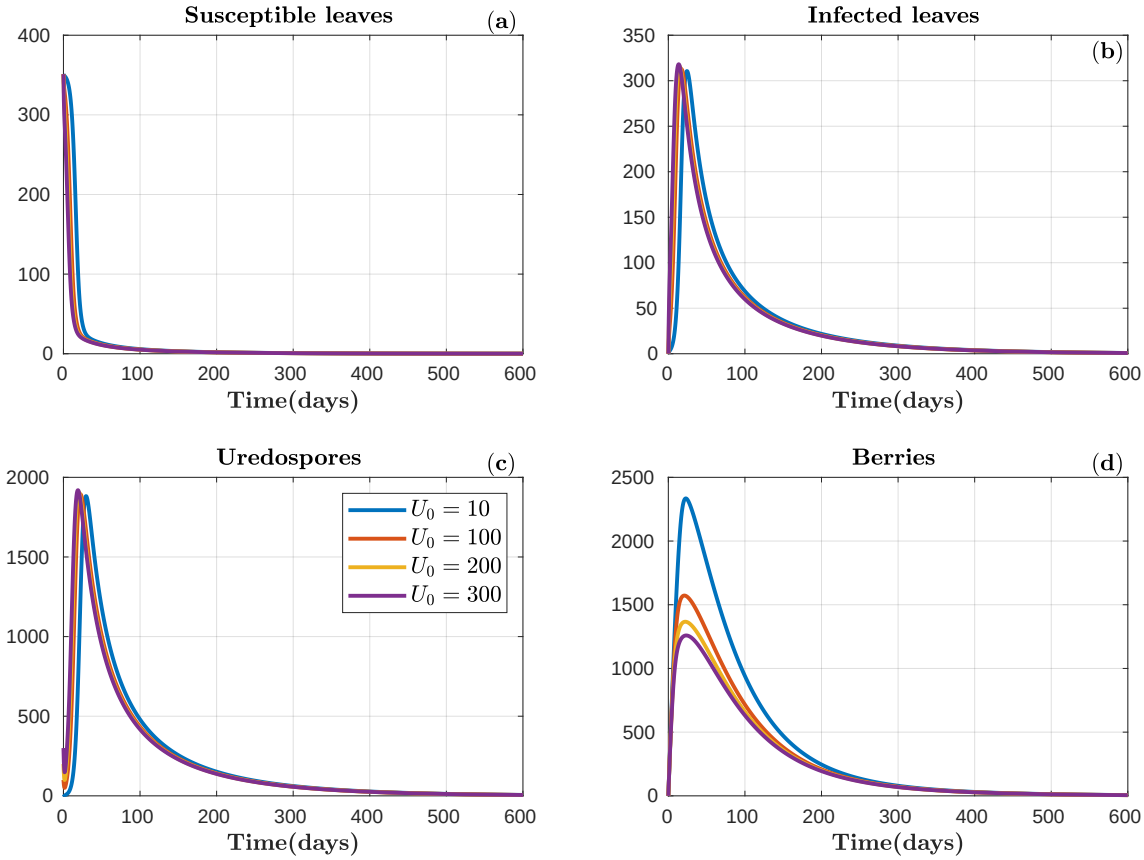

Figure 3.7: Destruction of the plantation by CLR. Simulations of model (3.1) for $\mathcal{R}_0 = 4$, using initial conditions (3.24) with $U_0 = 10$ (blue curves), $U_0 = 100$ (red curves), $U_0 = 200$ (yellow curves) and $U(0) = 300$ spores (purple curves): (a) susceptible leaves $J_S + M_S$, (b) infected leaves $J_L + J_I + M_L + M_I + M_R$, (c) uredospores U and (d) berries B. All parameter values are given in Table 3.4 except $\gamma_1 = 31.0856$ spores/leaf.day.

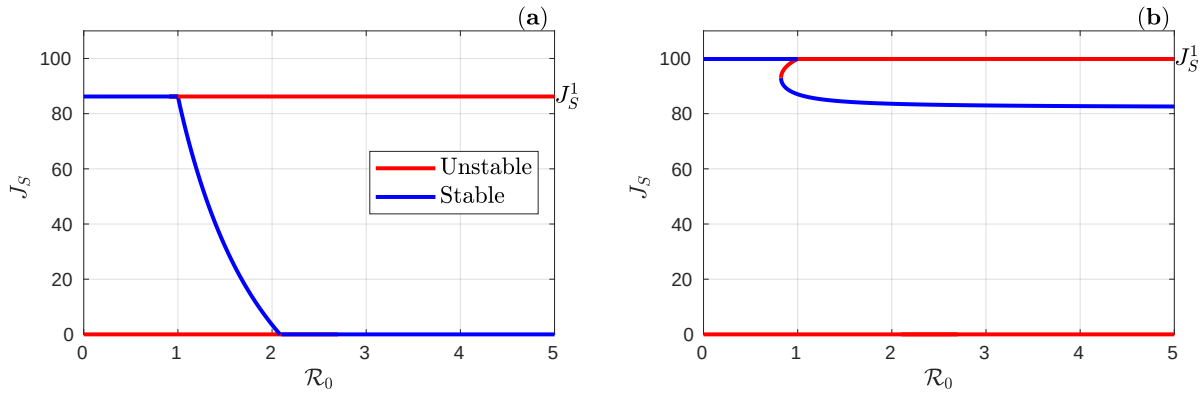

Figure 3.8: Subplots present the $(\mathcal{R}_0, J_S)$-bifurcation diagram with stable (blue curve) and unstable (red curve) equilibria of system (3.1). The bifurcation parameter is γ_1, $\mathcal{R}_0 = \zeta\gamma_1$ and $\gamma_2 = \eta\gamma_1$, with ζ defined in equation (3.20). Subplot (a) shows a forward bifurcation using parameter values in Table 3.4 except $\mu_M = 0.1236$/day leading to $\zeta = 3.676$ spores/leaf.day. Subplot (b) shows the backward bifurcation using parameter values in Table 3.1 except $d = 0.956$/day and $\eta = 0.3/20$ spores/leaf.day leading to $\zeta = 59.306$ spores/leaf.day.

in susceptible leaves.

3.5 Other types of bifurcation

Beside the forward and backward bifurcation diagrams presented in section 3.4. Figure 3.8 shows two different bifurcation diagrams. Subplot (a) presents a forward bifurcation, as in Figure 3.2, but where the endemic equilibrium disappears for large $\mathcal{R}_0$ values while the trivial equilibrium becomes stable. Subplot (b) presents a backward bifurcation, as in Figure 3.5, but where the endemic equilibrium persists for large $\mathcal{R}_0$ values.

3.6 Conclusion

In this paper, we proposed and analysed a mathematical model that describes the propagation of a fungal disease on a perennial plant. The originality of the model is the differentiation between young and mature leaves, to take into account the impact of host development on the aggressiveness of the pathogen. The model is applied to the particular case of coffee leaf rust in a coffee plantation. It is fairly generic and can be adapted to other fungal diseases for which the host age structure plays an important role.

We computed the disease-free and endemic equilibria and we studied their stability as a function of the basic reproduction number. We identified different bifurcation diagrams. They showed two behaviours for the model when the basic reproduction number is close to one. The first case is a forward bifurcation which corresponds to a stable disease free equilibrium when the basic reproduction number is less than one, and a stable endemic equilibrium when it is greater than one. The second case is a backward bifurcation in which, on top of the stable disease free equilibrium, there is a stable endemic equilibrium when the basic reproduction number is less than one. This means that, disease may persist even in these unfavourable conditions. Moreover, when the basic reproduction number is notably larger than one, be it in the forward or backward

bifurcation case, the endemic equilibrium may disappear and the trivial equilibrium then becomes stable, which corresponds to the destruction of the plantation.

All bifurcation cases allow to conclude that, when the basic reproduction number is greater that one, the disease can destroy the plantation and even when the basic reproduction number is less than one, the disease can persist. These results provide useful insights on the disease dynamics and its control. For instance, in order to eradicate a disease that spreads with basic reproduction number greater than one, it might not be sufficient to bring it below one, as an endemic state still persists. The basic reproduction number should be brought below the level of the saddle-node bifurcation to achieve effective disease control.

Chapter 4

Modelling coffee leaf rust dynamics to control its spread

In this chapter, we simplify the model in Chapter 3 by combining young and mature leaves into branches. Moreover, we distinguish between dry and rainy season and introduce spore dispersal. The model is obtained using the following hypotheses.

H_1: The model is based on a classical epidemiological model, in which the host population is subdivided by health status (healthy branches S, latent branches L, infectious branches I and leafless branches J), considering the crop branch as an individual. The model includes crop production (berries B) by branches during the rainy season. The infection being mediated by fungus spores (uredospore U) released in the plantation, their dynamics are also included.

H_2: The recruitment of healthy branches is constant.

H_3: The force of infection is density-dependent: it is proportional to the number of uredospores and inversely proportional to the total number of branches.

H_4: The model alternates dry and rainy seasons. The same model is used during both seasons, but with different parameter values: crop development and disease progression are reduced during the dry seasons.

H_5: Space is taken into account in this model. The branches are homogeneously distributed. The 1D dispersal of uredospores is considered.

H_6: The model uses a PDE formalism.

H_7: A parameter which reduces spore production is added to control the disease.

We then obtain a PDE model with six compartments. The objective of this second study is to understand the impact of spore diffusion and seasonality on the dynamics of CLR.

This work is published in *Mathematical Modelling of Natural Phenomena* [38]

Contents

Abstract: Coffee leaf rust (CLR) is one of the main diseases that affect coffee plantations worldwide. It is caused by the fungus *Hemileia vastatrix*. Damages induce severe yield losses (up to 70%). Its control mainly relies on cultural practices and fungicides, the latter having harmful ecological impact and important cost. Our goal is to understand the propagation of this fungus in order to propose a biocontrol solution, based on a mycoparasite that inhibits *H. vastatrix* reproduction. We develop and explore a spatio-temporal model that describes CLR propagation in a coffee plantation during the rainy and dry seasons. We show the existence of a solution and prove that there exists two threshold parameters, the dry and rainy basic reproduction numbers, that determine the stability of the equilibria for the dry and rainy season subsystems. To illustrate these theoretical results, numerical simulations are performed, using a non-standard finite method to integrate the pest model. We also numerically investigate the biocontrol impact. We determine its efficiency threshold in order to ensure CLR eradication.

Keywords: spatio-temporal model, coffee leaf rust, basic reproduction number, stability
MSC Classification: 35K57, 93D05, 65M06, 92D30

4.1 Introduction

Coffee is one of the most widely consumed beverages in the world; its trade satisfies the regular consumption of more than two billion people and exceeds 10$ billion worldwide [158]. Its cultivation is an important factor of social stability as it sustains the living of not less than twenty-five million small producers and their families worldwide by ICO [71]. The total production of all exporting countries in 2018 was more than 172 million 60-kilogram bags [71].

Coffee leaf rust (CLR) is a disease caused by a basidiomycete fungus, *Hemileia vastatrix*, that affects coffee trees. The fungus *H. vastatrix* is a compulsory parasite. In other words, it is a fungus that lives and develops only on coffee leaves. It attacks the lower leaves of the coffee tree and causes premature defoliation, which reduces the photosynthetic capacity and weakens the tree. Leaf fall causes abortion of a large part of the flowers and fruits, as well as desiccation of shoots. CLR is the most serious leaf disease of the coffee tree known to date [112]. It has direct and indirect economic impacts on coffee production. Direct impacts include decreased quantity and quality of yield. In some cases, more than 70% of the coffee production is lost [58]. Indirect impacts include increased costs to control the disease. Control methods include fungicide application [25], cultural practices [10] including stumping of diseased plants, the use of resistant cultivars [5], and biocontrol by fungal and bacterial parasites [166, 6]. These methods induce significant labour and material costs and, in the case of stumping, a year-long decline in production. To better control this fungus, it is necessary to understand the disease propagation and what conditions favour its development and dispersal.

The spread of crop diseases, in particular airborne pathogens such as fungi, has received a lot of attention from researchers. Among models that represent the pathogen spatial dispersal, one can cite the DDAL framework that focuses on the deployment of susceptible and resistant crop hosts in an agricultural landscape [120]. Fewer models represent the pathogen spread by a diffusion term in partial differential equations (PDE). For instance, Sapoukhina et al. also study susceptible and resistant crop mixtures for a fungal disease propagated by airborne spores in a field [140], while Burie et al. explore the dynamical behaviour of mildew in a vineyard [23]. These disease dynamics are relevant for CLR modelling: they include a latency period, a sporulation period, spore dispersal and germination.

CLR models in the literature represent different scales, from the individual coffee bush to the country or even the continent. Avelino et al. investigate the factors (coffee tree characteristics, crop management patterns, environment) that affect CLR intensity in several plots in Honduras [11]. Bebber et al. determine the germination and infection risk depending on the climate in Colombia and neighbouring countries [15]. In contrast to these static approaches, Vandermeer et al. study the interaction between the regional and local dynamics of CLR model by representing the evolution of the proportion of infected bushes and farms [169]. Vandermeer et al. also represent the CLR dynamics in a coffee farm in Chiapas using an SI epidemiological model of the host [165]. In these two latter studies, the fungus life cycle is not represented. Some other models investigate CLR control. Vandermeer et al. look at the interaction between *H. vastatrix* and a mycoparasite *Lecanicillium lecanii* [166], while Arroyo et al. consider interactions with antifungal bacteria [6]. However, no existing CLR model considers *H. vastatrix* dynamics together with its interaction with the coffee host. In particular none considered the impact of CLR on berry production, which is the variable of agronomic interest.

Our aim is to understand the CLR propagation in a field and to propose a biocontrol solution

based on the *Lecanicillium lecanii* mycoparasite, by a mathematical modelling approach. Biocontrol methods are still in development but could provide ecologically friendly alternatives to fungicides, which can induce pest resistance. Moreover, biocontrol can be coupled with cultural practices and does not require host replacement as for resistant plant deployment. To achieve our goal, an original CLR model is needed, based on existing crop-fungus interaction models with diffusion [23, 140] and including berry production. As coffee growth is climate-dependent and harvest is seasonal, we have to develop a hybrid spatio-temporal PDE model.

This paper is organized as follows. Section 4.2 is devoted to the biological background and the formulation of the spatio-temporal CLR propagation model with two seasons per year, the dry and rainy seasons. Section 4.3 presents the stability analysis of the subsystems during the two seasons. In Section 4.4, numerical simulations are performed to illustrate and validate theoretical results. We also present numerical results when mycoparasites are used to control CLR spread. Finally, we conclude the paper and propose several possible perspectives for future work.

4.2 Coffee leaf rust dynamics

4.2.1 Biological background

The coffee tree is a perennial plant, belonging to the Rubiaceae family, which has persistent leaves [16]. The productivity stage (flowers and fruits) begins after 3 years and lasts for 20 years on average. Flowers appear at the end of branches and require a lot of humidity for their development [28]. The annual productivity period lasts 7 to 11 months depending on coffee species and cultivars, as well as climate. In the case of Cameroon, with a single rainy period per year from April to November, there is a single harvest between November and December [151].

The life cycle of *H. vastatrix* in favourable humidity and temperature conditions lasts 5 weeks on average [172]. Uredospores are dispersed by rain and wind. They germinate and penetrate through stomates on the underside of the leaf. This infection process requires 24 to 48 hours [116]. The first symptom is a pale yellow lesion that appears 1 to 3 weeks after infection. Sporulation, i.e. the production of Uredospores and teliospores, occurs 2 weeks to several months after infection [172]. A single lesion produces 4 to 6 crops of spores, releasing 300,000 to 400,000 Uredospores over a period of 3 to 5 months [116].

As most rust fungi, *H. vastatrix* produces Uredospores for asexual reproduction and teliospores for sexual reproduction. Teliospores do not infect coffee leaves and have no known host [136], so it is not established that there is an effective sexual reproduction cycle.

During the dry season, *H. vastatrix* survives primarily as mycelium in the living tissues of the coffee leaves. As infected leaves drop prematurely during the dry months, a large amount of potential inoculum for the next rainy season disappears. However, a few green leaves always persist. Moreover, uredospores can survive about 6 weeks, so there is always some viable inoculum to infect the newly formed leaves at the start of the next rainy season [5].

4.2.2 Model formulation

Based on this biological knowledge, we propose a spatio-temporal coffee–CLR interaction model within a coffee plantation. We represent space and uredospore diffusion inside a bounded domain. At each point in space, we describe the evolution of the number of coffee branches, according to their epidemiological state, based on the CLR life cycle: healthy, latent with spores germinating

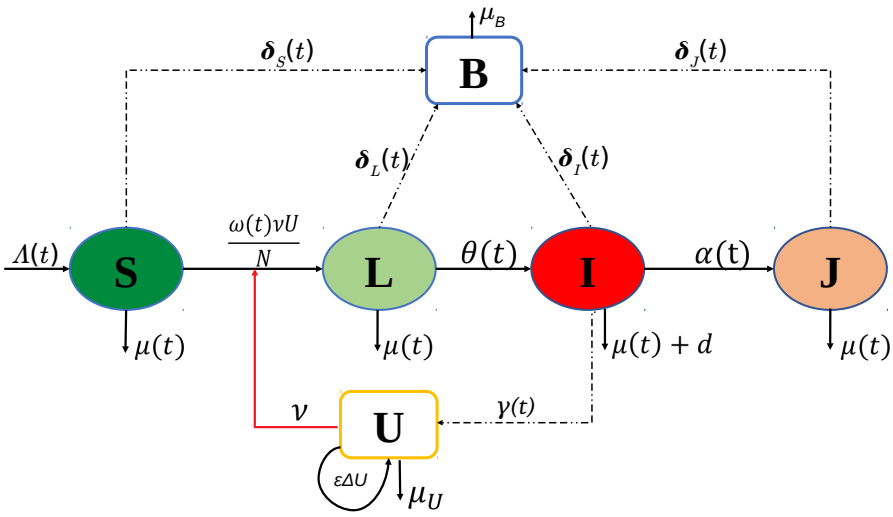

Figure 4.1: Diagram of the CLR propagation model in the coffee plantation corresponding to system (4.1). State variables are: healthy branches (S), latent branches (L), infectious branches (I), leafless branches (J), Uredospores (U) and berries (B). $\varepsilon\Delta U$ corresponds to uredospore diffusion.

or non sporulating lesions, infectious with sporulating lesions, and leafless at the end of the infection process. The infection of a branch corresponds to the infection of its leaves. We consider two periods: the rainy season during which berries are produced, and the dry season. This implies that most parameters are time-dependent, as they take two values according to the season.

We obtain the following model, that is illustrated in Figure 4.1:

$$\begin{cases} \partial_t S(t,x) &= \Lambda(t) - \frac{\omega(t)\nu U(t,x)}{N(t,x)} S(t,x) - \mu(t) S(t,x), \\ \partial_t L(t,x) &= \frac{\omega(t)\nu U(t,x)}{N(t,x)} S(t,x) - (\theta(t) + \mu(t)) L(t,x), \\ \partial_t I(t,x) &= \theta(t) L(t,x) - (\alpha(t) + \mu(t) + d) I(t,x), \\ \partial_t J(t,x) &= \alpha(t) I(t,x) - \mu(t) J(t,x), \\ \partial_t U(t,x) &= \varepsilon\Delta U(t,x) + \gamma(t) I(t,x) - (\nu + \mu_U) U(t,x), \\ \partial_t B(t,x) &= \delta_S(t) S(t,x) + \delta_L(t) L(t,x) + \delta_I(t) I(t,x) + \delta_J(t) J(t,x) - \mu_B B(t,x), \end{cases} \tag{4.1}$$

where $S(t,x)$, $L(t,x)$, $I(t,x)$, $J(t,x)$, $U(t,x)$ and $B(t,x)$ represent the densities of healthy branches, latent branches, infectious branches, leafless branches, Uredospores and berries respectively, at time t and location x defined in Ω, a simply connected bounded domain (of $\mathbb{R}$ or $\mathbb{R}^2$) with smooth boundary $\partial\Omega$. The densities are $/m$ or $/m^2$ depending on the choice of Ω. The total density of branches is $N(t,x) = S(t,x) + L(t,x) + I(t,x) + J(t,x)$.

The recruitment of healthy branches occurs at rate $\Lambda(t)$. Uredospores are deposited on leaves of all branches at rate ν and a fraction S/N lands on healthy branches. These spore covered healthy branches become latent branches with rate $\omega(t)$, which represents the germination ef-

ficacy, that is the number of healthy branches which become latent branches, per deposited spore. The latent branches become infectious at rate $\theta(t)$, where $1/\theta(t)$ corresponds to the latency period, and in turn become leafless branches at rate $\alpha(t)$, where $1/\alpha(t)$ corresponds to the sporulation period. All branches undergo natural mortality with baseline rate $\mu(t)$ and the infectious branches have an additional constant mortality rate d due to the disease. Uredospores are produced by infectious branches at rate $\gamma(t)$ and lose their ability to infect coffee branches at constant rate μ_U. Parameter ε is the uredospore diffusion coefficient. Berries are produced by all types of branches at different rates: $\delta_S(t) \geq \delta_L(t) \geq \delta_I(t) \geq \delta_J(t)$. They have a constant mortality rate μ_B. All parameters are assumed to be non negative.

Having two seasons, let us consider T the yearly period and τ the duration of the dry season. We set the initial time $t = 0$ at the beginning of a dry season. Then, for n years, we assume that time-dependent parameters $m(t)$, where $m(t) \in \{\Lambda(t), \omega(t), \theta(t), \alpha(t), \gamma(t), \mu(t)\}$, and $\delta_i(t)$, with $i \in \{S, L, I, J\}$, are constant during each season and can be written as follows:

$$m(t) = \begin{cases} m_D & \text{for} \quad t \in [nT, nT + \tau[, \\ m_R & \text{else,} \end{cases} \quad \text{and} \quad \delta_i(t) = \begin{cases} 0 & \text{for} \quad t \in [nT, nT + \tau[, \\ \bar{\delta}_i & \text{else,} \end{cases} \tag{4.2}$$

where D represents the dry season and R the rainy season.

Table 4.1 summarizes the biological meaning of parameter values for system (4.1).

Table 4.1: Description of parameters for system (4.1) – numerical values are used in section 4.4.

Symbol	Biological meaning	Value		Source
		Dry season (D)	Rainy season (R)	
Λ_p	Recruitment rate	6 day^{-1}	8 day^{-1}	Assumed
ω_p	Inoculum effectiveness	4.5%	5.5%	[131]
$\bar{\delta}_S$	Production rate of berries by S	0	0.7 day^{-1}	[71, 29]
$\bar{\delta}_L$	Production rate of berries by L	0	0.5 day^{-1}	[71, 29]
$\bar{\delta}_I$	Production rate of berries by I	0	0.3 day^{-1}	[71, 29]
$\bar{\delta}_J$	Production rate of berries by J	0	0.05 day^{-1}	[71, 29]
$1/\theta_p$	Latency period duration	30 days	21 days	[172]
μ_p	Mortality of mature branches	0.0134 day^{-1}	0.0034 day^{-1}	Assumed
$1/\alpha_p$	Sporulation period duration	150 days		[172]
γ_p	Production rate of Uredospores	$\in [0, 20]$ day^{-1}		[19]
μ_B	Mortality rate of berries	0.0021 day^{-1}		Assumed
d	Mortality rate due to the disease	0.056 day^{-1}		Assumed
ε	Diffusion coefficient	5000 m^2 day^{-1}		[23]
ν	Deposition rate	0.09 day^{-1}		[19]
μ_U	Mortality rate of Uredospores	0.015 day^{-1}		[92]

Initial conditions are $(\phi_S(x), \phi_L(x), \phi_I(x), \phi_J(x), \phi_U(x)) \in \left(L^2(\Omega)\right)^5$ where

$$\begin{cases} S(0,x) = \phi_S(x) > 0, \quad L(0,x) = \phi_L(x) \geq 0, \quad I(0,x) = \phi_I(x) \geq 0, \\ J(0,x) = \phi_J(x) \geq 0, \quad U(0,x) = \phi_U(x) \geq 0, \quad \forall x \in \Omega. \end{cases} \tag{4.3}$$

with $B(0,x) = 0 \; \forall x \in \Omega$. We assume that the harvest occurs instantaneously at the end of each rainy season. Thus $B(t,x)$ is brought back to 0 at $t = nT$, with other variables unchanged.

We suppose that the domain Ω is isolated, which implies that spores do not get in or out and that there is no interaction with the outside environment. To ensure this property, we assume

that there is a large enough buffer zone without coffee plants around the coffee plantation (hence around the domain Ω), so that no Uredospores are introduced from outside the plantation. Moreover, we neglect the spores that could potentially get out of the plantation. This absence of transfer is classically represented through the homogeneous Neumann boundary:

$$\frac{\partial U}{\partial \eta} = 0, \quad \text{on} \quad \partial\Omega \tag{4.4}$$

where η denotes the unit outward normal on $\partial\Omega$.

Remark 4.1. *When considered in one dimension, the space domain simply is an interval* $\Omega = [x_{\min}, x_{\max}]$*, whose boundary as considered in* (4.4) *is the pair of points* $\partial\Omega = \{x_{\min}, x_{\max}\}$*, and condition* (4.4) *becomes* $\frac{\partial U}{\partial x} = 0$ *in* $x = x_{\min}$ *and* $x = x_{\max}$*.*

4.3 Mathematical analysis

Herein, we present the basic properties of the subsystems of system (4.1), defined over each season. For any parameter m, we denote by m_p the seasonal constant value of the parameter m where $p = R$ for the rainy season and $p = D$ for the dry season. Replacing the value of every parameter $m(t)$ of system (4.1), with the corresponding constant value m_p with respect to the season, and removing the $\partial_t B$ equation since B is not present in the other equations of system (4.1), we obtain:

$$\begin{cases} \partial_t S = \Lambda_p - \dfrac{\omega_p \nu U}{N} S - \mu_p S, \\ \partial_t L = \dfrac{\omega_p \nu U}{N} S - (\theta_p + \mu_p) L, \\ \partial_t I \ = \theta_p L - (\alpha_p + \mu_p + d) I, \\ \partial_t J = \alpha_p I - \mu_p J, \\ \partial_t U - \varepsilon \Delta U = \gamma_p I - (\nu + \mu_U) U, \\ \dfrac{\partial U}{\partial \eta} = 0, \quad \text{on} \quad \partial\Omega, \\ S(0,x) = \phi_S, L(0,x) = \phi_L, I(0,x) = \phi_I, J(0,x) = \phi_J, U(0,x) = \phi_U, \forall x \in \Omega. \end{cases} \tag{4.5}$$

4.3.1 Basic properties

In this section, we will first establish positivity of the solutions if they exist in Lemma 4.1, their boundedness in Lemma 4.2, and finally their existence and uniqueness in Lemma 4.4. Through these, we obtain positivity, boundedness and global existence of solutions of subsystem (4.5) in Theorem 4.1.

In order to show positivity, we will be using the Lemma 2.2 defined in section 2.3.

Since the initial values are non-negative and the growth functions on the right-hand side of system (4.5) are assumed to be sufficiently smooth in $\mathbb{R}^5_+$, we have the following result over the positivity of a solution of subsystems (4.5), if it exists:

Lemma 4.1. *Any solution* $(S(t,x), L(t,x), I(t,x), J(t,x), U(t,x)) \in \left[C([0, \mathcal{T}_{max}) \times \bar{\Omega}) \cap C^{1,2}((0, \mathcal{T}_{max}) \times \Omega)\right]^5$ *of subsystems (4.5) is positive over* $[0, \mathcal{T}_{max})$*, the largest interval over which the solution of subsystems (4.5) exists.*

Proof of Lemma 4.1. For the positivity of S, L, I, J, let us define the supremum $t_1 = \sup\{t > 0,\ S(t,x) > 0,\ L(t,x) > 0,\ I(t,x) > 0,\ J(t,x) > 0,\ U(t,x) > 0\ \forall x \in \Omega\}$, and suppose $t_1 < \mathcal{T}_{max}$.

Using the definition of supremum, there does not exist $t \in [0, t_1)$ and $x \in \Omega$ such that any variable is equal to zero.

Among S, L, I, J, U, let us first consider S to be the variable such that there exists x with $S(t_1, x) = 0$, and let us define:

$$\lambda(t,x) = \exp\left(\int_0^t \frac{\omega_p \nu U(a,x)}{N(a,x)} da + \mu_p t\right).$$

One has:

$$\begin{aligned}\partial_t(\lambda(t,x)S(t,x)) &= \lambda(t,x)\left[\partial_t S(t,x) + \frac{\omega_p \nu U}{N} S(t,x) + \mu_p S(t,x)\right] \\ &= \Lambda_p \lambda(t,x) \\ &> 0\end{aligned}$$

where Λ_p is obtained from the expression of $\partial_t S(t,x)$ in subsystems (4.5). By integration of this expression over $[0, t_1]$, we obtain:

$$S(t_1,x)\lambda(t_1,x) - \phi_S(x)\lambda(0,x) > 0.$$

Since $\lambda(t_1,x) > 0$ and $\phi_S(x)\lambda(0,x) > 0$, we have $S(t_1,x) > 0$, which contradicts the hypothesis that $S(t_1,x) = 0$. Hence $S(t,x) > 0$ for all $(t,x) \in [0,t_1] \times \Omega$.

Also, the $\partial_t L$, $\partial_t I$ and $\partial_t J$ equations are linear scalar equations with forcing terms $\frac{\omega_p \nu U}{N} S$, $\theta_p L$ and $\alpha_p I$ that are positive over the interval $[0, t_1)$; hence $L(t_1,x)$, $I(t_1,x)$ and $J(t_1,x)$ are positive.

Hence, if $t_1 < \mathcal{T}_{max}$ as we supposed, we must have, for some x, $U(t_1,x) = 0$.

As $I(t,x) > 0$ over $[0,t_1]$, the last equation of subsystems (4.5) then gives rise to the following inequality system :

$$\begin{cases} \partial_t U - \varepsilon \Delta U \geq -(\nu + \mu_U)U, \quad (t,x) \in (0,t_1] \times \Omega \\ \frac{\partial U}{\partial \eta} \geq 0 \quad \text{on } \partial\Omega, \\ U(0,x) \geq 0, \quad \forall x \in \Omega. \end{cases} \tag{4.6}$$

Since $\nu + \mu_U$ is bounded in $[0,t_1] \times \Omega$, it follows from Lemma 2.2 that $U(t,x) > 0$ in $[0,t_1] \times \Omega$. This contradicts $U(t_1,x) = 0$, and hence the assumption $t_1 < \mathcal{T}_{max}$. Therefore all variables are positive for all times smaller than $\mathcal{T}_{max}$.

This achieves the proof. □

Lemma 4.2. *Let $(S,L,I,J,U) \in C^0\left(([0,\mathcal{T}_{\max}) \times \bar{\Omega}) \cap C^{1,2}([0,\mathcal{T}_{\max}) \times \Omega)\right)^5$ be the solution of subsystems (4.5) with bounded initial conditions. Then this solution is bounded, $\mathcal{T}_{\max} = +\infty$, $0 < N(t,x) = S + L + I + J \leq N_m$ and $0 < U(t,x) \leq U_m$, where:*

$$N_m = \max\left\{\frac{\Lambda_p}{\mu_p}, \|\phi\|_\infty\right\} \quad \text{and} \quad U_m = \max\left\{\max\{\Lambda_p/\mu_p, \|\phi\|_\infty\}\frac{\gamma_p}{(\nu + \mu_U)}, \|\phi_U\|_\infty\right\}.$$

Proof of Lemma 4.2. Let $\phi(x) = \phi_S(x) + \phi_L(x) + \phi_I(x) + \phi_J(x)$. The N-dynamics then satisfy:

$$\begin{cases} \partial_t N \leqslant \Lambda_p - \mu_p N, \quad (t,x) \in [0, \mathcal{T}_{\max}) \times \Omega \\ N(0,x) = \phi(x) \leqslant \|\phi\|_\infty = \max\limits_{x\in\Omega} \phi(x). \end{cases} \tag{4.7}$$

upon which we build the upper-bounding system

$$\begin{cases} \dfrac{dW_1}{dt} = \Lambda_p - \mu_p W_1, \\ W_1(0) = \|\phi\|_\infty. \end{cases} \tag{4.8}$$

The comparison principle then yields:

$$N(t,x) \leqslant W_1(t) = \frac{\Lambda_p}{\mu_p} + \left(\phi(x) - \frac{\Lambda_p}{\mu_p}\right) e^{-\mu_p t}$$

for all $(t,x) \in [0, \mathcal{T}_{\max}) \times \Omega$. Since $W_1(t) \leqslant \max\{\frac{\Lambda_p}{\mu_p}, \|\phi\|_\infty\}$ for $t \in [0,\infty)$, one has that $N(t,x)$ stays bounded and is hence defined for all times:

$$0 < N(t,x) \leqslant \max\left\{\frac{\Lambda_p}{\mu_p}, \|\phi\|_\infty\right\} = N_m, \quad \forall (t,x) \in [0,\infty) \times \Omega.$$

This upper-bound also holds for S, L, I and J which are integral parts of N.

From the upper-bound on I and the last equation of subsystems (4.5), we can deduce that:

$$\begin{cases} \partial_t U - \varepsilon \Delta U \leqslant \max\{\Lambda_p/\mu_p, \|\phi\|_\infty\}\gamma_p - (\nu + \mu_U)U, \quad (t,x) \in [0, \mathcal{T}_{max}) \times \Omega \\ U(0,x) = \phi_U(x) \leqslant \|\phi_U\|_\infty = \max\limits_{x\in\Omega} \phi_U(x), \\ \dfrac{\partial U}{\partial \eta} = 0, \quad x \in \partial\Omega, \end{cases} \tag{4.9}$$

and the upper-bounding system:

$$\begin{cases} \dfrac{dW_2}{dt} = \max\{\Lambda_p/\mu_p, \|\phi\|_\infty\}\gamma_p - (\nu + \mu_U)W_2, \\ W_2(0) = \|\phi_U\|_\infty. \end{cases} \tag{4.10}$$

It then follows that for all $(t,x) \in [0, \mathcal{T}_{\max}) \times \Omega$:

$$U(t,x) \leqslant W_2(t) = \max\{\Lambda_p/\mu_p, \|\phi\|_\infty\} \frac{\gamma_p}{(\nu + \mu_U)} + \left(\phi_U(x) - \max\{\Lambda_p/\mu_p, \|\phi\|_\infty\} \frac{\gamma_p}{(\nu + \mu_U)}\right) e^{-(\nu+\mu_U)t}.$$

Hence, as was done for N, we have:

$$U(t,x) \leqslant \max\left\{\max\{\Lambda_p/\mu_p, \|\phi\|_\infty\}\frac{\gamma_p}{(\nu + \mu_U)}, \|\phi_U\|_\infty\right\} = U_m, \quad \forall (t,x) \in [0,\infty) \times \Omega.$$

This completes the proof □

Now we prove existence and uniqueness of a local solution of subsystems (5). The idea is to write the system in the abstract form on a suitable Hilbert space and then to use the use the Hille-Yosida Theorem to conclude

We therefore introduce the linear space $\mathbf{H} = \left(\mathbf{L}^2(\Omega)\right)^5$ endowed with the usual inner product:

$$\|(y,z)\|_{\mathbf{H}} = \sum_{i=1}^{5}(y_i,z_i)_{\mathbf{L}^2(\Omega)}, \quad y=(y_1,y_2,y_3,y_4,y_5),\ z=(z_1,z_2,z_3,z_4,z_5);$$

$\mathbf{H}$ is a Hilbert space. Now define on $\mathbf{H}$ the linear operator A such that:

$$Ay = (\mu_p y_1, \mu_p y_2, \mu_p y_3, \mu_p y_4, -\varepsilon\Delta y_5), \tag{4.11}$$

with domain $D(A) = \left(\mathbf{L}^2(\Omega)\right)^4 \times \mathbf{H}^2_\eta(\Omega)$, where

$$\mathbf{H}^2_\eta(\Omega) := \{u \in \mathbf{H}^1(\Omega),\ \Delta u \in \mathbf{L}^2(\Omega),\ \frac{\partial U}{\partial \eta} = 0\}$$

Remark 4.2. *For $u \in \mathbf{H}^2_\eta(\Omega)$ the boundary condition $\frac{\partial U}{\partial \eta} = 0$ implies that*

$$\forall v \in \mathbf{H}^1(\Omega), \quad \int_\Omega -\Delta u\, v\, dx = \int_\Omega \nabla u \cdot \nabla v\, dx. \tag{4.12}$$

We will need the following result.

Lemma 4.3 ([121])**.** *Let ε be a positive real number. Let $f \in L^2(\Omega)$ and g the trace on $\partial\Omega$ of an element of $\mathbf{H}^1(\Omega)$. Assume that Ω is a bounded subset of $\mathbb{R}^N$, $N = 1, 2$ with smooth boundary and consider the following stationary boundary value problem:*

$$\begin{cases} u - \varepsilon\Delta\, u = f & a.e.\ on\ \Omega, \\ \frac{\partial u}{\partial \eta} = g & a.e.\ on\ \partial\Omega. \end{cases} \tag{4.13}$$

Then, the problem (4.13) has a unique solution $u \in H^1(\Omega)$. Moreover u belongs to $H^2(\Omega)$ and there exists a universal constant $M > 0$ that only depends on ε, N and Ω such that

$$\|u\|_{H^1(\Omega)} \leqslant M(\|f\|_{L^2(\Omega)} + \|g\|_{L^2(\partial\Omega)}).$$

We have the following result about the existence of solution of subsystems (4.5).

Lemma 4.4. *Assume that the initial conditions (4.3) holds, then there exists a unique local solution of problem (4.5) defined on $[0, \mathcal{T}_{\max}) \times \Omega$. More precisely:*

$$(S, L, I, J, U) \in C\left((0, \mathcal{T}_{\max}); D(A)\right) \cap C\left([0, \mathcal{T}_{\max}); \mathbf{H}\right) \cap C^1\left((0, \mathcal{T}_{\max}); \mathbf{H}\right);$$

Moreover,

$$(S, L, I, J, U) \in \left[C([0, \mathcal{T}_{max}) \times \bar{\Omega}) \cap C^{1,2}((0, \mathcal{T}_{max}) \times \Omega)\right]^5 \text{ if } (\phi_S, \phi_L, \phi_I, \phi_J, \phi_U) \in (C(\Omega))^4 \times L^2(\Omega)\ .$$

Proof of Lemma 4.4. System (4.5)-(4.3) can be written abstractly in the Hilbert space $\mathbf{H}$ in the following form:

$$\begin{cases} y'(t) = Ay(t) + F(y(t)), \quad t \geq 0, \\ y(0) = y_0 \in D(A), \end{cases} \tag{4.14}$$

where $y = (S, L, I, J, U)$, $y_0 = (\phi_S, \phi_L, \phi_I, \phi_J, \phi_U)$, Ay is defined as in Equation (4.11) and:

$$F(y) = \left(\Lambda_p - \frac{\omega_p \nu U}{N} S,\ \frac{\omega_p \nu U}{N} S - \theta_p L,\ \theta_p L - (\alpha_p + d) I,\ \alpha_p I,\ \gamma_p I - (\nu + \mu_U) U\right).$$

Note that, since Ω is bounded, for $y = (S, L, I, J, U) \in \mathbf{H}$, one has $F(y) \in \mathbf{H}$. Now let us show that the linear operator A is a maximal monotone operator on $\mathbf{H}$.

- $\forall\, v \in D(A)$, $(Av, v) = \sum_{i=1}^{4} \|v_i\|_{L^2}^2 - \varepsilon \int_\Omega \Delta u_5\, u_5 dx$. Since $u_5 \in H_\eta^2(\Omega)$, the identity (4.12) is satisfied with $v = u_5$ and one obtains that:

$$(Av, v) = \sum_{i=1}^{4} \|v_i\|_{L^2}^2 + \varepsilon \int_\Omega |\nabla u_5|^2 dx \ \geq 0,$$

  which implies that A is monotone.

- Now, let us show that $\forall v \in D(A), \exists u \in \mathbf{H},\ u + Au = v$. Let $v = (v_1, v_2, v_3, v_4, v_5) \in D(A)$. We are looking for $u = (u_1, u_2, u_3, u_4, u_5) \in D(A)$, such that $u + Au = v$. With this is mind, one has:

$$u + Au = v \iff (1 + \mu_p) u_i = v_i,\ i = 1, \ldots, 4 \quad \text{and} \quad \begin{cases} u_5 - \varepsilon \Delta\, u_5 = v_5 & \text{in} \quad \Omega, \\ u_5 \in H_\eta^2(\Omega). \end{cases}$$

  Therefore, for $i = 1, \ldots, 4$, $u_i = \frac{1}{1+\mu_P} v_i \in L^2(\Omega)$ and one obtains u_5 by solving the following elliptic problem:

$$\begin{cases} u_5 - \varepsilon \Delta\, u_5 = v_5 & \text{in} \quad \Omega, \\ \frac{\partial u_5}{\partial \nu} = 0 & \text{on} \quad \partial\Omega. \end{cases} \tag{4.15}$$

  According to Lemma 4.3, there exists a unique $u_5 \in H_\eta^2(\Omega)$ solution of (4.15) and A is maximal. By the Hille-Yosida theorem [121], we conclude that $-A$ is the infinitesimal generator of a C_0 semigroup of contractions on $\mathbf{H}$.

- We now show that F is Lipschitz continuous in both variables. Let $y = (S, L, I, J, U)$, $\tilde{y} = (\tilde{S}, \tilde{L}, \tilde{I}, \tilde{J}, \tilde{U}) \in \mathbf{H}$. Therefore, one has:

$$\begin{aligned} F(y) - F(\tilde{y}) = \Bigg(&\omega_p \nu \left(-\frac{U}{N} S + \frac{\tilde{U}}{\tilde{N}} \tilde{S}\right), \omega_p \nu \left(\frac{U}{N} S - \frac{\tilde{U}}{\tilde{N}} \tilde{S}\right) - \theta_p (L - \tilde{L}), \\ &\theta_p (L - \tilde{L}) - (\alpha_P + d)(I - \tilde{I}), \alpha_P (I - \tilde{I}), \gamma_p (I - \tilde{I}) - (\nu + \mu_U)(U - \tilde{U})\Bigg). \end{aligned}$$

  Since $\dot{N} = \Lambda_p - \mu_p N - dI \geq \Lambda_p - \mu_p N - dN$, we have $N(t, x) \geq \min(\frac{\Lambda_p}{\mu_p + d}, \tilde{\phi}(x))$. Moreover, according to Lemma 4.2, $\tilde{U}$ is bounded. This implies that $\frac{\tilde{U}}{N}$ is bounded. Similarly, $\frac{\tilde{U}}{\tilde{N}}$ is bounded. As $\frac{S}{N} \leq 1$, from the identity $\frac{U}{N} S - \frac{\tilde{U}}{\tilde{N}} \tilde{S} = \frac{U - \tilde{U}}{N} S - \frac{\tilde{U}}{\tilde{N}} (\tilde{S} - S) + \frac{\tilde{U} S}{N \tilde{N}} (\tilde{N} - N)$, we obtain:

$$\|F(y) - F(\tilde{y})\|_{\mathbf{H}} \leqslant K \|y - \tilde{y}\|_{\mathbf{H}},$$

  where K is a constant that depends on the constant $\omega_P, \nu, \theta_P, \alpha_P, d, \gamma_P$ and μ_U. Thus F is uniformly Lipschitz continuous on $\mathbf{H}$. Using the fact that the solution are positive, we can

now apply Theorem 1.6 page 189 of [121] and conclude that system (4.14) has a unique local strong solution on $[0, \mathcal{T}_{\max})$ in the sense that $(S, L, I, J, U) \in C\left((0, \mathcal{T}_{\max}); D(A)\right) \cap C\left([0, \mathcal{T}_{\max}); \mathbf{H}\right) \cap C^1\left((0, \mathcal{T}_{\max}); \mathbf{H}\right)$, we can also use the method present in [179] to conclude prove. This completes the proof.

□

Theorem 4.1. *Subsystems (4.5), with initial conditions in* $\mathbf{H}$ *that verify* $0 < \phi_S + \phi_L + \phi_I + \phi_J \leq N_m$, $0 \leq \phi_U \leq U_m$ *for all* $x \in \bar{\Omega}$, *admit a unique global solution in* $C\left((0,\infty); D(A)\right) \cap C\left([0,\infty); \mathbf{H}\right) \cap C^1\left((0,\infty); \mathbf{H}\right)$ *such that, for all* $(t, x) \in \mathbb{R}_+ \times \Omega$

$$S(t,x) > 0, \quad L(t,x) > 0, \quad I(t,x) > 0, \quad J(t,x) > 0, \quad 0 < N(t,x) \leqslant N_m, \quad 0 < U(t,x) \leqslant U_m$$

where $N_m = \max\left\{\frac{\Lambda_p}{\mu_p}, \|\phi\|_\infty\right\}$ *and* $U_m = \max\left\{\max\{\Lambda_p/\mu_p, \|\phi\|_\infty\}\frac{\gamma_p}{(\nu+\mu_U)}, \|\phi_U\|_\infty\right\}$

Proof of Theorem 4.1. Using Lemma 4.1, Lemma 4.2 and Lemma 4.4 we conclude the existence and uniqueness of bounded positive solution of subsystems (4.5) defined on $[0,\infty) \times \Omega$. we can conclude the proof of this theorem

□

4.3.2 Equilibria and their stability

Here, we compute the equilibria of subsystems (4.5) with $p = D$ or R and study their stability. Let

$$\mathcal{R}_0^{(p)} = \frac{\gamma_p}{(\nu+\mu_U)} \frac{\nu\omega_p}{(\theta_p+\mu_p)} \frac{\theta_p}{(\alpha_p+\mu_p+d)}$$

The expression $\mathcal{R}_0^{(p)}$ is derived in (4.38) in the proof of the local stability of the disease free equilibrium. It corresponds to the basic reproduction number in the dry ($p = D$) or rainy ($p = R$) season, since (i) $\frac{\gamma_p}{(\nu+\mu_U)}$ represents the mean number of new Uredospores generated by a single infectious branch and (ii) $\frac{\nu\omega_p}{(\theta_p+\mu_p)} \frac{\theta_p}{(\alpha_p+\mu_p+d)}$ measures the average number of new infectious branches generated by a single uredospore introduced in a completely susceptible field. We prove the following results for the stability of equilibria of subsystems (4.5).

Lemma 4.5.

1. *If* $\mathcal{R}_0^{(p)} < 1$ *the disease-free equilibrium (DFE)* $Q_p^0 = \left(\frac{\Lambda_p}{\mu_p}, 0, 0, 0, 0\right)$ *is locally asymptotically stable (LAS).*
2. *If* $\mathcal{R}_0^{(p)} > 1$ *and close to one, the DFE is unstable and there exists a unique positive endemic equilibrium* $Q_p^* = (S_p^*, L_p^*, I_p^*, J_p^*, U_p^*)$, *where*

$$\begin{aligned} I_p^* &= \frac{\Lambda_p(\nu+\mu_U)(\mathcal{R}_0^{(p)}-1)}{\gamma_p\omega_p\nu - d(\nu+\mu_U)}, \quad S_p^* = \frac{\Lambda_p - dI_p^*}{\mu_p\mathcal{R}_0^{(p)}}, \\ L_p^* &= \frac{(\alpha_p+\mu_p+d)}{\theta_p} I_p^*, \quad J_p^* = \frac{\alpha_p}{\mu_p} I_p^* \quad \text{and} \quad U_p^* = \frac{\gamma_p}{(\nu+\mu_U)} I_p^* \end{aligned} \tag{4.16}$$

which is locally asymptotically stable.

Proof of Lemma 4.5. The proof is given in Appendix (Section 4.6). □

Using Lyapunov theory and LaSalle's principle [88], we prove the global stability of the DFE, which implies that the CLR will dwindle until extinction, whatever the initial number of Uredospores and infectious branches.

Theorem 4.2. *If $\mathcal{R}_0^{(p)} < 1$, the DFE Q_p^0 of subsystems (4.5) is globally asymptotically stable (GAS).*

Proof of Theorem 4.2. Consider the function

$$V_1 = a_1 L + b_1 I + c_1 J + d_1 U. \tag{4.17}$$

where a_1, b_1, c_1 and d_1 are positive constants to be chosen later. Consider then the following Lyapunov function candidate:

$$W_1 = \int_\Omega V_1 dx = \int_\Omega (a_1 L + b_1 I + c_1 J + d_1 U) dx, \tag{4.18}$$

where Ω is the spatial domain defined above.

Let us consider the set $\mathcal{V} = C\left((0,\infty); \left(\mathbf{L}^2(\Omega)\right)^3 \times \mathbf{H}^2_\eta(\Omega)\right) \cap C\left([0,\infty); (\mathbf{L}^2(\Omega))^4\right) \cap C^1\left((0,\infty); (\mathbf{L}^2(\Omega))^4\right)$. For any solution $(L, I, J, U) \in \mathcal{V}$ of subsystems (4.5) with positive initial condition $(\phi_L(x), \ldots, \phi_U(x))$, $W_1(L, ..., U)$ is positive. Also, $W_1 = 0$ if and only if $(L, I, J, U) = (0, 0, 0, 0)$ on Ω.

The time derivative of the Lyapunov function W_1 along the trajectories of subsystems (4.5) satisfies:

$$\frac{dW_1}{dt} = \int_\Omega \dot{V}_1(L, I, J, U) dx. \tag{4.19}$$

From equation (4.17), one has that

$$\begin{aligned} \dot{V}_1 &= a_1 \frac{\partial L}{\partial t} + b_1 \frac{\partial I}{\partial t} + c_1 \frac{\partial J}{\partial t} + d_1 \frac{\partial U}{\partial t}, \\ &= a_1 \left(\frac{\omega_p \nu U}{N} S - (\theta_p + \mu_p) L\right) + b_1 (\theta_p L - (\alpha_p + \mu_p + d) I) + c_1 (\alpha_p I - \mu_M J) \\ &\quad + d_1 (\gamma_p I - (\nu + \mu_U) U) + d_1 \varepsilon \Delta U. \end{aligned} \tag{4.20}$$

Now, using the fact that $\frac{S}{N} \leqslant 1$, equation (4.20) becomes:

$$\dot{V}_1 \leqslant (-a_1(\theta_p+\mu_p)+b_1\theta_p)L+(-b_1(\alpha_p+\mu_p+d)+c_1\alpha_p+d_1\gamma_p)I+(-d(\nu+\mu_U)+a_1\omega_p\nu)U-c_1\mu_p J+d_1\varepsilon\Delta U. \tag{4.21}$$

Then, the positive constants a_1, b_1, c_1 and d_1 are chosen such that:

$$\begin{cases} -a_1(\theta_p + \mu_p) + b_1\theta_p = 0, \\ -b_1(\alpha_p + \mu_p + d) + c_1\alpha_p + d_1\gamma_p = 0, \\ -d_1(\nu + \mu_U) + a_1\omega_p\nu = 0. \end{cases} \tag{4.22}$$

Solving the above system (4.22) yields:

$$a_1 = \theta_p, \quad b_1 = \theta_p + \mu_p, \quad d_1 = \frac{\theta_p \omega_p \nu}{\nu + \mu_U} \quad \text{and} \quad c_1 = \frac{(\theta_p + \mu_p)(\alpha_p + \mu_p + d)}{\alpha_p}(1 - \mathcal{R}_0^{(p)}).$$

Note that $\mathcal{R}_0^{(p)} < 1$ ensures that $c_1 > 0$. Replacing the above expressions of a_1, b_1, c_1 and d_1

into equation (4.21), yields:

$$\dot{V}_1 \leqslant -c_1\mu_p J + d_1\varepsilon\Delta U. \tag{4.23}$$

Then equation (4.19) becomes:

$$\frac{dW_1}{dt} \leqslant -\int_\Omega c_1\mu_p J dx + d_1\varepsilon\int_\Omega \Delta U dx.$$

From the Neumann bounded condition $\frac{\partial U}{\partial \eta} = 0$, one has that:

$$\int_\Omega \Delta U dx = \int_{\partial\Omega} \frac{\partial U}{\partial \eta} = 0. \tag{4.24}$$

Thus, if $\mathcal{R}_0^{(p)} < 1$ one has:

$$\frac{dW_1}{dt} \leqslant -\int_\Omega c_1\mu_p J dx. \tag{4.25}$$

Thus, $\mathcal{R}_0^{(p)} < 1$ ensures that $\frac{dW_1}{dt} \leqslant 0$ for all $L, I, J, U \geq 0$.

The domain $\Gamma_\rho = \{(L, I, J, U) \in \mathcal{V} : W_1(L, I, J, U) \leq \rho\}$, $\rho > 0$, is compact and includes the origin. Moreover, it is positively $\mathcal{V}-$invariant with respect the last four equations of subsystems (4.5). In fact, if the initial condition $(\phi_L, \phi_I, \phi_J, \phi_U) \in \Gamma_\rho$, we have

$$\frac{dW_1(L, I, J, U)}{dt} \leq 0 \Rightarrow W_1(L, I, J, U) \leq W_1(\phi_L, \phi_I, \phi_J, \phi_U) \leq \rho$$

Also, $\frac{dW_1}{dt} = 0$ if and only if $J = 0$, which from subsystems (4.5) is satisfied over a time interval of non-zero length only if $L = 0$, $I = 0$ and $U = 0$. Then it is easy to see that the largest invariant set defined over $\mathcal{E} = \{(L, I, J, U) \in \mathcal{V} : \frac{dW_1(L,I,J,U)}{dt} = 0\}$ is the singleton $\{(0, 0, 0, 0)\}$. Therefore, using LaSalle-Krasowski invariant principle [[54], Theorem 2] and the LAS in Lemma 4.5, one can conclude that $(L, I, J, U) = (0, 0, 0, 0)$ is GAS when $\mathcal{R}_0^{(p)} < 1$. Similar proofs adapting Lasalle's principle for PDE can be found in [152, 174].

Replacing of the value $U = 0$ into the first equation of subsystems (4.5) yields:

$$\dot{S} = \Lambda_p - \mu_p S. \tag{4.26}$$

The above equation (4.26) has a unique equilibrium $S_p^0 = \frac{\Lambda_p}{\mu_p}$, which is GAS. Hence, since the solutions of subsystems (4.5) are bounded, $S(x, t) \to S_p^0$. Thus, one can conclude that the DFE $Q_p^0 = (S_p^0, 0, 0, 0, 0)$ is globally asymptotically stable for subsystems (4.5). This concludes the proof. □

4.3.3 Comparison of the dynamics in the dry and rainy seasons

The objective of this section is to compare the dynamics of subsystems (4.5) during the rainy and dry seasons. To this end, we first compare the basic reproduction numbers $\mathcal{R}_0^{(D)}$ and $\mathcal{R}_0^{(R)}$, and the number of infectious branches at the endemic equilibrium I_R^* and I_D^*. The former will indicate if and when CLR can persist within the coffee plantation, and the latter the intensity of the infection.

Simple biological hypotheses give the relation between the parameter values during the dry and rainy seasons. They mainly rely on the fact that some mechanims require humid conditions:

coffee tree growth is faster during the rainy season ($\Lambda_D \leqslant \Lambda_R$), germination occurs mostly during the rainy season ($\omega_D \leqslant \omega_R$), the lesion progresses faster during the rainy season ($\theta_D \leqslant \theta_R$) and the mortality rate of the branches is higher during the dry season (as a consequence of harvest, which always damages some branches) i.e ($\mu_R \leqslant \mu_D$). Hence, we have:

$$\Lambda_D \leqslant \Lambda_R, \quad \omega_D \leqslant \omega_R, \quad \theta_D \leqslant \theta_R, \quad \mu_R \leqslant \mu_D, \quad \gamma_D = \gamma_R \quad and \quad \alpha_D = \alpha_R. \tag{4.27}$$

4.3.3.1 Comparison of the basic reproduction numbers

Herein we compare the basic reproduction numbers of the subsystems:

$$\mathcal{R}_0^{(R)} = \frac{\gamma_R}{(\nu+\mu_U)} \frac{\nu\theta_R\omega_R}{(\theta_R+\mu_R)(\alpha_R+\mu_R+d)} \quad \text{and} \quad \mathcal{R}_0^{(D)} = \frac{\gamma_D}{(\nu+\mu_U)} \frac{\nu\theta_D\omega_D}{(\theta_D+\mu_D)(\alpha_D+\mu_D+d)}.$$

Using (4.27), one has:

$$\mathcal{R}_0^{(D)} \leqslant \mathcal{R}_0^{(R)}. \tag{4.28}$$

This means that the GAS of the DFE Q_R^0 during the rainy season implies the GAS of the DFE Q_D^0 during the dry season and the existence and local asymptotic stability of the endemic equilibrium Q_D^* during the dry season implies the existence and local asymptotic stability of the endemic equilibrium Q_R^* during the rainy season. Biologically speaking, if the disease is present during the dry season, it will be also present during the rainy season while, if the disease is absent during the rainy season, it will be also absent during the dry season.

4.3.3.2 Comparison of the infectious branches at the endemic level

To compare the disease at the endemic level, both basic reproduction numbers need to be greater than one, $1 < \mathcal{R}_0^{(p)}$ for $p = D$ and R. The expression of I_p^* depends on the parameters identified in (4.27). The partial derivatives of I_p^* with respect to parameters Λ_p, ω_p, θ_p and μ_p are:

$$\frac{\partial I_p^*}{\partial \Lambda_p} = \frac{(\nu+\mu_U)(\mathcal{R}_0^{(p)}-1)}{\gamma_p\omega_p\nu - d(\nu+\mu_U)} > 0, \quad \frac{\partial I_p^*}{\partial \omega_p} = \frac{\gamma_p\nu(\theta_p(\alpha_p+\mu_p)+\mu_p(\alpha_p+\mu_p+d))}{[\gamma_p\omega_p\nu - d(\nu+\mu_U)](\theta_p+\mu_P)(\alpha_p+\mu_p+d)} > 0,$$
$$\frac{\partial I_p^*}{\partial \theta_p} = \frac{\gamma_p\nu\omega_p\mu_p}{(\omega_p+\mu_p)} > 0, \quad \frac{\partial I_p^*}{\partial \mu_p} = -\frac{\gamma_p\nu\omega_p\theta_p(\theta_p+2\mu_p+\alpha_p d)}{[\gamma_p\omega_p\nu - d(\nu+\mu_U)](\theta_p+\mu_P)(\alpha_p+\mu_p+d)} < 0.$$

This shows that I_p^* is an increasing function if Λ_p, ω_p, θ_p and a decreasing function of μ_p. Now, using (4.27), we can deduce that:

$$I_R^* > I_D^*. \tag{4.29}$$

Therefore, if it reached equilibrium, the CLR would be more severe during the rainy season than during the dry season.

4.4 Numerical simulations

Herein, we present the results of numerical simulations of system (4.1) using a non standard finite difference method [108] presented in Appendix (Section 4.7). We take $T = 365$ days and $\tau = 120$ days which correspond to the durations of the year and the dry season in Cameroon, respectively. We set $\Omega = [0, 100]$ meters. We consider that initially all branches are healthy, that

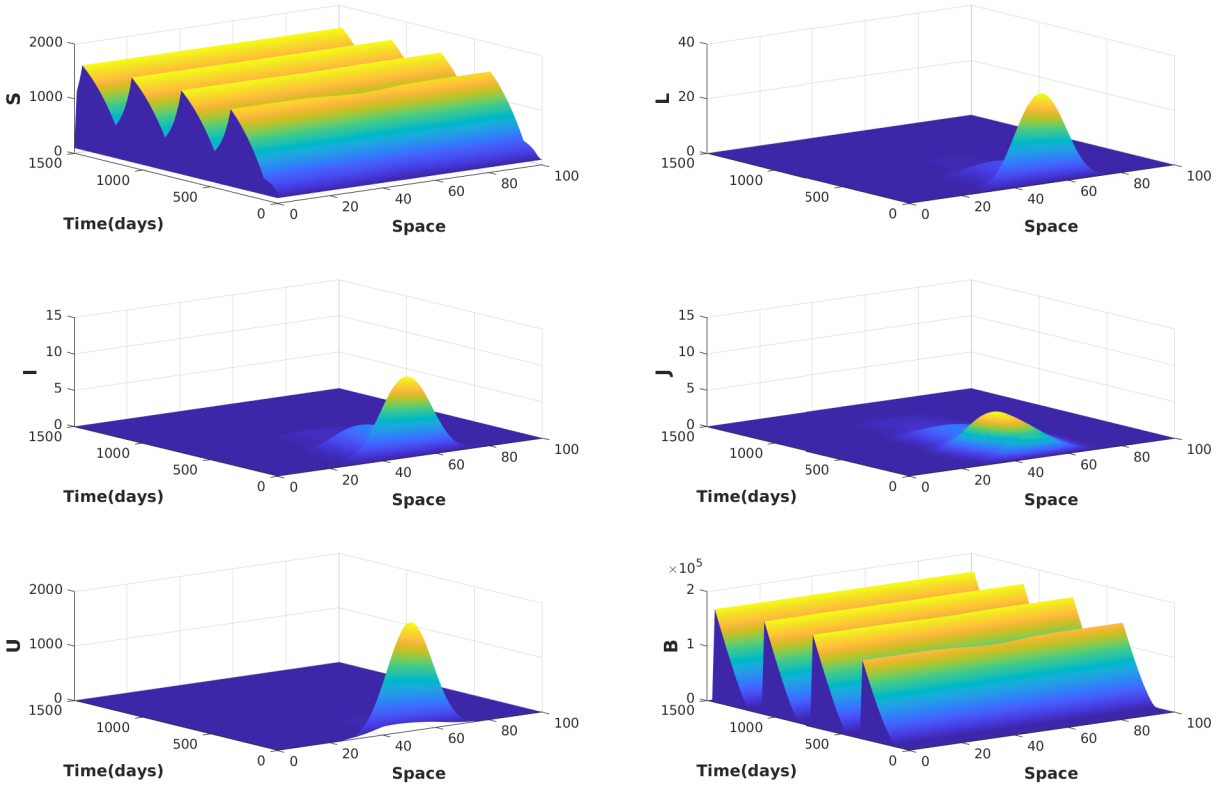

Figure 4.2: Spatio-temporal simulation of system (4.1,4.4,4.30) when $\gamma_D = \gamma_R = 1.5$, which leads to $\mathcal{R}_0^{(D)} = 0.52$ and $\mathcal{R}_0^{(R)} = 0.95$. All other parameter values are given in Table 4.1. Subplots represent healthy branches S, latent branches L, infectious branches I, leafless branches J, Uredospores U and berries B.

Uredospores are concentrated in the middle of the plantation and that there are no berries, so the initial conditions are, $\forall x \in \Omega$:

$$\begin{cases} S_0(x) = 100, \quad L_0(x) = I_0(x) = J_0(x) = 0, \\ U_0(x) = 2000 \sin^{14}(\frac{\pi x}{100}) \\ B_0(x) = 0. \end{cases} \tag{4.30}$$

Table 4.1 summarizes the parameter values for system (4.1) used for numerical simulations. We suppose that γ_p and α_p have the same value during the dry and rainy seasons.

4.4.1 CLR dynamics

We first choose $\gamma_p = 1.5$ for $p = D$ and R, so that $\mathcal{R}_0^{(D)} = 0.52$ and $\mathcal{R}_0^{(R)} = 0.95$. Figure 4.2 presents the spatio-temporal evolution of system (4.1) with these parameters in domain Ω during time interval $[0, 1500]$ days. Uredospores are initially present in the middle of the Ω interval, which induces local CLR infection during the first year. Subsequently, the infection dies out, as L, I, J and U go to 0. The S and B variables regain their healthy levels, corresponding to the stationary periodic disease-free solution. This illustrates Theorem 4.2: since $\mathcal{R}_0^{(D)}$ and $\mathcal{R}_0^{(R)}$ are smaller than one, the disease should vanish during both the dry and rainy seasons; we see here that connecting both seasons preserves this property.

Then we choose $\gamma_p = 8$ for $p = D$ and R, so that $\mathcal{R}_0^{(R)} = 5.09$ and $\mathcal{R}_0^{(D)} = 2.77$. In this

case, we have shown in Lemma 4.5 that the endemic equilibria exist and is locally asymptotically stable during both seasons. Numerical results are shown in Figure 4.3. One can observe that the peaks of the infectious branches and Uredospores flatten very quickly compared to the other variables. The convergence towards the endemic stationary solution is clear at the beginning of the third year (after 1000 days approximately). Oscillations are observed, as the endemic equilibrium is higher during the rainy season (subsystem (4.5) with $p = R$) than the dry season (subsystem (4.5) with $p = D$). Note that Uredospores hardly reach the edges of the plantation during the first year, so that healthy branches are produced in large quantity, contrary to the middle of the plantation where Uredospores directly infect branches, which limits growth. Hence, when the Uredospores reach the edges during the second year, there is a large infection peak at the edges, which contrasts with the middle of the plantation.

Figure 4.4 is a temporal representation of Figure 4.3 for three different values of x taken in the centre of the domain ($x = 50$m, yellow curve), on the border ($x = 1$m, blue curve) and in-between ($x = 25$m, red curve). Convergence towards the stationary endemic solution can also be observed here, as all curves overlap for the three x values at the end of the third year and on. At the centre of the domain, the system very rapidly converges towards this stationary solution, but it takes a year for $x = 25$m. On the border of the domain, branches remain susceptible during almost two years. Then the number of latent L and infectious I branches peak, as Uredospores U, initially in the centre of the domain, reach its borders. These peaks occur during the second rainy season. However, no such peak is observed for leafless branches J. Indeed, the number of leafless branches starts to increase at the end of the second rainy season (around time $t = 600$ days), but the arrival of the dry season reduces the number of branches before it can peak very high. Solutions then oscillate between the endemic equilibria of the dry and rainy seasons (purple and green dashed lines, respectively). Infection has a negative impact on the production, which is reduced to less than a third of its value without disease.

These simulations allow to conclude that the dynamics of system (4.1), can be inferred from the dynamics of subsystems (4.5) during the dry and rainy seasons.

4.4.2 Control of CLR

Integrated pest management currently used for the control of CLR [3] relies on the following methods:

- cultural practices, including stumping of diseased plants, shading, spore traps [5];
- chemical control by copper, triazole or dithiocarbamate fungicides [25];
- genetic control based on wild rust-resistant *Coffea* species [5];
- biological control based on *Hemileia vastatrix* natural enemies, e.g. mycoparasites such as *Lecanicillium lecanii* [26, 168], or antagonistic bacteria such as *Pseudomonas putida* P286 and *Bacillus thuringiensis B157* [61, 62]; it can also rely on natural allies of the crop such as benefic endophytes [147, 146].

Biological control is a potentially powerful tool for managing coffee leaf rust that allows organic certification. Therefore, we introduced in this study a mycoparasite (a parasitic fungus whose host is another fungus), *Lecanicillium lecanii*, known to hamper the reproduction of *H. vastatrix*. In our model, this biocontrol agent reduces the production of Uredospores by infectious

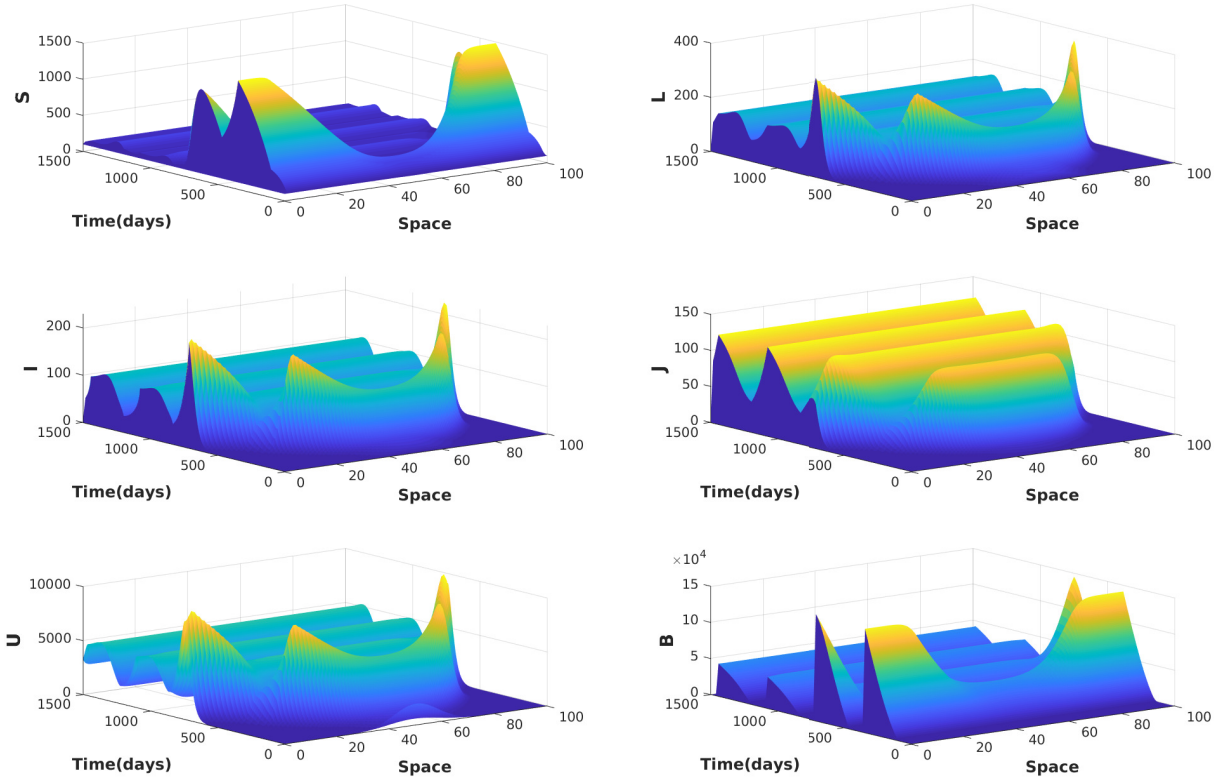

Figure 4.3: Spatio-temporal simulation of system (4.1,4.4,4.30) when $\gamma_D = \gamma_R = 8$, which leads to $\mathcal{R}_0^{(R)} = 5.09$ and $\mathcal{R}_0^{(D)} = 2.77$. All other parameter values are given in Table 4.1. Subplots represent healthy branches S, latent branches L, infectious branches I, leafless branches J, Uredospores U and berries B.

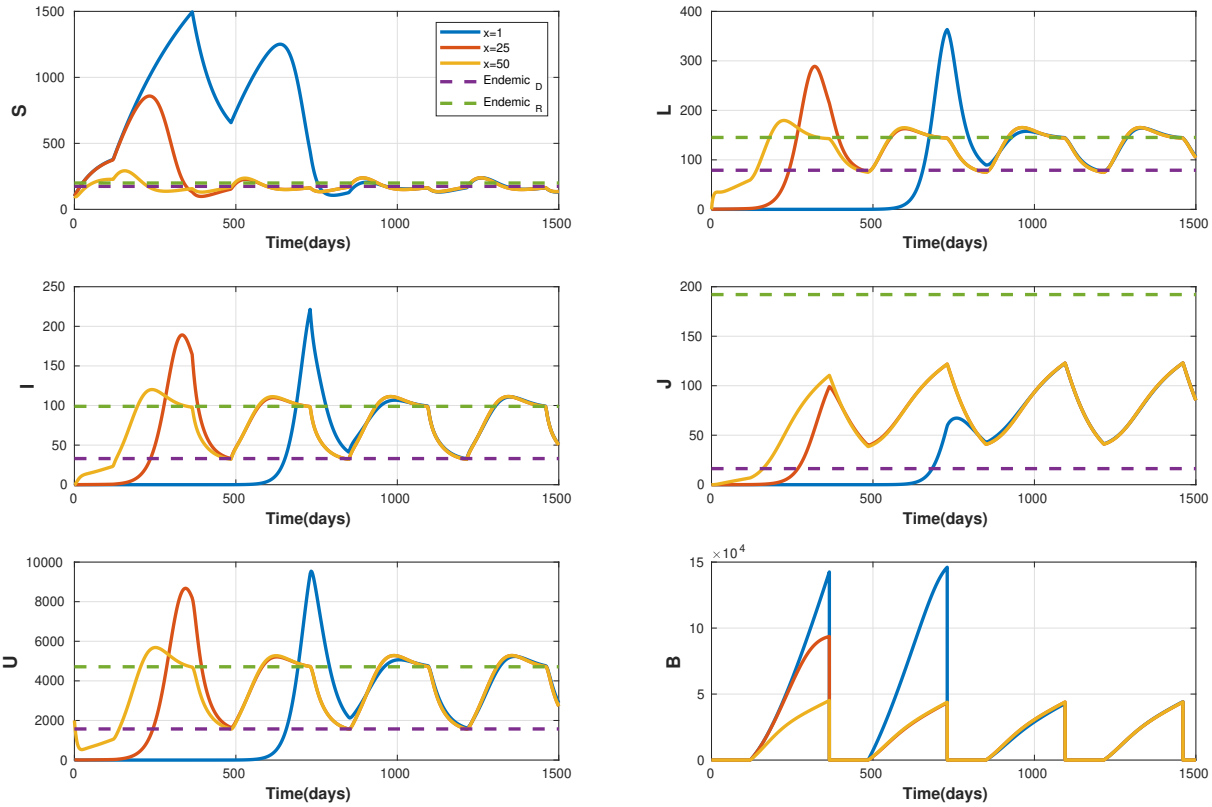

Figure 4.4: Temporal simulation, for three values of x, of system (4.1,4.4,4.30) when $\gamma_D = \gamma_R = 8$, which leads to $\mathcal{R}_0^{(R)} = 5.09$ and $\mathcal{R}_0^{(D)} = 2.77$ (as in Figure 4.3). All other parameter values are given in Table 4.1. x is chosen in the centre of the domain (yellow curve), on the border (blue curve) and in-between (red curve). Subplots represent healthy branches S, latent branches L, infectious branches I, leafless branches J, Uredospores U and berries B.

branches with an efficiency q. The production rate of Uredospores γ_p hence becomes $(1-q)\gamma_p$ and system (4.5) becomes:

$$\begin{cases} \partial_t S = \Lambda_p - \frac{\omega_p \nu U}{N} S - \mu_p S, \\ \partial_t L = \frac{\omega_p \nu U}{N} S - (\theta_p + \mu_p) L, \\ \partial_t I \ = \theta_p L - (\alpha_p + \mu_p + d) I, \\ \partial_t J = \alpha_p I - \mu_p J, \\ \partial_t U = \varepsilon \Delta U + (1-q)\gamma_p I - (\nu + \mu_U) U. \end{cases} \tag{4.31}$$

The basic reproduction numbers of system (4.31), for $p = D$ and R, are then:

$$\mathcal{R}_0^{(p)} = \frac{(1-q)\gamma_p \nu}{(\nu + \mu_U)} \frac{\theta_p \omega_p}{(\theta_p + \mu_P)(\alpha_p + \mu_p + d)}. \tag{4.32}$$

The higher the biocontrol efficiency q, the lower the reproduction numbers. So high enough values of q should allow to control the disease.

We simulated system (4.31) for different values of biocontrol efficiency q over 8 years. Figure 4.5 presents the temporal evolution of the state variables (S, L, I, J, U, B) integrated over domain Ω. Table 4.2 provides the reproduction numbers defined in equation (4.32), as well as the berry production and production loss during the 8th year, the latter being computed by reference to the disease-free case $q = 1$.

- $q = 0$ corresponds to no control (red curves) and $\mathcal{R}_0^{(R)} > \mathcal{R}_0^{(D)} > 1$, as in previous Section 4.4.1. The yield loss is as high as 80.1%.

- For a 50% efficiency (cyan curves), which still corresponds to $\mathcal{R}_0^{(R)} > \mathcal{R}_0^{(D)} > 1$, the number of spores U drops as expected, as the mycoparasite hampers the production of spores. So the number of healthy branches S increases. However, the number of latent L, infectious I and leafless J branches, barely change. Indeed, the production of latent branches depends on the product SU. The production of berries B then increases, as it is mostly driven by the healthy branches, but the yield loss is still high at 68.2%.

- For a 70% efficiency (magenta curves), corresponding to $\mathcal{R}_0^{(R)} > 1 > \mathcal{R}_0^{(D)}$, these observations are amplified: spores seriously drop; healthy branches and berries largely increase; latent, infectious and leafless branches decrease. The yield loss is 33.5%.

- For a 75% efficiency (black curves), also corresponding to $\mathcal{R}_0^{(R)} > 1 > \mathcal{R}_0^{(D)}$, infection remains very low, leading to an acceptable 6.0% yield loss.

- An 76% efficiency (blue curves), still corresponding to $\mathcal{R}_0^{(R)} > 1 > \mathcal{R}_0^{(D)}$, almost yields the same results as a perfect efficiency ($q = 1$). Infection is almost negligible, so the yield loss is as low as 1.8%.

- $q = 1$ (green curves) corresponds to a perfect (and unrealistic) efficiency, with $\mathcal{R}_0^{(R)} = \mathcal{R}_0^{(D)} = 0$, leading to the disease extinction and no yield loss.

Hence a 75% biocontrol efficiency is enough to sustain the berry production in the plantation, with a negligible yield loss. Higher efficiencies, moreover, achieve disease eradication.

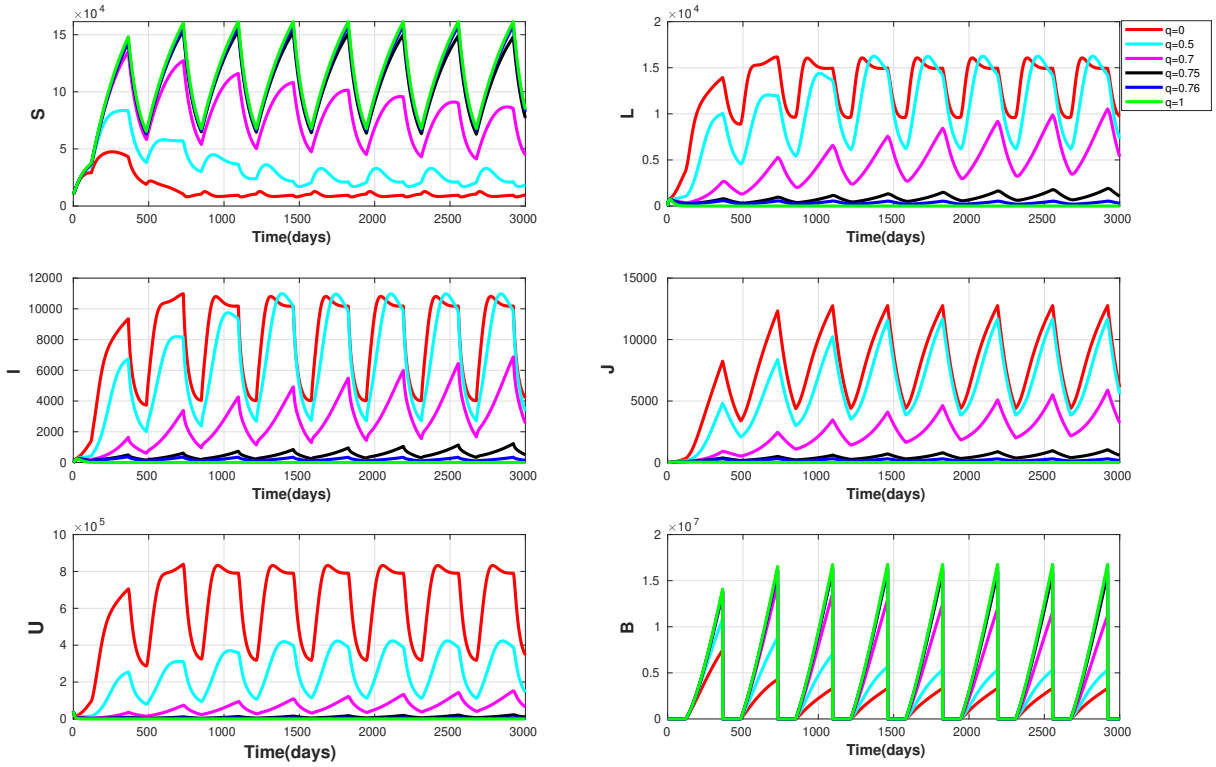

Figure 4.5: Temporal simulations, for various efficiencies q of the biocontrol mycoparasite, of controlled system (4.31,4.4,4.30) when $\gamma_D = \gamma_R = 8$. All other parameter values are given in Table 4.1. Subplots represent healthy branches S, latent branches L, infectious branches I, leafless branches J, Uredospores U and berries B, these variables being integrated over domain Ω.

Table 4.2: Impact of biocontrol efficiency q on reproduction numbers, defined in (4.32), and on berry production during the 8th and last year.

Biocontrol efficiency	$q = 0$	$q = 0.5$	$q = 0.7$	$q = 0.75$	$q = 0.76$	$q = 1$
$\mathcal{R}_0^{(D)}$	2.77	1.38	0.83	0.69	0.66	0
$\mathcal{R}_0^{(R)}$	5.09	2.54	1.52	1.27	1.22	0
Number of berries $\times 10^5$	33.2	53.1	111	157	164	167
Yield loss (%)	80.1	68.2	33.5	6.0	1.8	0

4.5 Conclusion

In this paper, we have proposed and analysed a PDE model that describes the dispersal of CLR in a coffee plantation during the rainy and dry seasons and its behaviour over time. Furthermore, we computed the disease-free and endemic equilibria of the two subsystems defined during the rainy and dry seasons. We showed that the basic reproduction numbers during the two seasons can determine the dynamics of global model: when the basic reproduction number is less than one during the rainy season, then CLR globally decreases till extinction; when it is greater than one for the dry season, then CLR persists.

We implemented a biocontrol in our model, corresponding to a mycoparasite such as *Lecanicillium lecanii*, which hampers CLR reproduction at all times. This solution was tested in Mexico [26] but is still under development. A rather high biocontrol efficiency (75% at least) is necessary in our model to control the disease, but lower efficiencies still improve coffee production notably. Moreover, the mycoparasite is applied all year round, so it is not easily implemented in practice and it involves important costs. It would be interesting to study when to deploy the mycoparasite in a cost-efficient way. An ideal mycoparasite should sustain the dry season and efficiently control CLR, so that the coffee plantation during the rainy season would suffer reasonable yield losses. In further work, we will also include cultural management and other biocontrol agents, in particular natural endophytes which are affordable for growers starting a new plantation.

Several extensions to this work are considered: (i) adding a stage structure on the coffee branches; (ii) simplifying the model, using an impulsive formalism for the dry season as in [96, 182], in order to obtain analytical results on the global model behaviour; (iii) solving an optimal control problem, consisting in maximising coffee production while minimising the control costs.

4.6 Appendix: Mathematical analysis

Proof of Lemma 4.5

1. *Local stability of the disease-free equilibrium*
   Let (S, L, I, J, U) be a solution of subsystems (4.5). Then, according to Kiehöfer [81], this solution can be written in the following form:

$$(S, L, I, R, U) = Q_p^0 + (W_1, W_2, W_3, W_4, W_5), \quad x \in \Omega, \quad t > 0. \tag{4.33}$$

   With this in mind, subsystems (4.5) can be written in the following compact form:

$$\frac{\partial W}{\partial t} = \mathcal{D}\Delta W + F(W), \tag{4.34}$$

   where $\mathcal{D} = \text{diag}(0, 0, 0, 0, 0, \varepsilon)$. The linearisation of subsystems (4.34) in the neighbourhood of Q_p^0 is:

$$\frac{\partial W}{\partial t} = \mathcal{D}\Delta W + L(Q_p^0)W, \tag{4.35}$$

   where $L(Q_p^0)$ is the Jacobian matrix at the DFE Q_p^0 of subsystems (4.5) in the absence of

diffusion, that is:

$$L(Q_p^0) = \begin{pmatrix} -\mu_p & 0 & 0 & 0 & -\omega_p\nu \\ 0 & -(\theta_p+\mu_p) & 0 & 0 & \omega_p\nu \\ 0 & \theta_p & -(\alpha_p+\mu_p+d) & 0 & 0 \\ 0 & 0 & \alpha_p & -\mu_p & 0 \\ 0 & 0 & \gamma_p & 0 & -(\nu+\mu_U) \end{pmatrix}.$$

Let g_j, $j \in \mathbb{N}$, be the j^{th} eigenfunction of operator $-\Delta$ with Neumann boundary conditions, so that:

$$\begin{cases} -\Delta g_j = \lambda_j g_j & \text{in } \Omega, \\ \dfrac{\partial g_j}{\partial \eta} \mid_{\partial\Omega} = 0 & \text{on } \partial\Omega, \end{cases} \tag{4.36}$$

where λ_j are the associated eigenvalues verifying $0 = \lambda_0 < \lambda_1 < \lambda_2 < \dots$

According to [81], the expanded expression of W in equation (4.35) can be written as:

$$W = \sum_{j=0}^{\infty} Y_j(t) g_j(x),$$

where each $Y_j(t) \in \mathbb{R}^5$. Substituting this expression into equation (4.35) yields:

$$\frac{dY_j}{dt} = (L(Q_p^0) - \lambda_j \mathcal{D}) Y_j. \tag{4.37}$$

Thus, the DFE Q_p^0 is stable if and only if each $Y_j(t) \to 0$ when $t \to \infty$, that is, if and only if all the eigenvalues of matrix $H_j = L(Q_p^0) - \lambda_j \mathcal{D}$ have negative real parts. Matrix H_j can be written in the following form:

$$H_j = \begin{pmatrix} -\mu_p & 0 & 0 & 0 & -\omega_p\nu \\ 0 & -(\theta_p+\mu_p) & 0 & 0 & \omega_p\nu \\ 0 & \theta_p & -(\alpha_p+\mu_p+d) & 0 & 0 \\ 0 & 0 & \alpha_p & -\mu_p & 0 \\ 0 & 0 & \gamma_p & 0 & -(\nu+\mu_U+\varepsilon\lambda_j) \end{pmatrix}.$$

The characteristic polynomial of matrix H_j is given by

$$P_1(X) = (X+\mu_p)^2 (X^3 + a_2 X^2 + a_1 X + a_0)$$

where

$$\begin{cases} a_2 = \theta_p + 2\mu_p + \alpha_p + d + \nu + \mu_U + \varepsilon\lambda_j \\ a_1 = (\theta_p+\mu_p)(\alpha_p+\mu_p+d+\nu+\mu_U+\varepsilon\lambda_j) + (\alpha_p+\mu_p+d)(\nu+\mu_U+\varepsilon\lambda_j) \\ a_0 = (\theta_p+\mu_p)(\alpha_p+\mu_p+d)(\nu+\mu_U+\varepsilon\lambda_j) - \gamma_p\theta_p\omega_p\nu \end{cases}$$

Firstly one can observe that $a_2 > 0$, $a_1 > 0$ and

$$a_0 = (\theta_p+\mu_p)(\alpha_p+\mu_p+d)(\nu+\mu_U+\varepsilon\lambda_j)\left(1 - \frac{\gamma_p\theta_p\omega_p\nu}{(\theta_p+\mu_p)(\alpha_p+\mu_p+d)(\nu+\mu_U+\varepsilon\lambda_j)}\right)$$

Hence $a_0 > 0$ if $\frac{\gamma_p\theta_p\omega_p\nu}{(\theta_p+\mu_p)(\alpha_p+\mu_p+d)(\nu+\mu_U+\varepsilon\lambda_j)} < 1$, which is satisfied for all (non negative) λ_j if it is satisfied for $\lambda_0 = 0$. The condition $a_0 > 0$ then leads to:

$$\mathcal{R}_0^{(p)} = \frac{\gamma_p\theta_p\omega_p\nu}{(\theta_p+\mu_p)(\alpha_p+\mu_p+d)(\nu+\mu_U)} < 1. \tag{4.38}$$

Secondly, the expression

$$\begin{aligned} a_2a_1 - a_0 = {} & (\alpha_p+\mu_p+d+\nu+\mu_U+\varepsilon\lambda_j)(\theta_p+\mu_p)^2 + (\theta_p+\mu_p)(\alpha_p+\mu_p+d+\nu+\mu_U+\varepsilon\lambda_j) \\ & + (\alpha_p+\mu_p+d)(\nu+\mu_U+\varepsilon\lambda_j)) + \gamma_p\theta_p\omega_p\nu > 0 \end{aligned}$$

Using the fact that $a_2 > 0$, $a_1 > 0$, $a_0 > 0$ and $a_2a_1 > a_0$, the Routh–Hurwitz stability criterion indicates that all the eigenvalues of matrix H_j have negative real parts. Hence the DFE Q_p^0 of subsystems (4.5) is LAS if and only $\mathcal{R}_0^{(p)} < 1$.

2. *Existence and local stability of the endemic equilibrium Q^**

Suppose that $\mathcal{R}_0^{(p)} > 1$. The expression (4.16) of the endemic equilibrium can easily be established as the solution of a set of linear equations, derived from equating the right-hand side of equation (4.5) to zero. We first prove that I_p^* and S_p^* are positive. Recall that:

$$I_p^* = \frac{\Lambda_p(\nu+\mu_U)(\mathcal{R}_0^{(p)}-1)}{\gamma_p\omega_p\nu - d(\nu+\mu_U)} \quad \text{and} \quad S_p^* = \frac{\Lambda_p(\gamma_p\omega_p\nu - d(\nu+\mu_U)\mathcal{R}_0^{(p)})}{\mu_p\mathcal{R}_0^{(p)}(\gamma_p\omega_p\nu - d(\nu+\mu_U))}.$$

Note that:

$$\begin{aligned} \mathcal{R}_0^{(p)} > 1 &\Rightarrow \frac{\gamma_p\omega_p\nu\theta_p}{(\nu+\mu_U)(\theta_p+\mu_p)(\alpha+\mu_p+d)} > 1, \\ &\Rightarrow d < \frac{\gamma_p\omega_p\nu\theta_p}{(\nu+\mu_U)(\theta_p+\mu_p)} - \alpha_p - \mu_p, \\ &\Rightarrow d < \frac{\gamma_p\omega_p\nu\theta_p}{(\nu+\mu_U)(\theta_p+\mu_p)}, \\ &\Rightarrow d(\nu+\mu_U) < \frac{\gamma_p\omega_p\nu\theta_p}{(\theta_p+\mu_p)} < \gamma_p\omega_p\nu \\ &\Rightarrow \gamma_p\omega_p\nu - d(\nu+\mu_U) > 0, \\ &\Rightarrow I_p^* > 0. \end{aligned}$$

Now using the fact that $\frac{\theta_p d}{(\theta_p+\mu_p)(\alpha_p+\mu_p+d)} < 1$, one has:

$$\begin{aligned} \frac{\gamma_p\omega_p\nu\theta_p d(\nu+\mu_U)}{(\nu+\mu_U)(\theta_p+\mu_p)(\alpha_p+\mu_p+d)} < \gamma_p\omega_p\nu &\Rightarrow (\nu+\mu_U)\mathcal{R}_0^{(p)} < \gamma_p\omega_p\nu, \\ &\Rightarrow \gamma_p\omega_p\nu - d(\nu+\mu_U)\mathcal{R}_0^{(p)} > 0 \\ &\Rightarrow S_p^* > 0 \end{aligned}$$

This concludes the existence of the endemic equilibrium.

Second, we investigate the local stability of the endemic equilibrium, using the following theorem.

Theorem 4.3 (Castillo-Chavez and Song [27]). *Consider the following ordinary differential equations, with a parameter ψ:*

$$\frac{dx}{dt} = f(x,\psi), \quad f : \mathbb{R}^n \times \mathbb{R}^n\mathbb{R}^n \quad \text{and} \quad f \in C^2(\mathbb{R}^n \times \mathbb{R}). \tag{4.39}$$

Without loss of generality, it is assumed that 0 is an equilibrium for system (4.39) for all values of the parameter ψ, that is $f(0,\psi) \equiv 0$ for all ψ. Assume

A_1: *$A = D_x f(0,0) = (\frac{\partial f_i}{\partial x_j}(0,0))$ is the linearization matrix of system (4.39) around the equilibrium 0 with ψ evaluated at 0. Zero is a simple eigenvalue of A and all other eigenvalues of A have negative real parts;*

A_2: *Matrix A has a nonnegative right eigenvector u and a left eigenvector v corresponding to the zero eigenvalue. Let f_k be the k^{th} component of f and*

$$a = \sum_{k,i,j=1}^{n} v_k u_i u_j \frac{\partial^2 f_k}{\partial z_i \partial z_j}(0,0), \quad \text{and} \quad b = \sum_{k,i=1}^{n} v_k u_i \frac{\partial^2 f_k}{\partial z_i \partial \psi}(0,0).$$

The local dynamics of (4.39) around 0 are totally determined by a and b.

(a) $a > 0$, $b > 0$. When $\psi < 0$ with $\|\psi\| \ll 1$, 0 is locally asymptotically stable, and there exists a positive unstable equilibrium; when $0 < \psi \ll 1$, 0 is unstable and there exists a negative and locally asymptotically stable equilibrium;

(b) $a < 0$, $b < 0$. When $\psi < 0$ with $\|\psi\| \ll 1$, 0 is unstable; when $0 < \psi \ll 1$, 0 is locally asymptotically stable, and there exists a positive unstable equilibrium;

(c) $a > 0$, $b < 0$. When $\psi < 0$ with $\|\psi\| \ll 1$, 0 is unstable, and there exists a locally asymptotically stable negative equilibrium; when $0 < \psi \ll 1$, 0 is stable, and a positive unstable equilibrium appears;

(d) $a < 0$, $b > 0$. When ψ changes from negative to positive, 0 changes its stability from stable to unstable. Correspondingly a negative unstable equilibrium becomes positive and locally asymptotically stable.

In order to apply this theorem, subsystems (4.5) can be written as follows, with $z = (S, L, I, J, U)$:

$$\begin{cases} \dfrac{\partial_t z_1}{\partial t} = F_1 = \Lambda_p - \mu_p z_1 - \dfrac{\omega_p \nu z_5}{z_1 + z_2 + z_3 + z_4}, \\ \dfrac{\partial_t z_2}{\partial t} = F_2 = \dfrac{\omega_p \nu z_5}{z_1 + z_2 + z_3 + z_4} - (\theta_p + \mu_p) z_2, \\ \dfrac{\partial_t z_3}{\partial t} = F_3 = \theta_p z_2 - (\alpha + \mu_p + d) z_3, \\ \dfrac{\partial_t z_4}{\partial t} = F_4 = \alpha_p z_3 - \mu_p z_4, \\ \dfrac{\partial_t z_5}{\partial t} - \varepsilon \Delta z_5 = F_5 = \gamma_p z_3 - (\nu + \mu_U) z_5, \end{cases} \tag{4.40}$$

Solving $\mathcal{R}_0^{(p)} = 1$, we obtain the following bifurcation value for parameter ω_p:

$$\omega_p^* = \frac{(\mu_p + \theta)(\alpha_p + \mu_p + d)(\nu + \mu_U)}{\nu \gamma_p \theta_p}.$$

We linearise this system at the DFE Q_p^0, as previously in equation (4.37), setting ω_p to ω_p^*. We need to determine the eigenvalues of matrix $L_{\omega_p^*} - \lambda_j \mathcal{D}$, where λ_j is an eigenvalue of the Laplacian operator $-\Delta$ (simplified notation $L_{\omega_p^*}$ is used instead of $L_{\omega_p^*}(Q_p^0)$). With $\lambda_j = \lambda_0 = 0$, the matrix admits $\beta_0 = 0$ as eigenvalue, the other eigenvalues still having a negative real part. For the other λ_j, all eigenvalues have negative real parts. So assumption A_1 of theorem 4.3 is verified.

Let us now verify assumption A_2. We need to compute the left and right eigenvectors of matrix $L_{\omega_p^*} - \lambda_j \mathcal{D}$ associated with the eigenvalue β. The left eigenvector, denoted by $v = (v_1, v_2, v_3, v_4, v_5)$, satisfies the following equation:

$$v(L_{\omega_p^*} - \lambda_j \mathcal{D} - \beta \mathbf{I}) = \mathbf{0},$$

where $\mathbf{I}$ and $\mathbf{0}$ are the identity matrix and null vector of dimension 5, respectively. For $\beta = \beta_0 = 0$ one has:

$$\begin{pmatrix} v_1 & v_2 & v_3 & v_4 & v_5 \end{pmatrix} \begin{pmatrix} -\mu_p & 0 & 0 & 0 & -\omega_p^* \nu \\ 0 & -(\theta_p + \mu_p) & 0 & 0 & \omega_p^* \nu \\ 0 & \theta_p & -(\alpha_p + \mu_p + d) & 0 & 0 \\ 0 & 0 & \alpha_p & -\mu_p & 0 \\ 0 & 0 & \gamma_p & 0 & -(\nu + \mu_U + \varepsilon \lambda_j) \end{pmatrix} = \begin{pmatrix} 0 & 0 & 0 & 0 & 0 \end{pmatrix}$$

which gives:

$$\begin{cases} v_1 = 0, \\ v_2 = \dfrac{\gamma_p \theta_p}{(\mu_p + \theta_p)(\alpha_p + \mu_p + d)} v_5, \\ v_3 = \dfrac{\gamma_p}{(\alpha_p + \mu_p + d)} v_5, \\ v_4 = 0, \\ v_5 > 0. \end{cases}$$

Similarly the right eigenvector of matrix $L_{\omega_p^*} - \lambda_j \mathcal{D}$, denoted by $u = (u_1, u_2, u_3, u_4, u_5)^T$, satisfies the following equation:

$$(L_{\omega_p^*} - \lambda_j \mathcal{D} - \beta \mathbf{I}) u = \mathbf{0}.$$

For $\beta = \beta_0 = 0$, one has:

$$\begin{pmatrix} -\mu_p & 0 & 0 & 0 & -\omega_p^* \nu \\ 0 & -(\theta_p + \mu_p) & 0 & 0 & \omega_p^* \nu \\ 0 & \theta_p & -(\alpha_p + \mu_p + d) & 0 & 0 \\ 0 & 0 & \alpha_p & -\mu_p & 0 \\ 0 & 0 & \gamma_p & 0 & -(\nu + \mu_U + \varepsilon \lambda_j) \end{pmatrix} \begin{pmatrix} u_1 \\ u_2 \\ u_3 \\ u_4 \\ u_5 \end{pmatrix} = \begin{pmatrix} 0 \\ 0 \\ 0 \\ 0 \\ 0 \end{pmatrix},$$

which gives:

$$\begin{cases} u_1 = -\dfrac{\omega_p^*\nu}{\mu}u_5, \\ u_2 = \dfrac{\omega_p^*\nu}{\mu+\theta}u_5, \\ u_3 = \dfrac{\omega_p^*\nu\theta}{(\mu+\theta)(\alpha_p+\mu_p+d)}u_5, \\ u_4 = \dfrac{\alpha_p\omega_p^*\nu\theta_p}{(\mu_p+\theta_p)(\alpha_p+\mu_p+d)}u_5, \\ u_5 > 0. \end{cases}$$

Let us now compute a, defined in assumption A_2 of theorem 4.3, for system (4.40):

$$a = \sum_{i,j,k=1}^{5} v_k u_i u_j \frac{\partial^2 F_k}{\partial z_i \partial z_j}(Q_p^0, \omega_p^*).$$

The only terms that are non null correspond to:

$$\frac{\partial^2 F_2}{\partial z_i \partial z_5}(Q_p^0, \omega_p^*) = v_2 \frac{\partial^2 F_2}{\partial z_5 \partial z_j}(Q_p^0, \omega_p^*) = -\frac{\omega_p \nu^*}{S^0} \quad \text{for } i,j = 2,3,4.$$

Substituting these terms into the expression of a, one obtains:

$$\begin{aligned} a &= v_2 \left[2u_2u_5 \frac{\partial^2 F_2}{\partial z_2 \partial z_5}(Q_p^0, \omega_p^*) + 2u_3u_5 \frac{\partial^2 F_2}{\partial z_3 \partial z_5}(Q_p^0, \omega_p^*) + 2u_4u_5 \frac{\partial^2 F_2}{\partial z_4 \partial z_5}(Q_p^0, \omega_p^*) \right], \\ &= -v_2u_5(u_2+u_3+u_4)\frac{\omega_p^*\nu}{S^0} < 0. \end{aligned}$$

Let us now compute b, defined in assumption A_2 of theorem 4.3, for system (4.40):

$$b = \sum_{k,i=1}^{5} v_k u_i \frac{\partial^2 F_k}{\partial z_i \partial \omega_p}(Q_p^0, \omega_p^*).$$

The only term that is non null corresponds to:

$$\frac{\partial^2 F_2}{\partial z_5 \partial \omega_p}(Q_p^0, \omega_p^*) = \frac{\nu}{S_0}.$$

Substituting this term into the expression of b, one obtains:

$$\begin{aligned} b &= v_2u_5 \frac{\partial^2 F_2}{\partial z_5 \partial \omega_p}(Q_p^0, \omega_p^*) \\ &= v_2u_5 \frac{\nu}{S_0} > 0. \end{aligned}$$

Thus, $a < 0$ and $b > 0$. Using Theorem 4.3, we conclude that when bifurcation parameter changes from $\omega_p < \omega_p^*$ to $\omega_p^* < \omega_p$, *i.e.* the basic reproduction number changes from $\mathcal{R}_0^{(p)} < 1$ to $\mathcal{R}_0^{(p)} > 1$, the DFE changes from GAS to unstable. Moreover, when the basic reproduction number is close to one, the endemic equilibrium Q_P^* appears and is locally asymptotically stable. This completes the proof.

4.7 Appendix: Numerical scheme

4.7.1 Discretization of model system

Herein, we develop a non-standard finite difference scheme that is consitent with the dynamics of the continous PDE model system (3.1). To do so, model system (3.1) can be written in the following compact form

$$\frac{\partial P}{\partial t} = D\frac{\partial^2 P}{\partial^2 x} - A_0(P)P + A_1, \tag{4.41}$$

where

$$P = (S, L, I, R, B_e, U)^T, \quad D = diag(0, 0, 0, 0, 0, \varepsilon), \quad A_1 = (\Lambda, 0, 0, 0, 0, 0)^T,$$

and

$$A_0(P) = \begin{pmatrix} \mu_M + \mu(t) + \frac{\omega\nu U}{N} & 0 & 0 & 0 & 0 & 0 \\ -\frac{\omega\nu U}{N} & (1-q)\theta + \mu_M + \mu(t) & 0 & 0 & 0 & 0 \\ 0 & -(1-q)\theta & \alpha + \mu_M + d + \mu(t) & & 0 & 0 \\ 0 & 0 & -\alpha & \mu_M + \mu(t) & 0 & 0 \\ -\delta_1(t) & -\delta_2(t) & -\delta_3(t) & -\delta_4(t) & \mu_e & 0 \\ 0 & 0 & -\gamma & 0 & 0 & (\nu + \mu_U) \end{pmatrix}.$$

For the temporal discretization, we replace the continous time variable $t \in [0, \infty)$ by the discretes variables $t_n = ndt$, $n \in \mathbb{Z}$ where dt is the temporal step size. Also, for the spatial discretiztion, the continous space variable $x \in \Omega$ is replaced by the discrete variables, $x_j = jdx$, $j \in \mathbb{Z}$ where dx is the spatial step size. With this is mind, one has

$$\frac{\partial P}{\partial t} = \frac{P_j^{n+1} - P_j^n}{\psi(dt)} + o(\psi(dt)), \tag{4.42}$$

and

$$\frac{\partial^2 P}{\partial^2 t} = \frac{P_{j+1}^n - 2P_j^n + P_{j-1}^n}{(dx)^2} + o(dx)^2). \tag{4.43}$$

Now, plugging Eqs.(4.42) and (4.43) in Eq. (4.41), gives

$$\frac{P_j^{n+1} - P_j^n}{\psi(dt)} = D\frac{P_{j+1}^n - 2P_j^n + P_{j-1}^n}{(dx)^2} - A_0(P_j^n)P_j^{n+1} + A_1 \tag{4.44}$$

Which can be rewritten as follows:

$$P_j^{n+1} = \mathcal{A}_1^{-1}\mathcal{A}_2(P_{j+1}^n + P_{j-1}^n) + \mathcal{A}_1^{-1}\mathcal{A}_3 P_j^n + \mathcal{A}_1^{-1}A_1, \tag{4.45}$$

where

$$\mathcal{A}_1 = \begin{pmatrix} C_1 & 0 & 0 & 0 & 0 & 0 \\ O_1 & C_2 & 0 & 0 & 0 & 0 \\ 0 & O_2 & C_3 & 0 & 0 & 0 \\ 0 & 0 & O_3 & C_4 & 0 & 0 \\ O_4 & O_5 & O_6 & 0_7 & C_5 & 0 \\ 0 & 0 & O_8 & 0 & 0 & C_6 \end{pmatrix}, \quad \mathcal{A}_2 = diag(0,0,0,0,0,d_U)$$

and

$$\mathcal{A}_3 = diag(1,1,1,1,1,1-2d_U),$$

with

$$\begin{cases} C_1 = 1+\psi(dt)[\mu_M+\mu(t)+\dfrac{\omega\nu U}{N}], \quad C_2 = 1+\psi(dt)((1-q)\theta+\mu_M+\mu(t)), \\ C_3 = 1+\psi(dt)(\alpha+\mu_M+d+\mu(t)), \quad C_4 = 1+\psi(dt)(\mu_M+\mu(t)), \quad d_U = \dfrac{\varepsilon\psi(dt)}{(dx)^2}, \\ C_5 = 1+\psi(dt)\mu_e, \quad C_6 = 1+\psi(dt)(\nu+\mu_U), \\ O_1 = -\psi(dt)\dfrac{\omega\nu U}{N}, \quad O_2 = -\psi(dt)(1-q)\theta, \quad O_3 = -\psi(dt)\alpha, \quad O_4 = \psi(dt)\delta_1(t), \\ O_5 = \psi(dt)\delta_2(t), \quad O_6 = \psi(dt)\delta_3(t), \quad O_7 = \psi(dt)\delta_4(t) \quad \text{and} \quad O_8 = \psi(dt)\gamma \end{cases}$$

Now, using the notation of P defined in Eq.(4.41), and after the calculation of $\mathcal{A}^{-1}$, we obtain the following for model system (4.45) :

$$\begin{cases} S_j^{n+1} = \dfrac{1}{C_1}S_j^n + \dfrac{\Lambda}{C_1}, \\ L_j^{n+1} = -\dfrac{O_1}{C_1C_2}S_j^n + \dfrac{1}{C_2}L_j^n - \dfrac{\Lambda O_1}{C_1C_2}, \\ I_j^{n+1} = \dfrac{O_1O_2}{C_1C_2C_3}S_j^n - \dfrac{O_2}{C_2C_3}L_j^n + \dfrac{1}{C_3}I_j^n + \dfrac{\Lambda O_1O_2}{C_1C_2C_3}, \\ R_j^{n+1} = -\dfrac{O_1O_2O_3}{C_1C_2C_3C_4}S_j^n + \dfrac{O_2O_3}{C_2C_3C_4}L_j^n - \dfrac{O_3}{C_3C_4}I_j^n + \dfrac{1}{C_4}R_j^n - \dfrac{\Lambda O_1O_2O_3}{C_1C_2C_3C_4}, \\ B_{ej}^{n+1} = \xi_1 S_j^n + \xi_2 L_j^n - \dfrac{(C_4O_6 - O_3O_7)}{C_3C_4C_5}I_j^n - \dfrac{O_7}{C_4C_5}R_j^n + \dfrac{1}{C_5}B_{ej}^n + \xi_1\Lambda, \\ U_j^{n+1} = -\dfrac{O_1O_2O_8}{C_1C_2C_3C_6}S_j^n + \dfrac{O_2O_8}{C_2C_3C_6}L_j^n - \dfrac{O_8}{C_3C_6}I_j^n + \dfrac{1-2d_U}{C_6}U_j^n + \dfrac{d}{C_6}(U_{j-1}^n + U_{j+1}^n) - \dfrac{\Lambda O_1O_2O_8}{C_1C_2C_3C_6}, \end{cases} \tag{4.46}$$

where

$$\xi_1 = \frac{-C_4O_4C_2C_3 + C_4O_1O_5C_3 - C_4O_1O_2O_6 - O_1O_2O_3O_7}{C_1C_2C_3C_4C_5}$$

and

$$\xi_2 = \frac{-C_3C_4O_5 + C_4O_2O_6 - O_2O_3O_7}{C_2C_3C_4C_5}$$

4.7.2 Discretization of boundary conditions

The discretization of the Neumann boundary conditions gives the following systems

$$\begin{cases} \dfrac{P_1^{n+1} - P_1^n}{\psi(dt)} = \dfrac{D}{(dx)^2}(P_2^n - 2P_1^n + P_0^n), \\ \\ P_2^n = P_0^n, \end{cases} \tag{4.47}$$

and

$$\begin{cases} \dfrac{P_{Ne+1}^n - P_1^n}{\psi(dt)} = \dfrac{D}{(dx)^2}(P_{Ne+2}^n - 2P_{Ne+1}^n + P_{Ne}^n), \\ \\ P_{Ne+2}^n = P_{Ne}^n, \end{cases} \tag{4.48}$$

Combining Eq.(4.47) and Eq.(4.48) yields

$$\begin{cases} P_1^{n+1} = (Id - 2\mathcal{A}_2)P_1^n + 2\mathcal{A}_2 P_2^n, \\ \\ P_{Ne+1}^{n+1} = (Id - 2\mathcal{A}_2)P_{Ne+1}^n + 2\mathcal{A}_2 P_{Ne}^n, \end{cases} \tag{4.49}$$

Using the notation of P defined in Eq.(4.41), Eq.4.49 can be writteen as follows:

$$\begin{cases} S_1^{n+1} = S_1^n, \quad L_1^{n+1} = L_1^n, \quad I_1^{n+1} = I_1^n, \quad R_1^{n+1} = R_1^n, \quad B_{e1}^{n+1} = B_{e1}^n \\ U_1^{n+1} = (1 - 2d_U)U_1^n + 2d_U U_2^n, \quad S_{Ne+1}^{n+1} = S_{Ne+1}^n, \\ L_{Ne+1}^{n+1} = L_{Ne+1}^n, \quad I_{Ne+1}^{n+1} = I_{Ne+1}^n, \quad R_{Ne+1}^{n+1} = R_{Ne+1}^n, \\ B_{eNe+1}^{n+1} = B_{eNe+1}^n, \quad U_{Ne+1}^{n+1} = (1 - 2d_U)U_{Ne+1}^n + 2d_U U_{Ne}^n, \end{cases} \tag{4.50}$$

4.7.3 Consistence of scheme

The numerical scheme (4.46) is consistent if $d_U \leq \dfrac{1}{2}$ where $d_U = \dfrac{\varepsilon\psi(dt)}{(dx)^2}$

Taking $\psi(dt) = \dfrac{e^{Mt} - 1}{M}$, $M = \max\{\mu_M, \mu_M + (1-q)\theta, \mu_M + \alpha + d, \mu_U + \nu, \mu_{Be}\}$, we have the result.

Chapter 5

Impulsive modelling of rust dynamics and hyperparasite releases for biocontrol

In this chapter, the model is seasonal, but does not distinguish between young and mature leaves. It includes the dynamics of a biocontrol agent with impulsive releases. The model is obtained using the following hypotheses.

H_1: The model is based on a classical epidemiological model, in which the host population is subdivided by health status (healthy leaves S and infected leaves I), considering the crop leaf as an individual. The model includes crop production (flowers F and berries B) by leaves during the rainy season and harvest at the end of the season. The infection being mediated by fungus spores (uredospore U) released in the plantation, their dynamics are also included.

H_2: The recruitment of healthy leaves is constant.

H_3: The force of infection is density-dependent: it is proportional to the number of uredospores and inversely proportional to the total number of leaves.

H_4: The model alternates dry and rainy seasons. The dynamics are continuous during the rainy seasons and represented by discrete events during the dry seasons.

H_5: Space is not explicitly taken into account in this model, uredospores are homogeneously distributed on leaves.

H_6: The model uses an impulsive differential equations (IDE) formalism.

H_7: The model includes the dynamics of hyperparasites (P) which feed on uredospores. Hyperparasites are released one or several times per rainy season.

We then obtain an IDE model with five compartments. The aim of this last study is to implement a biocontrol strategy of CLR based on hyperparasites.

The work presented in this chapter is based on preliminary results published in *IFAC-PapersOnLine1* [37] and presented in Appendix A.1. In this preliminary work the impact of control is represented by adding an extra negative term in the dynamics of uredospores. We then, use optimal control to maximise the yield and reduce the cost of control.

Contents

Abstract: Fungal diseases cause serious damages in crop worldwide. In particular, coffee leaf rust (CLR), caused by fungus *Hemileia vastatrix* attacks coffee leaves and reduces coffee yield. This paper presents a multi-seasonal model of the CLR development in the coffee plantation with continuous dynamics during the rainy season and a discrete event to represent the simpler dynamics during the dry season. Biological control using hyperparasites through one or more discrete introduction events over the year is then added. Analytical and semi-numerical studies are performed to identify how much and how frequently hyperparasites need to be introduced through the definition of a threshold value, as a function of various parameters. We show that the best strategy to efficiently control the disease depends on the hyperparasite mortality: low mortality parasites need be released only once a year, while high mortality parasites should be released more frequently to ensure their persistence in the plantation. This work hence provides qualitative and quantitative bases for the deployment of hyperparasite-based biocontrol, a promising alternative to fungicides for rust control.

Highlights:

- Original impulsive model of multi-seasonal fungal disease dynamics
- Explicit dynamics of hyperparasites, acting as predators of spores
- Hyperparasite-based biocontrol can drastically reduce disease impact on crop production
- Hyperparasite release frequency modulates the control efficiency

Keywords: crop protection, coffee leaf rust, hybrid model, seasonality, Floquet theory, stability

5.1 Introduction

Many of the most serious crop diseases are caused by fungi such as rusts [3]. Mathematical models of fungal diseases have received a lot of attention from researchers. For instance, Pivonia at al. studied the seasonal appearance of rusts in the United States, in particular soybean rust, thanks to a general disease model [124]. Rimbaud et al. investigated how the spatial deployment of resistant cultivars affects the resistance efficiency and durability, using a demogenetic model, for a seasonal crop infected by a fungal-like pathogen [134]. Fleming used a mathematical model to prove that a complex of polyphagous non-synchronised predators and parasites is likely to control only low-density cereal rust populations, but the author also proved that control at low rust density can delay epidemic development and thus substantially reduce yield losses [49]. Mammeri et al. studied the impact of spatial heterogeneities on the spread and control of grapevine powdery mildew [97], but only during a cropping season. There are fewer models of fungal diseases that target perennial hosts. For instance, Ravigné et al. looked at the impact of sexual and asexual reproduction on the epidemiological dynamics and showed that they could induce cyclic persistence of the disease, as it can observed for banana Sigatoka diseases [130]. Desprez-Loustau et al. developed a seasonal eco-evolutionary model of oak powdery mildew in Europe, based on a within-season and between-season transmission trade-off, which captures the main features of the disease, that is seasonality and pathogen species coexistence [36].

Plant growth and disease spread may be affected by seasonal patterns, which then need to be included in epidemiological models. It is the case of crops cultivated in temperate climates or tropical regions that alternate dry and rainy seasons. As the dynamics can substantially differ between the seasons with possibly rapid transitions, impulsive or semi-discrete models have been developed for several plant fungal diseases, as for oak powdery mildew in the study cited above. Among these models, one can also cite Tankam-Chedjou et al. who built a model to describe and control the dynamics of a banana soilborne pest in a multi-seasonal framework, optimising the fallow period durations between cropping seasons [155]. Periodic patterns are not necessarily linked to seasonality and can also be due to impulsive control strategies introduced in the epidemiological models. For instance, in the biological control framework, Nundloll et al. studied the periodic release of predators, natural enemies of the plant pest of interest, and determined the minimal predator rate required to eradicate the pest [115]. Xinzhu et al. formulated and analysed a model with continuous cultural control and with impulsive cultural control strategies such as replanting and/or removing diseased plants; they concluded that impulsive removing of diseased plants is more efficient and more economical than continuous removing [105]. Nembot et al. developed a model of cocoa black pod rot disease, caused by *Phytophthora megakarya*, and showed the impact of periodic impulsive sanitary harvests on the disease dynamics [113]. Semi-discrete models are hence particularly appropriate for seasonal plant and pathogen dynamics, as well as impulsive control strategies.

Control methods used to fight fungal diseases include chemical fungicide application, cultural practices, and the use of resistant cultivars [145]. These methods induce significant labour and/or material costs. Moreover, chemical fungicides are harmful to the environment [82], potentially also to farmers and consumers [70]; in addition, they may affect non-target organisms and induce pest resistance [76]. Therefore, researchers are currently investigating alternative control methods such as biocontrol [75, 6]. Several biological agents have been tested to control fungal plant diseases, among which various bacteria. Antagonist bacteria such as *Bacillus* species make

plants more resistant to fungal infections [144, 68, 148, 34]. Other investigations on biocontrol focused on hyperparasites, which are parasites whose host is often an insect pest but can also be a fungus. For example, several insects such as *Mycodiplosis* (Diptera) [67] and fungi such as *Lecanicillium lecanii* (previously called *Verticillium lecanii*) [104, 55] feed on rust spores.

As a foundation for our model, we considered coffee leaf rust (CLR), which is caused by a fungus, *Hemileia vastatrix*. It attacks the lower leaves of the coffee tree and causes premature defoliation, which reduces the photosynthetic capacity and weakens the tree. Leaf fall causes abortion of a large part of the flowers and fruits, as well as desiccation of shoots. It has direct and indirect economic impacts on coffee production. Direct impacts include decreased quantity and quality of yield. In some cases, more than 70% of the coffee production is lost [58, 8]. Indirect impacts include increased costs to control the disease.

The fungus *Hemileia vastatrix* is a basidiomycete, which, like most fungi, produces spores (used for reproduction). Its control is achieved similarly to that of other fungal diseases. For instance, the antagonist bacteria *Bacillus subtilis*, isolated from the rhizosphere of coffee crops, largely reduced the growth of CLR (up to 68%) under in vitro conditions [34]. The fungus *Cladosporium hemileiae*, inhibits the evolution of *H. vastatrix* mycelium [149]. The fungus *Lecanicillium lecanii* [168] and the insect *Mycodiplosis* [139, 63] can feed on spores. In all these biocontrol studies, the dose and time of application of the bacteria or hyperparasites affected their effectiveness in controlling coffee leaf rust development. In this work, we chose to focus on a *Mycodiplosis*-like hyperparasite, which was reported as a promising biocontrol agent and paid special attention to the quantity and frequency of the releases. To this aim, mathematical modelling can help identifying when and how to release a biocontrol agent.

Our goal in this paper is to control a fungal disease in the field, by means of hyperparasite releases, using a mathematical modelling approach. To achieve this goal, we extend an original impulsive CLR model that we previously developed [37]. In particular, we explicitly represent the hyperparasite dynamics, the latter acting as predators of spores. Moreover, we consider in this work discrete releases of the hyperparasite instead of a continuous control.

This paper is organised as follows. Section 5.2 is devoted to the formulation of the impulsive model of CLR, with continuous dynamics during the rainy seasons and discrete events for the dry seasons. It also presents the mathematical analysis of the model using Floquet theory and simulations of this impulsive model to illustrate the theoretical results. In Section 5.3, we introduce the biocontrol in the model, based on hyperparasite yearly releases. We semi-analytically study the stability of the control model to obtain the stability regions as functions of parameter values. Section 5.4 presents the impact of multiple yearly releases of hyperparasites, with contrasting results according to the value of the hyperparasite mortality rate. The last Section 5.5 concludes the paper with a discussion of the main results and possible perspectives for future work.

5.2 Coffee leaf rust dynamics

5.2.1 Modelling of CLR

In this section, we formulate a mathematical model for the CLR in the coffee plantation. To do so, we consider the dynamics of fungus during the production season, which corresponds to the rainy season for some countries, through ordinary differential equations; while the non-

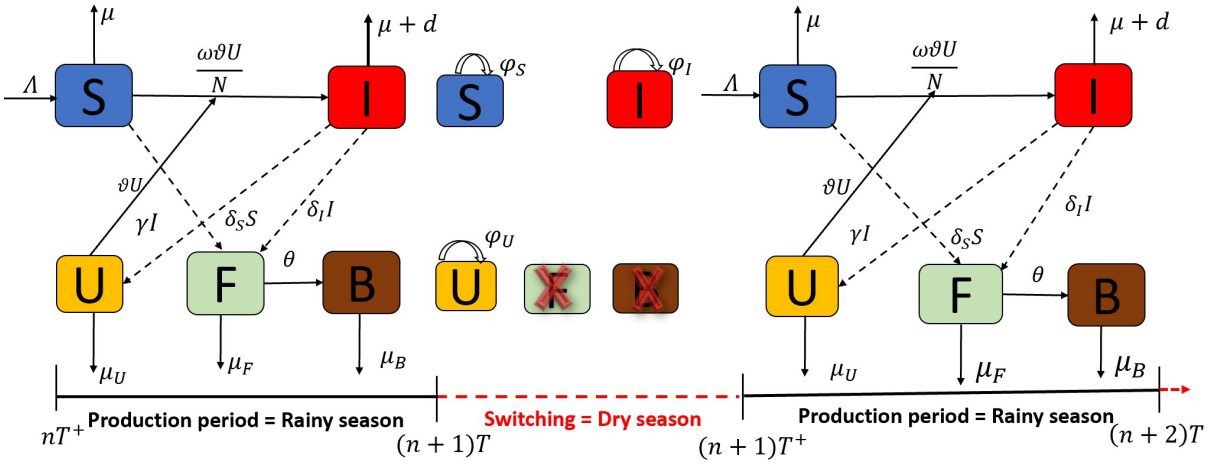

Figure 5.1: Diagram of the CLR multi-seasonal model. Model equations are given in system (5.1). State variables are: healthy leaves (S), infectious leaves (I), uredospores (U), flowers (F) and berries (B). T corresponds to the length of rainy season and n the year number.

production period, which is the dry season, is represented by impulses since the dynamics are simpler during that period. More precisely, we consider that in a coffee plantation we can find: susceptible leaves S, which are healthy leaves that have not (yet) been attacked, infected leaves I, uredospores U, which the fungus *H. vastatrix* uses for its asexual reproduction, flowers F and berries B.

During the production period with length $T > 0$ which represents the rainy season, the recruitment of healthy leaves occurs at rate Λ. Uredospores are deposited on leaves of all leaves at rate ν. When the conditions are favourable, they germinate with efficiency rate ω and the susceptible leaves become infected leaves. All leaves undergo natural mortality with baseline rate μ and the infected leaves have an additional mortality rate d due to the disease. Uredospores are produced by infected leaves at rate γ and lose their ability to infect coffee leaves at constant rate μ_U. Susceptible and infected leaves produce the flowers with constant rate δ_S and δ_I respectively and $\delta_S > \delta_I$. The flowers become berries at rate θ. At the end of the production period, harvest occurs instantaneously and we consider that the dry season or non-production period can be summarised in a discrete time event due to the slow growth of leaves during the dry season. The impact of harvest and dry season reduces the number of susceptible leaves, infected leaves and uredospores with rates φ_S, φ_I and φ_U respectively. Using the fact that uredospores lose their ability to infect quickly, we assume that φ_U is very close to 0. The representation of this evolution in the coffee plantation over a multi-year period, gives the multi-seasonal model, given in Figure 5.1, with the continuous dynamics during the rainy season and switching event for the dry season.

Using flowchart in Figure 5.1, we can write the following impulsive differential system:

Rainy season for $t \neq nT$:

$$\begin{cases} \dot{S} = \Lambda - \omega\nu U\dfrac{S}{N} - \mu S, \\ \dot{I} = \omega\nu U\dfrac{S}{N} - (\mu + d)I, \\ \dot{U} = \gamma I - (\nu + \mu_U)U, \\ \dot{F} = \delta_S S + \delta_I I - (\theta + \mu_F)F, \\ \dot{B} = \theta F - \mu_B B; \end{cases} \tag{5.1}$$

Dry season:

$$\begin{cases} S(nT^+) = \varphi_s S(nT), \\ I(nT^+) = \varphi_I I(nT), \\ U(nT^+) = \varphi_U U(nT), \\ F(nT^+) = 0; \\ B(nT^+) = 0. \end{cases}$$

where $S(t)$, $I(t)$, $U(t)$, $F(t)$, $B(t)$ and $N(t) = S(t) + I(t)$ represent the number of healthy leaves, infected leaves, uredospores, flowers, berries and total number of leaves, respectively, at time t; with $0 < \varphi_S, \varphi_I, \varphi_U < 1$ and φ_U close to 0.

5.2.2 Mathematical analysis

Herein, we first presented basic properties of the model (5.1). Secondly, the periodic disease free solution is computed and its stability is proven. Finally, numerical simulations are performed to illustrate our mathematical results.

5.2.2.1 Basic properties of the model

Let $\mathbb{R}^5_+ = \{X \in \mathbb{R}^5, X \geq 0\}$. Denote by $f = (f_1, f_2, f_3, f_4, f_5)$ the map given by the right-hand side of system (5.1) when $t \neq nT$, and consider the initial conditions $(S(0), I(0), U(0), F(0), B(0)) \in \mathbb{R}^*_+ \times \mathbb{R}^4_+$.

The solutions of system (5.1) are non-negative. Indeed, suppose that one of the variables, that we will denote x, is equal to 0 at some instant, with all the others being non-negative. A quick analysis shows that $\dot{x} \geq 0$, so that x cannot become negative. This implies that the solutions are non-negative.

By adding the first and second equations of system (5.1), we obtain the dynamics of total leaves which satisfies:

$$\begin{cases} \dot{N} = \Lambda - \mu N - dI, \ t \neq nT; \\ N(nT^+) \leq \varphi_S N(nT). \end{cases} \tag{5.2}$$

From equation (5.2), and using the non-negativity of variable I, we obtain $\Lambda - (\mu + d)N \leq \dot{N} \leq \Lambda - \mu N$ and $N(nT^+) \leq \varphi_S N(nT)$. It follows that $\min(\Lambda/(\mu + d), N(0)) \leq N(t) \leq \max(\Lambda/\mu, N(0)) = \Gamma_N$, which implies that $S, I \leq \Gamma_N$. For $\Lambda/(\mu + d) < N(0) < \Lambda/\mu$, replacing S and I by this upper bound value in the uredospore and flower dynamics, we obtain the following

systems:

$$\begin{cases} \dot{U} \leq \gamma\dfrac{\Lambda}{\mu} - (\nu+\mu_U)U, & t \neq nT; \\ U(nT^+) = \varphi_U U(nT); \end{cases} \tag{5.3}$$

$$\begin{cases} \dot{F} \leq \delta_S\dfrac{\Lambda}{\mu} + \delta_I\dfrac{\Lambda}{\mu} - (\theta+\mu_F)F, & t \neq nT; \\ F(nT^+) = 0. \end{cases} \tag{5.4}$$

Identifying the values where the upper bounds of (5.3) and (5.4) are equal to 0, one has $U(t) \leq \max(\frac{\gamma\Lambda}{\mu(\nu+\mu_U)}, U(0))$ and $F(t) \leq \max(\frac{\Lambda(\delta_S+\delta_I)}{\mu(\theta+\mu_F)}, F(0))$. Replace the upper bound of F in the berry dynamics, we obtain

$$\begin{cases} \dot{B} \leq \theta\dfrac{\Lambda(\delta_S+\delta_I)}{\mu(\theta+\mu_F)} - \mu_B U, & t \neq nT; \\ B(nT^+) = 0. \end{cases} \tag{5.5}$$

Identifying the values where the upper bounds of (5.5) is equal to 0, one has $B(t) \leq \max(\frac{\Lambda\theta(\delta_S+\delta_I)}{\mu(\theta+\mu_F)\mu_B}, B(0))$. Hence, we have shown the boundedness of S, I, U, F and B. Also the region given by

$$G = \Big\{(S,I,U,F,B) \in \mathbb{R}^5_+ \mid S(t)+I(t) \leq \frac{\Lambda}{\mu},\ U(t) \leq \frac{\gamma\Lambda}{\mu(\nu+\mu_U)}, \\ F(t) \leq \frac{\Lambda(\delta_S+\delta_I)}{\mu(\theta+\mu_F)}, B(t) \leq \frac{\Lambda\theta(\delta_S+\delta_I)}{\mu(\theta+\mu_F)\mu_B}\Big\}$$

is positively invariant for impulsive system (5.1).

The solutions of system (5.1) are piecewise continuous functions $X : \mathbb{R}_+ \to \mathbb{R}^4_+$. The non-null constant parameter Λ, allows to the variable N remain not close to zero and the smooth properties of the right side of system (5.1) guarantee the existence and uniqueness of positive solutions of system (5.1).

Since the berry state variables F and B is not present in the other equations of system (5.1), we do no need to consider F and B in the rest of the mathematical analysis. We then analyse this new system:

$$\begin{cases} \dot{S} = \Lambda - \dfrac{\omega\nu U}{N}S - \mu S, & t \neq nT; \\ \dot{I} = \dfrac{\omega\nu U}{N}S - (\mu+d)I, & t \neq nT; \\ \dot{U} = \gamma I - (\nu+\mu_U)U, & t \neq nT; \\ S(nT^+) = \varphi_S S(nT); \\ I(nT^+) = \varphi_I I(nT); \\ U(nT^+) = \varphi_U U(nT). \end{cases} \tag{5.6}$$

5.2.2.2 Periodic disease free solution and its stability

The periodic disease free solution (PDFS) occurs when $I = 0$ and $U = 0$. Replacing these values in system (5.6), we obtain

$$\begin{cases} \dot{S} = \Lambda - \mu S, \ t \neq nT; \\ S(nT^+) = \varphi_S S(nT). \end{cases}$$

Solving the above equation for $t \in (nT, (n+1)T]$, yields

$$S(t) = \frac{\Lambda}{\mu} + \left(S(nT^+) - \frac{\Lambda}{\mu} \right) e^{-\mu(t-nT)}. \tag{5.7}$$

This implies that for $t = (n+1)T$, one has

$$S((n+1)T) = \frac{\Lambda}{\mu} + \left(S(nT^+) - \frac{\Lambda}{\mu} \right) e^{-\mu T}.$$

Using the impulsive condition $S((n+1)T^+) = \varphi_S S((n+1)T)$ yields

$$S((n+1)T^+) = \varphi_S \left(\frac{\Lambda}{\mu} + (S(nT^+) - \frac{\Lambda}{\mu}) e^{-\mu T} \right). \tag{5.8}$$

The fixed point of equation (5.8) is given by

$$S(nT^+) = \frac{\Lambda \varphi_S (1 - e^{-\mu T})}{\mu (1 - \varphi_S e^{-\mu T})} > 0. \tag{5.9}$$

Substituting the value of $S(nT^+)$ into equation (5.7), for $t \in (nT, (n+1)T]$, the solution is

$$S^T(t) = \frac{\Lambda}{\mu} \left[1 - \frac{(1 - \varphi_S) e^{\mu T}}{e^{\mu T} - \varphi_S} e^{-\mu(t-nT)} \right]. \tag{5.10}$$

Finally, the PDFS is $X^T(t)$=$(S^T(t), 0, 0)$, where $S^T(t)$ is defined above.

For the stability, we first study the local stability of the PDFS $X^T(t)$ using small amplitude perturbation methods. For that, let us denote $\tilde{X}(t) = X(t) - X^T(t)$, where $X(t) = (S(t), I(t), U(t))^T$ and $\tilde{X}(t)$ is understood to be small amplitude perturbations. Substituting the expression of $\tilde{X}(t)$ in system (5.6) gives

$$\begin{cases} \dot{\tilde{S}} = -\dfrac{\omega \nu \tilde{U}}{\tilde{N} + S^T(t)} (\tilde{S} + S^T(t)) - \mu \tilde{S}, & t \neq nT; \\ \dot{\tilde{I}} = \dfrac{\omega \nu \tilde{U}}{\tilde{N} + S^T(t)} (\tilde{S} + S^T(t)) - (\mu + d) \tilde{I}, & t \neq nT, \\ \dot{\tilde{U}} = \gamma \tilde{I} - (\nu + \mu_U) \tilde{U}, & t \neq nT; \\ \tilde{S}(nT^+) = \varphi_S \tilde{S}(nT); \\ \tilde{I}(nT^+) = \varphi_I \tilde{I}(nT); \\ \tilde{U}(nT^+) = \varphi_U \tilde{U}(nT). \end{cases} \tag{5.11}$$

where $\tilde{N}(t) = \tilde{S}(t) + \tilde{I}(t)$ and $N^T(t) = S^T(t)$.

The linearization of system (5.11) in the neighbourhood of $0_{\mathbb{R}^3}$ is

$$\begin{cases} \dot{\tilde{X}}(t) = A\tilde{X}(t),\ t \neq nT; \\ \tilde{X}(nT^+) = diag(\varphi_S, \varphi_I, \varphi_U)\tilde{X}(nT); \end{cases} \tag{5.12}$$

where

$$A = \begin{pmatrix} -\mu & 0 & -\omega\nu \\ 0 & -(\mu+d) & \omega\nu \\ 0 & \gamma & -(\nu+\mu_U) \end{pmatrix}.$$

Solving the first equation of system (5.12) for $t \in (0, T]$ yields

$$\tilde{X}(t) = \Phi_A(t)\tilde{X}(0^+), \tag{5.13}$$

where

$$\Phi_A(t) = e^{At} = \begin{pmatrix} e^{-\mu t} & * & * \\ 0 & \psi_{22}(t) & \psi_{23}(t) \\ 0 & \psi_{32}(t) & \psi_{33}(t) \end{pmatrix}$$

and

$$\begin{cases} \psi_{22}(t) = \dfrac{1}{2\beta}\left[(\beta + k_1 - k_2)e^{\lambda_1 t} + (\beta - k_1 + k_2)e^{\lambda_2 t}\right], \\ \psi_{23}(t) = \dfrac{\nu\omega}{\beta}\left[-e^{\lambda_1 t} + e^{\lambda_2 t}\right], \psi_{32}(t) = \dfrac{\gamma}{\beta}\left[-e^{\lambda_1 t} + e^{\lambda_2 t}\right], \\ \psi_{33}(t) = \dfrac{1}{2\beta}\left[(\beta - k_1 + k_2)e^{\lambda_1 t} + (\beta + k_1 - k_2)e^{\lambda_2 t}\right], \end{cases}$$

with

$$\begin{cases} k_1 = \mu + d, \quad k_2 = \nu + \mu_U, \\ \alpha = k_1 + k_2, \quad \beta = \sqrt{(k_1 - k_2)^2 + 4\gamma\omega\nu}, \\ \lambda_1 = -\dfrac{\alpha}{2} - \dfrac{\beta}{2} \text{ and } \lambda_2 = -\dfrac{\alpha}{2} + \dfrac{\beta}{2}. \end{cases}$$

Using the impulsive conditions $\tilde{X}(nT^+) = diag(\varphi_S, \varphi_I, \varphi_U)\tilde{X}(nT)$, the solution given by equation (5.13) becomes

$$\tilde{X}(nT^+) = diag(\varphi_S, \varphi_I, \varphi_U)\Phi_A(T)\tilde{X}((n-1)T^+). \tag{5.14}$$

From the above equation, the monodromy matrix $M = diag(\varphi_S, \varphi_I, \varphi_U)\Phi_A(T)$, *i.e.*

$$M = \begin{pmatrix} \varphi_S e^{-\mu T} & * & * \\ 0 & \varphi_I\psi_{22}(T) & \varphi_I\psi_{23}(T) \\ 0 & \varphi_U\psi_{32}(T) & \varphi_U\psi_{33}(T) \end{pmatrix}.$$

Due to the block-triangular form of monodromy matrix M, there is no need to calculate the exact form of $(*)$ for the following analysis.

The Floquet multipliers of the monodromy matrix M are given by $\chi_1 = \varphi_S e^{-\mu T} < 1$ and the eigenvalues of the sub-matrix

$$M_1 = \begin{pmatrix} \varphi_I\psi_{22}(T) & \varphi_I\psi_{23}(T) \\ \varphi_U\psi_{32}(T) & \varphi_U\psi_{33}(T) \end{pmatrix}. \tag{5.15}$$

The PDFS $X^T(t)$ is locally asymptotically stable if the Floquet multipliers of the monodromy matrix M stay inside the unit circle, which is equivalent to the Floquet multipliers of sub-matrix M_1 staying inside the unit circle. To obtain this result, the submonodromy matrix M_1 needs to satisfy the following Jury conditions [173]:

$$\begin{cases} -\operatorname{Tr}(M_1) - \det(M_1) < 1, \\ \det(M_1) < 1, \\ \operatorname{Tr}(M_1) - \det(M_1) < 1, \end{cases} \tag{5.16}$$

where

$$\begin{cases} \operatorname{Tr}(M_1) = \varphi_I \psi_{22}(T) + \varphi_U \psi_{33}(T), \\ \det(M_1) = \varphi_I \varphi_U \left(\psi_{22}(T)\psi_{33}(T) - \psi_{23}(T)\psi_{32}(T)\right). \end{cases}$$

Using the hypothesis $\varphi_U \to 0$, conditions (5.16) hold if and only if $\mathcal{R} = \varphi_I \psi_{22}(T) < 1$. Finally, we obtain the following Lemma for local stability.

Lemma 5.1. *The PDFS $X^T(t)$ is locally asymptotically stable provided that $\mathcal{R} < 1$ and unstable else, where*

$$\mathcal{R} = \frac{\varphi_I}{2\beta}\left[(\beta + k_1 - k_2)e^{\lambda_1 T} + (\beta - k_1 + k_2)e^{\lambda_2 T}\right]. \tag{5.17}$$

Moreover, the following result about the global asymptotic stability of the PDFS $X^T(t)$ of system (5.6) holds.

Theorem 5.1. *The PDFS $X^T(t)$ of system = (5.6) is globally asymptotically stable if $\mathcal{R} < 1$ and unstable else.*

Proof of Theorem 5.1. Let us prove the global attractivity of the PDFS $X^T(t)$. Consider the following subsystem:

$$\begin{cases} \dot{I} = \dfrac{\omega\nu U}{N} S - (\mu + d)I, & t \neq nT; \\ \dot{U} = \gamma I - (\nu + \mu_U)U, & t \neq nT; \\ I(nT^+) = \varphi_I I(nT); \\ U(nT^+) = \varphi_U U(nT). \end{cases} \tag{5.18}$$

The trivial solution of system (5.18) is $(0, 0)$ and the system is cooperative because $\partial I/\partial U = \frac{\omega\nu S}{N} > 0, \partial U/\partial I = \gamma > 0$. As $S(t)/N(t) < 1$, one has that system (5.18) is upper bounded by the following cooperative system:

$$\begin{cases} \dot{I}_1 = \omega\nu U_1 - (\mu + d)I_1, & t \neq nT; \\ \dot{U}_1 = \gamma I_1 - (\nu + \mu_U)U_1, & t \neq nT; \\ I_1(nT^+) = \varphi_I I_1(nT); \\ U_1(nT^+) = \varphi_U U_1(nT). \end{cases} \tag{5.19}$$

Applying Kamke's theorem [33], one has that $I(t) \leq I_1(t), U(t) \leq U_1(t)$ when $I_1(0) = I(0)$ and $U_1(0) = U(0)$. When $\mathcal{R} < 1$, using the previous result of local stability, $(I_1(t), U_1(t)) \to (0^+, 0^+)$. Then, one has

$$(I_1(t), U_1(t)) \to (0^+, 0^+) \Rightarrow (I(t), U(t)) \to (0^+, 0^+).$$

Since $U \to 0^+$, for any arbitrary positive ε_U there exists $t_0 > 0$ such that for $t \geq t_0$, $U(t) \leq \varepsilon_U$. Using non-negativity of the solutions and the fact that $S(t)/N(t) \leq 1$ into the first equation of system (5.6), one has :

$$\Lambda - \omega\nu\varepsilon_U - \mu S(t) \leq \dot{S}(t) \leq \Lambda - \mu S(t)$$

Applying the comparison principle on the above differential inequalities and using the impulsive condition, one has $S_1(t) \leq S(t) \leq S_2(t)$, with $S_1(t)$ and $S_2(t)$ the solutions of the following impulsive differential equations respectively:

$$\begin{cases} \dot{S}_1 = \Lambda - \omega\nu\varepsilon_U - \mu S_1, \ t \neq nT; \\ S_1(nT^+) = \varphi_S S_1(nT), \end{cases}$$

and

$$\begin{cases} \dot{S}_2 = \Lambda - \mu S_2, \ t \neq nT; \\ S_2(nT^+) = \varphi_S S_2(nT). \end{cases}$$

One can observe that $S_1(t) \to S^T_{\varepsilon_U}(t)$ and $S_2(t) \to S^T(t)$ asymptotically. This implies that

$$S^T_{\varepsilon_U}(t) \leq S(t) \leq S^T(t). \tag{5.20}$$

Since we can write ε_U as small as we want using the fact that $U(t) \to 0$, we obtain $S^T_{\varepsilon_U}(t) \to S^T(t)$ when $\varepsilon_U \to 0$. Finally, using (5.20), one has that $S(t) \to S^T(t)$. Which implies that the PDFS is globally attractive. In other words, independently from the initial conditions (S_0, I_0, U_0), one has that

$$(S(t), I(t), U(t)) \to (S^T(t), 0, 0)$$

This concludes the proof of global asymptotic stability. □

5.2.3 Numerical simulations of CLR dynamics

Herein, we present the results of numerical simulations of system (5.1) using ode45 in Matlab to integrate the differential equations during the rainy seasons, with the impulses giving each year's initial conditions. We take $T = 250$ days, which is the length of rainy season in Cameroon [151] and also corresponds to the length of coffee production period. For the simulations, we suppose that all leaves are initially healthy, which means that $I(0) = 0$ leaf, with $S(0) = 500$ leaves. Infection is initiated by uredospores, with $U(0) = 3000$ spores. There are no flowers and berries initially, $F(0) = 0$ flower and $B(0) = 0$ berry, because simulations start at the beginning of the production period. The initial conditions are then

$$(S(0), I(0), U(0), F(0), B(0)) = (500, 0, 3000, 0, 0). \tag{5.21}$$

Table 5.1 summarises the parameter definitions and values used in this paper and that this the calculation of the values of some parameters values.

- The maturation of flowers takes 180 days, which represents stage I + stage II + stage III presented by Torres Castillo et al [159], then the maturation rate is $\theta = 1/180 \approx 0.0055$/day.
- In the coffee tree, a node produces 30 flowers during the owering period ([31], page 59).

Table 5.1: Description and values of parameters for system (5.22).

Symbol	Biological meaning	Value	Source
T	Rainy season duration	250 days	[151]
Λ	Recruitment rate of S	8 leaves/day	Assumed
ω	Germination rate	0.065 leaves/spore	[180, 131]
μ	Mortality rate of leaves	0.0034/day	Assumed
γ	Sporulation rate by I	2 spores/leaf.day	[19]
d	Mortality rate due to CLR	0.056/day	Assumed
ν	Deposition rate	0.09/day	[19]
μ_U	Mortality rate of U	0.015/day	Assumed
φ_S	Reduction rate of S	0.7	Assumed
φ_I	Reduction rate of I	0.4	Assumed
φ_U	Reduction rate of U	0.1	Assumed
δ_S	Flower production rate by S	0.08 flowers/leaf.day	[28]
δ_I	Flower production rate by I	0.04 flowers/leaf.day	[28]
μ_F	Mortality rate of F	$2,4 \times 10^{-3}$/day	[31]
θ	Maturation of F	0.0055/day	[159]
μ_B	Mortality rate of B	$2,4 \times 10^{-3}$/day	[31]
Λ_P	Yearly released quantity of P	*variable* predators	Assumed
a	Consumption rate	*variable* spores/predator.day	Assumed
e	Biomass transformation rate	0.7 predators/spore	Assumed
K	Saturation constant of P	100000 spores	Assumed
μ_P	Mortality rate of P	0.003 & 0.1/day	Assumed
φ_P	Reduction rate of P	0.3	Assumed

Each node has 2 leaves, so a leaf corresponds to 15 flowers. The production of flowers in the model is hence $\delta_S = 0.08$ flowers/leaf.day, we suppose $\delta_I = 0.04$ flowers/leaf.day due to the disease which reduce the production of flowers by the infected leaves.

- In ([31], page 28), on 100 flowers 65 set fruit after pollination. This implies $e^{-180\mu_F} = 0.65$, computation gives $\mu_F = 2.4 \times 10^{-3}$/day. We suppose that the berries have the same mortality rate, then $\mu_B = 2.4 \times 10^{-3}$/day.

In Theorem 5.1, we show that when the spectral radius $\mathcal{R}$ is greater than one, the periodic disease free solution (PDFS) is unstable. In this case, CLR can establish itself, which is confirmed by the solid curve of Figure 5.2, drawn for $\mathcal{R} = 2.53 > 1$.

The dashed curve of Figure 5.2, drawn for $\mathcal{R} = 0.27 < 1$, shows that, for the initial conditions considered, the number of infected leaves and uredospores converges towards zero. The system then converges to the PDFS. We can observe in subplot (a) that, once the stationary regime is established, there are considerably less healthy leaves with endemic CLR (solid curve) than when CLR disappears (dashed curve). The same phenomenon can be observed in subplot (d), which represents the berry trajectories. At the end of the 6^{th} year, the number of berries is 9844 without disease (dashed curve) and 4290 with disease (solid curve), indicating a yield loss larger than 56% due to CLR.

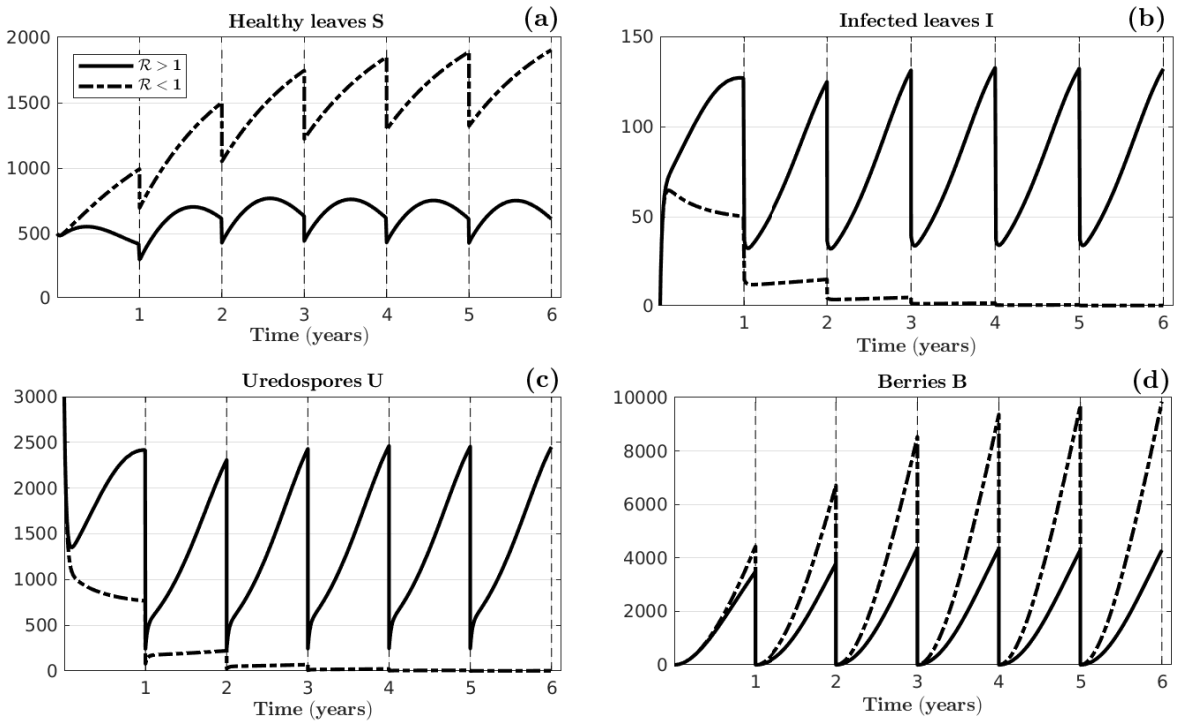

Figure 5.2: Impact of CLR on the production of coffee berries. The plots present the trajectories of impulsive differential system (5.6) when the PDFS is stable (dashed curve, $\gamma = 1.6$ spores/leaf.day $\Rightarrow \mathcal{R} = 0.27 < 1$) and when the PDFS is unstable (solid curve, default value $\gamma = 2$ spores/leaf.day $\Rightarrow \mathcal{R} = 2.53 > 1$). Subplots represent: (a) healthy leaves S, (b) infectious leaves I, (c) uredospores U and (d) berries B. Remaining parameter values are given in Table 5.1 and initial conditions by (5.21).

5.3 Biocontrol of CLR using hyperparasites

To limit the impact of CLR on coffee berry production, we now introduce a biocontrol agent in the model, more specifically an hyperparasite such as *Mycodiplosis*, which consumes uredospores of *H. vastatrix*. The new model is then an extension of system (5.6), to which we add an equation for the hyperparasites (or predators) P, that prey on the uredospores with consumption rate a, biomass transformation rate e and mortality rate μ_P. A proportion φ_P survives the dry season. Our aim is to identify how many and when to release hyperparasites in order to control CLR. In this section, we assume that a quantity Λ_P of hyperparasites is released once a year, at the start of the production season. This translates into a Λ_P jump in the hyperparasite population at each switching moment. The model with biocontrol is then given by

$$\begin{array}{ll} \text{Rainy season for } t \neq nT: & \text{Dry season:} \\ \begin{cases} \dot{S} = \Lambda - \omega\nu U\frac{S}{N} - \mu S; \\ \dot{I} = \omega\nu U\frac{S}{N} - (\mu + d)I; \\ \dot{U} = \gamma I - (\nu + \mu_U)U - aP\frac{U}{K+U}; \\ \dot{P} = eaP\frac{U}{K+U} - \mu_P P; \\ \dot{F} = \delta_S S + \delta_I I - (\theta + \mu_F)F, \\ \dot{B} = \theta F - \mu_B B. \end{cases} & \begin{cases} S(nT^+) = \varphi_s S(nT); \\ I(nT^+) = \varphi_I I(nT); \\ U(nT^+) = \varphi_U U(nT); \\ P(nT^+) = \varphi_P P\,(nT) + \Lambda_P; \\ F(nT^+) = 0. \\ B(nT^+) = 0. \end{cases} \end{array} \tag{5.22}$$

System (5.22) has the same properties as system (5.6) for the existence, uniqueness, non-negativity and boundedness of solutions. We pursue the mathematical analysis and simulations of system (5.22) without the $\dot{F}$ and $\dot{B}$ equations, since berry variable B is not present in the other equations.

5.3.1 Controlled periodic disease free solution and its stability

The controlled periodic disease free solution (cPDFS) occurs when $I = 0$ and $U = 0$. The healthy leaves dynamics are unchanged compared to the PDFS and still satisfy (5.10) while the hyperparasite dynamics are

$$\begin{cases} \dot{P} = -\mu_P P,\ t \neq nT; \\ P(nT^+) = \varphi_P P(nT) + \Lambda_P,\ t = nT. \end{cases} \tag{5.23}$$

Solving equation (5.23) yields

$$P((n+1)T) = P(nT^+)e^{-\mu_P T}.$$

Combined, the above equation and the impulsive condition give

$$P((n+1)T^+) = \varphi_P P(nT^+)e^{-\mu_P T} + \Lambda_P.$$

Then, solving for the fixed point of the above discrete equation and using the dynamics of hyperparasites at the cPDFS yields

$$P^T(t) = \frac{\Lambda_P}{1 - \varphi_P e^{-\mu_p T}} e^{-\mu_P(t-nT)}. \tag{5.24}$$

Thus, the cPDFS for system (5.22) is $Y^T(t) = (S^T(t), 0, 0, P^T(t))$, where $S^T(t)$ and $P^T(t)$ are given in equation (5.10) and (5.24), respectively. We have the following result for the global stability of cPDFS.

Lemma 5.2. *The cPDFS $Y^T(t) = (S^T(t), 0, 0, P^T(t))$ of system (5.22) is globally asymptotically stable when $\mathcal{R} < 1$.*

Proof of Lemma 5.2. Let $\tilde{Y}(t) = Y(t) - Y^T(t)$ where $Y(t) = (S(t), I(t), U(t), P(t))$ and $\tilde{Y}(t)$ is understood as to be small amplitude perturbations. Substituting the expression of $\tilde{Y}(t)$ in the system (5.6) gives

$$\begin{cases} \dot{\tilde{S}} = -\dfrac{\omega\nu\tilde{U}}{\tilde{N} + S^T(t)}(\tilde{S} + S^T(t)) - \mu\tilde{S}, & t \neq nT; \\ \dot{\tilde{I}} = \dfrac{\omega\nu\tilde{U}}{\tilde{N} + S^T(t)}(\tilde{S} + S^T(t)) - (\mu + d)\tilde{I}, & t \neq nT; \\ \dot{\tilde{U}} = \gamma\tilde{I} - (\nu + \mu_U)\tilde{U} - a(\tilde{P} + P^T(t))\dfrac{\tilde{U}}{K + \tilde{U}}, & t \neq nT; \\ \dot{\tilde{P}} = ea(\tilde{P} + P^T(t))\dfrac{\tilde{U}}{K + \tilde{U}} - \mu_P\tilde{P}, & t \neq nT; \\ \tilde{S}(nT^+) = \varphi_S\tilde{S}(nT); \\ \tilde{I}(nT^+) = \varphi_I\tilde{I}(nT); \\ \tilde{U}(nT^+) = \varphi_U\tilde{U}(nT); \\ \tilde{P}(nT^+) = \varphi_P\tilde{P}(nT); \end{cases} \tag{5.25}$$

where $\tilde{N}(t) = \tilde{S}(t) + \tilde{I}(t)$ and $N^T(t) = S^T(t)$.

The linearisation of system (5.25) around $0_{\mathbb{R}^4}$ is

$$\begin{cases} \dot{\tilde{Y}}(t) = G(t)\tilde{Y}(t), & t \neq nT; \\ \tilde{Y}(nT^+) = diag(\varphi_S, \varphi_I, \varphi_U, \varphi_P)\tilde{Y}(nT); \end{cases} \tag{5.26}$$

where

$$G(t) = \begin{pmatrix} -\mu & 0 & -\omega\nu & 0 \\ 0 & -(\mu + d) & \omega\nu & 0 \\ 0 & \gamma & -(\nu + \mu_U) - \frac{aP^T(t)}{K} & 0 \\ 0 & 0 & \frac{eaP^T(t)}{K} & -\mu_P \end{pmatrix}.$$

Solving system (5.26) for $t \in (0, T]$ yields $\tilde{Y}(t) = \Phi_G(t)\tilde{Y}(0^+)$, with $\Phi_G(t)$ the fundamental matrix that satisfies

$$\frac{d\Phi_G(t)}{dt} = G(t)\Phi_G(t),$$

where $\Phi_G(0) = I$. Re-ordering the variables as follows, $(\tilde{S}, \tilde{P}, \tilde{I}, \tilde{U})$, we note that the system is block-triangular. The stability is then determined by considering separately $(\tilde{S}, \tilde{P})$ and the pair $(\tilde{I}, \tilde{U})$. The Floquet multipliers for the first two are $\varphi_S e^{-\mu T}$ and $\varphi_P e^{-\mu_P T}$, which are smaller than one. With this in mind, the stability of system (5.26) reduces to the stability of the following sub-system

$$\begin{cases} \dot{\tilde{Y}}_1(t) = G_1(t)\tilde{Y}_1(t), & t \neq nT; \\ \tilde{Y}(nT^+) = diag(\varphi_I, \varphi_U)\tilde{Y}(nT); \end{cases} \tag{5.27}$$

where

$$Y_1(t) = (I(t), U(t)) \quad \text{and} \quad G_1(t) = \begin{pmatrix} -(\mu + d) & \omega\nu \\ \gamma & -(\nu + \mu_U) - \frac{aP^T(t)}{K} \end{pmatrix}.$$

One can observe that

$$G_1(t) < B = \begin{pmatrix} -(\mu + d) & \omega\nu \\ \gamma & -(\nu + \mu_U) \end{pmatrix}.$$

The monodromy matrix associated to matrix B is the matrix M_1 given in equation (5.15), which is stable if $\mathcal{R} < 1$, where $\mathcal{R}$ is given in equation (5.17). Using the fact that system (5.27) is cooperative, we can conclude that, when $\mathcal{R} < 1$, the cPDFS $Y^T(t)$ is globally asymptotically stable, which implies that CLR dwindles until extinction. □

5.3.2 Semi-numerical analysis of the controlled model

In order to analyse system (5.22) when $\mathcal{R} > 1$, we need to compute the monodromy matrix associated with matrix $G_1(t)$. This is done by numerically solving the linear system (5.27) using the initial conditions $\tilde{Y}_1(0^+) = (1, 0)$ and $\tilde{Y}_1(0^+) = (0, 1)$. The two solutions evaluated at time T are put together to obtain the fundamental matrix. Then we use the impulsive condition to obtain the monodromy matrix.

The monodromy matrix associated with $\tilde{Y}_1$ is

$$M_{G_1} = \begin{pmatrix} \varphi_I & 0 \\ 0 & \varphi_U \end{pmatrix} \Phi_{G_1}(T).$$

We analyse the spectral radius $\mathcal{R}_c$ of this matrix and check that it is smaller than one for the local stability of the cPDFS $Y^T(t)$ of system (5.22). We term this method "semi-numerical" as it requires numerical computations, but not extensive simulations of the system [56].

In Figure 5.3, we plot the threshold level of the spectral radius $\mathcal{R}_c = 1$ of controlled system (5.22) for parameter pairs (Λ_P, a) (subplot (a)) and (ν, γ) (subplot (b)), as well as the threshold stability level $\mathcal{R} = 1$ of uncontrolled system (5.1) for parameter pair (ν, γ). In subplot (a), the regions below and above the blue curve are, respectively, the unstable and stable regions of the cPDFS of controlled system (5.22). As expected, stability of the cPDFS is guaranteed for large values of the yearly quantity of predators released Λ_P, and of the predator consumption rate a. Also, when the predator capacity to consume uredospores is higher, less predators are needed for the extinction of the disease, and vice versa. The blue dot corresponds to parameter values ensuring a stable cPDFS, values that are used for the blue curve in subplot (b).

In subplot (b), as in subplot (a), the blue curve separates the unstable and stable regions of the cPDFS of the controlled system; moreover, the black curve separates these two regions for the uncontrolled system. The parameter region between these two curves hence represents the gain obtained by adding the biocontrol: in this region, CLR goes extinct with biocontrol, but persists without. Subplot (b) shows that, in order to eliminate CLR through the proposed biocontrol effort, the sporulation and deposition rate should not be too large.

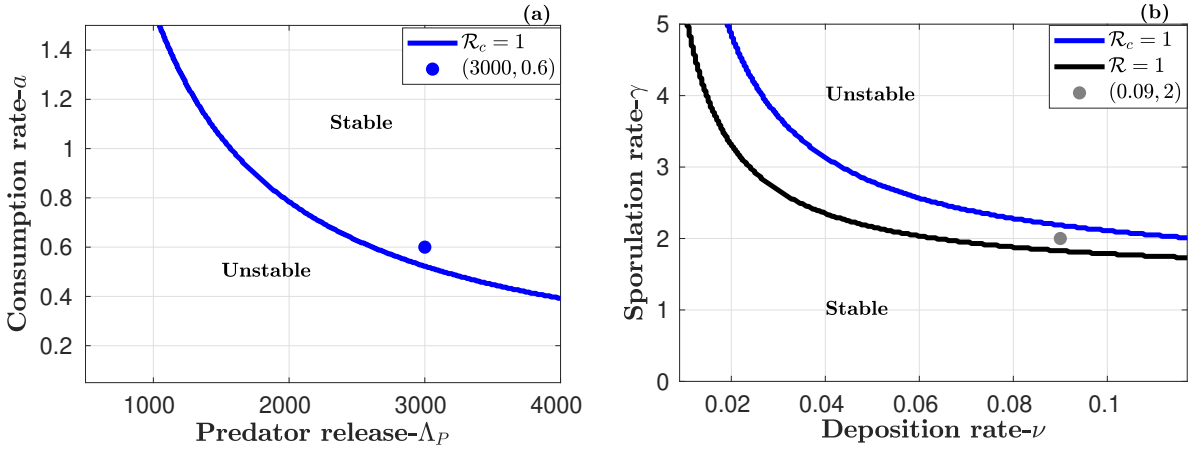

Figure 5.3: Stability regions of periodic disease free solutions as functions of model parameters. Blue curves represent the threshold $\mathcal{R}_C = 1$ separating the stable and unstable regions of the model with predator (5.22), for different values of parameter pair (Λ_P, a) in subplot (a) and (ν, γ) in subplot (b); moreover, the black curve $\mathcal{R} = 1$ in subplot (b) separates the stable and unstable regions of the model without predator (5.1). The blue dot in subplot (a) corresponds to the (Λ_P, a) values used for the blue curve in subplot (b). Similarly, the grey dot in subplot (b) corresponds to the default (ν, γ) values used for the blue curve in subplot (a). Remaining parameter values are given in Table 5.1.

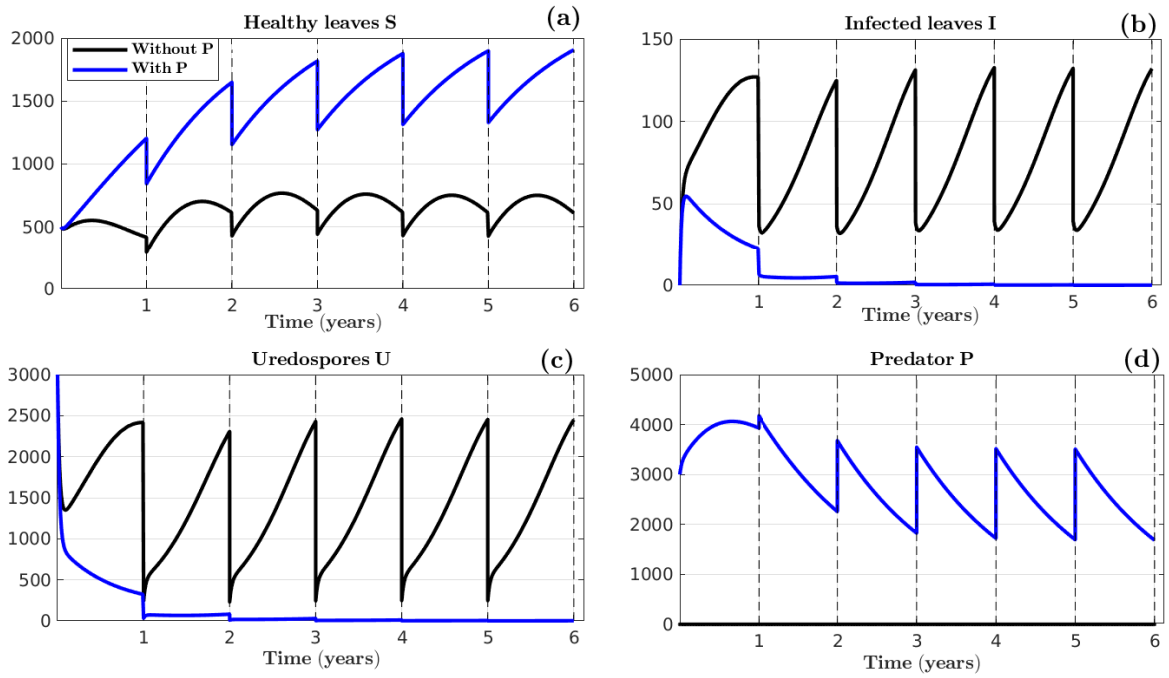

Figure 5.4: Impact of biocontrol on the system dynamics. 6-year simulations of model (5.1) without predator (black curve) and model (5.22) with predator (blue curve), using initial conditions (5.28): (a) healthy leaves S; (b) infected leaves I; (c) uredospores U and (d) predator (hyperparasites) P. All parameter values are given in Table 5.1 and correspond to $\mathcal{R} = 2.53 > 1$.

5.3.3 Asymptotic behaviour for yearly releases

Herein, we investigate the asymptotic behaviour of system (5.22) when predators are released once a year at the beginning of each production period. To do so, we consider the parameter values given by the two dots in the stability regions of Figure 5.3. We point out that the gray dot in subplot (b) of Figure 5.3 is in the instability region of system (5.22) without control which means that the CLR would persist in the coffee plantation if unchecked. We consider the initial condition given in equation (5.21), adding the initial release of predators $P(0^+) = \Lambda_P = 3000$, which yields

$$(S(0^+), I(0^+), U(0^+), P(0^+), F(0^+), B(0^+)) = (500, 0, 3000, 3000, 0, 0). \tag{5.28}$$

Figure 5.4 compares the temporal dynamics of system (5.1) without control (black curves) and model (5.22) with control (blue curves). From this figure, one can observe that under the actions of biocontrol, the number of healthy leaves increases and becomes stationary (see Figure 5.4(a)), while the number of infectious leaves and uredospores dwindles until extinction (see Figures 5.4(b) and (c)). During the first year, the quantity of predators (hyperparasites) increases through uredospore consumption. From the second year on, the number of uredospores is very close to zero, so that the solution is close to the cPDFS. Biocontrol using hyperparasites reduces drastically CLR in the coffee plantation.

5.4 Multiple releases of hyperparasites per year

In this section, we suppose that the yearly quantity Λ_P of hyperparasites is released at different times over the year: it is uniformly divided into m releases of size $\frac{\Lambda_P}{m}$, with release interval $\frac{T}{m}$. We thus obtain an impulsive model with a new switching condition for the predator, given by

$$
\begin{aligned}
&\text{Rainy season for } t \neq nT: \\
&\begin{cases}
\dot{S} = \Lambda - \omega\nu U\dfrac{S}{N} - \mu S; \\
\dot{I} = \omega\nu U\dfrac{S}{N} - (\mu + d)I; \\
\dot{U} = \gamma I - (\nu + \mu_U)U - aP\dfrac{U}{K+U}; \\
\dot{P} = eaP\dfrac{U}{K+U} - \mu_P P, \qquad t \neq nT + \dfrac{j}{m}T; \\
\dot{F} = \delta_S S + \delta_I I - (\theta + \mu_F)F \\
\dot{B} = \theta F - \mu_B B.
\end{cases} \\
&\text{Predator releases for } j \in \{1, ..., m-1\}: \\
&P\left(nT + \frac{j}{m}T^+\right) = P\left(nT + \frac{j}{m}T\right) + \frac{\Lambda_P}{m}; \\
&\text{Dry season:} \\
&\begin{cases}
S(nT^+) = \varphi_s S(nT); \\
I(nT^+) = \varphi_I I(nT); \\
U(nT^+) = \varphi_U U(nT); \\
P(nT^+) = \varphi_P P\,(nT) + \dfrac{\Lambda_P}{m}; \\
F(nT^+) = 0 \\
B(nT^+) = 0.
\end{cases}
\end{aligned}
\tag{5.29}
$$

System (5.29) has the same properties as system (5.6) for the existence, uniqueness, non-negativity, and boundedness of solution. We made the mathematical analysis of system (5.29) without $\dot{F}$ and $\dot{B}$ equations, since B is not present in other equations.

5.4.1 Multiple release controlled periodic disease free solution and its stability

To compute the multiple release controlled periodic disease free solution (m-cPDFS), we only consider the first year for readability purposes, which means that $t \in (0, T]$. The m-cPDFS of biocontrol system (5.29) occurs when $I = 0$ and $U = 0$, so healthy leaf dynamics are unchanged compared to the PDFS and still satisfy (5.10); the hyperparasite dynamics are

$$
\begin{cases}
\dot{P} = -\mu_P P, & t \neq nT; \\
P\left(\dfrac{j}{m}T^+\right) = P\left(\dfrac{j}{m}T\right) + \dfrac{\Lambda_P}{m}, & \text{for } j = 1, \ldots, m-1; \\
P(T^+) = \varphi_P P\left(\dfrac{(m-1)}{m}T\right) + \dfrac{\Lambda_P}{m}.
\end{cases}
\tag{5.30}
$$

Solving equation $\dot{P} = -\mu_P P$ for $t \in]\frac{jT}{m}, \frac{(j+1)T}{m}]$ we obtain

$$P(t) = P\left(\frac{jT^+}{m}\right) e^{-\mu_P\left(t-\frac{jT}{m}\right)}. \tag{5.31}$$

Using equation (5.31) and the second equation of (5.30) we have

$$P\left(\frac{(j+1)}{m}T^+\right) = P\left(\frac{jT^+}{m}\right) e^{-\mu_P \frac{T}{m}} + \frac{\Lambda_P}{m}.$$

For $j = 0$

$$P\left(\frac{T^+}{m}\right) = P\left(0^+\right) e^{-\mu_P \frac{T}{m}} + \frac{\Lambda_P}{m}.$$

For $j = 1$

$$\begin{aligned} P\left(\frac{2T^+}{m}\right) &= \left(P\left(0^+\right) e^{-\mu_P \frac{T}{m}} + \frac{\Lambda_P}{m}\right) e^{-\mu_P \frac{T}{m}} + \frac{\Lambda_P}{m}; \\ &= P\left(0^+\right) e^{-\mu_P \frac{2T}{m}} + \frac{\Lambda_P}{m} e^{-\mu_P \frac{T}{m}} + \frac{\Lambda_P}{m}. \end{aligned}$$

For $j = 2$

$$P\left(\frac{3T^+}{m}\right) = P\left(0^+\right) e^{-\mu_P \frac{3T}{m}} + \frac{\Lambda_P}{m} \sum_{i=0}^{2} e^{-\mu_P \frac{iT}{m}}.$$

Generally, for all $j = 0, ...m-1$

$$\begin{aligned} P\left(\frac{jT^+}{m}\right) &= P\left(0^+\right) e^{-\mu_P \frac{jT}{m}} + \frac{\Lambda_P}{m} \sum_{i=0}^{j-1} e^{-\mu_P \frac{iT}{m}}; \\ &= P\left(0^+\right) e^{-\mu_P \frac{jT}{m}} + \frac{\Lambda_P}{m} \left(\frac{1 - e^{-\mu_P \frac{jT}{m}}}{1 - e^{-\mu_P \frac{T}{m}}}\right), \end{aligned}$$

in particular for $j = m-1$, that is

$$P\left(\frac{(m-1)T^+}{m}\right) = P\left(0^+\right) e^{-\mu_P \frac{(m-1)T}{m}} + \frac{\Lambda_P}{m} \left(\frac{1 - e^{-\mu_P \frac{(m-1)T}{m}}}{1 - e^{-\mu_P \frac{T}{m}}}\right).$$

Using this latter expression and the third equation of (5.30), we obtain

$$P\left(T^+\right) = \varphi_P \left[P\left(0^+\right) e^{-\mu_P T} + \frac{\Lambda_P}{m} \left(\frac{e^{-\mu_P \frac{T}{m}} - e^{-\mu_P T}}{1 - e^{-\mu_P \frac{T}{m}}}\right)\right] + \frac{\Lambda_P}{m}.$$

The value for which $P\left(T^+\right) = P\left(0^+\right)$ is

$$P\left(0^+\right) = \frac{\Lambda_P}{m} \left[\frac{\varphi_P \left(e^{-\mu_P \frac{T}{m}} - e^{-\mu_P T}\right) + 1 - e^{-\mu_P \frac{T}{m}}}{\left(1 - \varphi_P e^{-\mu_P T}\right)\left(1 - e^{-\mu_P \frac{T}{m}}\right)}\right].$$

So we can conclude that, for $t \in]\frac{jT}{m}, \frac{(j+1)T}{m}]$, the m-cPDFS is given by $Z^T(t) =$

$(S^T(t), 0, 0, P^T_{m,j}(t))$, with $S^T(t)$ given by equation (5.10) and

$$P^T_{m,j}(t) = \left[P\left(0^+\right) e^{-\mu_P \frac{jT}{m}} + \frac{\Lambda_P}{m} \left(\frac{1 - e^{-\mu_P \frac{jT}{m}}}{1 - e^{-\mu_P \frac{T}{m}}} \right) \right] e^{-\mu_P \left(t - \frac{jT}{m}\right)}, \tag{5.32}$$

$P(0^+)$ being defined above.

Then, the m-cPDFS is $Z^T(t) = (S^T(t), 0, 0, P^T_{m,j}(t))$, for $t \in]\frac{jT}{m}, \frac{(j+1)T}{m}]$, where $S^T(t)$ is given by (5.10) and $P^T_{m,j}(t)$ by

$$P^T_{m,j}(t) = \left[P\left(0^+\right) e^{-\mu_P \frac{jT}{m}} + \frac{\Lambda_P}{m} \left(\frac{1 - e^{-\mu_P \frac{jT}{m}}}{1 - e^{-\mu_P \frac{T}{m}}} \right) \right] e^{-\mu_P \left(t - \frac{jT}{m}\right)}, \tag{5.33}$$

with

$$P\left(0^+\right) = \frac{\Lambda_P}{m} \left[\frac{\varphi_P \left(e^{-\mu_P \frac{T}{m}} - e^{-\mu_P T} \right) + 1 - e^{-\mu_P \frac{T}{m}}}{\left(1 - \varphi_P e^{-\mu_P T}\right) \left(1 - e^{-\mu_P \frac{T}{m}}\right)} \right]. \tag{5.34}$$

Lemma 5.3. *The m-cPDFS $Z^T(t) = (S^T(t), 0, 0, P^T_{m,j}(t))$ of controlled model with multiple releases, is globally asymptotically stable when $\mathcal{R} < 1$*

Proof of Lemma 5.3. The proof is similar to the proof of Lemma 5.2 which holds for one release per year. □

To present the impact of the multiple release strategy on CLR control, we first compute a proxy of the control intensity over the season, namely the yearly average number of hyperparasites present in the plantation for the m-cPDFS. This quantity depends on m, the number of hyperparasite releases per year.

The yearly average number of hyperparasites for the m-cPDFS is computed over the interval $[0, T]$ as follows:

$$g(m) = \int_0^T P^T(t)dt = \sum_{j=0}^{m-1} \int_{\frac{jT}{m}}^{\frac{(j+1)T}{m}} P^T_{m,j}(t)dt.$$

Replacing $P^T_{m,j}(t)$ by its expression in equation (5.33), we obtain

$$\begin{aligned}
g(m) &= \sum_{j=0}^{m-1} \int_{\frac{jT}{m}}^{\frac{(j+1)T}{m}} \left[P\left(0^+\right) e^{-\mu_P \frac{jT}{m}} + \frac{\Lambda_P}{m} \left(\frac{1 - e^{-\mu_P \frac{jT}{m}}}{1 - e^{-\mu_P \frac{T}{m}}} \right) \right] e^{-\mu_P \left(t - \frac{jT}{m}\right)}(t)dt; \\
&= \sum_{j=0}^{m-1} \left[P\left(0^+\right) e^{-\mu_P \frac{jT}{m}} + \frac{\Lambda_P}{m} \left(\frac{1 - e^{-\mu_P \frac{jT}{m}}}{1 - e^{-\mu_P \frac{T}{m}}} \right) \right] \int_{\frac{jT}{m}}^{\frac{(j+1)T}{m}} e^{-\mu_P \left(t - \frac{jT}{m}\right)}(t)dt; \\
&= \sum_{j=0}^{m-1} \left[P\left(0^+\right) e^{-\mu_P \frac{jT}{m}} + \frac{\Lambda_P}{m} \left(\frac{1 - e^{-\mu_P \frac{jT}{m}}}{1 - e^{-\mu_P \frac{T}{m}}} \right) \right] \left[\frac{1 - e^{-\mu_P \frac{T}{m}}}{\mu_P} \right].
\end{aligned}$$

Replacing $P(0^+)$ by its expression in equation (5.34), we obtain

$$\begin{aligned}
g(m) &= \sum_{j=0}^{m-1}\left[\frac{\Lambda_P}{m}\left(\frac{\varphi_P\left(e^{-\mu_P\frac{T}{m}}-e^{-\mu_P T}\right)+1-e^{-\mu_P\frac{T}{m}}}{(1-\varphi_P e^{-\mu_P T})\left(1-e^{-\mu_P\frac{T}{m}}\right)}\right)e^{-\mu_P\frac{jT}{m}}\right] \\
&\quad+\sum_{j=0}^{m-1}\left[\frac{\Lambda_P}{m}\left(\frac{1-e^{-\mu_P\frac{jT}{m}}}{1-e^{-\mu_P\frac{T}{m}}}\right)\right]\left[\frac{1-e^{-\mu_P\frac{T}{m}}}{\mu_P}\right], \\
&= \frac{\Lambda_P}{m\mu_P}\sum_{j=0}^{m-1}\left[\frac{\varphi_P\left(e^{-\mu_P\frac{T}{m}}-e^{-\mu_P T}\right)+1-e^{-\mu_P\frac{T}{m}}}{(1-\varphi_P e^{-\mu_P T})}e^{-\mu_P\frac{jT}{m}}+1-e^{-\mu_P\frac{jT}{m}}\right], \\
&= \frac{\Lambda_P}{m\mu_P}\left[\left(\frac{\varphi_P\left(e^{-\mu_P\frac{T}{m}}-e^{-\mu_P T}\right)+1-e^{-\mu_P\frac{T}{m}}}{(1-\varphi_P e^{-\mu_P T})}\right)\left(\frac{1-e^{-\mu_P T}}{1-e^{-\mu_P\frac{T}{m}}}\right)\right. \\
&\quad\left.+m-\frac{1-e^{-\mu_P T}}{1-e^{-\mu_P\frac{T}{m}}}\right], \\
&= \frac{\Lambda_P}{m\mu_P}\left[\left(\frac{(\varphi_P-1)e^{-\mu_P\frac{T}{m}}}{(1-\varphi_P e^{-\mu_P T})}\right)\left(\frac{1-e^{-\mu_P T}}{1-e^{-\mu_P\frac{T}{m}}}\right)+m\right].
\end{aligned}$$

Simplifying this expression, we finally obtain

$$g(m) = \left(\frac{-\Lambda_P(1-\varphi_P)(1-e^{-\mu_P T})}{\mu_P\left(1-\varphi_P e^{-\mu_P T}\right)}\right)\frac{1}{m(e^{\mu_P\frac{T}{m}}-1)}+\frac{\Lambda_P}{\mu_P}.$$

Then,

$$g(m) = \int_0^T P^T(t)dt = \sum_{j=0}^{m-1}\int_{\frac{jT}{m}}^{\frac{(j+1)T}{m}} P^T_{m,j}(t)dt = \frac{\Gamma}{m(e^{\mu_P\frac{T}{m}}-1)}+\frac{\Lambda_P}{\mu_P}, \tag{5.35}$$

with

$$\Gamma = \frac{-\Lambda_P(1-\varphi_P)(1-e^{-\mu_P T})}{\mu_P\left(1-\varphi_P e^{-\mu_P T}\right)}.$$

Differentiating $g(m)$ with respect to m, one has

$$g'(m) = \frac{\Gamma e^{\mu_P\frac{T}{m}}\left(e^{-\mu_P\frac{T}{m}}+\frac{\mu_P T}{m}-1\right)}{m^2(e^{\mu_P\frac{T}{m}}-1)^2}.$$

Since $e^{-\mu_P\frac{T}{m}}$ is always larger than its first order approximation $1-\frac{\mu_P T}{m}$ for $\frac{T}{m}>0$, all factors are positive except Γ, so that $g'(m)<0$. This allows to conclude that the yearly average number of hyperparasites decreases with the number of releases per year, without CLR (quantity computed for the m-cPDFS). One might then think that spreading Λ_P over several releases is less efficient than releasing everything at the beginning of the season. This is investigated below through simulation.

We use two contrasted predator mortality rates to simulate the solution $P^T_{m,j}(t)$ in the m-cPDFS. Subplots (a) and (b) of Figure 5.5 present the simulation of $P^T_{m,j}(t)$ for various release frequencies and for both mortality rates over three years; they illustrate the important impact these two factors on the m-cPDFS.

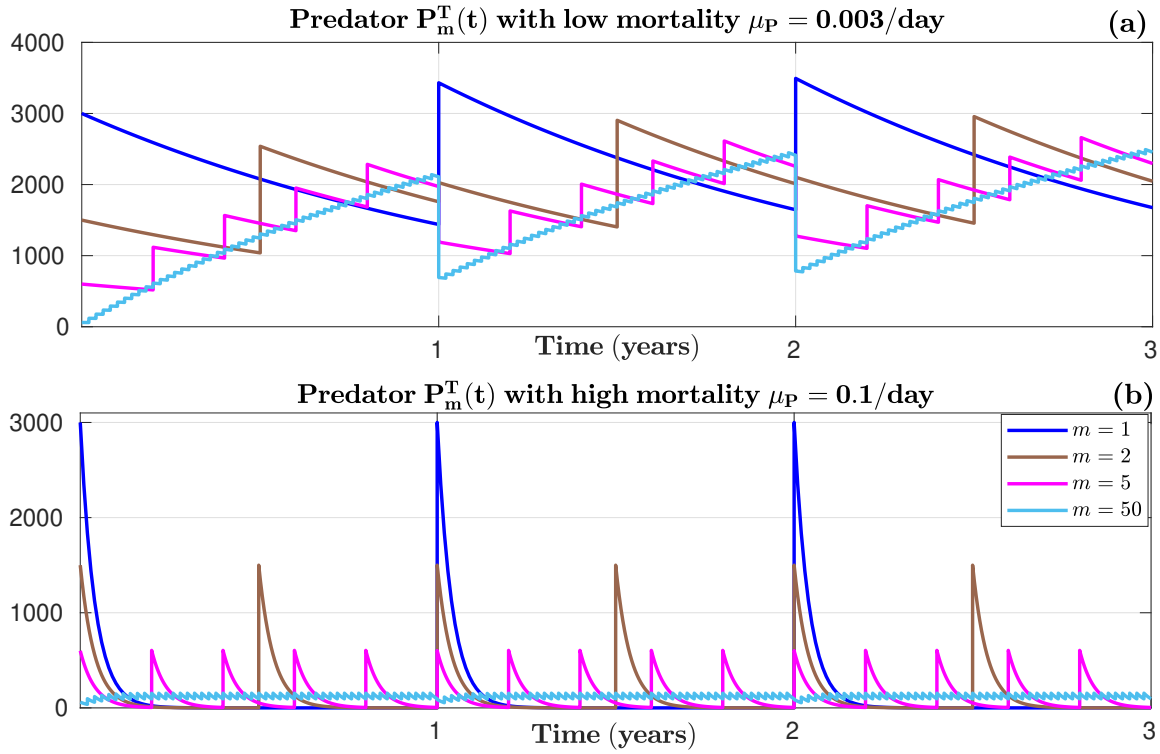

Figure 5.5: Impact of the predator mortality and its release frequency on its dynamics without CLR. The plots present the predator dynamics of the m-cPDFS (multiple release controlled periodic disease free solution) of system (5.29) for: (a) the default low mortality rate $\mu_P = 0.003/day$; and (b) a high mortality rate $\mu_P = 0.1/day$. Various release frequencies are plotted: $m = 1$ (blue curve), $m = 2$ (brown curve), $m = 5$ (magenta curve) and $m = 50$ (light blue curve) releases per year. Initial condition is $P(0^+)$ given in (5.34), so the solutions are periodic. The yearly released quantity is $\Lambda_P = 3000$ predators. Remaining parameter values are given in Table 5.1.

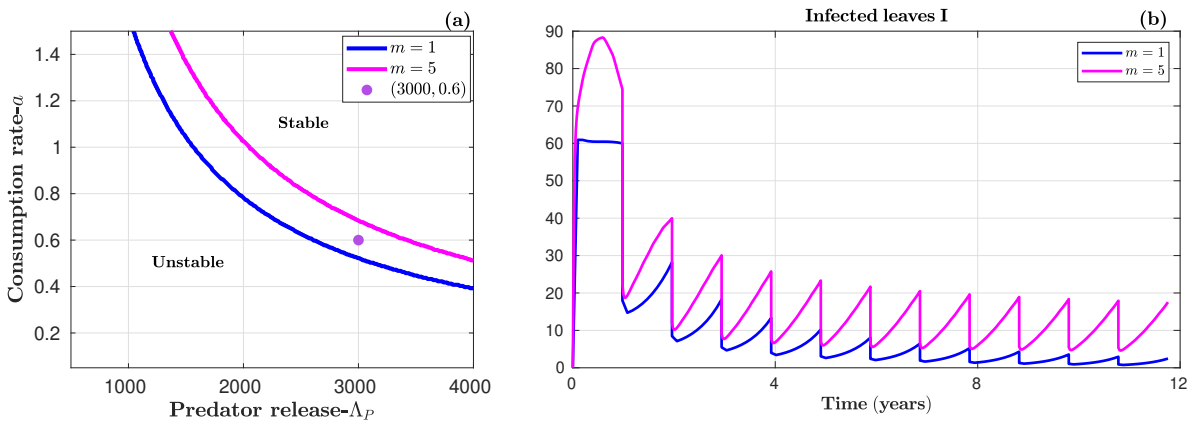

Figure 5.6: Impact of release frequency on the stability for low predator mortality rate $\mu_P = 0.003$/day. Subplot (a) presents the stable and unstable regions of the m-cPDFS of system (5.29) according to parameter pair (Λ_P, a). The regions are separated by $\mathcal{R}_{c,m} = 1$ for $m = 1$ (blue curve) or $m = 5$ (magenta curve) releases/year. Subplot (b) shows the dynamics of infected leaves I for parameter values ($\Lambda_P = 3000$ predators, $a = 0.6$ spores/predator.day) corresponding to the purple dot in subplot (a). Remaining parameter values are given in Table 5.1 and initial conditions by (5.36).

5.4.2 Impact of release frequency on CLR control

Herein, we present the impact of the yearly hyperparasite release frequency on CLR control. This is first done using the semi-numerical analysis of the model with multiple releases, to show the (Λ_p, a)-stability region of the m-cPDFS (as in Figure 5.3), for different values of the release number m. Secondly, we present simulations of the dynamic behaviour of system (5.29).

In all simulations, the epidemiological parameters are set to their value in Table 5.1. The only parameters that vary are the ones related to the hyperparasites: Λ_p, a, μ_p and m. As in Figure 5.5, we use two contrasted values for the predator mortality μ_p, the low and high values representing respectively a favourable and unfavourable environment for the hyperparasites.

Moreover, we consider that an initial hyperparasite release occurs at time 0 with the usual initial conditions (5.21) for the other variables, so that

$$(S(0^+), I(0^+), U(0^+), P(0^+), F(0^+), B(0^+)) = (500, 0, 3000, \frac{\Lambda_P}{m}, 0, 0) \tag{5.36}$$

5.4.2.1 Impact on stability

Herein, we present the impact of the yearly release frequency on the m-cPDFS stability of controlled system (5.29), for the two contrasted predator mortality rates depicted in Figure 5.5. Only two release frequencies are considered, $m = 1$ and $m = 5$ releases per year, as results obtained for $m = 5$ also hold for higher frequencies.

Case 1 – Less frequent is more effective (low mortality rate $\mu_P = 0.003$/day) In subplot (a) of Figure 5.6, $\mathcal{R}_{c,1} = 1$ for $m = 1$ (blue curve) and $\mathcal{R}_{c,5} = 1$ for $m = 5$ (magenta curve) separate the instability (below) and stability (above) regions of the m-cPDFS of controlled system (5.29), when parameters (Λ_P, a) vary. The stability region is greater for $m = 1$ than for $m = 5$, that is when the yearly release frequency is lower.

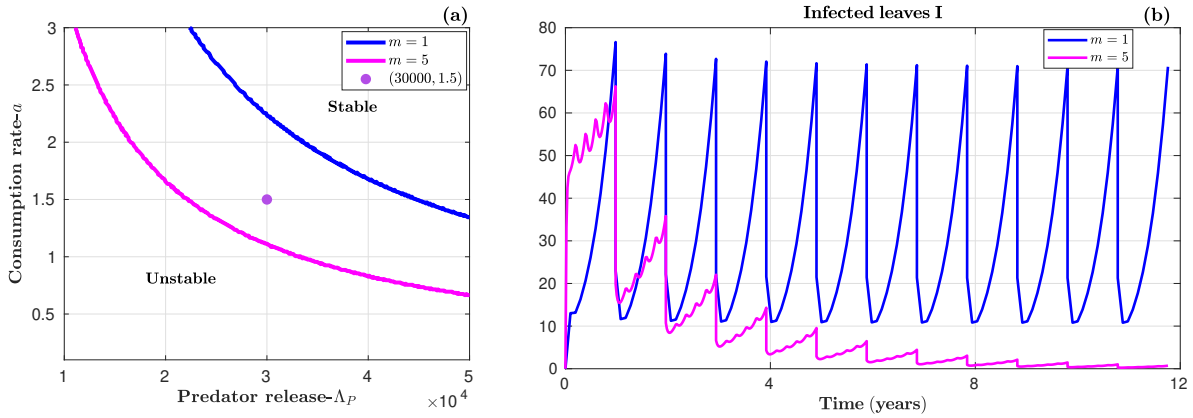

Figure 5.7: Impact of release frequency on the stability for high predator mortality rate $\mu_P = 0.1$/day. Subplot (a) presents the stable and unstable regions of the m-cPDFS of system (5.29) according to parameter pair (Λ_P, a). The regions separated by $\mathcal{R}_{c,m} = 1$ for $m = 1$ (blue curve) or $m = 5$ (magenta curve) releases/year. Subplot (b) shows the dynamics of infected leaves I for parameter values ($\Lambda_P = 30000$ predators, $a = 1.5$ spores/predator.day) corresponding to the purple dot in subplot (a). Remaining parameter values are given in Table 5.1 and initial conditions by (5.36)

Subplot (b) of Figure 5.6 illustrates the long term dynamics (over 12 years) of the infected leaves of system (5.29), with initial conditions (5.36), for parameter values $\Lambda_P = 3000$ predators and $a = 0.6$ spores/predator.day, which correspond to the purple dot in subplot (a). As expected from subplot (a), CLR goes extinct for one release per year (blue curve), while it persists for five releases per year (magenta curve).

Therefore, if the hyperparasite mortality is very low, the best strategy for eradicating CLR is to release hyperparasites once a year at the beginning of the season, implying that releasing less frequently in larger quantity is the most effective. This is consistent with the control intensity proxy computed in equation (5.35), which is higher for lower frequencies.

Case 2 – More frequent is more effective (high mortality rate $\mu_P = 0.1$/day) Figure 5.7 is built as Figure 5.6, but for a high predator mortality. In subplot (a), as opposed to what is observed for low mortality, the stability region is greater for $m = 5$ than for $m = 1$, that is when the yearly release frequency is higher.

Subplot (b) is plotted with parameter values $\Lambda_P = 30000$ predators and $a = 1.5$ spores/predator.day, which correspond to the purple dot in subplot (a). As expected from subplot (a), CLR extinction is achieved for five releases per year but not for one release per year. Infected leaves I behave quite differently. For $m = 1$, I decrease at the beginning of each year and then increase sharply; indeed, the hyperparasite population is large at the beginning of the year, but declines sharply due to the high mortality rate (see Figure 5.5(b)), so that CLR is not kept in check. By contrast, for $m = 5$, hyperparasites do not stay close to 0 for long so that no large increase of I occurs.

For high predator mortality, the best strategy to control CLR is to release hyperparasites five times per year, meaning that more frequent releases are better. This conclusion was not obvious, considering that the control intensity proxy computed in equation (5.35) is lower for more frequent releases.

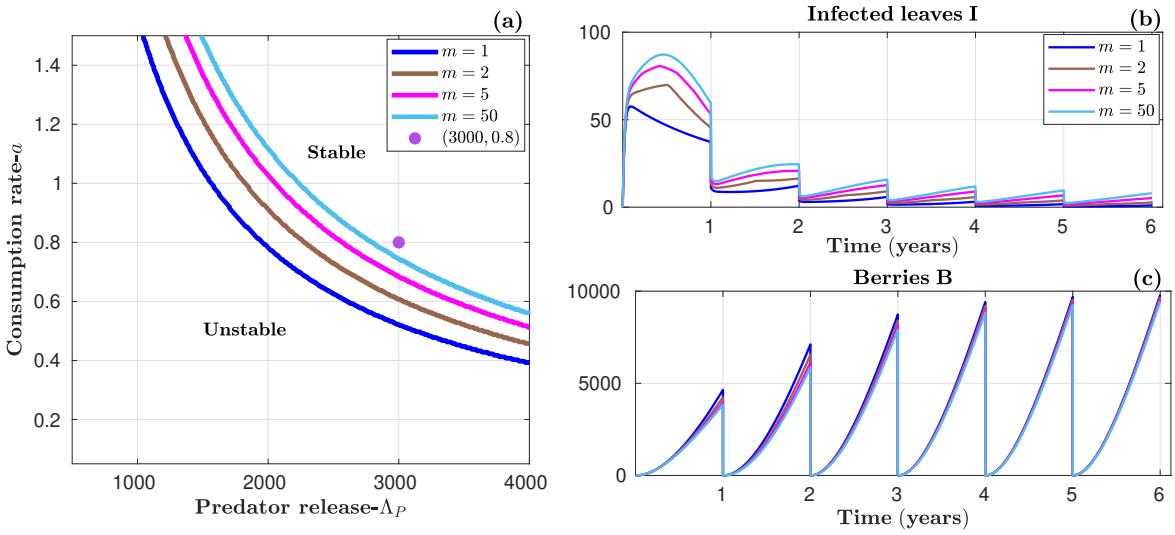

Figure 5.8: Impact of release frequency on the transient dynamics with low predator mortality. Subplot (a) presents the stable and unstable regions of the m-cPDFS of system (5.29) according to parameter pair (Λ_P, a). The regions are separated by $\mathcal{R}_{c,m} = 1$ for $m = 1$ (blue curve), $m = 2$ (brown curve), $m = 5$ (magenta curve) or $m = 50$ (light blue curve) releases/year. Subplots (b) and (c) show the dynamics of infected leaves I and berries B for parameter values ($\Lambda_P =$ 3000 predators, $a = 0.8$ spores/predator.day) corresponding to the purple dot in subplot (a). Remaining parameter values are given in Table 5.1 and initial conditions by (5.36).

5.4.2.2 Impact on transient dynamics

Herein, we still look at the impact of the yearly release frequency, for the same contrasted predator mortality rates, but we focus on the first years and assume that the m-cPDFS of controlled system (5.29). Four frequency values are considered, namely $m = 1, 2, 5, 50$ releases per year.

Case 1 – Less frequent is faster (low mortality rate $\mu_P = 0.003$/day) Just as Figure 5.6(a), subplot (a) of Figure 5.8 displays the instability (below) and stability (above) regions of the m-cPDFS of controlled system (5.29). These regions are separated by $\mathcal{R}_{c,1} = 1$ for $m = 1$ release/year (blue curve), $\mathcal{R}_{c,2} = 1$ for $m = 2$ releases/year (brown curve), $\mathcal{R}_{c,5} = 1$ for $m = 5$ releases/year (magenta curve) and $\mathcal{R}_{c,50} = 1$ for $m = 50$ releases/year (light blue curve). Subplot (a) confirms that for low hyperparasite mortality, the best strategy for controlling CLR is to release the hyperparasites once a year at the beginning of the season.

Figure 5.8 also shows the temporal evolution of infected leaves (subplot (b)) and berries (subplot (c)), using initial conditions (5.36) and parameter values $\Lambda_P = 3000$ predators and $a = 0.8$ spores/predator.day. These parameter values, which correspond to the purple dot in subplot (a), ensure that the m-CPDFS is stable for all four values of the release frequency m. In subplot (b), we can observe that the disease is driven to extinction for $m = 1$ (blue curve). For $m = 5$ (magenta curve) and $m = 50$ (light blue curve), the number of infected leaves after six years is still notably greater than zero (less notably so for $m = 2$, brown curve). However, if we increase the number of years, the extinction will be observed for all values of m.

Subplot (c) shows that the number of berries at the end of each year decreases when m increases. This confirms our previous result: the best strategy for low hyperparasite mortality is

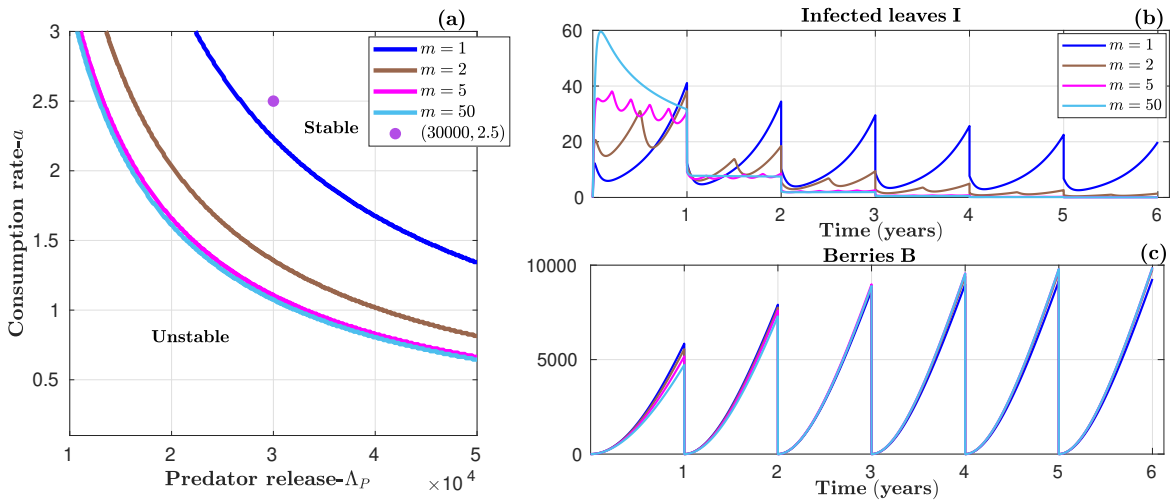

Figure 5.9: Impact of release frequency on the transient dynamics with high predator mortality. Subplot (a) presents the stable and unstable regions of the m-cPDFS of system (5.29) according to parameter pair (Λ_P, a). The regions are separated by $\mathcal{R}_{c,m} = 1$ for $m = 1$ (blue curve), $m = 2$ (brown curve), $m = 5$ (magenta curve) or $m = 50$ (light blue curve) releases/year. Subplots (b) and (c) show the dynamics of infected leaves I and berries B for parameter values ($\Lambda_P = 30000$ predators, $a = 2.5$ spores/predator.day) corresponding to the purple dot in subplot (a). Remaining parameter values are given in Table 5.1 and initial conditions by (5.36).

to few releases per year.

Case 2 – Best strategy depends on the horizon (high mortality rate $\mu_P = 0.1$) As expected for high hyperparasite mortality, in subplot (a) of Figure 5.9, the $\mathcal{R}_{c,m} = 1$ curves, delimiting the stable and unstable regions of the m-cPDFS, are in reverse order compared to Figure 5.8(a). However, we should note that $\mathcal{R}_{c,5} = 1$ (magenta curve) and $\mathcal{R}_{c,50} = 1$ (light blue curve) are almost indistinguishable, implying that both strategies are almost equivalent in terms of eradication success.

Subplots (b) and (c) of Figure 5.9 are built using parameter values $\Lambda_P = 30000$ predators and $a = 2.5$ spores/predator.day, which correspond to the purple dot in subplot (a)). In subplot (b), we observe CLR extinction in all cases but for $m = 1$, for which extinction takes longer. In the latter case, the high mortality rate drives the hyperparasite population to very small values very quickly so that it is absent for most of the season, which slows down the control process.

To better explain the impact of the high hyperparasite mortality on berries depicted in subplot (c), we consider the number of berries at the end of each season and thus we obtain Table 5.2. The majority of parameter values of the model are certainly assumed, but this qualitative study shows the effectiveness of the biocontrol of CLR using hyperparasite

In terms of berry production, the best strategy from the first year to the second year is to release the hyperparasites once. From year 3 to year 4, the highest berry production occurs with $m = 5$ releases per year. From year 5 and on, the production increases with the release frequency, which is the result expected in the case of high predator mortality. However, except for $m = 1$, the berry production numbers are then almost all identical since CLR is nearly eradicated. Therefore, the best release strategy depends on the time horizon considered.

Table 5.2: Berry production at the end of each season, for different yearly release frequencies and high predator mortality. Production values correspond to subplot (c) of Figure 5.9. The optimal production for each year is enhanced in bold.

	Releases per year			
	$m = 1$	$m = 2$	$m = 5$	$m = 50$
year 1	**5845**	5554	5131	4717
year 2	**7906**	7756	7600	7290
year 3	8663	8866	**8985**	8897
year 4	8987	9399	**9568**	9553
year 5	9159	9657	9793	**9796**
year 6	9270	9785	9876	**9880**

5.4.2.3 Summary

From the four cases described above, we can conclude that the best hyperparasite release strategy, in terms of CLR control and berry production, strongly depends on hyperparasite characteristics, namely its mortality rate (μ_P) and its uredospore consumption rate (a). Both parameters determine the yearly released quantity of hyperparasites (Λ_P) needed to control CLR. Moreover, the mortality rate has an impact on the best hyperparasite release frequency (m). On the long run, more frequent is more effective for high hyperparasite mortality, and vice versa for low mortality. On the shorter run however, less frequent may also be better for high mortality.

5.5 Discussion

In this work, we built an original impulsive model of coffee leaf rust dynamics in a coffee plantation, in which the non production (dry) season takes the form of an impulse, it is based in a previous study [38]. There are few CLR models in the literature and they represent different geographical scales, from the individual coffee bush to the country or even the continent. Bebber et al. determined the germination and infection risk depending on the climate in Colombia and neighbouring countries, based upon existing experimental data [15]. In contrast to these static approaches, Vandermeer et al. studied the interaction between the regional and local dynamics of CLR model by representing the evolution of the proportion of infected bushes and farms [169]. Vandermeer et al. also represented the CLR dynamics in a coffee farm in Chiapas using an SI (susceptible–infected) epidemiological model of the host and concluded that the network approach can be a useful way of gaining qualitative insight about disease dynamics in space [165].

The originality of our model, compared to the dynamical approaches above, is the hybrid formalism that is particularly suited to describe the seasonality of coffee and rust dynamics, as well as impulsive biocontrol. Floquet theory was used to compute stability thresholds for the periodic disease free solution. The initial coffee leaf rust model was then coupled with the dynamics of predator-like hyperparasites, as recommended by Zambolin [180] for alternative biocontrol methods; this resulted in a controlled impulsive model. The semi-numerical analysis of this controlled impulsive model allowed to conclude that hyperparasite-based biocontrol can drastically reduce coffee leaf rust. Moreover, we studied how successful biocontrol implementation depends on hyperparasite characteristics, in particular its mortality.

We set the study in a framework where the yearly released quantity of hyperparasites is fixed and only its release frequency varies. We deemed this comparison relevant since, whatever the

release strategy, the same yearly budget may be allocated to biocontrol agents.

Low and high hyperparasite mortality rates were considered to represent different environmental situations and hyperparasite characteristics. High mortality occurs if the hyperparasite is a specialist parasite like *Mycodiplosis* [67], which means that it only consumes CLR uredospores, or if it is a generalist hyperparasite whose alternate food sources are absent; in both cases, the hyperparasite quickly dies out in absence of CLR. Low mortality occurs for generalist hyperparasites in a rich environment. Most hyperparasites of *H. vastatrix* in the literature have alternative preys. For example, the *Lecanicillium lecanii* fungus is a CLR hyperparasite that could be used for biocontrol [168, 143], and it is also a pathogen of plant-parasitic nematodes [57]. Hence, both low and high mortality situations could occur in the field.

For low mortality rates, the best strategy is to release the hyperparasites once a year at the beginning of the production season. This strategy is efficient because it is the one that ensures the largest average hyperparasite density over the year, hyperparasites being always present because of the low mortality rate. However, the cost of such a large release at the beginning of the production season, on top of all the actions that need to be taken for coffee farming at that same time (such as fertiliser and manure application, or trimming of dry or excess leaves), can put too large a financial burden on the coffee producer. This problematic represents a well-known trade-off between yield and affordability in farming practices. Another potential problem is that massively advising farmers to adopt these practices could cause an excessive increase in the local demand of hyperparasites, and consequently a shortage in the market. For both these reasons, a strategy considering two releases could be recommended, even though it is less cost-efficient.

When the hyperparasite mortality rate is high, the best strategy depends on the horizon. For the first year, the most efficient approach is to have a large release at the beginning of the season in order to have an immediate massive impact. For the subsequent years, 5 and then 50 releases per year are advocated in Table 5.2. However, there is little difference in berry production between 5 and 50 releases in years 5 and 6. Moreover, the eradication success is almost identical for both strategies in terms of yearly released quantity of hyperparasites needed to control CLR (see Figure 5.9(a)). Considering the burden and cost associated with having 50 interventions over the production season, five yearly releases should be preferred to 50. Releasing predators twice a year may appear slightly suboptimal in terms of eradication success. It is however fairly close to the berry production achieved when releases occur five times per year and it is less labour consuming. In terms of cost-effectiveness, two releases per year might then be a good compromise. This result is complementary to the results of Henk et al [67], which shows that the larvae of some *Mycodiplosis* species can feed on spores of rust fungi and their frequency play an important role.

In the present work, we have focused our attention on one family of strategies: those that repeat themselves every year and are evenly spread over the production season, with a first release at the beginning of each year. Potential generalisations are numerous, but could not be considered here. One could for example choose to change strategy every year; this would seem to be a good idea if we look at Table 5.2, where we would choose to have a large single release the first year, and potentially five releases per year after that. One could also choose not to have a first release at the beginning of the year, but later in the season, or to have a larger release at the beginning of the year and then some smaller ones during the year. Finally, hyperparasites could be released in reaction to peaks of uredospore densities in the plantation, so as to maximise their impact; the latter approach however requires close monitoring of the disease in the plantation.

In addition to them potentially being more efficient, these approaches have the advantage of not imposing the full burden of acquiring hyperparasites at the beginning of the season.

The continuous part of our model contains most elements that we deem relevant, keeping it reasonably small and tractable. However, uredospore germination and mycelium formation depend on various environmental factors [10], such as temperature [35]. Introducing meteorological data in our model would allow for a better description of the day-to-day dynamics, but constant parameters gives a fairly good representation of the average dynamics for our purpose.

The hybrid model we developed is able to describe the dynamics of other fungal diseases that attack leaves of perennial plants. It appears as a promising tool to explore the efficiency of biocontrol strategies based on the impulsive release of hyperparasites. The impulsive component of the model presented in this work corresponds to plants that are harvested once a year; such is the case in temperate climate or in tropical climate with dry and rainy seasons. However, this model can be perfectly adapted to other countries without such contrasted seasons, where there are more than one harvest per year. In this case, several impulses can occur over the year, corresponding to partial harvests only, and not seasonality. The conclusions that we have drawn for CLR might not translate to other pathogen-plant pairs in other contexts, beyond our analytical results; a full semi-analytical study and numerical simulations should be performed for each case.

Chapter 6

General conclusion

Contents

6.1 Summary of main results

This thesis focused on the mathematical modelling and biocontrol of the dynamics of fungal diseases applied to the particular case of CLR and its impact on coffee production. The main objective was to develop rigorous mathematical models of plant-pathogen interactions, and also to develop an efficient and long-lasting control strategy that reduces the fungal development and preserves the yield. We reviewed literature about the impact of pest and fungal diseases, the biology of *H. vastatrix* and coffee tree in Chapter 1. This chapter also presents existing mathematical models of plant pathogens and particularly of CLR. In Chapter 2, we presented the mathematical tools used in the thesis. The main contributions of the work are found in Chapters 3, 4 and 5. Chapter 3 is based on a manuscript in revision in *Journal of Mathematical Biology*. Chapter 4 is built on a paper published in *Mathematical Modelling of Natural Phenomena* [38]. Chapter 5 is a manuscript in revision in *Mathematical Biosciences*, which is an extension of a paper published in *IFAC-PapersOnLine* [37] and given in Appendix A.

In our first contribution, presented in Chapter 3, we proposed and analysed a mathematical model that describes the propagation of a fungal disease on a perennial plant using an ODE model. The model is based on classical epidemiological models and its originality is the differentiation between young and mature leaves. Our aim was to understand the host-pathogen interactions and study the impact of host development on the aggressiveness of the pathogen. We proved that the model exhibits complex asymptotic properties, that differ from classical epidemiological models: a basic reproduction number smaller than one is insufficient to eradicate the disease as it could persist even though it could not invade, and a basic reproduction number greater than one does not guarantee the persistence of the disease, as large values could result in the destruction of the plantation.

Our second contribution, presented in Chapter 4, consisted in proposing and analysing a PDE model describing the disease propagation in the plantation, differentiating the rainy and dry seasons. The main goal was to understand the impact of seasonality on the propagation

of the fungal disease in order to propose a biocontrol solution, based on a hyperparasite that inhibits the fungus reproduction. We computed the equilibria of the two subsystems, defined during the rainy and dry seasons. We proved that the basic reproduction numbers during the two seasons could determine the dynamics of the full model: when the basic reproduction number is less than one during the rainy season, then CLR globally decreases until extinction; when it is greater than one for the dry season, then CLR persists. We showed that a rather high biocontrol efficiency (75% at least) is necessary in our model to control the disease, but lower efficiencies still improve coffee production notably.

In our last contribution, presented in Chapter 5, we developed a multi-seasonal model, alternating continuous crop-fungus dynamics during the rainy seasons and discrete events to represent the simpler dynamics during the dry seasons. The originality of our model, compared to the dynamical approaches above, is the hybrid formalism that is particularly suited to describe the seasonality of coffee and rust dynamics, as well as impulsive biocontrol. Our goal was to develop a biocontrol strategy based on the impulsive release of hyperparasites in the plantation. We used semi-numerical analysis to show that the best hyperparasite release strategy strongly depends on the hyperparasite characteristics, namely its mortality rate and its uredospore consumption rate. Both parameters determine the yearly released quantity of hyperparasites needed to control the disease. Moreover, we showed that the mortality rate has an impact on the best hyperparasite release frequency. On the long run, more frequent is more effective for high hyperparasite mortality, and vice versa for low mortality. On the shorter run however, less frequent may also be better for high mortality.

6.2 Perspectives

We identified two main extensions for this modelling work: the first one based on intra-guild predation and the second one on the deployment of resistant cultivars.

In this thesis, the biological control we proposed to control coffee leaf rust focused on the deployment of hyperparasites that prey on *H. vastarix* uredospores, such as fungus *L. lecanii* [168] and *Mycodiplosis* insect [139]. According to Chapter 5, the mortality rate of hyperparasites determines how often they need to be released in the plantation. The growth of *L. lecanii* is favoured by the same climatic conditions as *H. vastatrix*. Moreover *L. lecanii* is a generalist [48], so it can survive in the plantation in the absence of *H. vastarix* uredospores. Its mortality should hence be relatively low in a coffee plantation affected by coffee leaf rust. Based on our findings, it could then be released in the plantation at a low frequencies. However, because *L. lecanii* is a generalist, it may select other preys, such as green coffee scales [166], decreasing the effectiveness of the control. The *Mycodiplosis* larva is a specialist, that only feeds on *H. vastarix* uredospores [67]. However, these larvae are eaten by the *Azteca sericeasur* ant [63, 89], so their mortality may be significant. In that case, according to our findings, they should be released fairly frequently. Based on field studies in Puerto Rico and Mexico, Hajian-Forooshani at al. suggested that the joint presence of both *L. lecanii* and *Mycodiplosis* may provide control for *H. vastarix*, with varying outcomes depending on the community composition. It would be interesting to extend our work and investigate intra-guild predation, including the dynamics of both predators in the coffee leaf rust model.

In this thesis, we did not make a difference between the coffee varieties arabica and robusta. The arabica variety represents 70% of the global production, while robusta accounts for less

than 30%. Indeed arabica has a higher agronomic value, but it is more susceptible to CLR than robusta. Therefore, developing CLR resistant coffee varieties with a suitable agronomic value is a current challenge. Most resistant varieties are obtained by combining arabica and robusta varieties, some are listed in Subsection 1.2.3. Several genes providing resistance to strains of the fungus *H. vastatrix* were identified in several coffee varieties [128, 129]. However, the fungus *H. vastatrix*, like many others, is adapting to these resistant varieties, necessitating the development of new resistant plants or management strategies that reduce or slow the resistance breakdown. Many modelling studies proposed control methods based on resistant plants, mixing or alternating resistant and susceptible plants in space and/or time to preserve the resistance efficiency on the long run [133, 45]. Indeed, the extensive use of resistant plants increases the selection pressure on virulent pathogens, that can overcome the plant resistance. However, reducing the use of resistant plants may face acceptability issues, as resistant plants provide better returns in the short term [114]. Moreover, strategies are better suited for annual crops. Replacing coffee plants is particularly challenging for farmers because it takes an average of four years to produce coffee. It is hence particularly interesting to gain some knowledge based on theoretical studies in the case of coffee leaf rust, to help the deployment of resistant varieties with mixtures of plants carrying different resistances the most promising approach for perennial plants..

Appendix A

Ifac paper

Contents

This work is published in *IFAC-PapersOnLine* [37]

A.1 Optimal control of the impulsive model of the propagation of the coffee leaf rust

Abstract: This paper presents the dynamics and optimal control of the coffee leaf rust (CLR) over the coffee plantation with impulsive effect, which represents the non production period of coffee. Our aim is to estimate the damage cause by the CLR and the optimal control the propagation of the CLR during many years using the biological control. We show the existence of solution and prove using Floquet theory that there exist the threshold calling basic reproduction number, that determine the stability of solutions. Numerical simulations are performed to illustrate the theoretical results. This paper deals with the problem of modelling and optimal control of the coffee leaf rust (CLR) in a coffee plantation. We first formulate and analyze a mathematical model for the propagation of CLR with impulsive effect, which represents the non-production period of coffee. Then, the CLR control is formulated and solved as an optimal control, showing how a biological control strategy can be implemented in a coffee plantation to reduce the damage caused by CLR, therefore increasing the coffee production. Numerical simulations are performed to illustrate and validate the theoretical results.

Keywords: Epidemiological modeling; Impulsive system; Floquet theory; Stability; Optimal control, *Hemileia vastatrix*.

A.1.1 Introduction

Coffee is one of the most widely consumed beverages in the world, with their consumption in 2019/20 being estimated at 168 million 60-kilogram bags [72]. Its cultivation is widespread in almost all the countries of the tropic and is an important factor of social stability as it supports no less than twenty-five million small producers and their families worldwide. However, due to the climate of these areas, multiple coffee diseases have persisted for several years. Among these pests, the Coffee Leaf Rust (CLR) is considered the most important leaf disease known to this day for being one of the most devastating pathogens. It is caused by the fungus *Hemileia vastatrix*, first discovered in Sri Lanka in 1869, and nowadays present in the majority of the coffee-growing regions of the world. The pathogenic principle behind CLR is that it causes premature defoliation, which reduces the photosynthetic capacity of coffee leaves, inducing severe yield losses to the sector (up to 70%).

The dynamics of CLR is complex due to the multiple interactions between the plant host and the pathogen in the environment. A better understanding of such CLR dynamics can significantly improve the accuracy of the models, which can be then analyzed through theoretical studies and numerical simulations. Many efforts have been and are still being devoted to the modeling of the propagation of CLR [165]. However, none of them take into account the impulsive effect in the dynamics. Considering discrete events in the model—such as harvesting—could allow for a more comprehensive representation of the plantation process, providing in turn a more precise framework for pest treatment. In this regard, several works have used ordinary impulsive differential equations for representing population dynamics in ecology and epidemiology in the recent years [96, 154, 156, 40].

The capacity to accurately model the time evolution of coffee plantations allows not only to effectively predict trends in the process, but also to act on them. In this context, optimal control theory has proven to be a powerful tool for investigating potential control strategies in pest treatment [1, 178, 18]. Such approaches are commonly based on the well-known PMP (Pontryagin's maximum principle) [125]: for a given cost function to maximize, this theory can provide necessary (and often sufficient) conditions for optimality of control strategies in systems of ordinary differential equations, partial differential equations and hybrid systems with given constraints [39].

The present contribution offers an impulsive perspective to the modeling of the propagation of CLR in a coffee plantation. We first formulate and analyze a non-controlled impulsive model for the propagation of CLR, for which we compute the periodic disease-free solution (PDFS) and a threshold parameter $\mathcal{R}$. Then, we conduct an in-depth analysis of the global asymptotic stability of the PDFS when $\mathcal{R} < 1$, and we perform numerical simulations to illustrate the theoretical results. Furthermore, we devise an extended model that considers a biological control for pest treatment, intended to maximize the coffee production while minimizing the damages undergone by the CLR. The latter objective is written as an Hybrid OCP (Optimal Control Problem), for which we propose an analogous problem in continuous form, which allows to obtain numerical solutions with Bocop [20]. Later on, we provide a numerical solution of an optimal trajectory of the system for a relevant set of parameters and initial conditions. As a result, we show that a cost-effective inoculative biological control can successfully contain the damages on a coffee plantation.

A.1.2 The model and its basic properties

A.1.2.1 Mathematical Modeling of coffee leaf rust

In this section, we formulate a mathematical model for the propagation of the CLR in the coffee plantation. To do so, we consider the dynamics of fungus during the production season—which corresponds to the rainy season for some countries—through ordinary differential equations; and during the non-production period—which is the dry season for some countries—represented by the impulsive effect. More precisely, we consider that in a coffee plantation we can find: susceptible branches S, infected branches I and urediniospores U. During the production period with length $T > 0$, the recruitment of healthy branches occurs at rate Λ. Urediniospores are deposited on leaves of all branches at rate ν, and a fraction S/N lands on susceptible branches. When the conditions are favorable, urediniospores germinate with efficiency rate ω and the susceptible branches becomes infected branches. All branches undergo natural mortality with baseline rate μ and the infected branches have an additional mortality rate d due to the disease. Urediniospores are produced by infected branches at rate γ and lose their ability to infect coffee branches at constant rate μ_U. Susceptible and infected branches produce the berries with constant rate δ_S and δ_I, respectively. At the end of the production period, harvest occurs instantaneously and we consider that the dry season or non-production period corresponds to the time when the number of branches at the end of the production period switches, this switch due to the fact that harvesting reduces the number of susceptible branches, infected branches and urediniospores with rates φ_S, φ_I and φ_U respectively. Using the fact that urediniospores lose their ability to infect fastly, we assume that φ_U is very close to 0. The model is given by the following hybrid system:

$$\begin{cases} \dot{S} = \Lambda - \dfrac{\omega\nu U}{N}S - \mu S, \ t \neq nT; \\ \dot{I} = \dfrac{\omega\nu U}{N}S - (\mu + d)I, \ t \neq nT; \\ \dot{U} = \gamma I - (\nu + \mu_U)U, \ t \neq nT; \\ \dot{B} = \delta_S S + \delta_I I - \mu_B B, \ t \neq nT; \\ S(nT^+) = \varphi_S S(nT); \\ I(nT^+) = \varphi_I I(nT); \\ U(nT^+) = \varphi_U U(nT); \\ B(nT^+) = 0. \end{cases} \tag{A.1}$$

where $S(t)$, $I(t)$, $U(t)$ and $N(t) = S(t) + I(t)$ represent the number of susceptible branches, infected branches, urediniospores and total branches, respectively at time t. With $0 < \varphi_I \leq \varphi_S < 1$ and $\varphi_U > 0$ but close to 0.

Table A.1 summarizes the biological meaning and the values of parameter of model (A.1).

A.1.2.2 Basic properties of the model

Let $\mathbb{R}^4_+ = \{X \in \mathbb{R}^4, X \geq 0\}$. Denote by $f = (f_1, f_2, f_3, f_4)$ the map given by the right-hand side of system (A.1), and consider the initial conditions

$$(S(0), I(0), U(0), B(0)) \in \mathbb{R}^4_+, \ S(0) > 0. \tag{A.2}$$

Table A.1: Description and values of parameters for system (A.1)

	Biological meaning	Value
Λ	Recruitment of S	50/day
ω	Inoculum effectiveness	6.5% [131]
μ	Mortality rate of branches	0.0034/day
γ	Production rate of spores	$\in [0, 20]$/day
d	Mortality rate due to CLR	0.056/day
ν	Deposition rate	0.09/day [19]
μ_U	Mortality rate of spores	0.015/day
φ_S	Reduction rate of S	0.7/day
φ_I	Reduction rate of I	0.4/day
φ_U	Reduction rate of spores	0.001/day

The solutions of system (A.1) are positives. Indeed, suppose that one of the variables, that we will denote x, is equal to 0 at some instant, with all the others being non-negative. A quick analysis shows that $\dot{x} \geq 0$ cannot become negative. This implies that $x(t) \geq 0$. Then, the solutions are positive. The solutions of system (A.1) are piecewise continuous functions $X : \mathbb{R}_+ \to \mathbb{R}^4_+$, X is continuous on $(nT, (n+1)T]$, $n \in \mathbb{N}$ and $X(nT^+) = \lim_{t \to nT^+} X(t)$. Clearly, the smooth properties of f guarantee the existence and uniqueness of positive solutions of system (A.1). By adding the first and second equations in system (A.1), we see that the dynamics of total branches satisfies

$$\begin{cases} \dot{N} = \Lambda - \mu N - dI, \ t \neq nT \\ N(nT^+) \leq \varphi_S N(nT). \end{cases} \tag{A.3}$$

From the equation (A.3), and using the positivity of the variables of the model, we have $\dot{N} \leq \Lambda - \mu N$ and $N(nT^+) \leq \varphi_S N(nT)$. It follows that $0 \leq \lim_{t \to \infty} N(t) \leq \frac{\Lambda}{\mu}$. Then, the following region

$$G = \left\{ (N, U) \in \mathbb{R}^2_+ \mid N(t) \leq \frac{\Lambda}{\mu}, \ U(t) \leq \frac{\gamma \Lambda}{\mu(\nu + \mu_U)} \right\}. \tag{A.4}$$

is positively invariant by system (A.1).

A.1.3 Mathematical analysis

Herein, we present the mathematical analysis of system (A.1). Since the state variable of berries B is not present in the other equations of system (A.1), we do not consider it in the mathematical analysis.

A.1.3.1 Periodic desease free solution and its stability

The periodic disease free solution (PDFS) occurs when $I = 0$ and $U = 0$. Replacing these values in the impulsive differential equation (IDE) (A.1), we obtain

$$\dot{S} = \Lambda - \mu S, \ t \neq nT; \quad S(nT^+) = \varphi_S S(nT). \tag{A.5}$$

The resolution of the first equation of system (A.5) gives:

For $t \in (nT, (n+1)T]$

$$S(t) = \frac{\Lambda}{\mu} + \left(S(nT^+) - \frac{\Lambda}{\mu}\right) e^{-\mu(t-nT)}. \tag{A.6}$$

This implies that

$$S((n+1)T) = \frac{\Lambda}{\mu} + \left(S(nT^+) - \frac{\Lambda}{\mu}\right) e^{-\mu T}. \tag{A.7}$$

Using the impulsive condition $S((n+1)T^+) = \varphi_S S((n+1)T)$ yields

$$S((n+1)T^+) = \varphi_S \left(\frac{\Lambda}{\mu} + (S(nT^+) - \frac{\Lambda}{\mu})e^{-\mu T}\right). \tag{A.8}$$

The fixed point of the equation (A.8) is given by

$$S(nT^+) = \frac{\Lambda\varphi_S(1-e^{-\mu T})}{\mu(1-\varphi_S e^{-\mu T})} > 0. \tag{A.9}$$

Substituting the value of $S(nT)$ into the equation (A.6), for $t \in (nT, (n+1)T]$ one has

$$S^P(t) = \frac{\Lambda}{\mu}\left[1 - \frac{(1-\varphi_S)e^{\mu T}}{e^{\mu T} - \varphi_S} e^{-\mu(t-nT)}\right]. \tag{A.10}$$

Finally, the PDFS is $X^P(t)$=$(S^P(t), 0, 0)$, where $S^P(t)$ is defined as in equation (A.10).

A.1.3.2 Stability of the PDFS

We first study the local stability of $X^P(t)$ using small amplitude pertubation methods. Let us denote $\tilde{X}(t) = X(t) - X^P(t)$ where $X(t) = (S(t), I(t), U(t))^T$ and $\tilde{X}(t)$ is understood to be small amplitude pertubations. Substituting the expression of $\tilde{X}(t)$ in the system (A.1) gives

$$\begin{cases} \dot{\tilde{S}} = -\dfrac{\omega\nu\tilde{U}}{\tilde{N} + S^P(t)}(\tilde{S} + S^P(t)) - \mu\tilde{S},\ t \neq nT; \\ \dot{\tilde{I}} = \dfrac{\omega\nu\tilde{U}}{\tilde{N} + S^P(t)}(\tilde{S} + S^P(t)) - (\mu+d)\tilde{I},\ t \neq nT; \\ \dot{\tilde{U}} = \gamma\tilde{I} - (\nu + \mu_U)\tilde{U},\ t \neq nT; \\ \tilde{S}(nT^+) = \varphi_S\tilde{S}(nT); \\ \tilde{I}(nT^+) = \varphi_I\tilde{I}(nT); \\ \tilde{U}(nT^+) = \varphi_U\tilde{U}(nT). \end{cases} \tag{A.11}$$

where $\tilde{N}(t) = \tilde{S}(t) + \tilde{I}(t)$ and $N^P(t) = S^P(t)$. The linearization of system (A.11) gives

$$\begin{cases} \dot{\tilde{X}}(t) = A\tilde{X}(t),\ t \neq nT; \\ \tilde{X}(nT^+) = diag(\varphi_S, \varphi_I, \varphi_U)\tilde{X}(nT); \end{cases} \tag{A.12}$$

where

$$A = \begin{pmatrix} -\mu & 0 & -\omega\nu \\ 0 & -(\mu+d) & \omega\nu \\ 0 & \gamma & -(\nu+\mu_U) \end{pmatrix}.$$

Solving the system (A.12) yields $\tilde{X}(t) = \Phi(t)\tilde{X}(0)$, where $\Phi(0) = I$ with I being the identity matrix of dimension 3 and $\Phi(t)$ the fundamental matrix that satisfies $\frac{d\Phi(t)}{dt} = A\Phi(t)$. A calculation gives

$$\Phi(t) = \begin{pmatrix} e^{-\mu t} & \psi_{12}(t) & \psi_{13}(t) \\ 0 & \psi_{22}(t) & \psi_{23}(t) \\ 0 & \psi_{32}(t) & \psi_{33}(t) \end{pmatrix}, \tag{A.13}$$

where

$$\begin{cases} \psi_{22}(t) = \dfrac{1}{2\beta}\left[(\beta + k_1 - k_2)e^{\lambda_1 t} + (\beta - k_1 + k_2)e^{\lambda_2 t}\right], \\ \psi_{23}(t) = \dfrac{\nu\omega}{\beta}\left[-e^{\lambda_1 t} + e^{\lambda_2 t}\right], \psi_{32}(t) = \dfrac{\gamma}{\beta}\left[-e^{\lambda_1 t} + e^{\lambda_2 t}\right], \\ \psi_{33}(t) = \dfrac{1}{2\beta}\left[(\beta - k_1 + k_2)e^{\lambda_1 t} + (\beta + k_1 - k_2)e^{\lambda_2 t}\right]. \end{cases} \tag{A.14}$$

with

$$\begin{cases} k_1 = \mu + d, \quad k_2 = \nu + \mu_U, \\ \alpha = k_1 + k_2, \quad \beta = \sqrt{(k_1 - k_2)^2 + 4\gamma\omega\nu}, \\ \lambda_1 = -\dfrac{\alpha}{2} - \dfrac{\beta}{2} \text{ and } \lambda_2 = -\dfrac{\alpha}{2} + \dfrac{\beta}{2}. \end{cases} \tag{A.15}$$

Using the impulsive conditions, one obtains the impulsive matrix $\tilde{X}(nT^+) = diag(\varphi_S, \varphi_S, \varphi_U)\tilde{X}(nT)$. Finally, the solution of system (A.12) becomes

$$\tilde{X}(t) = diag(\varphi_S, \varphi_I, \varphi_U)\Phi(t)\tilde{X}(0). \tag{A.16}$$

From the above equation, the monodromy matrix is $M = diag(\varphi_S, \varphi_I, \varphi_U)\Phi(T)$, i.e

$$M = \begin{pmatrix} \varphi_S e^{-\mu T} & \varphi_S \xi_1(T) & \varphi_S \xi_2(T) \\ 0 & \varphi_I \psi_{22}(T) & \varphi_I \psi_{23}(T) \\ 0 & \varphi_U \psi_{32}(T) & \varphi_U \psi_{33}(T) \end{pmatrix}. \tag{A.17}$$

The Floquet multipliers of the matrix M is given by $\chi_1 = \varphi_S e^{-\mu T} < 1$ and the multipliers of the submatrix

$$M_1 = \begin{pmatrix} \varphi_I \psi_{22}(T) & \varphi_I \psi_{23}(T) \\ \varphi_U \psi_{32}(T) & \varphi_U \psi_{33}(T) \end{pmatrix}. \tag{A.18}$$

Then, the PDFS $X^P(t)$ is locally asymptotically stable if the eigenvalues of matrix M_1 stay in the unit cycle, which need to satisfy verify the following Jury conditions [173]:

$$\begin{cases} -tr(M_1) - \det(M_1) < 1, \\ \det(M_1) < 1, \\ tr(M_1) - \det(M_1) < 1, \end{cases} \tag{A.19}$$

where

$$\begin{cases} tr(M_1) = \varphi_I \psi_{22}(T) + \varphi_U \psi_{33}(T), \\ \det(M_1) = \varphi_I \varphi_U \left(\psi_{22}(T)\psi_{33}(T) - \psi_{23}(T)\psi_{32}(T)\right), \end{cases} \tag{A.20}$$

The conditions (A.19) hold if $\varphi_U \to 0$ and $\varphi_I \psi_{22}(T) < 1$. Finally, one has the following lemmama.

Lemma A.1. *The PDFS $X^P(t)$ is locally asympototically stable provided that $\mathcal{R} < 1$ where*

$$\mathcal{R} = \frac{\varphi_I}{2\beta}\left[(\beta + k_1 - k_2)e^{\lambda_1 T} + (\beta - k_1 + k_2)e^{\lambda_2 T}\right]. \tag{A.21}$$

We have the following result about the global stability of the PDFS of the system (A.1).

Theorem A.1. *The PDFS $X^P(t)$ of the system (A.1) is globally asympototically stable in region G provided that $\mathcal{R} < 1$.*

Proof of Theorem A.1. We will prove the global attractivity of the PDFS $X^P(t)$. Consider the subsystem following:

$$\begin{cases} \dot{I} = \dfrac{\omega\nu U}{N} S - (\mu + d)I, \ t \neq nT; \\ \dot{U} = \gamma I - (\nu + \mu_U)U, \ t \neq nT; \\ I(nT^+) = \varphi_I I(nT), \ U(nT^+) = \varphi_U U(nT). \end{cases} \tag{A.22}$$

The trivial solution of system (A.22) is $(0, 0)$ and the solution $(S(t), I(t), U(t)) \in G$. The system (A.22) is cooperative because ($\frac{\partial I}{\partial U} = \frac{\omega\nu S}{N} > 0, \frac{\partial U}{\partial I} = \gamma > 0$) and using the fact that $\frac{S(t)}{N(t)} < 1$, one has the following cooperative system:

$$\begin{cases} \dot{I}_1 = \omega\nu U_1 - (\mu + d)I_1, \ t \neq nT; \\ \dot{U}_1 = \gamma I_1 - (\nu + \mu_U)U_1, \ t \neq nT; \\ I_1(nT^+) = \varphi_I I_1(nT), \ U_1(nT^+) = \varphi_U U_1(nT). \end{cases} \tag{A.23}$$

Applying the Kamke's theorem [33], one has that $I(t) \leq I_1(t), U(t) \leq U_1(t)$. The asymptotically, system (A.23) behaves like the system (A.22) [[64]], when $\mathcal{R}_0 < 1$. Then, one has

$$I_1(t), U_1(t) \to 0^+ \Rightarrow I(t), U(t) \to 0^+. \tag{A.24}$$

Since $U \to 0^+$, for any arbitrary positive ε_U there exists a $t_0 > 0$ such that for $t \geq t_0$, $U(t) \leq \varepsilon_U$. Using the positivity of the solutions and the fact that $S(t)/N(t) \leq 1$ into the first equation of system (A.1), one has :

$$\Lambda - \omega\nu\varepsilon_U - \mu S(t) \leq \dot{S}(t) \leq \Lambda - \mu S(t) \tag{A.25}$$

Applying the comparison theorem on the above differential inequalities, one has $S_1(t) \leq S(t) \leq S_2(t)$, where for $t \in]nT; (n+1)T]$,

$$\begin{cases} S_1(t) = \dfrac{\Lambda - \omega\nu\varepsilon_U}{\mu}\left[1 - \dfrac{(1-\varphi_S)e^{\mu T}}{e^{\mu T} - \varphi_S} e^{-\mu(t-nT)}\right], \\ S_2(t) = \dfrac{\Lambda}{\mu}\left[1 - \dfrac{(1-\varphi_S)e^{\mu T}}{e^{\mu T} - \varphi_S} e^{-\mu(t-nT)}\right], \end{cases} \tag{A.26}$$

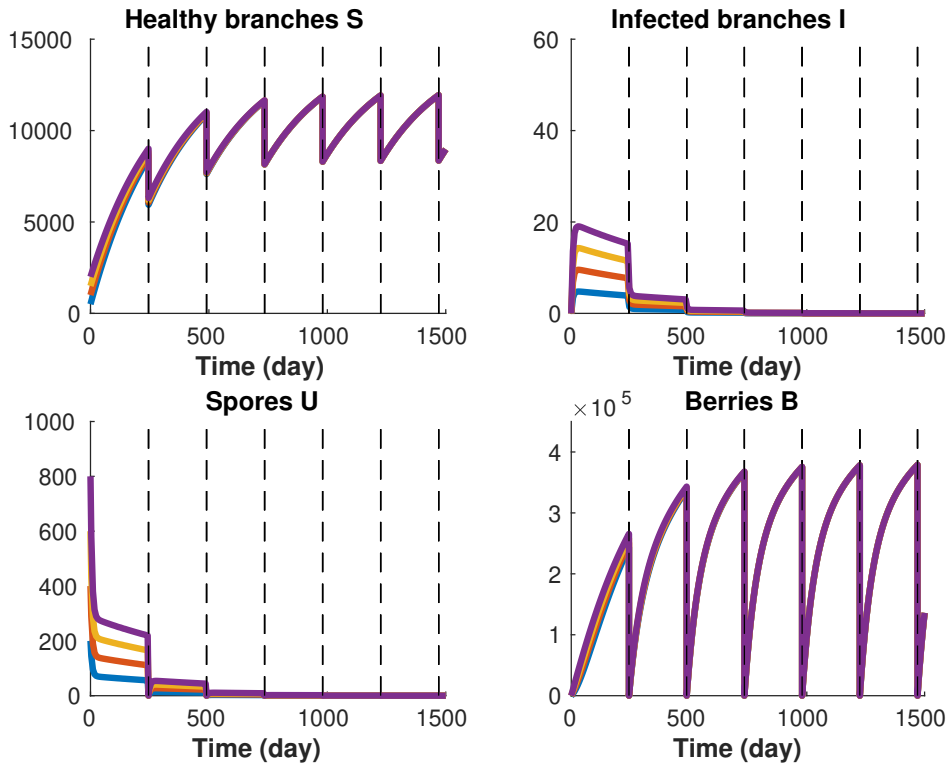

Figure A.1: Trajectories of system (A.1) when $\gamma = 1.6$ (so that $\mathcal{R}_0 = 0.36$). All other parameter values are given in Table A.1.

with S_1 and S_2 the solutions of the following impulsive differential equations:

$$\dot{S}_1 = \Lambda - \omega\nu\varepsilon_U - \mu S_1,\ t \neq nT;\ S_1(nT^+) = \varphi_S S_1(nT), \tag{A.27}$$

$$\dot{S}_2 = \Lambda - \mu S_2,\ t \neq nT;\ S_2(nT^+) = \varphi_S S_2(nT), \tag{A.28}$$

One can observe that $S_2(t) \to S^P(t)$ if $\varepsilon_U \to 0$ and $S_2(t) \to S^P(t)$, which implies that $S(t) \to S^P(t)$ asympototically. In the orther words, independently from the initial value $(S_0, I_0, U_0) \in G$, one has that

$$(S(t), I(t), U(t)) \to (S^P(t), 0, 0) \tag{A.29}$$

This concludes the proof. □

Numerical results for the global stability of the PDFS and persistence are present in Figure A.1 and A.2 respectively. To do so, we consider the initial conditions $(S_0, U_0) \in [(500, 200), (1000, 400), (1500, 600), (2000, 800)]$, $I_0 = 0$ and $B_0 = 0$. Figure A.1 shows that, for different initial conditions, the number of infected branches and urediniospores converge towards zero, which is the state free disease. Additionally, we can observe that the trajectories of susceptible branches and berries becomes stationary after three seasons, as proved in Theorem A.1. Although the persistence has not be proved analytically, numerical results in Figure A.2 tend to show that the persistence of the CLR appears for system (A.1) when $\mathcal{R}_0 = 5.7 > 1$. From Figures A.1 and A.2 one can deduce that, during the disease free period (when $\mathcal{R}_0 < 1$), the

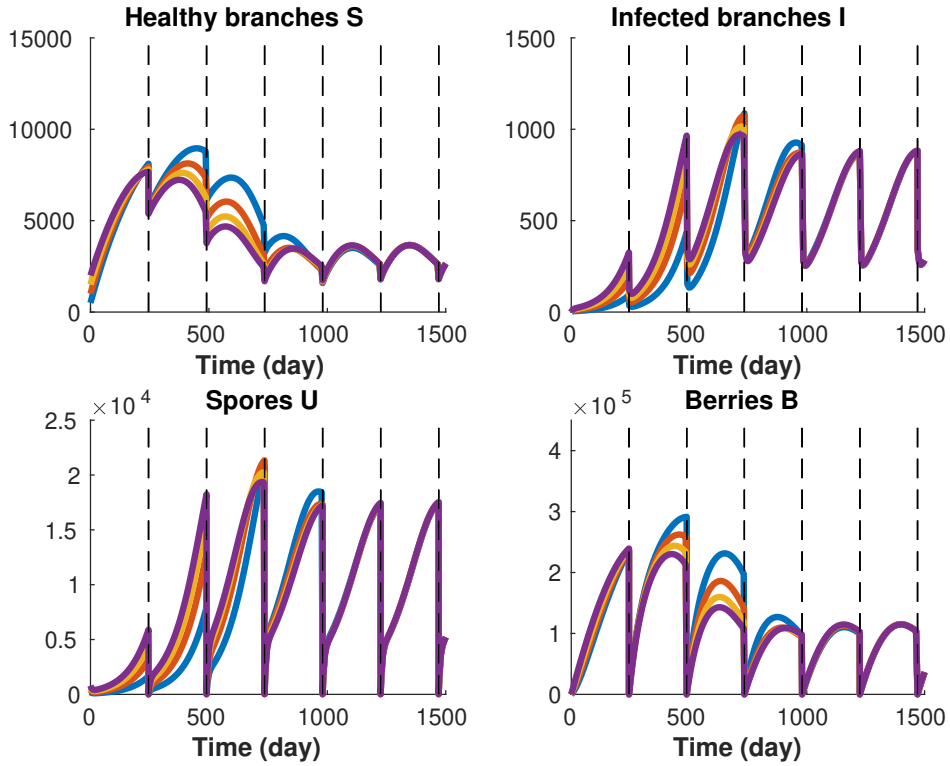

Figure A.2: Trajectories of system (A.1) for different initial condition, when $\gamma = 2.1$ (so that $\mathcal{R}_0 = 5.7 > 1$). All other parameter values are given in Table A.1.

number of berries is 378910, during the persistence of disease state (when $\mathcal{R}_0 > 1$) the number of berries is 117698. Then, one can conclude that the yield lost due to the CLR is estimate at $68,93\%$. Thus, one can ask the following question, how to reduce the damage caused by the CLR in coffee plantation.

A.1.4 Optimal control

A.1.4.1 Optimal problem

Many different methods are commonly used in CLR control, with varying levels of environmental impact. Herein, we choose the biological control, because it is a potentially powerful tool for managing coffee leaf rust that allows organic certification. This biological control uses natural enemies, e.g. mycoparasites such as *Lecanicillium lecanii* [26, 168]. The goal is to introduce the mycoparasite in the plantation so that it will consume the urediniospores. This method represents the inoculative biological control and is denoted by v. The new system with control $v(t)$ is the first system(A.1) where equation U changes to

$$\dot{U} = \gamma I - (\nu + \mu_U)U - v, \; t \neq nT; \tag{A.30}$$

where $v(t) \in [0, v_{max}]$, with v_{max} the maximum value of the biological control. Given k seasons of duration T, we are interested in maximizing the net revenue, which is directly proportional to the amount of grains of coffee at the end of each season

$$\sum_{j=1}^{k} B(jT), \tag{A.31}$$

and inversely proportional to the usage of the control treatment throughout the whole period

$$\int_0^{kT} v \, dt. \tag{A.32}$$

Thus, we define the cost function to maximize representing the profit for a time period $[0, kT]$, given by

$$J(v) = \alpha_B \sum_{j=1}^{k} B(jT) - \alpha_v \int_0^{kT} v \, dt, \tag{A.33}$$

where α_B and α_v are the market prices per coffee grain and per spore, respectively. By using the relation

$$B(jT) = \int_{(j-1)T}^{jT} (\delta_S S + \delta_I I - \mu_B B) \, dt, \tag{A.34}$$

which takes into account that $B(jT^+) = 0$, we can rewrite the cost function as

$$J(v) = \int_0^{kT} \Big(\alpha_B(\delta_S S + \delta_I I - \mu_B B) - \alpha_v v \Big) \, dt. \tag{A.35}$$

Then, we define the Hybrid Optimal Control Problem

$$\begin{cases} \textit{maximize} & J(v) \\ \textit{subject to} & \textit{dynamics of system (A.30)}, \\ & \textit{initial conditions (A.2)}, \\ & v(\cdot) \in \mathcal{V}, \end{cases} \tag{HOCP}$$

with $\mathcal{V}$ being the set of admissible controllers, which are Lebesgue measurable real-valued functions defined on the interval $[0, kT]$ and satisfying the constraint $v(t) \in [0, v_{max}]$. We notice that $v(t)$ appears linearly in the dynamics (A.30), and, since $S = 0$ is repulsive, $S + I > 0$ for any trajectory, which means that the dynamics cannot blow up in finite time (and so all trajectories remain in a compact set). An analytical computation of an hybrid optimal control can be derived through the Hybrid Maximum Principle [39], a generalization of the classical PMP (Pontryagin's Maximum Principle). For (HOCP), we define the state $x = (S, I, U, B)$ and adjoint state $p = (p_S, p_I, p_U, p_B)$, and so the Hamiltonian is written as

$$H(x, p, p_0, v) = \langle \lambda, f(x, v) \rangle - p_0 f^0(x, v) \tag{A.36}$$

where $f^0(x, v) = \alpha_B \dot{B} - \alpha_v v$, which corresponds to the integrand of the cost function $J(v)$, f is the right-hand side of (A.30), and $p_0 \leq 0$. According to the Maximum Principle, the optimal control $v(t)$ should maximize the Hamiltonian along the optimal trajectory. Since H is linear in the control, the solution of (HOCP) becomes

$$v_{opt}(t) = \begin{cases} 0 & \textit{if } \phi(x, p) < 0; \\ v_{max} & \textit{if } \phi(x, p) > 0; \\ v_{sing}(t) & \textit{if } \phi(x, p) = 0. \end{cases} \tag{A.37}$$

where $\phi(x, p)$ is the switching function defined as

$$\phi(x, p) \doteq \frac{\partial H}{\partial v}, \tag{A.38}$$

and $v_{sing}(t)$ is called a singular control. According to (A.37), any solution of (HOCP) is a concatenation of bangs and singular arcs. A singular arc occurs when the switching function ϕ vanishes over some subinterval of time, and can be obtained by successively differentiating ϕ until the control v can be computed explicitly in terms of the state and adjoint state. However, a more detailed description of the control law is often hard to obtain, due to the presence of the adjoint state p in the singular arc v_{sing} and in the switching function $\phi(x, p)$. One way to help understand the structure of the optimal control is to simulate numerical trajectories using direct methods, by approximating the problem by a finite dimensional optimization problem. Nevertheless, the use of optimal control solvers is usually restricted to continuous systems. Thus, in order to be able to apply such methods, we rewrite (HOCP) in a continuous form.

A.1.4.2 Problem in continuous form

(HOCP) can be rewritten in the continuous form by defining k set of states $x_n = (S_n, I_n, U_n, B_n)$ and k controls $v_n(t)$, with dynamics defined for $t \in [0, T]$ as

$$\begin{cases} \dot{S_n} = \Lambda - \omega\nu U_n \dfrac{S_n}{S_n + I_n} - \mu S_n, \\ \dot{I_n} = \omega\nu U_n \dfrac{S_n}{S_n + I_n} - (\mu + d) I_n, \\ \dot{U_n} = \gamma I_n - (\nu + \mu_U) U_n - v_n, \\ \dot{B_n} = \delta_S S_n + \delta_I I_n - \mu_B B_n, \end{cases} \tag{A.39}$$

for $n = 1, \ldots, k$, with boundary conditions

$$\begin{cases} S_1(0) = S_0 > 0, \ I_1(0) = I_0 \geq 0, \\ U_1(0) = U_0 \geq 0, \ B_1(0) = B_0 > 0 \\ S_{n+1}(0) = \varphi_s S_n(T), \ I_{n+1}(0) = \varphi_I I_n(T), \\ U_{n+1}(0) = \varphi_U U_n(T), \ B_{n+1}(0) = 0. \end{cases} \tag{A.40}$$

for $n = 1, \ldots, k-1$. Then, the cost function becomes

$$J_c(v_1, \ldots, v_k) = \alpha_B \sum_{n=0}^{k} B_n(T) - \alpha_v \sum_{n=0}^{k} \int_0^T v_n \, dt, \tag{A.41}$$

and the resulting continuous optimal control problem is

$$\begin{cases} \textit{maximize} & J_c(v_1, \ldots, v_k) \\ \textit{subject to} & \textit{dynamics of system (A.39)}, \\ & \textit{boundary conditions (A.40)}, \\ & v_n(\cdot) \in \mathcal{V}, \ \textit{for } n = 1, \ldots, k. \end{cases} \tag{COCP}$$

While this new OCP includes the boundary conditions relating the consecutive set of states x_n, there are no terminal conditions on (HOCP) which means that the set of admissible controllers is not empty. Thus, existence of a solution for (COCP)—and therefore for (HOCP)—holds by Filippov's theorem [2].

A.1.4.3 Numerical results

Figure A.3 presents the results of a numerical simulation performed with Bocop of the optimal control and the optimal trajectory for problem (HOCP). In this Figure, we compare an open-loop strategy ($v \equiv 0$) with $\mathcal{R}_0 > 1$, and the same initial conditions with the optimal control. For the latter case, the biological treatment succesfully erradicates the pest. The optimal strategy is characterized by a bang control $v \equiv v_{max}$ during an initial period of time in the first season, followed by a singular arc in which the use of the pest treatment is gradually reduced until no further control is applied. Indeed, the optimal control exploits the fact that both U and I are greatly reduced at the end of each season due to harvesting, to economize on pest treatment. After that, no further control is required. The latter pattern has also been observed for different set of parameters and initial conditions defined in the previous section. In general, the treatment

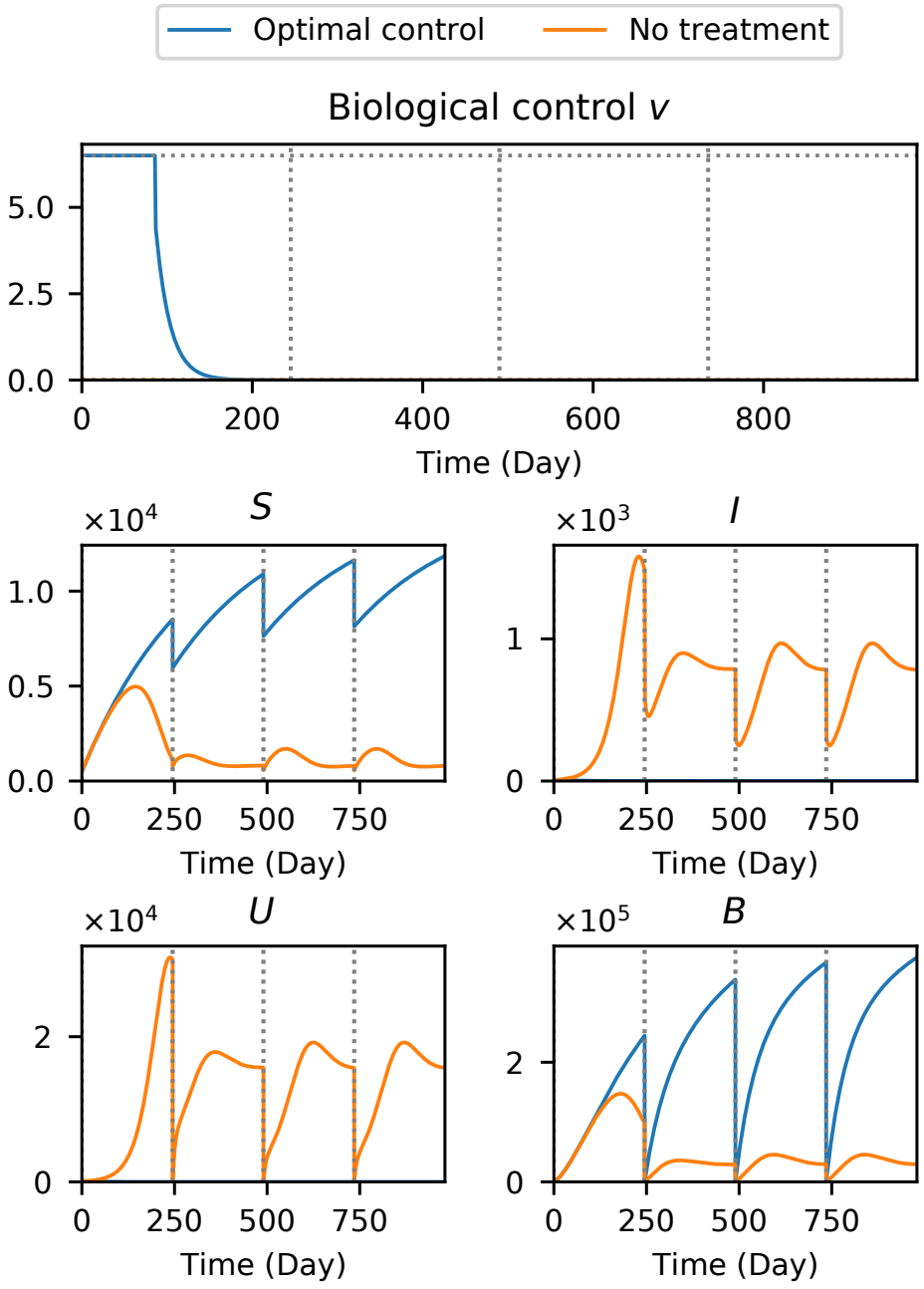

Figure A.3: Trajectories of HCOP (A.30) when $\gamma = 2.1$ (so that $\mathcal{R}_0 = 5.7$ without control). The maximum control $v_{max} = 6.5$. All other parameter values are given in Table A.1. Initial conditions are set to $S(0) = 500$, $U(0) = 200$, $I(0) = B(0) = 0$.

is applied rather for an initial interval of the season, followed by a a decrease that takes the control to $v \equiv 0$. As a conclusion for the analyzed particular case, coffee producers should maximize the quantity of mycoparasitic (between given boundaries) roughly only during the beginning of the first year, while discontinuing the treatment in posterior seasons. Naturally, the instant at which the treatment should be turned off is strongly linked to the initial conditions, and so each case requires a specific analysis.

A.1.5 Conclusion

This paper presented a comprehensive, impulsive model for the transmission dynamics of the CLR within a coffee plantation. The model has been analyzed to gain insight into its qualitative dynamics. Using the Floquet theory, we have found that there exists a threshold parameter that determines the extinction and persistence of CLR in a coffee plantation. Later on, we presented a controlled model based on an inoculative biological control, for which we defined an OCP targeting the maximization of the net revenue of a coffee plantation. For such problem, we performed a numerical analysis for a relevant set of parameters and initial conditions, intended to provide guidance in how to control the damages caused by CLR. In a follow-up of this work, we will perform a more detailed pest treatment analysis by proposing different control strategies including the dynamics of the mycoparasite in the model.

List of Publications and talks

Paper 1 C. Djuikem, F. Grognard, R. T. Wafo, S. Bowong, S. Touzeau. Modelling coffee leaf rust dynamics to control its spread. *Mathematical Modelling of Natural Phenomena*, 26(16):25, 2021. https://doi.org/10.1051/mmnp/2021018.

- **Talk 1**: International Conference on Mathematical Methods and Models in Biosciences (BIOMATH 2019) | Jun 16 – Jun 22 | Będlewo | Poland | Conference grant awarded | Oral presentation: Modelling and controlling fungus *Hemileia vastatrix*, a coffee pest. https://hal.inria.fr/hal-02309454

Paper 2 C. Djuikem, F. Grognard, S. Touzeau. Impulsive modelling of rust dynamics and hyperparasite releases for biocontrol. In revision for *Mathematical Biosciences*, September 2022.

- **Talk 2**: Conference on Mathematical Population Dynamics, Ecology and Evolution (MPDEE 2021) | Apr 26 – Apr 30 | CIRM | Marseille | France | Virtual oral presentation: Impulsive model and hyperparasite-based biocontrol of coffee leaf rust propagation. https://hal.inria.fr/hal-03456344.
- **Talk 3**: 7th IFAC Conference on Analysis and Design of Hybrid Systems (ADHS 2021) | July 7 – July 9 | Brussels | Belgium | Virtual oral presentation: Mathematical modelling and optimal control of the seasonal coffee leaf rust propagation. https://hal.inria.fr/hal-03274865.
- **Conference paper**: C. Djuikem, A. G. Yabo, F. Grognard, S. Touzeau. Mathematical modelling and optimal control of the seasonal coffee leaf rust propagation. *IFAC-PapersOnLine*, 54(5):193-198, 2021. https://doi.org/10.1016/j.ifacol.2021.08.497.

Paper 3 C. Djuikem, F. Grognard, S. Touzeau. Bifurcation analysis in an epidemiological model of fungal crop disease. In revision for *Journal of Mathematical Biology*, August 2022.

- **Talk 4**: 12th European Conference on Mathematical and Theoretical Biology (ECMTB 2022) | Sept 19 – Sept 23 | Heidelberg | Germany | Oral presentation: Bifurcation analysis in a coffee leaf rust epidemiological model. https://ecmtb2022.org/wp-content/uploads/sites/18/2022/07/list_of_talks.pdf

Bibliography

[1] Z. Abbasi, I. Zamani, A. H. A. Mehra, M. Shafieirad, and A. Ibeas. Optimal control design of impulsive sqeiar epidemic models with application to covid-19. *Chaos, Solitons and Fractals*, 139:110054, 2020. doi:10.1016/j.chaos.2020.110054. (Cited on page 124.)

[2] A. A. Agrachev and Y. Sachkov. *Control theory from the geometric viewpoint*, volume 87. Springer Science & Business Media, 2013. (Cited on page 134.)

[3] G. N. Agrios. *Plant Pathology*. Academic Press, San Diego, USA, 4 edition, 1997. URL: https://books.google.fr/books?id=CnzbgZgby60C&lpg=PP1&ots=FrFqseYEpg&lr&hl=fr&pg=PP1#v=onepage&q&f=false. (Cited on pages 1, 75 and 91.)

[4] L. F. Aristizábal and M. A. Johnson. Monitoring coffee leaf rust (hemileia vastatrix) on commercial coffee farms in hawaii: Early insights from the first year of disease incursion. *Agronomy*, 12(5):1134, 2022. doi:10.3390/agronomy12051134. (Cited on page 7.)

[5] P. A. Arneson. Coffee rust, 2000. The Plant Health Instructor (updated 2011). URL: http://www.apsnet.org/edcenter/intropp/lessons/fungi/Basidiomycetes/Pages/CoffeeRust.aspx, doi:10.1094/PHI-I-2000-0718-02. (Cited on pages 5, 9, 61, 62 and 75.)

[6] J. Arroyo-Esquivel, F. Sanchez, and L. A. Barboza. Infection model for analyzing biological control of coffee rust using bacterial anti-fungal compounds. *Mathematical Biosciences*, 307:13–24, 2019. doi:10.1016/j.mbs.2018.10.009. (Cited on pages 17, 61 and 91.)

[7] J. Avelino, S. Cabut, B. Barboza, M. Barquero, R. Alfaro, C. Esquivel, J.-F. Durand, and C. Cilas. Topography and crop management are key factors for the development of american leaf spot epidemics on coffee in costa rica. *Phytopathology*, 97(12):1532–1542, 2007. doi:10.1094/PHYTO-97-12-1532. (Cited on page 4.)

[8] J. Avelino, M. Cristancho, S. Georgiou, P. Imbach, L. Aguilar, G. Bornemann, P. Läderach, F. Anzueto, A. J. Hruska, and C. Morales. The coffee rust crises in colombia and central america (2008–2013): impacts, plausible causes and proposed solutions. *Food Security*, 7(2):303–321, 2015. doi:10.1007/s12571-015-0446-9. (Cited on pages 7, 9 and 92.)

[9] J. Avelino, S. Gagliardi, I. Perfecto, M. Isaac, T. Liebig, J. Vandermeer, I. Merle, Z. Hajian-Forooshani, and N. Motisi. Tree effects on coffee leaf rust at field and landscape scales. *Plant Disease*, Jan. 2022. doi:10.1094/PDIS-08-21-1804-FE. (Cited on page 17.)

[10] J. Avelino, L. Willocquet, and S. Savary. Effects of crop management patterns on coffee rust epidemics. *Plant pathology*, 53(5):541–547, 2004. doi:10.1111/j.1365-3059.2004.01067.x. (Cited on pages 17, 61 and 118.)

[11] J. Avelino, H. Zelaya, A. Merlo, A. Pineda, M. Ordóñez, and S. Savary. The intensity of a coffee rust epidemic is dependent on production situations. *Ecological modelling*, 197(3-4):431–447, 2006. doi:10.1016/j.ecolmodel.2006.03.013. (Cited on pages 16, 33 and 61.)

[12] D. Bainov and P. Simeonov. *Impulsive differential equations: periodic solutions and applications*, volume 66. CRC Press, 1993. (Cited on pages 23, 24 and 25.)

[13] BBC News: Guatemala's coffee rust 'emergency' devastates crops, 2013. [accessed 21/10/2022]. URL: https://www.bbc.com/news/world-latin-america-21392257. (Cited on pages 3 and 18.)

[14] E. M. Beasley, N. Aristizábal, E. M. Bueno, and E. R. White. Spatially explicit models predict coffee rust spread in fragmented landscapes. *Landscape Ecology*, 37(8):2165–2178, 2022. doi:10.1007/s10980-022-01473-1. (Cited on page 17.)

[15] D. P. Bebber, Á. D. Castillo, and S. J. Gurr. Modelling coffee leaf rust risk in Colombia with climate reanalysis data. *Philosophical Transactions of the Royal Society B: Biological Sciences*, 371(1709):20150458, 2016. doi:10.1098/rstb.2015.0458. (Cited on pages 17, 34, 61 and 116.)

[16] J. A. M. Bedimo, B. P. Dufour, C. Cilas, and J. Avelino. Effets des arbres d'ombrage sur les bioagresseurs de Coffea arabica. *Cahiers Agricultures*, 21(2-3):89–97, 2012. doi:10.1684/agr.2012.0550. (Cited on page 62.)

[17] J. M. Bedimo, I. Njiayouom, D. Bieysse, M. N. Nkeng, C. Cilas, and J.-L. Notteghem. Effect of shade on arabica coffee berry disease development: Toward an agroforestry system to reduce disease impact. *Phytopathology*, 98(12):1320–1325, 2008. doi:10.1094/PHYTO-98-12-1320. (Cited on page 3.)

[18] S. Belbas and W. Schmidt. Optimal control of impulsive volterra equations with variable impulse times. *Applied mathematics and computation*, 214(2):353–369, 2009. doi:10.1016/j.amc.2009.04.066. (Cited on page 124.)

[19] K. R. Bock. Dispersal of uredospores of Hemileia vastatrix under field conditions. *Transactions of the British Mycological Society*, 45(1):63–74, 1962. doi:10.1016/S0007-1536(62)80035-7. (Cited on pages 36, 64, 100 and 126.)

[20] BOCOP: an open source toolbox for optimal control, 2017. URL: http://bocop.org. (Cited on page 124.)

[21] P. M. Boonekamp. Are plant diseases too much ignored in the climate change debate? *European Journal of Plant Pathology*, 133(1):291–294, 2012. doi:10.1007/s10658-011-9934-8. (Cited on page 33.)

[22] J. B. Burie, A. Calonnec, and A. Ducrot. Singular perturbation analysis of travelling waves for a model in phytopathology. *Mathematical Modelling of Natural Phenomena*, 1(1):49–62, 2006. doi:10.1051/mmnp:2006003. (Cited on page 12.)

[23] J.-B. Burie, A. Calonnec, and M. Langlais. Modeling of the invasion of a fungal disease over a vineyard. In *Mathematical Modeling of Biological Systems*, volume 2, pages 11–21. Springer, 2008. doi:10.1007/978-0-8176-4556-4_2. (Cited on pages 12, 14, 33, 61, 62 and 64.)

[24] J.-B. Burie and A. Ducrot. A field scale model for the spread of fungal diseases in crops: the example of a powdery mildew epidemic over a large vineyard. *Mathematical Methods in the Applied Sciences*, 38(17):3720–3737, 2015. doi:10.1002/mma.3312. (Cited on page 12.)

[25] A. Capucho, L. Zambolim, U. Lopes, and N. Milagres. Chemical control of coffee leaf rust in coffea canephora cv. conilon. *Australasian Plant Pathology*, 42(6):667–673, 2013. doi:10.1007/s13313-013-0242-y. (Cited on pages 9, 61 and 75.)

[26] G. Carrion and V. Rico-Gray. Mycoparasites on the coffee rust in Mexico. *Fungal Diversity*, 11(5):49–60, 10 2002. URL: https://www.fungaldiversity.org/fdp/sfdp/FD_11_49-60.pdf. (Cited on pages 75, 80 and 132.)

[27] C. Castillo-Chavez and B. Song. Dynamical models of tuberculosis and their applications. *Mathematical Biosciences & Engineering*, 1(2):361, 2004. doi:10.3934/mbe.2004.1.361. (Cited on pages 23 and 83.)

[28] G. Champéroux. *Manuel du planteur de café laotien*. CIRAD-IRCC, IRCC, Montpellier, 1991. URL: http://agritrop.cirad.fr/345484/. (Cited on pages 4, 5, 62 and 100.)

[29] A. Charrier and J. Berthaud. Botanical classification of coffee. In *Coffee*, pages 13–47. Springer, 1985. doi:10.1007/978-1-4615-6657-1_2. (Cited on pages 36 and 64.)

[30] A. Charrier and A. B. Eskes. *Botany and Genetics of Coffee*, chapter 2, pages 25–56. John Wiley & Sons, Ltd, 2004. doi:/10.1002/9783527619627.ch2. (Cited on page 4.)

[31] M. N. Clifford and K. C. Willsons, editors. *Coffee: botany, biochemistry and production of beans and beverage*. Springer, New York, 1985. doi:10.1007/978-1-4615-6657-1. (Cited on pages 5, 11, 99 and 100.)

[32] J. S. Coleman. Leaf development and leaf stress: increased susceptibility associated with sink-source transition. *Tree Physiology*, 2(1-2-3):289–299, 12 1986. arXiv:https://academic.oup.com/treephys/article-pdf2/1-2-3/289/4594414/2-1-2-3-289.pdf, doi:10.1093/treephys/2.1-2-3.289. (Cited on page 33.)

[33] W. A. Coppel. *Stability and asymptotic behavior of differential equations*. Heath, 1965. (Cited on pages 98 and 129.)

[34] S. Daivasikamani et al. Biological control of coffee leaf rust pathogen, hemileia vastatrix berkeley and broome using bacillus subtilis and pseudomonas fluorescens. *Journal of Biopesticides*, 2(1):94–98, 2009. URL: http://wwww.jbiopest.com. (Cited on pages 10 and 92.)

[35] E. De Jong, A. Eskes, J. Hoogstraten, and J. Zadoks. Temperature requirements for germination, germ tube growth and appressorium formation of urediospores of hemileia vastatrix. *Netherlands Journal of Plant Pathology*, 93(2):61–71, 1987. doi:10.1007/BF01998091. (Cited on page 118.)

[36] M.-L. Desprez-Loustau, F. M. Hamelin, and B. Marçais. The ecological and evolutionary trajectory of oak powdery mildew in Europe. In K. Wilson, A. Fenton, and D. Tompkins, editors, *Wildlife Disease Ecology: Linking Theory to Data and Application*, Ecological Reviews, chapter 15, page 429–457. Cambridge University Press, 2019. doi:10.1017/9781316479964.015. (Cited on pages 12, 33 and 91.)

[37] C. Djuikem, A. Gabriel Yabo, F. Grognard, and S. Touzeau. Mathematical modelling and optimal control of the seasonal coffee leaf rust propagation. *IFAC-PapersOnLine*, 54(5):193–198, 2021. 7th IFAC Conference on Analysis and Design of Hybrid Systems ADHS 2021. doi:10.1016/j.ifacol.2021.08.497. (Cited on pages 89, 92, 119 and 123.)

[38] C. Djuikem, F. Grognard, R. Tagne Wafo, S. Touzeau, and S. Bowong. Modelling coffee leaf rust dynamics to control its spread. *Mathematical Modelling of Natural Phenomena*, 16:26, 2021. doi:10.1051/mmnp/2021018. (Cited on pages 34, 59, 116 and 119.)

[39] A. V. Dmitruk and A. M. Kaganovich. The hybrid maximum principle is a consequence of pontryagin maximum principle. *Systems & Control Letters*, 57(11):964–970, 2008. doi:10.1016/j.sysconle.2008.05.006. (Cited on pages 124 and 133.)

[40] A. d'Onofrio. Stability properties of pulse vaccination strategy in seir epidemic model. *Mathematical biosciences*, 179(1):57–72, 2002. doi:10.1016/S0025-5564(02)00095-0. (Cited on page 124.)

[41] e-Krishi Shiksha. Diseases of coffee. [accessed 15/9/2022]. URL: http://ecoursesonline.iasri.res.in/mod/page/view.php?id=9675. (Cited on pages 2, 3 and 4.)

[42] M. El Jarroudi, H. Karjoun, L. Kouadio, and M. El Jarroudi. Mathematical modelling of non-local spore dispersion of wind-borne pathogens causing fungal diseases. *Applied Mathematics and Computation*, 376:125107, 2020. doi:10.1016/j.amc.2020.125107. (Cited on page 12.)

[43] A. Eskes. *Incomplete resistance to coffee leaf rust (Hemileia vastatrix)*. Wageningen University and Research, 1983. (Cited on page 11.)

[44] A. Eskes, M. Mendes, and C. Robbs. Laboratory and field studies on parasitism of hemileia vastatrix with verticillium lecanii and v. leptobactrum. *Café, Cacao, Thé (Francia) v. 35 (4) p. 275-282*, 1991. (Cited on page 10.)

[45] F. Fabre, J.-B. Burie, A. Ducrot, S. Lion, Q. Richard, and R. Djidjou-Demasse. An epi-evolutionary model for predicting the adaptation of spore-producing pathogens to quantitative resistance in heterogeneous environments. *Evolutionary applications*, 15(1):95–110, 2022. doi:10.1111/eva.13328. (Cited on page 121.)

[46] Climate change fans spread of pests and threatens plants and crops, new fao study. [accessed 15/9/2022]. URL: https://www.fao.org/news/story/en/item/1402920/icode/. (Cited on page 1.)

[47] FAOSTAT: Cameroon, agricultural land, 2016. [Online; accessed August 3, 2022]. URL: https://www.fao.org/faostat/en/#country/32. (Cited on page 2.)

[48] M. Fazeli-Dinan, R. Talaei-Hassanloui, and M. Goettel. Virulence of the entomopathogenic fungus lecanicillium longisporum against the greenhouse whitefly, trialeurodes vaporariorum and its parasitoid encarsia formosa. *International Journal of Pest Management*, 62(3):251–260, 2016. doi:10.1080/09670874.2016.1182228. (Cited on page 120.)

[49] R. A. Fleming. The potential for control of cereal rust by natural enemies. *Theoretical Population Biology*, 18(3):374–395, 1980. doi:10.1016/0040-5809(80)90060-X. (Cited on pages 12, 13, 33 and 91.)

[50] J. Flood. *Coffee wilt disease*. CABI, 2010. (Cited on page 3.)

[51] Fortune Business Insights. Gree coffee market size, share & covid-19 impact analysis. [accessed 15/9/2022]. URL: https://www.fortunebusinessinsights.com/green-coffee-market-106635. (Cited on page 2.)

[52] Y. Fotso Fotso. *Modelling, analysis and control of coffee berry borer*. Theses, Université de Dschang (Cameroun), Jan. 2022. URL: https://hal.archives-ouvertes.fr/tel-03608463. (Cited on page 2.)

[53] D. Fróna, J. Szenderák, and M. Harangi-Rákos. The challenge of feeding the world. *Sustainability*, 11(20):5816, 2019. doi:10.3390/su11205816. (Cited on page 1.)

[54] L. Galbusera, M. P. E. Marciandi, P. Bolzern, and G. Ferrari-Trecate. Control schemes based on the wave equation for consensus in multi-agent systems with double-integrator dynamics. In *2007 46th IEEE Conference on Decision and Control*, pages 1498–1503. IEEE, 2007. doi:10.1109/CDC.2007.4434358. (Cited on page 72.)

[55] W. Gams and A. Van Zaayen. Contribution to the taxonomy and pathogenicity of fungicolous verticillium species. i. taxonomy. *Netherlands Journal of Plant Pathology*, 88(2):57–78, 1982. doi:10.1007/BF01977339. (Cited on page 92.)

[56] B. Ghosh, F. Grognard, and L. Mailleret. Natural enemies deployment in patchy environments for augmentative biological control. *Applied Mathematics and Computation*, 266:982–999, 2015. doi:10.1016/j.amc.2015.06.021. (Cited on pages 26 and 104.)

[57] M. S. Goettel, M. Koike, J. J. Kim, D. Aiuchi, R. Shinya, and J. Brodeur. Potential of Lecanicillium spp. for management of insects, nematodes and plant diseases. *Journal of Invertebrate Pathology*, 98(3):256–261, 2008. Special Issue for SIP 2008. doi:10.1016/j.jip.2008.01.009. (Cited on page 117.)

[58] G. Grée. Epidemiology of coffee leaf rust in the Eastern Highlands. *Coffee Research Institute Newsletter*, 2:16–20, 1993. URL: https://agritrop.cirad.fr/399280/. (Cited on pages 61 and 92.)

[59] F.-M. Gumpert, H. Geiger, and U. Stähle. A mathematical model of the epidemics in homogeneous and heterogeneous host stands/ein mathematisches modell für epidemien in homogenen und heterogenen wirtsbeständen. *Zeitschrift für Pflanzenkrankheiten und Pflanzenschutz/Journal of Plant Diseases and Protection*, pages 206–215, 1987. URL: https://www.jstor.org/stable/43383228. (Cited on page 12.)

[60] S. Hacquard, B. Petre, P. Frey, A. Hecker, N. Rouhier, and S. Duplessis. The poplar-poplar rust interaction: insights from genomics and transcriptomics. *Journal of pathogens*, 2011, 2011. doi:10.4061/2011/716041. (Cited on page 33.)

[61] F. Haddad, L. A. Maffia, E. S. G. Mizubuti, and H. Teixeira. Biological control of coffee rust by antagonistic bacteria under field conditions in Brazil. *Biological Control*, 49(2):114–119, 2009. doi:10.1016/j.biocontrol.2009.02.004. (Cited on page 75.)

[62] F. Haddad, R. M. Saraiva, E. S. G. Mizubuti, R. S. Romeiro, and L. A. Maffia. Antifungal compounds as a mechanism to control Hemileia vastatrix by antagonistic bacteria. *Tropical Plant Pathology*, 38(5):398–405, 2013. doi:10.1590/S1982-56762013000500004. (Cited on pages 10 and 75.)

[63] Z. Hajian-Forooshani, I. S. Rivera Salinas, E. Jiménez-Soto, I. Perfecto, and J. Vandermeer. Impact of regionally distinct agroecosystem communities on the potential for autonomous control of the coffee leaf rust. *Environmental Entomology*, 45(6):1521–1526, 10 2016. arXiv:https://academic.oup.com/ee/article-pdf/45/6/1521/8660201/nvw125.pdf, doi:10.1093/ee/nvw125. (Cited on pages 10, 92 and 120.)

[64] J. Hale. *Ordinary differential equations, 1969*. Wiley-Interscience, New York, 1969. (Cited on page 129.)

[65] W. H. Hamer. *Epidemic disease in England: the evidence of variability and of persistency of type*. Bedford Press, 1906. (Cited on page 11.)

[66] Hawaii Department of Agriculture Divisions. Board of agriculture expands coffee quarantine to o'ahu and lana'i. [accessed 20/10/2022]. URL: https://hdoa.hawaii.gov/blog/main/nr21-08coffeequarantineexpanded/. (Cited on pages 3, 4 and 7.)

[67] D. Henk, D. Farr, and M. Aime. Mycodiplosis (diptera) infestation of rust fungi is frequent, wide spread and possibly host specific. *Fungal Ecology*, 4(4):284–289, 2011. doi:10.1016/j.funeco.2011.03.006. (Cited on pages 10, 18, 92, 117 and 120.)

[68] A. Heydari, M. Pessarakli, et al. A review on biological control of fungal plant pathogens using microbial antagonists. *Journal of biological sciences*, 10(4):273–290, 2010. doi:10.3923/jbs.2010.273.290. (Cited on page 92.)

[69] F. D. Hinnah, P. C. Sentelhas, F. R. Alves Patrício, R. N. Paiva, and M. V. Parenti. Performance of a weather-based forecast system for chemical control of coffee leaf rust. *Crop Protection*, 137:105225, 2020. doi:10.1016/j.cropro.2020.105225. (Cited on page 17.)

[70] P. Hrelia, C. Fimognari, F. Maffei, F. Vigagni, R. Mesirca, L. Pozzetti, M. Paolini, and G. C. Forti. The genetic and non-genetic toxicity of the fungicide vinclozolin. *Mutagenesis*, 11(5):445–453, 1996. doi:10.1093/mutage/11.5.445. (Cited on page 91.)

[71] International Coffee Organization. Coffee production by exporting countries. [accessed 23/2/202]. URL: http://www.ico.org/prices/po-production.pdf. (Cited on pages 61 and 64.)

[72] International Coffee Organization. World coffee consumption, 2020. [accessed 12/11/2020]. URL: http://www.ico.org/prices/new-consumption-table.pdf. (Cited on page 124.)

[73] D. Jackson, J. Skillman, and J. Vandermeer. Indirect biological control of the coffee leaf rust, hemileia vastatrix, by the entomogenous fungus lecanicillium lecanii in a complex coffee agroecosystem. *Biological Control*, 61(1):89–97, 2012. doi:10.1016/j.biocontrol.2012.01.004. (Cited on page 10.)

[74] J. Jaramillo, E. Muchugu, F. E. Vega, A. Davis, C. Borgemeister, and A. Chabi-Olaye. Some like it hot: the influence and implications of climate change on coffee berry borer (hypothenemus hampei) and coffee production in east africa. *PloS one*, 6(9):e24528, 2011. doi:10.1371/journal.pone.0024528. (Cited on page 2.)

[75] M. J. Jeger, P. Jeffries, Y. Elad, and X.-M. Xu. A generic theoretical model for biological control of foliar plant diseases. *Journal of Theoretical Biology*, 256(2):201–214, 2009. doi:10.1016/j.jtbi.2008.09.036. (Cited on page 91.)

[76] M. J. Jeger, P. J. Wijngaarden, and R. F. Hoekstra. Adaptation to the cost of resistance in a haploid clonally reproducing organism: The role of mutation, migration and selection. *Journal of Theoretical Biology*, 252(4):621–632, 2008. doi:10.1016/j.jtbi.2008.02.023. (Cited on page 91.)

[77] John Megahan. Life cycle of the coffee leaf rust. [accessed 8/9/2022]. URL: https://feralatlas.supdigital.org/poster/coffee-rust-spreads-together-with-coffee-plantations. (Cited on page 8.)

[78] J.-C. Kamgang. *Contribution à la stabilisation des systèmes mécaniques: contribution à l'étude de la stabilité des modèles épidémiologiques*. PhD thesis, Université Paul Verlaine-Metz, 2003. URL: https://hal.univ-lorraine.fr/tel-01749936. (Cited on page 40.)

[79] J. C. Kamgang and G. Sallet. Computation of threshold conditions for epidemiological models and global stability of the disease-free equilibrium (dfe). *Mathematical biosciences*, 213(1):1–12, 2008. doi:10.1016/j.mbs.2008.02.005. (Cited on page 42.)

[80] W. O. Kermack and A. G. McKendrick. A contribution to the mathematical theory of epidemics. *Proceedings of the royal society of london. Series A, Containing papers of a mathematical and physical character*, 115(772):700–721, 1927. doi:10.1098/rspa.1927.0118. (Cited on page 11.)

[81] H. Kielhöfer. Stability and semilinear evolution equations in Hilbert space. *Archive for Rational Mechanics and Analysis*, 57(2):150–165, 1974. doi:10.1007/BF00248417. (Cited on pages 80 and 81.)

[82] M. Komárek, E. Čadková, V. Chrastnỳ, F. Bordas, and J.-C. Bollinger. Contamination of vineyard soils with fungicides: a review of environmental and toxicological aspects. *Environment international*, 36(1):138–151, 2010. doi:10.1016/j.envint.2009.10.005. (Cited on page 91.)

[83] A. Koutouleas, H. J. L. Jørgensen, B. Jensen, J.-P. B. Lillesø, A. Junge, and A. Ræbild. On the hunt for the alternate host of Hemileia vastatrix. *Ecology and Evolution*, 9(23):13619–13631, 2019. doi:10.1002/ece3.5755. (Cited on page 33.)

[84] A. Kushalappa, M. Akutsu, S. Oseguera, G. Chaves, C. Melles, J. Miranda, and G. Bartolo. Equations for predicting the rate of coffee rust development based on net survival ratio for monocyclic process of hemileia vastatrix *Coffea arabica*. *Fitopatologia Brasileira (Brazil)*, 1984. URL: https://www.apsnet.org/publications/phytopathology/backissues/Documents/1983Articles/Phyto73n01_96.PDF. (Cited on page 16.)

[85] A. Kushalappa, G. Chaves, et al. An analysis of the development of coffee rust in the field. *Fitopatologia Brasileira*, 5(1):95–103, 1980. (Cited on page 16.)

[86] A. C. Kushalappa. Linear models applied to variation in the rate of coffee rust development. *Journal of Phytopathology*, 101(1):22–30, 1981. doi:https://doi.org/10.1111/j.1439-0434.1981.tb03317.x. (Cited on page 16.)

[87] A. C. Kushalappa and B. E. Albertus. *Coffee rust: Epidemiology, resistance and management*. CRC Press, Florida, USA, 1989. (Cited on pages 3 and 9.)

[88] J. P. LaSalle. *The stability of dynamical systems*, volume 25. Siam, 1976. (Cited on page 71.)

[89] K. Li, J. H. Vandermeer, and I. Perfecto. Disentangling endogenous versus exogenous pattern formation in spatial ecology: a case study of the ant azteca sericeasur in southern mexico. *Royal Society open science*, 3(5):160073, 2016. doi:10.1098/rsos.160073. (Cited on page 120.)

[90] T. Liebig, F. Ribeyre, P. Läderach, H.-M. Poehling, P. van Asten, and J. Avelino. Interactive effects of altitude, microclimate and shading system on coffee leaf rust. *Journal of Plant Interactions*, 14(1):407–415, 2019. doi:10.1080/17429145.2019.1643934. (Cited on page 10.)

[91] T.-K. Lim and W. Z. W. Nik. Mycoparasitism of the coffee rust pathogen, hemileia vastatrix, by verticillium psalliotae in malaysia. *Pertanika.*, 6(2):23–25, 1983. doi:http://agris.upm.edu.my:8080/dspace/handle/0/13206. (Cited on page 10.)

[92] U. Lopes, L. Zambolim, P. Neto, H. Duarte, J. Ribeiro, A. Souza, and F. Rodrigues. Silicon and Triadimenol for the management of coffee leaf rust. *Journal of Phytopathology*, 162, 02 2014. doi:doi:10.1111/jph.12166. (Cited on page 64.)

[93] J. A. Lucas, N. J. Hawkins, and B. A. Fraaije. The evolution of fungicide resistance. *Advances in applied microbiology*, 90:29–92, 2015. doi:10.1016/bs.aambs.2014.09.001. (Cited on page 9.)

[94] L. V. Madden and F. Van Den Bosch. A population-dynamics approach to assess the threat of plant pathogens as biological weapons against annual crops: Using a coupled differential-equation model, we show the conditions necessary for long-term persistence of a plant disease after a pathogenic microorganism is introduced into a susceptible annual crop. *BioScience*, 52(1):65–74, 2002. doi:10.1641/0006-3568(2002)052[0065:APDATA]2.0.CO;2. (Cited on page 15.)

[95] M. Mahfud, M. A. ZA, S. Meon, and J. Kadir. In vitro and in vivo tests for parasitism of verticillium psalliotae treschow on hemileia vastatrix berk. and br. *Malaysian Journal of Microbiology*, 2(1):46–50, 2006. doi:10.21161/MJM.210608. (Cited on page 10.)

[96] L. Mailleret and F. Grognard. Global stability and optimisation of a general impulsive biological control model. *Mathematical Biosciences*, 221(2):91–100, 2009. doi:10.1016/j.mbs.2009.07.002. (Cited on pages 80 and 124.)

[97] Y. Mammeri, J. Burie, M. Langlais, and A. Calonnec. How changes in the dynamic of crop susceptibility and cultural practices can be used to better control the spread of a fungal pathogen at the plot scale? *Ecological Modelling*, 290:178–191, 2014. Special Issue of the 4th International Symposium on Plant Growth Modeling, Simulation, Visualization and Applications (PMA'12). doi:10.1016/j.ecolmodel.2014.02.017. (Cited on pages 12, 33 and 91.)

[98] L. Manuel, P. Talhinhas, V. Varzea, and J. Neves-Martins. Characterization of colletotrichum kahawae isolates causing coffee berry disease in angola. *Journal of phytopathology*, 158(4):310–313, 2010. doi:10.1111/j.1439-0434.2009.01613.x. (Cited on page 3.)

[99] D. Masaba and J. M. Waller. Coffee berry disease: the current status. *Coffee berry disease: the current status.*, pages 237–249, 1992. (Cited on page 3.)

[100] A. Maublanc and L. Roger. Une nouvelle rouille du caféier au Cameroun. *Bulletin de la Société Mycologique de France*, 50:193–202, 1934. (Cited on page 4.)

[101] A. Maupetit, R. Larbat, M. Pernaci, A. Andrieux, C. Guinet, A.-L. Boutigny, B. Fabre, P. Frey, and F. Halkett. Defense compounds rather than nutrient availability shape aggressiveness trait variation along a leaf maturity gradient in a biotrophic plant pathogen. *Frontiers in Plant Science*, 9, 2018. doi:10.3389/fpls.2018.01396. (Cited on pages 12 and 33.)

[102] S. McCook and J. Vandermeer. The big rust and the red queen: Long-term perspectives on coffee rust research. *Phytopathology*, 105(9):1164–1173, 2015. doi:10.1094/PHYTO-04-15-0085-RVW. (Cited on page 9.)

[103] J. McDonald. A preliminary account of a disease of green coffee berries in kenya colony. *Transactions of the British Mycological Society*, 11(1):145–154, 1926. doi:10.1016/S0007-1536(26)80033-6. (Cited on page 3.)

[104] K. Mendgen. Growth of verticillium lecanii in pustules of stripe rust (puccinia striiformis). *Phytopathologische Zeitschrift*, 102(3-4):301–309, 1981. doi:10.1111/j.1439-0434.1981.tb03391.x. (Cited on page 92.)

[105] X. Meng and Z. Li. The dynamics of plant disease models with continuous and impulsive cultural control strategies. *Journal of Theoretical Biology*, 266(1):29–40, 2010. doi:10.1016/j.jtbi.2010.05.033. (Cited on pages 13 and 91.)

[106] I. Merle. *Effets du microclimat sur le développement de l'épidémie de rouille orangée du caféier Arabica (Hemileia vastatrix-Coffea arabica) dans une gamme de situations de production*. PhD thesis, Université de Montpellier, 2019. (Cited on pages 18 and 34.)

[107] I. Merle, P. Tixier, E. de Melo Virginio Filho, C. Cilas, and J. Avelino. Forecast models of coffee leaf rust symptoms and signs based on identified microclimatic combinations in coffee-based agroforestry systems in costa rica. *Crop Protection*, 130:105046, 2020. doi:10.1016/j.cropro.2019.105046. (Cited on page 17.)

[108] R. E. Mickens. Nonstandard finite difference schemes for reaction-diffusion equations. *Numerical Methods for Partial Differential Equations: An International Journal*, 15(2):201–214, 1999. doi:10.1080/1023619021000000807. (Cited on pages 28 and 73.)

[109] L. C. Monaco et al. Consequences of the introduction of coffee rust into brazil. *The genetic basis of epidemics in agriculture*, pages 57–71, 1977. (Cited on page 9.)

[110] L. B. Mondiale. Agriculture et alimentation. [accessed 14/9/2022]. URL: https://www.banquemondiale.org/fr/topic/agriculture/overview. (Cited on page 1.)

[111] D. Moore, G. D. Robson, and A. P. J. Trinci. *21st Century Guidebook to Fungi*. Cambridge University Press, 2000. doi:10.1017/CBO9780511977022. (Cited on page 11.)

[112] R. A. Muller, D. Berry, J. Avelino, and D. Bieysse. *Coffee Diseases*, chapter 4, pages 491–545. John Wiley & Sons, Ltd, 2008. URL: https://onlinelibrary.wiley.com/doi/abs/10.1002/9783527619627.ch18, doi:10.1002/9783527619627.ch18. (Cited on page 61.)

[113] C. Nembot, P. Takam Soh, G. M. Ten Hoopen, and Y. Dumont. Modeling the temporal evolution of cocoa black pod rot disease caused by phytophthora megakarya. *Mathematical Methods in the Applied Sciences*, 41(18):8816–8843, 2018. doi:10.1002/mma.5206. (Cited on pages 13 and 91.)

[114] S. Nilusmas, M. Mercat, T. Perrot, C. Djian-Caporalino, P. Castagnone-Sereno, S. Touzeau, V. Calcagno, and L. Mailleret. Multi-seasonal modelling of plant-nematode interactions reveals efficient plant resistance deployment strategies. *Evolutionary applications*, 13(9):2206–2221, 2020. doi:10.1111/eva.12989. (Cited on page 121.)

[115] S. Nundloll, L. Mailleret, and F. Grognard. Two models of interfering predators in impulsive biological control. *Journal of Biological Dynamics*, 4(1):102–114, 2010. doi:10.1080/17513750902968779. (Cited on pages 13 and 91.)

[116] F. J. Nutman, F. M. Roberts, and R. T. Clarke. Studies on the biology of hemileia vastatrix berk. & br. *Transactions of the British Mycological Society*, 46(1):27–44, 1963. doi:10.1016/S0007-1536(63)80005-4. (Cited on pages 33 and 62.)

[117] E.-C. Oerke. Crop losses to pests. *The Journal of Agricultural Science*, 144(1):31–43, 2006. (Cited on page 1.)

[118] T. O. of Economic Complexity (OEC). Historical data, 2017. [Online; accessed August 3, 2022]. URL: https://oec.world/en/profile/country/cmr#yearly-trade. (Cited on page 2.)

[119] C.-V. Pao. *Nonlinear parabolic and elliptic equations*. Springer Science & Business Media, 2012. (Cited on page 26.)

[120] J. Papaïx, K. Adamczyk-Chauvat, A. Bouvier, K. Kiêu, S. Touzeau, C. Lannou, and H. Monod. Pathogen population dynamics in agricultural landscapes: The Ddal modelling framework. *Infection, Genetics and Evolution*, 27:509–520, 2014. (Cited on pages 12 and 61.)

[121] A. Pazy. *Semigroups of linear operators and applications to partial differential equations*, volume 44. Springer Science & Business Media, 2012. (Cited on pages 26, 27, 68, 69 and 70.)

[122] F. Pellegrin, B. Seivert, F. Kohler, C. Van Bercie, and B. Boccas. La rouille orangée du caféier Arabica en Nouvelle Calédonie : historique et épidémiologie. *Café, Cacao, Thé*, 27(1):27–40, 1983. URL: https://www.documentation.ird.fr/hor/fdi:03582. (Cited on pages 18 and 34.)

[123] D. R. Pereira, D. H. Nadaleti, E. C. Rodrigues, A. D. da Silva, M. R. Malta, S. P. de Carvalho, and G. R. Carvalho. Genetic and chemical control of coffee rust (hemileia vastatrix b erk et b r.): impacts on coffee (coffea arabica l.) quality. *Journal of the Science of Food and Agriculture*, 101(7):2836–2845, 2021. doi:10.1002/jsfa.10914. (Cited on page 9.)

[124] S. Pivonia and X. Yang. Relating epidemic progress from a general disease model to seasonal appearance time of rusts in the united states: Implications for soybean rust. *Phytopathology*, 96(4):400–407, 2006. doi:10.1094/PHYTO-96-0400. (Cited on pages 12, 33 and 91.)

[125] L. S. Pontryagin. *Mathematical theory of optimal processes*. Routledge, 2018. (Cited on page 124.)

[126] N. S. Prakash, J. Devasia, Jayarama, and R. K. Aggarwal. Chapter 8 - coffee industry in india: Production to consumption—a sustainable enterprise. In V. R. Preedy, editor, *Coffee in Health and Disease Prevention*, pages 61–70. Academic Press, San Diego, 2015. doi:10.1016/B978-0-12-409517-5.00008-5. (Cited on page 2.)

[127] S. Rahman, A. R. Anik, and J. R. Sarker. Climate, environment and socio-economic drivers of global agricultural productivity growth. *Land*, 11(4):512, 2022. doi:10.3390/land11040512. (Cited on page 1.)

[128] D. Ramiro, A. Jalloul, A.-S. Petitot, M. F. Grossi De Sá, M. P. Maluf, and D. Fernandez. Identification of coffee wrky transcription factor genes and expression profiling in resistance responses to pathogens. *Tree Genetics & Genomes*, 6(5):767–781, 2010. doi:10.1007/s11295-010-0290-1. (Cited on page 121.)

[129] D. A. Ramiro, O. Guerreiro-Filho, and P. Mazzafera. Phenol contents, oxidase activities, and the resistance of coffee to the leaf miner leucoptera coffeella. *Journal of chemical ecology*, 32(9):1977–1988, 2006. doi:10.1007/s10886-006-9122-z. (Cited on page 121.)

[130] V. Ravigné, V. Lemesle, A. Walter, L. Mailleret, and F. M. Hamelin. Mate limitation in fungal plant parasites can lead to cyclic epidemics in perennial host populations. *Bulletin of mathematical biology*, 79(3):430–447, 2017. doi:10.1007/s11538-016-0240-7. (Cited on pages 12, 33 and 91.)

[131] R. W. Rayner. Germination and penetration studies on coffee rust (Hemileia vastatrix B. & Br.). *Annals of Applied Biology*, 49(3):497–505, 1961. doi:10.1111/j.1744-7348.1961.tb03641.x. (Cited on pages 36, 64, 100 and 126.)

[132] R. Razafindramamba. Biologie de la rouille du caféier. *Revue de Mycologie*, 23:177–200, 1958. URL: https://www.documentation.ird.fr/hor/fdi:11779. (Cited on page 33.)

[133] L. Rimbaud, F. Fabre, J. Papaïx, B. Moury, C. Lannou, L. G. Barrett, and P. H. Thrall. Models of plant resistance deployment. *Annual Review of Phytopathology*, 59:125–152, 2021. doi:10.1146/annurev-phyto-020620-122134. (Cited on page 121.)

[134] L. Rimbaud, J. Papaïx, L. G. Barrett, J. J. Burdon, and P. H. Thrall. Mosaics, mixtures, rotations or pyramiding: What is the optimal strategy to deploy major gene resistance? *Evolutionary Applications*, 11(10):1791–1810, 2018. doi:10.1111/eva.12681. (Cited on pages 12, 33 and 91.)

[135] C. Rodrigues Jr, A. Bettencourt, and L. Rijo. Races of the pathogen and resistance to coffee rust. *Annual review of phytopathology*, 13(1):49–70, 1975. doi:10.1146/annurev.py.13.090175.000405. (Cited on page 10.)

[136] C. J. Rodrigues Jr. Coffee rusts: history, taxonomy, morphology, distribution and host resistance. *Fitopatologia Brasileira*, 15:5–9, 1990. (Cited on pages 9 and 62.)

[137] R. Ross. *The prevention of malaria*. John Murray, 1911. (Cited on page 11.)

[138] M. A. Rutherford and N. Phiri. Pests and diseases of coffee in eastern africa: A technical and advisory manual. *Wallingford, UK: CAB International*, 2006. URL: https://fa2q.net/sites/cooperativeknowledge.info/files/resource/U3071CoffeeManual.pdf. (Cited on pages 2, 3 and 4.)

[139] E. Santiago-Elena, E. J. Zamora-Macorra, M. Zamora-Macorra, and K. G. Elizalde-Gaytan. Interaction between mycodiplosis and hemileia vastatrix in three scenarios of coffee crop management (coffea arabica). *Revista mexicana de fitopatología*, 38(3):320–336, 2020. doi:10.18781/r.mex.fit.2005-2. (Cited on pages 10, 92 and 120.)

[140] N. Sapoukhina, Y. Tyutyunov, I. Sache, and R. Arditi. Spatially mixed crops to control the stratified dispersal of airborne fungal diseases. *Ecological Modelling*, 221(23):2793–2800, 2010. doi:10.1016/j.ecolmodel.2010.08.020. (Cited on pages 12, 33, 61 and 62.)

[141] M. Saubin, S. de Mita, X. Zhu, B. Sudret, and F. Halkett. Impact of ploidy and pathogen life cycle on resistance durability. *Peer Community in Evolutionary Biology*, Aug. 2021. URL: https://hal.archives-ouvertes.fr/hal-03610230, doi:10.24072/pcjournal.10. (Cited on page 10.)

[142] G. H. Sera, C. H. S. de Carvalho, J. C. de Rezende Abrahão, E. A. Pozza, J. B. Matiello, S. R. de Almeida, L. Bartelega, and D. M. dos Santos Botelho. Coffee leaf rust in brazil: Historical events, current situation, and control measures. *Agronomy*, 12(2), 2022. doi:10.3390/agronomy12020496. (Cited on pages 10 and 11.)

[143] R. Setiawati, A. Widiastuti, A. Wibowo, and A. Priyatmojo. Variability of lecanicillium spp. mycoparasite of coffee leaf rust pathogen (hemileia vastatrix) in indonesia. *Pakistan Journal of Biological Sciences: PJBS*, 24(5):588–598, 2021. doi:10.3923/pjbs.2021.588.598. (Cited on page 117.)

[144] J. Shafi, H. Tian, and M. Ji. Bacillus species as versatile weapons for plant pathogens: a review. *Biotechnology & Biotechnological Equipment*, 31(3):446–459, 2017. doi:10.1080/13102818.2017.1286950. (Cited on page 92.)

[145] E. G. Sharvelle. *Plant disease control*. The AVI Publishing Company, 1979. (Cited on pages 9, 10 and 91.)

[146] H. F. Shiomi, H. S. A. Silva, I. S. d. Melo, F. V. Nunes, and W. Bettiol. Bioprospecting endophytic bacteria for biological control of coffee leaf rust. *Scientia Agricola*, 63:32–39, 2006. doi:10.1590/S0103-90162006000100006. (Cited on pages 10 and 75.)

[147] H. S. A. Silva, J. P. Tozzi, C. R. F. Terrasan, and W. Bettiol. Endophytic microorganisms from coffee tissues as plant growth promoters and biocontrol agents of coffee leaf rust. *Biological Control*, 63(1):62–67, 2012. doi:10.1016/j.biocontrol.2012.06.005. (Cited on page 75.)

[148] V. Singh and B. Deverall. Bacillus subtilis as a control agent against fungal pathogens of citrus fruit. *Transactions of the British Mycological Society*, 83(3):487–490, 1984. doi:10.1016/S0007-1536(84)80045-5. (Cited on page 92.)

[149] R. L. Steyaert. Cladosporium hemileiae n. spec. un parasite de l'hemileia vastatrix berk. et br. *Bulletin de la Société Royale de Botanique de Belgique/Bulletin van de Koninklijke Belgische Botanische Vereniging*, 63(Fasc. 1):46–48, 1930. URL: https://www.jstor.org/stable/20791606. (Cited on pages 10 and 92.)

[150] C. Struck. Infection strategies of plant parasitic fungi. In B. Cooke, D. G. Jones, and B. Kaye, editors, *The Epidemiology of Plant Diseases*, pages 117–137. Springer, Dordrecht, 2006. doi:10.1007/1-4020-4581-6_4. (Cited on page 11.)

[151] J.-B. Suchel. Quelques remarques à propos de la répartition des pluies au Cameroun durant la période sèche 1969-1973. *Hommes et Terres du Nord*, 3(1):24–28, 1983. (Cited on pages 62, 99 and 100.)

[152] C. Tadmon and S. Foko. Modeling and mathematical analysis of an initial boundary value problem for hepatitis b virus infection. *Journal of Mathematical Analysis and Applications*, 474(1):309–350, 2019. doi:10.1016/j.jmaa.2019.01.047. (Cited on page 72.)

[153] P. Talhinhas, D. Batista, I. Diniz, A. Vieira, D. N. Silva, A. Loureiro, S. Tavares, A. P. Pereira, H. G. Azinheira, L. Guerra-Guimarães, et al. The coffee leaf rust pathogen hemileia vastatrix: one and a half centuries around the tropics. *Molecular plant pathology*, 18(8):1039, 2017. doi:10.1111/mpp.12512. (Cited on page 7.)

[154] A. T. Tamen, Y. Dumont, J.-J. Tewa, S. Bowong, and P. Couteron. A minimalistic model of tree–grass interactions using impulsive differential equations and non-linear feedback

functions of grass biomass onto fire-induced tree mortality. *Mathematics and Computers in Simulation*, 133:265–297, 2017. doi:10.1016/j.matcom.2016.03.008. (Cited on page 124.)

[155] I. Tankam-Chedjou, F. Grognard, J. J. Tewa, and S. Touzeau. Optimal and sustainable management of a soilborne banana pest. *Applied Mathematics and Computation*, 397:125883, 2021. doi:10.1016/j.amc.2020.125883. (Cited on pages 13 and 91.)

[156] I. Tankam-Chedjou, S. Touzeau, L. Mailleret, J. J. Tewa, and F. Grognard. Modelling and control of a banana soilborne pest in a multi-seasonal framework. *Mathematical biosciences*, 322:108324, 2020. doi:10.1016/j.mbs.2020.108324. (Cited on page 124.)

[157] B. S. Tchienkou-Tchiengang, I. Tankam-Chedjou, I. V. Yatat-Djeumen, and J. J. Tewa. Multi-seasonal modelling of the african maize stalk borer with assessment of crop residue management. *Applied Mathematical Modelling*, 114:379–407, 2023. URL: https://www.sciencedirect.com/science/article/pii/S0307904X22004474, doi:https://doi.org/10.1016/j.apm.2022.09.025. (Cited on page 13.)

[158] V. M. Toledo and P. Moguel. Coffee and sustainability: the multiple values of traditional shaded coffee. *Journal of Sustainable Agriculture*, 36(3):353–377, 2012. (Cited on page 61.)

[159] N. E. Torres Castillo, E. M. Melchor-Martínez, J. S. Ochoa Sierra, R. A. Ramirez-Mendoza, R. Parra-Saldívar, and H. M. Iqbal. Impact of climate change and early development of coffee rust – an overview of control strategies to preserve organic cultivars in mexico. *Science of The Total Environment*, 738:140225, 2020. doi:10.1016/j.scitotenv.2020.140225. (Cited on pages 5, 99 and 100.)

[160] V. Valencia, L. García-Barrios, E. J. Sterling, P. West, A. Meza-Jiménez, and S. Naeem. Smallholder response to environmental change: Impacts of coffee leaf rust in a forest frontier in mexico. *Land Use Policy*, 79:463–474, 2018. doi:10.1016/j.landusepol.2018.08.020. (Cited on page 3.)

[161] F. Van den Bosch, J. Metz, and J. Zadoks. Pandemics of focal plant disease, a model. *Phytopathology*, 89(6):495–505, 1999. doi:10.1094/PHYTO.1999.89.6.495. (Cited on page 12.)

[162] P. Van den Driessche and J. Watmough. Reproduction numbers and sub-threshold endemic equilibria for compartmental models of disease transmission. *Mathematical biosciences*, 180(1-2):29–48, 2002. doi:10.1016/s0025-5564(02)00108-6. (Cited on pages 21, 22, 40 and 42.)

[163] J. Van der Plank. Chapter 7 - analysis of epidemics. In J. HorsfallO and A. Dimond, editors, *Plant Pathology*, pages 229–289. Academic Press, 1960. doi:10.1016/B978-0-12-395678-1.50013-8. (Cited on pages 11 and 12.)

[164] J. Van der Plank. Dynamics of epidemics of plant disease: Population bursts of fungi, bacteria, or viruses in field and forest make an interesting dynamical study. *Science*, 147(3654):120–124, 1965. (Cited on page 11.)

[165] J. Vandermeer, Z. Hajian-Forooshani, and I. Perfecto. The dynamics of the coffee rust disease: an epidemiological approach using network theory. *European Journal of Plant Pathology*, 150(4):1001–1010, 2018. doi:10.1007/s10658-017-1339-x. (Cited on pages 17, 34, 61, 116 and 124.)

[166] J. Vandermeer, D. Jackson, and I. Perfecto. Qualitative dynamics of the coffee rust epidemic: educating intuition with theoretical ecology. *BioScience*, 64(3):210–218, 2014. doi:10.1007/s10658-017-1339-x. (Cited on pages 17, 61 and 120.)

[167] J. Vandermeer and A. King. Consequential classes of resources: Subtle global bifurcation with dramatic ecological consequences in a simple population model. *Journal of theoretical biology*, 263(2):237–241, 2010. doi:10.1016/j.jtbi.2009.12.006. (Cited on page 17.)

[168] J. Vandermeer, I. Perfecto, and H. Liere. Evidence for hyperparasitism of coffee rust (Hemileia vastatrix) by the entomogenous fungus, Lecanicillium lecanii, through a complex ecological web. *Plant Pathology*, 58(4):636–641, 2009. doi:10.1111/j.1365-3059.2009.02067.x. (Cited on pages 10, 75, 92, 117, 120 and 132.)

[169] J. Vandermeer and P. Rohani. The interaction of regional and local in the dynamics of the coffee rust disease. *arXiv*, 1407.8247, 2014. doi:10.48550/arXiv.1407.8247. (Cited on pages 17, 61 and 116.)

[170] J. Waller. Control of coffee diseases. In *Coffee*, pages 219–229. Springer, 1985. (Cited on page 2.)

[171] J. Waller, M. Bigger, and R. Hillocks. World coffee production. In *Coffee pests, diseases and their management*, pages 17–33. CABI Wallingford UK, 2007. (Cited on pages 2, 3 and 4.)

[172] J. M. Waller. Coffee rust—epidemiology and control. *Crop Protection*, 1(4):385–404, 1982. doi:10.1016/0261-2194(82)90022-9. (Cited on pages 33, 36, 62 and 64.)

[173] H. Wang. *Mathematical modeling I-preliminary*. Bookboon, 2012. (Cited on pages 25, 98 and 128.)

[174] J. Wang, J. Yang, and T. Kuniya. Dynamics of a pde viral infection model incorporating cell-to-cell transmission. *Journal of Mathematical Analysis and Applications*, 444(2):1542–1564, 2016. (Cited on page 72.)

[175] R. Ward, D. Gonthier, and C. Nicholls. Ecological resilience to coffee rust: Varietal adaptations of coffee farmers in copán, honduras. *Agroecology and Sustainable Food Systems*, 41(9-10):1081–1098, 2017. doi:10.1080/21683565.2017.1345033. (Cited on page 3.)

[176] Wikipedia. Hemileia vastatrix. [accessed 12/9/2022]. URL: https://en.wikipedia.org/wiki/Hemileia_vastatrix. (Cited on page 7.)

[177] J. N. Wintgens, editor. *Coffee: Growing, processing, sustainable production. A guidebook for growers, processors, traders and researchers.* Wiley, 2009. doi:10.1002/9783527619627. (Cited on pages 2, 4, 5, 10 and 33.)

[178] K. Wong and W. Tang. Optimal control of switched impulsive systems with time delay. *The ANZIAM Journal*, 53(4):292–307, 2012. doi:10.1017/S1446181112000284. (Cited on page 124.)

[179] A. Yagi. *Abstract parabolic evolution equations and their applications*. Springer Science & Business Media, 2009. (Cited on page 70.)

[180] L. Zambolim. Current status and management of coffee leaf rust in brazil. *Tropical Plant Pathology*, 41(1):1–8, 2016. doi:10.1007/s40858-016-0065-9. (Cited on pages 33, 36, 100 and 116.)

[181] B. Zewdie, A. J. Tack, B. Ayalew, G. Adugna, S. Nemomissa, and K. Hylander. Temporal dynamics and biocontrol potential of a hyperparasite on coffee leaf rust across a landscape in arabica coffee's native range. *Agriculture, Ecosystems & Environment*, 311:107297, 2021. doi:10.1016/j.agee.2021.107297. (Cited on pages 10, 17 and 18.)

[182] W. Zhu. Global exponential stability of impulsive reaction–diffusion equation with variable delays. *Applied Mathematics and Computation*, 205(1):362–369, 2008. doi:10.1016/j.amc.2008.08.018. (Cited on page 80.)